Author:
Li, Yunfei

Title:
Cartilage Degeneration and Subchondral Bone Microarchitecture in Hip Osteoarthritis and Osteoporosis

A Regional, Zonal, and Compartmental Comparison

Cartilage Degeneration and Subchondral Bone Microarchitecture in Hip Osteoarthritis and Osteoporosis:

A Regional, Zonal, and Compartmental Comparison

李云飞

Yunfei Li

A dissertation submitted to the University of Bristol in accordance with the requirements of the degree of Doctor of Philosophy in the Translational Health Sciences, Bristol Medical School, Faculty of Health Sciences

July 2021

39228 Words

For my beloved family

致我亲爱的家人

ABSTRACT

Osteoporosis (OP) and Osteoarthritis (OA) are two of the most common musculoskeletal diseases in the ageing population. This study aimed at a comprehensive comparison of subchondral bone and cartilage changes between OP and OA, in order to better understand their commonalities and differences and provide new information on the pathological process of OA.

Femoral heads with OP (N=7) and OA (N=31) were collected from patients undergoing arthroplasty surgeries. Osteochondral plugs were extracted from different regions of the femoral heads according to the severity of cartilage degradation assessed by a new macroscopic and a modified OARSI microscopic grading system. Plugs were scanned by micro-computed tomography and it was shown that subchondral bone with early cartilage degradation in OA was similar to those in OP in terms of both microarchitecture and matrix mineralisation, in both subchondral plate and trabecular bone. In contrast, subchondral bone in OA with advanced cartilage degradation was sclerotic and hypo-mineralised. These data indicate that subchondral bone remodelling in OA is a biphasic process and at an early stage it may have similar features to those seen in OP. Moreover, subchondral trabecular bone was more mineralised than the subchondral plate in both OP and OA, and the relationships among trabecular bone volume fraction, material density, and apparent density were similar in OP and different stages of OA.

Chondrocytes expressing MMP13 and ADAMTS4 were located mainly in the upper zone(s) of cartilage in both OP and OA as shown by immunohistochemistry. The percentage of degradative chondrocytes in different zones of cartilage in OA exhibited a significant variation with the severity of cartilage degradation. The percentage was significantly lower in OP in all zones compared to various stages of OA, but exhibited greater heterogeneity. The correlations between expression of degradative enzymes by chondrocytes and subchondral bone properties in OP and OA were statistically significant for only a few parameters examined, and the correlations were generally weak. Based on these data a novel model of cartilage degradation in OA was proposed, in which biochemical disruption is more important in early stages while mechanical wear is critical in advanced stages.

AUTHOR'S DECLARATION

I declare that the work in the dissertation was carried out in accordance with the requirements of the Regulation and Code of Practice for Research Degree Programmes at the University of Bristol and that it has not been submitted for any other academic award. Except for where indicated by specific references in the text, the research presented is my own work. Work done in collaboration with, or with the assistance of, others, is indicated as such. Any views expressed in the dissertation are those of the author.

Yunfei Li

July 2021

ACKNOWLEDGEMENT

I would like to thank my supervisors, Dr Mohammed Sharif and Professor Ashley Blom, for their generous support, guidance, and advice throughout the four challenging years. The work would not have been possible without their help and dedicated supervision.

I would like to thank the China Scholarship Council and University of Bristol for the financial support they provided for this PhD programme.

I am grateful to my fellow students, Ms Yulia Liem, Mr Haroon Ahmed and Ms Grace Matilda Sellers at Bristol Medical School, who helped with some of the experiments and data analysis as indicated in the thesis. I would like to acknowledge those who provided invaluable academic advice and technical support during my project, Professor John Tarlton, Dr Khadija Ourradi, Dr Candida Tasman, Dr Erika Kague, Dr Ali Bienemann, Dr Lisa Boulter, Ms Debbie Martin, and Professor Claire Perks at University of Bristol; Professor Zaitunnatakhin Zamli at the International Islamic University Malaysia; Dr Enrico Dall'Ara at University of Sheffield; Dr Ngee Han Lim and Dr Bryony Stott at University of Oxford; and Mr Simon Florio at the Severn Pathology. I want to express my sincere thanks to our lab administration team, especially Ms Emma Foose and Mr Tom Hathway, who were always there for my logistic needs.

My thanks also go to patients who supported the research by agreeing to participate and donating their surgically removed joint specimens. The very well organised and efficient tissue collection would not have been possible without the help from the outstanding surgeons at the Southmead Hospital, Mr Niall Sullivan, Mr Mike Whitehouse, and Mr Bas Van Ooij.

Thank you, to every teacher, tutor, doctor, lecturer and professor that I met in my thirty years' education who together brought me here. Thank you, to all my classmates and friends, you have been very supportive during this journey and I hope the journey ahead.

My special thanks go to my mother and father, who raised me and unconditionally supported my education in the past thirty years. I am grateful to my parents-in-law, for treating me like their own son and encouraging me in the pursuit of a higher academic degree. I will always

remember my grand-parents, I am sure they would be happy seeing what I have achieved today. My dear wife, thank you for taking care of me and our lovely daughter through the most difficult times, I am a lucky man to have you by my side. My daughter, you are my world and I am sorry for not being there when you were born and for being missing from your life most of the time in the last two years.

PUBLICATIONS

A full-length peer-reviewed research article based on the data presented in Chapter 4 and Chapter 5 of this thesis has been published on the Journal of Orthopaedic Research.

Li, Y., Liem, Y., Dall'Ara, E., Sullivan, N., Ahmed, H., Blom, A., and Sharif, M. Subchondral bone microarchitecture and mineral density in human osteoarthritis and osteoporosis: A regional and compartmental analysis. Journal of Orthopaedic Research. 2021;1-13.

Conference abstracts based on the data generated from this PhD project are listed below.

Li, Y., Liem, Y., Dall'Ara, E., Fry, C., Sullivan, N., Tucker, D., Zamli, Z., Ahmed, H., Sellers, G.M., Blom, A. and Sharif, M. Regional and compartmentalized variation of subchondral bone mineralization and microarchitecture in hip osteoarthritis. Osteoarthritis Research Society International (OARSI): World Congress on Osteoarthritis (Vienna, Austria, 2020).

Li, Y., Y. Liem, N. Sullivan, D. Tucker, S. Florio, D. Martin, H. Ahmed, A. Blom, and M. Sharif. "Quick and accurate evaluation of cartilage histopathology on undecalcified osteochondral tissue. Osteoarthritis Research Society International (OARSI): World Congress on Osteoarthritis (Vienna, Austria, 2020).

Li, Y., H. Ahmed, E. Dall'ara, N. Sullivan, Y. Liem, D. Tucker, C. Fry, B. V. Ooij, A. Blom, and M. Sharif. Spatial variations of bone microarchitecture and mineralization in hip osteoarthritis and osteoporosis. European Alliance of Associations for Rheumatology (EULAR): Annual European Congress of Rheumatology (Frankfurt, Germany, 2020).

STATEMENT OF AUTHORSHIP

As stated in the publication listed below, as the first author of the publication Yunfei Li was responsible for the design of the study, acquisition of data, analysis and interpretation of data, drafting of manuscript, critical revision of manuscript, and approval of final manuscript. A description of contribution of other authors can be found in the publication.

Li, Y., Liem, Y., Dall'Ara, E., Sullivan, N., Ahmed, H., Blom, A., and Sharif, M. Subchondral bone microarchitecture and mineral density in human osteoarthritis and osteoporosis: A regional and compartmental analysis. Journal of Orthopaedic Research. 2021;1-13.

First Author signature: Date:

Supervisor signature: Date:

TABLE OF CONTENTS

LIST OF FIGURES

LIST OF TABLES

LIST OF ABBREVIATIONS

ACLT	Anterior cruciate ligament transection
ACP	Amorphous calcium phosphate
ADAMTS	A disintegrin and metalloproteinase with thrombospondin motifs
AGE	Advanced glycation end products
ALP	Alkaline phosphatase
ANOVA	Analysis of variance
BMC	Bone mineral content
BMD	Bone mineral density
BMI	Body mass index
BML	Bone marrow lesions
BMP	Bone morphogenic protein
BMU	Basic multicellular unit
BRC	Bone remodelling compartment
BS/BV	Specific bone surface (bone surface/bone volume)
BV/TV	Bone volume fraction (bone volume/tissue volume)
CMFDA	5-chloromethylfluorescein diacetate
Col I	Type I collagen
Col II	Type II collagen
Col III	Type IIII collagen
Col IX	Type IX collagen
Col VI	Type VI collagen
Col X	Type X collagen
Col XI	Type XI collagen
COMP	Cartilage oligomeric matrix protein
Conn.Dn	Connectivity density
CTAn	CT Analyzer software
CTX	C-terminal telopeptide of collagen
DAB	3, 3'-diaminobenzidine
DDR2	Discoindin domain receptor 2
DMOAD	Disease modifying osteoarthritis drug
DXA	Dual-energy X-ray absorptiometry
DZ	Deep zone
ECM	Extracellular matrix
EDTA	Ethylenediaminetetraacetic acid
ER	Oestrogen receptor
FOXO	Forkhead box O
FRAX	Fracture Risk Assessment Tool
GAG	Glycosaminoglycan
H&E	Hematoxylin and eosin
HGF	Hepatocyte growth factor
HHGS	Histologic/histochemical grading system

HRP	Horseradish peroxidase
HRT	Hormone replacement therapies
HTRA1	High temperature requirement A1
ICC	Intraclass correlation coefficient
ICRS	International Cartilage Repair Society
IGD	Interglobular domain
IGF	Insulin-like growth factor
IHC	Immunohistochemistry
IL	Interleukin
ITM	Inter-territorial matrix
JSN	Joint space narrowing
K-L	Kellgren and Lawrence grading
K-W	Kruskal-Wallis test
LOA	Limits of agreement
M-CSF	Macrophage colony stimulating factor
microCT	Micro-computer tomography
MMP	Matrix metalloproteinase
MRI	Magnetic resonance imaging
MZ	Middle zone
NCP	Non-collagenous protein
NGF	Nerve growth factor
NHS	National Health Services
NSAID	Non-steroidal anti-inflammatory drug
OA	Osteoarthritis
OARSI	Osteoarthritis Research Society International
OP	Osteoporosis
OPG	Osteoprotegerin
PBS	Phosphate buffered saline
PCM	Pericellular matrix
PCR	Polymerase chain reaction
PDGF	Platelet derived growth factor
PGE2	Prostaglandin E2
PI	Propidium iodide
PIICP	Procollagen II C-pro-peptide
PIINP	Procollagen II N-pro-peptide
Pl.Po	Plate porosity
Pl.Th	Plate thickness
PTH	Parathyroid hormone
QCT	Quantitative computed tomography
RAGE	Receptor for advanced glycation end-products
RANK	Receptor activator of nuclear factor NF-κB
RANKL	RANK ligand
ROI	Region of Interest
ROS	Reactive oxygen species

SASP	Senescence associated secretory phenotype
SBA	Subchondral bone attrition
SD	Standard deviation
SERM	Selective oestrogen receptor modulator
SIBLING	Small integrin-binding ligand N-linked glycoprotein
SLRP	Small leucine-rich proteoglycan
SMI	Structure model index
SZ	Superficial zone
Tb.N	Trabecular number
Tb.Sp	Trabecular separation
Tb.Th	Trabecular thickness
TGF	Transforming growth factor
TM	Territorial matrix
TMD	Tissue mineral density
TNF	Tumour necrosis factor
TRAP	Tartrate-resistant acid phosphatase
VEGF	Vascular endothelial growth factor
WHO	World Health Organisation
WOMAC	Western Ontario and McMaster Universities OA index

Chapter 1

Introduction

Osteoporosis (OP) and Osteoarthritis (OA) are two of the most common musculoskeletal diseases in the ageing population. OA is characterised by cartilage degeneration, subchondral bone sclerosis, synovial inflammation and osteophytes formation at diarthrodial joints, leading to pain and disability. OP is characterised by systemic loss of bone due to unbalanced bone resorption, leading to increased risk of fragility fractures. The relationship between the two conditions has been a topic of discussion for decades. While the historical view is that OP and OA are mutually exclusive diseases, recent evidence suggests an overlap between their pathophysiology. The purpose of this study is a comprehensive comparison of subchondral bone and the overlying cartilage in OP and OA, in order to build a more detailed knowledge of the commonalities and differences between the two diseases.

1.1 DIARTHRODIAL JOINT

A diarthrodial joint (**Figure 1.1A**), also known as synovial joint, consists of the two ends of adjacent bones which are covered by a layer of articular cartilage. The joint is protected and stabilised by joint capsule, ligaments, tendons and muscles. The inner layer of joint capsule is lined by a thin membrane called synovium or synovial membrane, which encloses the joint creating a cavity. The joint cavity is filled with synovial fluid that lubricates joint movements and provides nutrient for articular cartilage. Additional components such as meniscus may also present in specific joints like the knees.

A hip joint is composed of the proximal end of femur (femoral neck and femoral head) and acetabulum of pelvis (**Figure 1.1A, B**). It is a typical 'ball and socket' joint. The sphere-like femoral head is superiorly and medially contained by the cup-like acetabulum, bearing the weight of body and allowing movement of the lower limb. Hip OA and low-energy fracture of the femoral neck due to OP are both common in the elderly population (**Figure 1.1C, D**). Surgical treatments of these conditions, including total arthroplasty and hemiarthroplasty,

can provide readily available joint specimens. Therefore, the hip joint is a good candidate for clinical and translational research investigating and/or contrasting OP and OA.

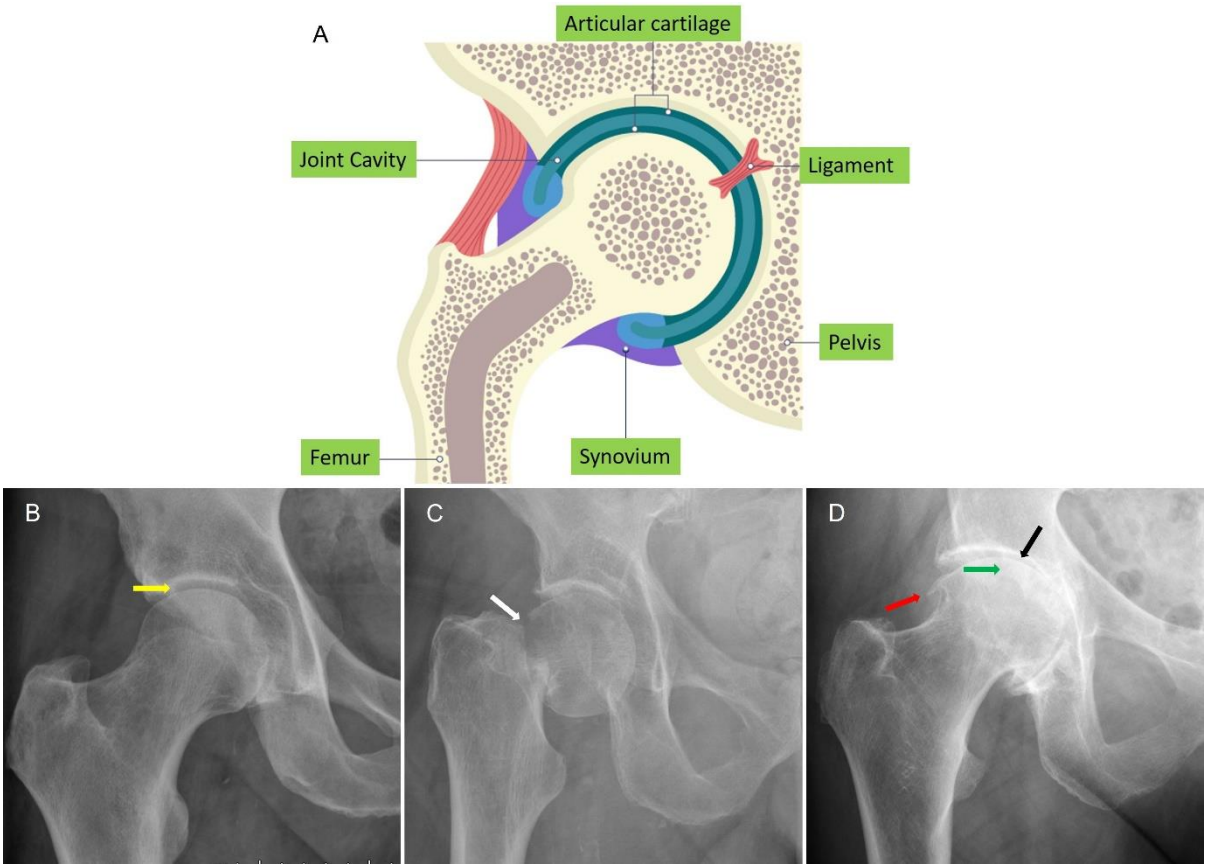

Figure 1.1. Hip joint. (A) Schematic illustration of hip joint. Hip joint is a 'ball and socket' joint consisting of the proximal end of femur and acetabulum of pelvis. Articular surfaces are covered by articular cartilage. The joint is protected and stabilised by joint capsule, ligaments, tendons and muscles. The inner layer of joint capsule is lined by synovium, which encloses the joint creating a cavity that is filled with synovial fluid. (B) X-ray of a healthy hip joint. A clear joint space (yellow arrow) between femoral head and acetabulum can be observed. (C) X-ray of fracture of the femoral neck (white arrow) due to OP. (D) X-ray of a hip joint with OA. Narrowing of joint space (black arrow), sclerosis of subchondral bone (green arrow) and growth of osteophytes (red arrow) can be observed. (A) was adapted from https://efmurgi.wordpress.com/2019/09/26/the-skeletal-system/ with modifications. (B), (C) and (D) were from the participants recruited in this study.

1.2 BASIC SCIENCES OF BONE

Bone is a multifunctional organ that provides mechanical support and protection, contributes to the mobility of body, and participates in metabolic homeostasis and hematopoiesis. These functions of bone are dependent on its hierarchical and adaptive architectures at molecular, ultrastructural, microstructural, and anatomical levels (1-3), and are tightly regulated by bone cells in response to various biochemical and biomechanical factors (4-7).

1.2.1 Composition, structure, and anatomy

1.2.1.1 Extracellular matrix

1.2.1.1.1 Collagen

Organic components account for 20 – 25% of bone wet weight, of which roughly 90% is attributed to type I collagen (Col I) (2). A mature Col I molecule is a heterotrimer consisting of two α1 chains and one α2 chain, which assemble into a long helix structure in the middle, with short non-helical telopeptides at the C- and N-terminus (**Figure 1.2A**) (8). Five Col I molecules are crosslinked in a quarter-staggered manner by various enzymatically or non-enzymatically generated bonds to form microfibrils (**Figure 1.2B**), which further aggregate laterally and longitudinally to constitute fibrils that are about 10μm in length and 150nm in diameter (**Figure 1.2C**) (8-12). Such arrangements yield the typical periodical appearance of collagen fibres under electron microscopy (**Figure 1.2C, D**). The holes between the ends of molecules and the lateral space between the neighbouring molecules are bound with water attracted by hydroxyprolines and filled with mineral crystals (**Figure 1.2B**) (8, 10, 13).

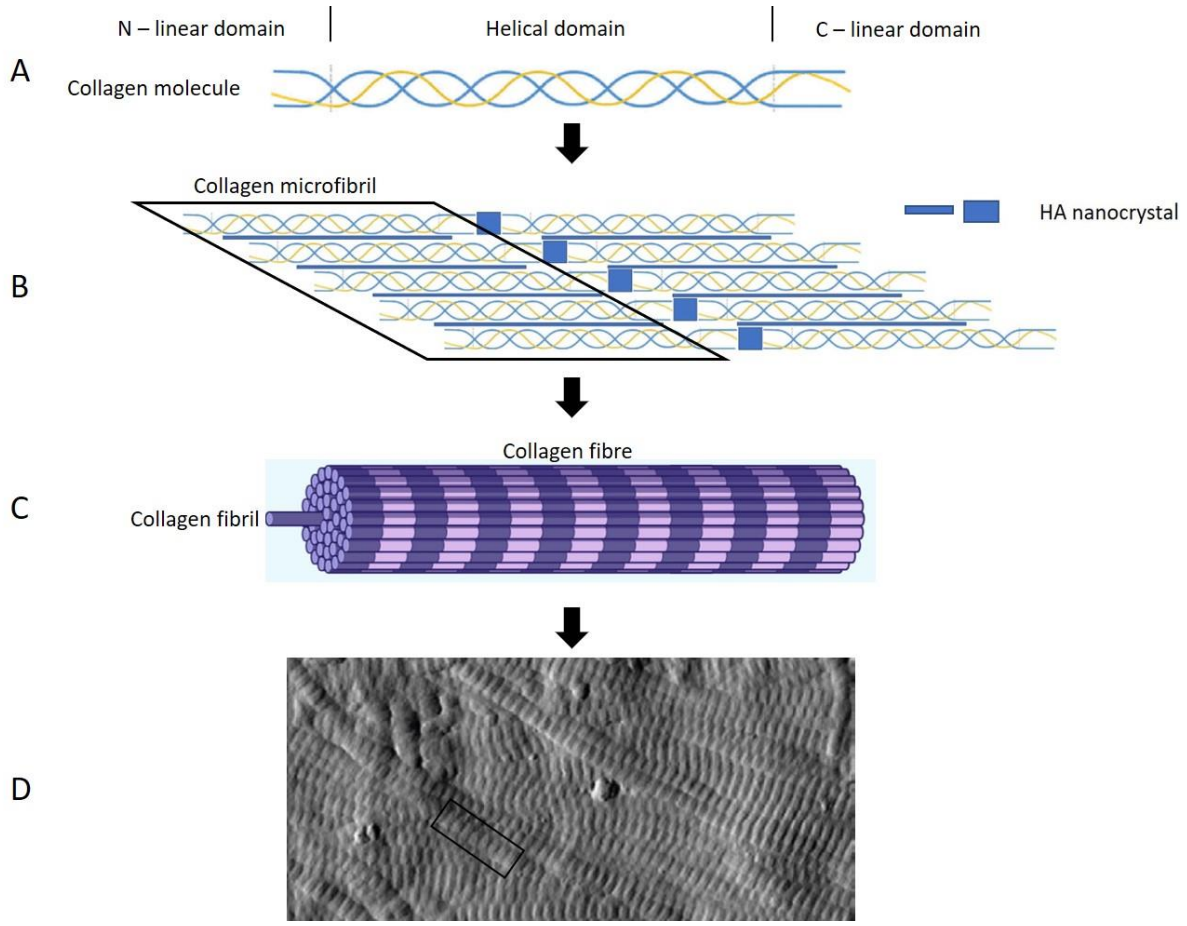

Figure 1.2. Type I collagen in bone extracellular matrix. (A) Mature type I collagen (Col I) molecule consists of two α1 chains and one α2 chain forming a long helical structure in the middle, with short linear domains at the C- and N-terminus. (B) Five Col I molecules are crosslinked in a quarter-staggered manner to form microfibrils, which further aggregate laterally and longitudinally to constitute fibrils. The spaces between molecules are filled with hydroxyapatite (HA) crystals. (C) Collagen fibrils assemble into fibres that have typical periodical appearances under electron microscopy (D). (A) and (B) were adapted from (693), (C) was adapted from (694) and (D) was adapted from (18) with modifications.

1.2.1.1.2 Minerals

Minerals account for about 65% of bone wet weight (14). Bone minerals are predominantly hydroxyapatite ($Ca_{10}(PO_4)_6(OH)_2$), which crystalises and grows laterally to develop a thin-plate shape that is orientated parallel to one another and to collagen fibrils (**Figure 1.2B**) (13, 15). The size of hydroxyapatite crystals in bone is approximately 30-50nm in length, 15-30nm in width and 2-10nm in thickness (9). The HA at crystal surfaces often exists in a unique dynamic phase. It is deficient in calcium (non-stoichiometry) with a Ca:P ratio lower than 1.67, and the hydroxyl and phosphate ions are substituted by carbonate (8, 15-17). Such chemical

impurities, together with the relatively small crystal size but large surface area, bestow bone minerals with the solubility needed for rapid resorption and release, allowing bone to continuously remodel itself and play a role in the regulation of acid-base homeostasis and calcium-phosphate metabolism (9, 12).

Mineral deposition in new bone is a biphasic process that follows the 'mineralisation law' (18-20). According to this law, upon the laying down of organic scaffold, hydroxyapatite is quickly deposited within the spaces of collagenous matrix. This primary rapid phase is responsible for approximately 70% of bone mineralisation at physiological conditions and lasts for up to 3 weeks. It is followed by a much slower secondary phase that is characterised by the maturation and growth of apatite crystals and takes months to years to complete. The exact mechanism of mineral deposition in collagen framework during bone formation is yet to be defined but nucleation of amorphous calcium phosphate (ACP) mediated by non-collagenous proteins (NCPs), Col I fibrils and water may be involved (9, 16, 21-23).

1.2.1.1.3 Others

NCPs represent a minor proportion of organic members in the extracellular matrix of bone, but are indispensable for bone biology. They include proteoglycans (e.g., hyaluronan, small leucine-rich proteoglycans (SLRPs) and versican), glycoproteins (e.g., alkaline phosphatase, fibronectin), proteins of the small integrin-binding ligand N-linked glycoprotein family (SIBLING, e.g., osteopontin, dentin matrix acidic phosphoprotein 1 (DMP), and sialoproteins), osteocalcin and osteonectin (24, 25). These proteins interact with bone cells, collagen fibrils, and/or minerals and herein participate in activities such as regulation of cell proliferation, modification of collagen framework, and deposition of minerals (22, 24).

Water occupies about 10% of bone wet weight (9). It comprises mobile water that is free-flowing in vascular, lacunar or canalicular systems, and structural water which is bound to or situated between collagen and mineral crystals (21, 26, 27). The former phase of water is important for transportation of nutrients, waste products and signalling molecules (28), while the bound water is critical for the organisation of collagen fibrils and apatite crystals, and contributes to the biomechanical properties of bone (15, 21, 29).

1.2.1.2 Ultrastructure

1.2.1.2.1 Haversian system

The ultrastructural unit of cortical bone is the osteon, also known as haversian system (**Figure 1.3A, B**) (3, 30). In the osteon, collagen fibres are orientated alternately in concentric layers known as lamellae, which enclose a central canal (haversian canal) containing a neurovascular bundle (**Figure 1.3A**) (31). In adult bone each osteon is about 1 – 10mm in length, 100 – 250μm in diameter (50μm for haversian canal) and has 20 – 25 laminar sheets (30). Haversian canals of adjacent osteons are connected by transversely running tunnels named Volkmann's canals (**Figure 1.3A**) (32). Though Volkmann's canals, the haversian vessels are connected to each other and to the local vascular plexus, allowing inter-osteonal communications and transportation (33). The interface between neighbouring lamellae is interspersed by holes (200-600μm^3 in volume) called lacunae (**Figure 1.3A**), in which osteocytes are embedded (34). They resemble a solar system spreading around the haversian canal. Lacunae are connected by tinny tunnels called canaliculi (100-700nm in diameter) in which cell processes are encapsulated to allow inter-cellular communications (35, 36). The lacuna-canalicular network plays a critical role in the mechano-transduction that induces bone remodelling and repair (36-41). Osteons are commonly orientated roughly along the direction of the primary mechanical force borne by the bone. For example, osteons in the diaphysis of femur are aligned roughly along the long axis with slight inclination (5° – 15°), as the femur is subjected to mainly vertical compression and some degree of torsion and bending (42). Individual osteons are separated from each other and from the interstitial area by their outer wall – the cement line (43). Between osteons lie the interstitial lamellae which comprise disorganised incomplete lamellae representing the remnants of previously resorbed bone (**Figure 1.3A**) (14). Osteons and interstitial bone are surrounded by circumferential lamellae which form the outer shell of cortical bone (**Figure 1.3A**).

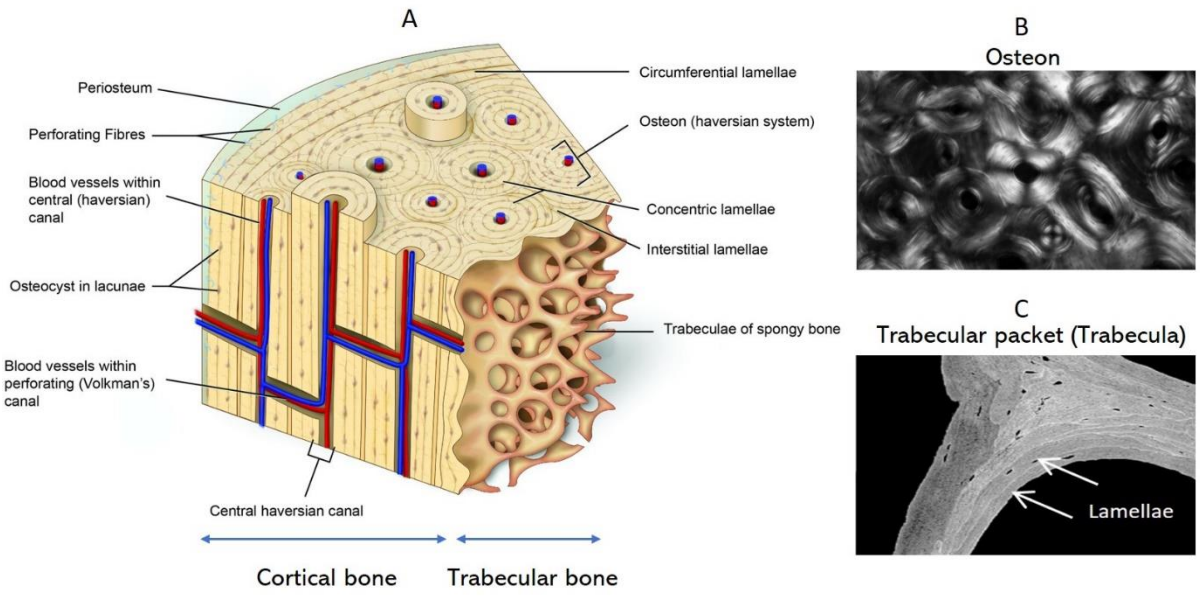

Figure 1.3. Ultra- and microstructure of bone. (A) Schematic presentation of bone structure. Bone processes a compact outer shell called cortical bone and a spongy-like inner structure called trabecular bone. The ultrastructural unit of cortical bone and trabecular bone is osteon and lamellar packet, respectively. The electron microscopy images of osteon and trabecular packet are shown in (B) and (C). Osteon consists of concentric lamellae surrounding the central canal, while lamellar packet consists of lamellae running along the direction of the trabecula. (A), (B) and (C) were adapted from (695), (30) and (18) respectively with modifications.

1.2.1.2.2 Trabecular packet

The ultrastructural unit of trabecular bone is lamellar packet, which is composed of parallel lamellae running along the direction of individual trabecula (**Figure 1.3C**) (31). Osteocyte lacunae and canaliculi are buried across the packets as in osteons, except that there is not a central canal for them to circle around.

1.2.1.3 Microstructure

1.2.1.3.1 Cortical bone

Bones possess a dense outer shell made of compact cortical bone (**Figure 1.3A**), the thickness of which varies between various types of bones and between different locations within bones (e.g., epiphysis or diaphysis of long bone). Cortical bone accounts for about 80% of total bone volume in human skeleton (31, 44). Cortical bone consists of harversian systems and

interstitial and circumferential lamellae arranged in a compact manner with limited porosity. Porosity of cortical bone (intra-cortical porosity) can be attributed to harversian and Volkmann's canals, osteocyte lacunae, canaliculi, resorption cavities, and holes where blood vessels penetrate the cortical shell into the medullary cavity (33, 45, 46). The inner walls of harversian and Volkmann's canals are termed intra-cortical surfaces. They are covered by a layer of osteoprogenitor cells (lining cells) (33) and represent locations of remodelling activities in cortical bone (46, 47). The external surface of cortical bone is covered by a membrane called periosteum which consists of an outer fibrous layer for protection and muscle attachments, and an inner osteogenic cell layer for bone growth and repair (48).

1.2.1.3.2 Trabecular bone

Inside the cortical shell is the trabecular bone (also called cancellous or spongy bone) that comprises of lamellar packets which assemble into rod- or plate-like struts (i.e., trabeculae) (**Figure 1.3A, C**) (49). Trabeculae stretch out from the internal surface of cortical bone and are connected to each other to form a spongy-like porous structure that is filled with bone marrow (14). Porosity of trabecular bone commonly refers to the volumetric ratio of the interspersed marrow space, which normally ranges around 70% (45, 47). Though trabecular bone contributes to only about 20% of total bone in human, it provides a relatively large surface area for bone remodelling which is important for mineral metabolism in physiological conditions (31, 47). These surfaces are covered by lining cells and can be further classified into those facing the medullary cavity (endosteum or endosteal surface) and those within the trabecular framework (trabecular surface) (30).

1.2.1.4 Gross anatomy

Adult human skeleton consists of 206 bones. Based on the shape, location and anatomical functions they can be subdivided in to 5 categories. Long bones are present at extremities of body such as femur of thigh, tibia of leg, radius of arm and phalanges of fingers. They are characterised by a long hollow shaft (diaphysis) and two relatively enlarged ends (epiphysis) with transitional areas (metaphysis). They act like levers to support muscular movements and bear the weight of body at lower limbs (31). Flat bones, such as occipital/frontal/parietal bones of cranium and ribs and sternum of chest, usually have a broad and strong surface to protect vital organs like brain, lungs, and those in the abdomen. Irregular bones include

vertebrae and sacrum which are the support of the axial skeleton. Short bones have roughly three equal dimensions and are often those connecting long bones at joints and facilitating joint movements, e.g., carpal bones of wrist and tarsal bones of ankle. Sesamoid bones are usually embedded in tendons subjected to stress and frictions, such as the patella in the quadricep femoris tendon of the knee joint. In diaphysis of long bone the central space often enlarges to form a medullary cavity, which is surrounded by a thin trabecular framework immediately beneath cortical bone. In other types of bone and the epiphysis of long bone, the internal space is often occupied completely by trabecular bone. Bones also develop anatomical marks symbolising their physical functions such as tuberosities and processes for tendon and muscle attachment, and grooves for the passage of ligaments, muscles, and neurovascular bundles.

1.2.2 Bone cells

1.2.2.1 Osteoblast

Osteoblasts are bone-forming cells (**Figure 1.4**). They originate from osteoprogenitors which are mesenchymal stem cells found in bone marrow or periosteum (14, 50). Upon stimulation by various growth factors, cytokines, hormones and biomechanical factors, osteoprogenitors at the site of bone formation proliferate and differentiate into osteoblasts (51, 52). These procedures are mediated primarily by the classic canonical Wnt/β-catenin signalling pathway, which is also important for osteoblast survival and function and regulates osteoclast activities indirectly through the RANK – RANKL – OPG pathway (see **Section 1.2.3.3**) (53, 54). Mature active osteoblasts resemble typical biological features of protein-producing cells – cuboidal shape with large nuclei, prominent Golgi apparatus, and extensive endoplasmic reticulum (55). Osteoblasts are also recognised by the expression of alkaline phosphatase (ALP) and osteocalcin, which play pivotal roles in the mineralisation process (56, 57). The level of these proteins in the circulation can be used as indicator of osteoblast number and bone formation (55, 58, 59). During bone formation, osteoblasts produce and secrete matrix components including Col I and proteoglycans to first construct an organic template/scaffold known as osteoid (60). This is followed by primary and secondary mineral deposition as mentioned in **Section 1.2.1.1.2**. Upon fulfilling their role in bone formation, a large proportion of osteoblasts progress to apoptosis. Of the remaining cells, some are transformed into bone

lining cells covering the quiescent bone surface, while others are embedded in the newly synthesised matrix and become osteocytes (61, 62). Bone lining cells have the osteogenic potential to convert back to active osteoblasts (63), a process that is implicated in the reversal phase in bone remodelling (see **Section 1.2.3.3**) (64).

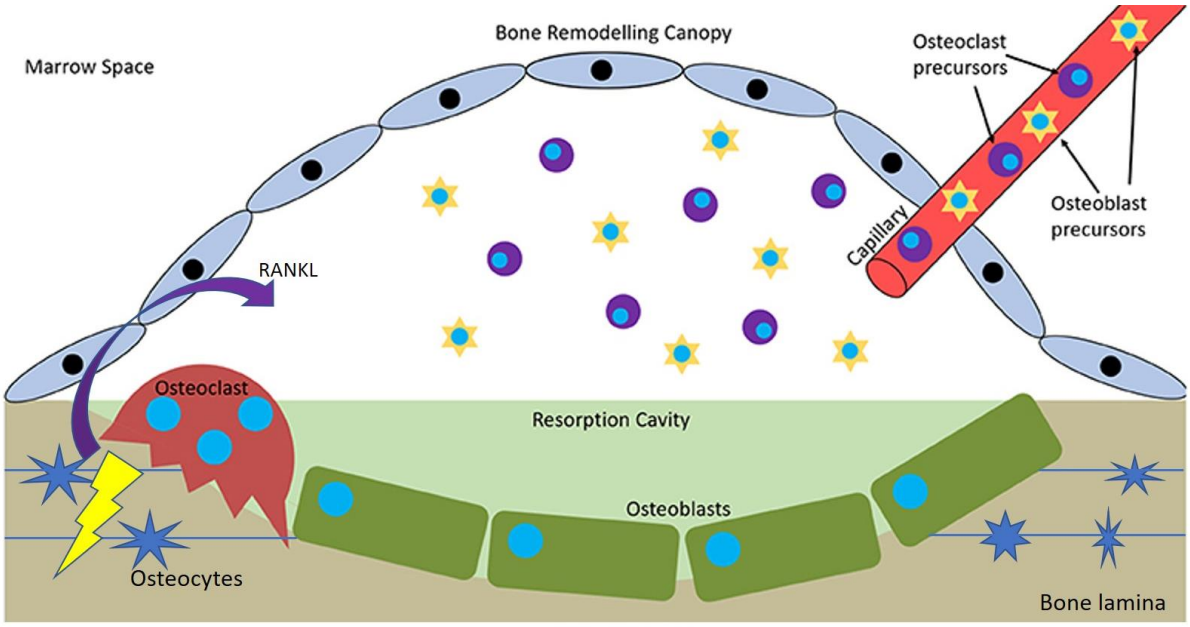

Figure 1.4. Basic multicellular unit and bone remodelling compartment. Upon stimulus by, for example, microdamage, RANKL can be released by osteocytes and stimulates relocation and differentiation of osteoclast progenitors at the site of remodelling. The lining cells are lifted to form the bone remodelling compartment where cells involved in the remodelling process are contained. These cells, including osteoclasts, osteoblasts, reversal cells (lining cells) and osteocytes, form a functional unit called basic multicellular unit. Mature osteoclasts resorb bone matrix, followed by a reversal step in which osteoblasts are recruited to the previously resorbed surface. Osteoblasts lay down newly synthesised osteoid which is then subjected to primary and secondary mineralisation. Osteoclasts die by apoptosis at the end of remodelling, while osteoblasts are buried in new bone and become osteocytes. Figure is adapted from (65) with modifications.

1.2.2.2 Osteocytes

During bone formation some osteoblasts are embedded in the lacunae in new matrix and become osteocytes (**Figure 1.4**). Osteocytes are mature bone cells and represent the largest population (>90%) of bone cells (66). Like neurons, osteocytes possess numerous projections

(processes) stretching out from the cell body and are in contact with the neighbouring companions through the canalicular system. Communications between osteocytes, and between osteocytes and other cells (osteoblasts, osteoclasts, lining cells and progenitors) on bone surfaces, are mediated via gap junctions formed by connexin 43 (66, 67), and via transport of soluble factors through canaliculi (40, 68). The primary function of osteocytes is to modulate bone homeostasis through regulation of bone resorption, formation and mineralisation in response to various stimuli, mainly growth factors, cytokines, hormones and mechanical stress (60, 61, 68, 69). Osteocytes are able to perceive changes in their biomechanical environment (e.g., motions, immobilisation, and injuries) either directly through cell and matrix deformation, or through alternations in the dynamics and streaming potentials of canalicular fluid (37, 68, 70-72). These biochemical and biomechanical simulations are transduced by osteocytes through various signalling pathways (e.g., Wnt/β-catenin) into biological regulators (e.g., RANKL/OPG, macrophage colony stimulating factor 1 (M-CSF)) that act on progenitors or mature osteoblasts and osteoclasts, either inhibiting or promoting bone formation and/or resorption (66, 73-75).

1.2.2.3 Osteoclast

Osteoclasts are responsible for bone resorption (**Figure 1.4**). Upon receiving osteocyte and/or osteoblast derived signals, hematopoietic monocyte-macrophage precursors in bone marrow or the circulation are recruited to the target bone area, where they fuse and differentiate into mature osteoclasts, a process called osteoclastogenesis (61, 68, 76, 77). Mature osteoclasts are multinucleated polarised cells with an apical membrane domain facing the bone surface and a basolateral membrane domain facing the cavities (marrow space, haversian canal, etc). The apical domain can be further divided into the peripheral ring-like sealing zone responsible for cell-bone attachment; the central ruffled border responsible for the secretion of protons (H^+) and proteinases needed for bone digestion; and the transition zone between the sealing zone and ruffled border. The apical domain encloses the resorption space and contains degraded bone matrix fragments within it (76). During bone resorption, protons pumped out from osteoclasts acidify the resorption space to allow dissolution of mineral crystals (60). This is followed by degradation of the exposed organic components by enzymes such as cathepsin

K, matrix metalloproteinases and tartrate-resistant acid phosphatase (TRAP) (78, 79). Once resorption is completed, osteoclasts end up dying by apoptosis (76).

1.2.3 Bone development, modelling and remodelling

1.2.3.1 Bone development

Development of bone includes two distinct processes: intramembranous ossification (skull, scapula, clavicle, etc) and endochondral ossification (e.g., long bones) (80-82). Intramembranous ossification relies on the establishment of primary ossification centre by a collection of mesenchymal cells, which differentiate into osteoblasts and then produce bone matrix. In endochondral ossification, however, the condensation of mesenchymal cells results in their differentiation into chondroblasts instead of osteoblasts. Chondroblasts produce a cartilaginous template for bone formation. Initially, osteoblasts appear at the outer surface of the template and build an osteal structure called the bone collar. This is accompanied by the hypertrophy and death of chondrocytes in the centre of cartilage and subsequent invasion of blood vessels, delivering osteoblast and osteoclast progenitors and triggering the formation of primary ossification centre. The primary ossification centre continuously expands radially and longitudinally. Later the secondary ossification centres occur at the distal ends of cartilage template in a similar way. Primary and secondary ossification centres join at the so-called growth plate. Cartilage at the upper part of growth plate keeps proliferating while at the bottom it becomes hypertrophic and is continuously resorbed and turned into bone. This ‘chase and run’ process is responsible for the longitudinal growth of long bone. At the time of skeletal maturity, growth plate is completely ossified and becomes the epiphyseal line.

1.2.3.2 Bone modelling

In the growing skeleton, modelling is the preliminary mechanism for bone to develop and optimise its shape and mass to meet the challenge of increasing body size and activities (5). Unlike remodelling (see next section), modelling is an uncoupled process involving either bone resorption (by osteoclasts) or formation (by osteoblasts) (83). A good example would be the enlargement of the medullary cavity of long bone by bone excavation from endosteal

surface, and the expansion of cortical bone by radial growth at the periosteal surface. These two simultaneous modelling procedures happen at different surfaces of bone and are independent from each other. These procedures result in the increasing diameter of long bones with relatively consistent thickness of the cortical shell. Bone growth via modelling is different from that via intramembranous or endochondral ossification in that modelling always happens on an existing bone surface, while the latter does not need an osteal template (83).

1.2.3.3 Bone remodelling

In the adult skeleton, remodelling is the key mechanism by which bone can adapt to the dynamic biomechanical demands, repair and renew itself, and participate in the mineral metabolism (84). The remodelling process, which takes months to complete, is a coordinated cycle of focal bone resorption and formation mediated by osteoclasts, the osteoblast lineage (osteoblasts, osteocytes, lining cells), and their progenitors (85). These cells form a functional group named basic multicellular unit (BMU) at the site of remodelling (**Figure 1.4**) (5, 86).

Initiation of bone remodelling is characterised by recruitment and differentiation of osteoclasts. The key regulator of this step is the signalling pathway involving the receptor activator of nuclear factor NF-κB (RANK), RANK ligand (RANKL), and osteoprotegerin (OPG) (76). RANKL is expressed by osteoblasts and/or osteocytes in response to biomechanical or biochemical stimuli (loading-unloading, microdamage/fracture, hormones, etc) (**Figure 1.4**) (55, 85). RANKL, either in secreted or membrane-bound form (87), binds to its receptor (RANK) expressed by progenitors of osteoclast, triggering their relocation to the remodelling site and subsequent activation/polarisation (88). This process can be antagonised by OPG, which is an osteoblast- and osteocyte-derived soluble decoy receptor for RANKL and therefore prevent its binding with RANK (89, 90). The RANKL/OPG ratio is an indicator of osteoclastogenic activities (85). Other factors such as M-CSF are also important for osteoclastogenesis (91).

Along with recruitment of osteoclasts, lining cells in the target bone area prepare the surface by lifting up to form a canopy and create the bone remodelling compartment (BRC) as a shelter for the ongoing remodelling process (**Figure 1.4**) (77, 92). Mature osteoclasts attach to the bone surface through the interactions between the sealing zone and bone matrix

components (77). Then they remove the enclosed bone matrix as described in **Section 1.2.2.3**, which is the second step of the bone remodelling cycle. The released fragments of matrix components such as C-terminal telopeptide of Col I (CTX-I) in serum or urine can be used as clinical marker for bone turnover status (93).

In physiological conditions, bone resorption and formation in each remodelling cycle is locally coupled, meaning that the amount of bone removed roughly equals the amount of bone formed (94-96). The 'coupling' is mediated by the so-called 'reversal' step through which osteoblasts are recruited to the resorbed bone surface (**Figure 1.4**) and then start laying down newly synthesised Col I (77). Molecular and cellular mechanism for the reversal step is yet to be defined. It is generally accepted that, as osteoclasts move along, the exposed destructed bone surface is covered by a layer of mononuclear cells, which are commonly described as the 'reversal cells' covering the 'reversal surface' (97). Reversal cells are suspected to be members of the osteoblast lineage, especially lining cells (98). Upon attraction to the exposed surface, these cells first clean up the resorption pit, followed by a phenotype change into osteogenic osteoblasts (64, 98-101). In the meantime, osteoclastogenesis and osteoclast function are suppressed and bone resorption gradually stops. A number of mechanisms have been suggested to be involved in the reversal process, including the bidirectional communication between osteoclasts and reversal cells through the membrane-bound ephrinB2/EphB4 signalling system, the growth factors and cytokines liberated from degraded bone matrix or released from osteoclasts, and morphological sensing of the resorbed cavity by reversal cells (77, 85).

The last step of the remodelling cycle, bone formation, starts with production of organic matrix by osteoblasts, which is followed by primary and secondary mineralisation as described in **Section 1.2.1.1.2**. The cement line symbolises the loci where bone resorption stops and formation begins (100).

1.2.4 Biomechanics

Bone is exposed to a variety of biomechanical challenges *in vivo*, including, but not limited to, compression, torsion, tension, shear and bending forces in daily activities. Bone must be strong to resist deformation in order to provide support and protection, yet it has to exhibit

some extent of flexibility so that it absorbs energy without fracture (43, 102). Bone's capability of meeting these mechanical demands comes from its hierarchical structure. More intriguingly, it is able to dynamically adjust its structure in response to the changes in these demands through modelling and remodelling, a process well known as the 'Wolff's law' (103).

At material level, minerals contribute to bone tissue strength and stiffness while collagens determine its ductility and toughness (104, 105). Completely demineralised bone is soft and easily deformed while fully deproteinated bone is strong but brittle, thus prone to fracture (106-108). An optimal trade-off is often achieved under physiological conditions. At apparent level, the strength and toughness of the entire bone specimen, including pores, canals, and marrow space, are determined not only by the mineral and collagen composition of the bone tissue itself, but also by the presented quantity and architectural arrangements of the bone tissue (109). This is illustrated in **Figure 1.5**. Given a fixed volume and architecture, bone that has a lower tissue mineralisation is less capable of weight bearing. However, given a fixed level of mineralisation, cortical bone that has thinner and more porous walls with smaller diameter, and trabecular bone that is thinner, less connected and rod-shaped, are generally less resistant to load.

Material and apparent mechanical properties of bone can be examined using a number of mechanical tests (110). A series of parameters, for example, elastic modulus (a measure of stiffness), ultimate stress (a measure of strength) and failure energy (a measure of fracture toughness), can be calculated by plotting stress (force applied per unit area) against strain (percentage deformation) to describe the mechanical properties of bone (110-112).

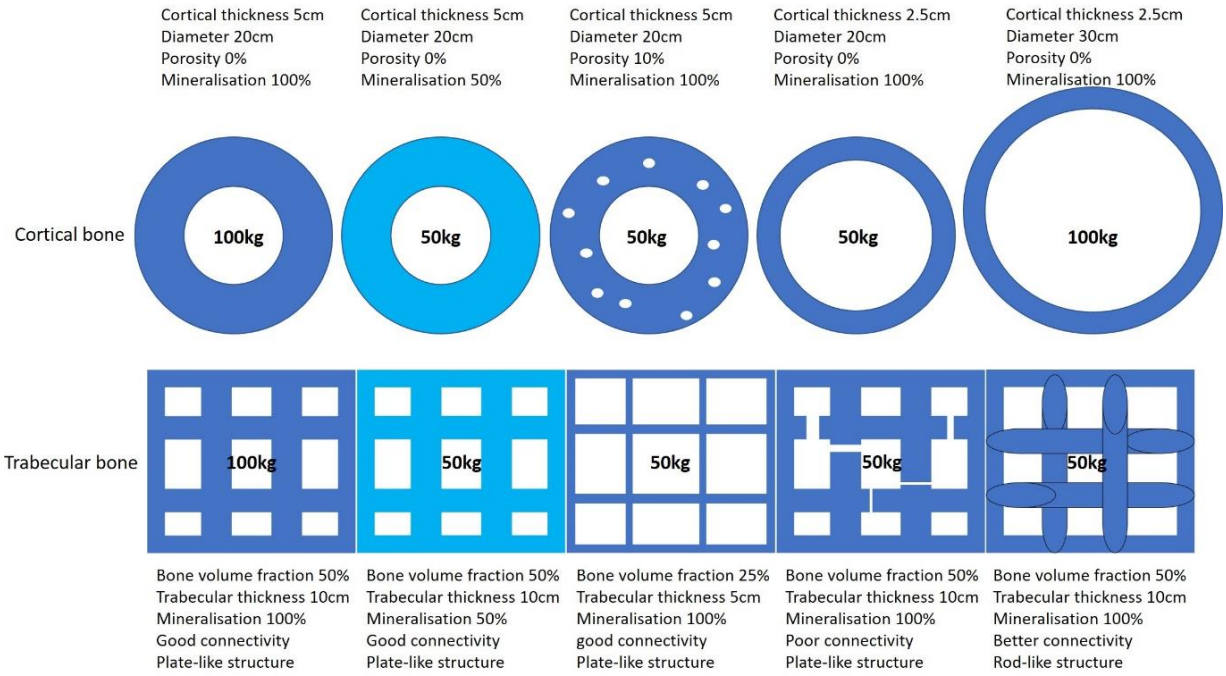

Figure 1.5. Determinants of bone strength at material and apparent levels. Graphs were created using Microsoft PowerPoint.

1.3 BASIC SCIENCES OF ARTICULAR CARTILAGE

Articular cartilage in diarthrodial joints is a layer of hyaline cartilage covering the surface of bone. It provides a cushion for joint loading (weight bearing) and prevents frictions between bones upon joint movements. In healthy conditions, articular cartilage is an avascular and aneural connective tissue composed of extracellular matrix (ECM) and cells (113). Its thickness in normal conditions varies between different joint types and also depends on the location within the joint, ranging from 2mm up to 8mm (114, 115).

1.3.1 Extracellular matrix

The ECM consists of mainly collagens (50% – 60% dry weight), proteoglycans (25% – 35% dry weight), NCPs and glycoproteins (15% – 20% dry weight), and water (65% – 80% wet weight) (116, 117).

1.3.1.1 Collagens

Type II collagen (Col II) (**Figure 1.6**) represents 90% to 95% of collagenous molecules and is the most abundant organic component in cartilage ECM (114). Col II is produced by chondrocytes as a precursor (procollagen). Upon secretion into ECM, the terminal globular domains (procollagen II C- and N-pro-peptide, PIICP and PIINP) of procollagen were removed by specific proteinases (118). Level of these globular domains retained in cartilage or released into biological fluid is an indicator of collagen synthesis (119, 120). Mature Col II is a homotrimer comprising three identical polypeptide α1 chains that intertwine to form a triple helical structure along most of the molecular length, with short linear sequences at both ends (118). The helical domain of Col II is resistant to enzymatic degradation by most proteinases, but is subjected to cleavage by collagenases. In cartilage matrix, Col II molecules stagger together to form fibrils through pyridinoline crosslinks anchoring linear C- and N-terminal telopeptides to triple helixes (118). The fibril formation further stabilises and strengthens collagen network, protecting it from thermal and mechanical dissociation and providing cartilage with resistance to deformation under tensile and shear forces (117).

Other collagens that present in articular cartilage include type I, VI, IX, X and XI, etc. They account for a much smaller proportion of the collagen pool but are indispensable to the ECM homeostasis. For example, type XI collagen (Col XI) interacts with Col II to construct heterotypic fibrils, where Col XI resides in the centre to regulate the size of collagen fibrils (117). Type IX collagen (Col IX) appears on the surface of fibrils and may act as a bridge between collagen and other macromolecules such as proteoglycans (121, 122). Type VI (Col VI) collagen is a non-fibrillar collagen mainly found in the pericellular matrix (123). It forms a complex with matrilin and small proteoglycans such as biglycan and decorin to build the scaffold and determine the mechanical properties of the pericellular matrix (124, 125). Type X collagen (Col X), which is abundant in the growth plate during skeletal development and symbolises the hypertrophy of cartilage and chondrocytes, is absent in adult healthy cartilage but re-occurs in disease conditions such as OA (126, 127).

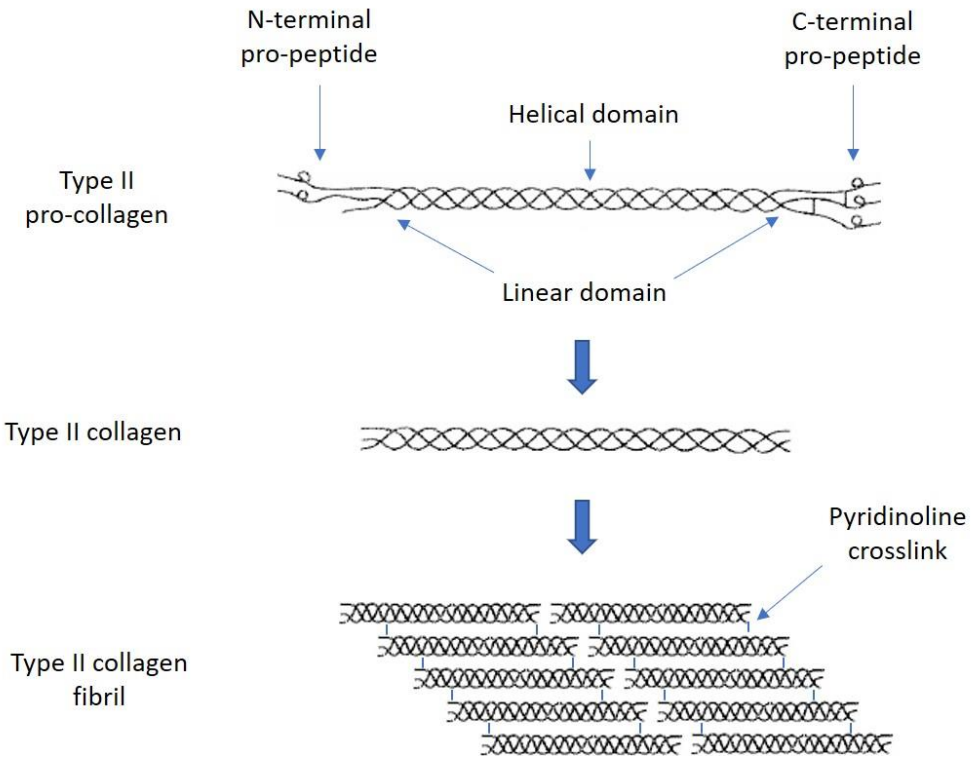

Figure 1.6. Type II collagen in cartilage extracellular matrix. Type II collagen (Col II) is produced as procollagen. Upon secretion into cartilage extracellular matrix, the terminal globular domains are removed. Mature Col II is a homotrimer comprising three identical α1 chains that intertwine to form a triple helical structure along most of the molecular length, with short linear sequences at both ends. Collagen molecules stagger together to form fibrils through pyridinoline crosslinks anchoring linear C- and N-terminal telopeptides to triple helixes. Figure was adapted from (696) with modifications.

1.3.1.2 Proteoglycans

Aggrecan is the dominant type of proteoglycan in cartilage (**Figure 1.7**) (115). Aggrecan consists of a core protein which is covalently bound by glycosaminoglycans (GAGs) forming a brush-like structure. There are three globular domains (G1, G2 and G3) on the aggrecan core protein (128, 129). The N-terminal G1 domain is linked to the G2 domain through an interglobular domain (IGD); and between the G2 and C-terminal G3 domain lies the GAG attaching region. GAGs attached to the core protein, mainly keratan sulfate and chondroitin sulfate, are long polysaccharide chains with repeating negatively charged disaccharides (114). In articular cartilage, aggrecan monomers tend to aggregate on a hyaluronan backbone by binding the link proteins through the G1 domain (116). Large aggrecan aggregates are entrapped within the collagen meshwork. Due to their negative charge and hydrophyllic

nature, aggrecans are able to absorb and preserve water in cartilage matrix. This process is critical as it generates an osmotic swelling pressure, which together with molecular charging repulsion gives cartilage its elasticity and resistance against compressive force (114, 129, 130). During joint movement, cartilage matrix functions like a sponge to repeatedly squeeze out and take back water. This procedure facilitates diffusion of soluble materials within cartilage, and promotes exchange of materials with synovial fluid, providing nutrients for cartilage (113, 131).

Another large proteoglycan found in cartilage is perlecan. It is exclusively located in the pericellular matrix, where it is implicated in the cell-matrix communications and mechano-transduction (132-134). There are also SLRPs in cartilage. They include decorin, biglycan, fibromodulin, and lumican, etc. They do not form aggregates but are often bound to other macromolecule such as Col II, Col VI and growth factors (117). They have a role in the stabilisation of collagen network, modulation of matrix homeostasis, and regulation of cell activities (117, 135, 136).

1.3.1.3 Others

Other organic components present in smaller amount in cartilage matrix include various NCPs and glycoproteins. Through its C-terminal domain, Cartilage oligomeric matrix protein (COMP) binds to Col II and influences fibril formation. It plays a role in both maintenance and degeneration of fibrillar network in articular cartilage, depending on its quantity relative to collagen (137-139). Matrilins and fibronectin interact with both chondrocytes and other matrix constituents, contributing to cell biology and organisation of the ECM (136, 140, 141).

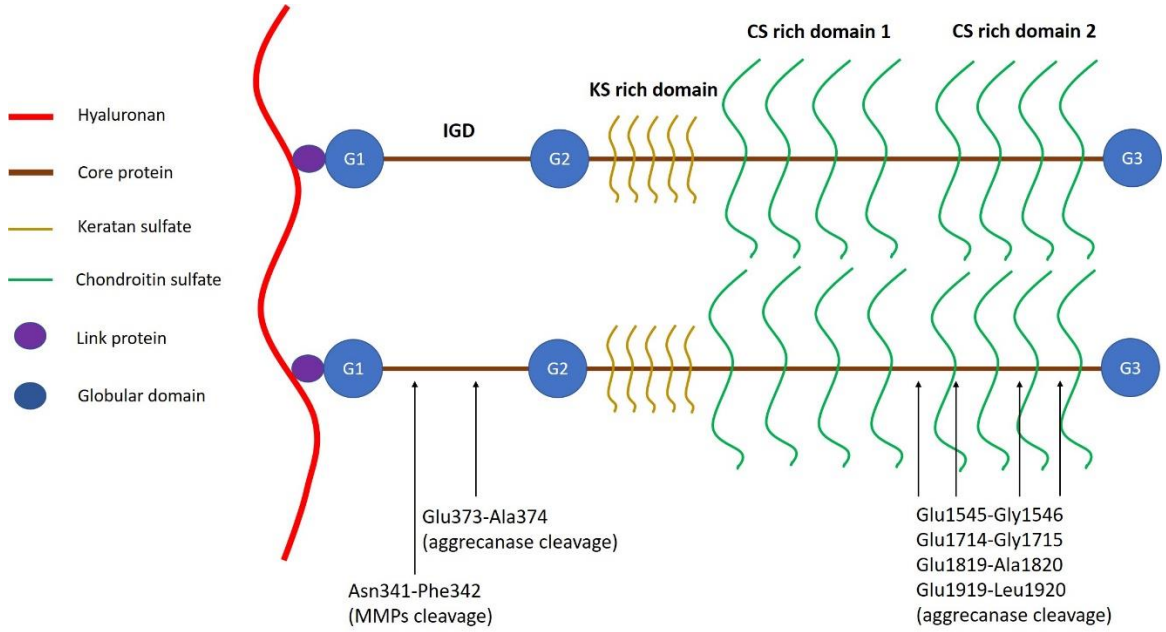

Figure 1.7. Aggrecan in cartilage extracellular matrix. An aggrecan monomer consists of three globular domains (G1, G2, G3), an interglobular domain (IGD), and a domain attached by various glycosaminoglycans (GAGs) such as keratan sulfate (KS) and chondroitin sulfate (CS). Aggrecan monomers aggregate on a hyaluronan backbone via link proteins. Aggrecan can be degraded by aggrecanases within the IGD and GAG-attaching domain, and by matrix metalloproteinases (MMPs) within the IGD. Figure was created using Microsoft PowerPoint.

1.3.2 Chondrocytes

The singular resident cell type in mature hyaline cartilage is chondrocytes. Chondrocytes are derived from chondroblasts, which are differentiated from mesenchymal cells within the mesoderm germ layer during skeletal development (142). In mature cartilage, chondrocytes are highly specialised and mitotically inactive cells accounting for about 1 – 2% of total cartilage volume (143).

The primary role of chondrocytes is to maintain cartilage homeostasis and repair damage, through controlled production and degradation of the ECM components. Chondrocyte metabolism is relatively low in normal conditions, which is consistent with the low turnover rate of collagen and proteoglycans (122, 144). The catabolic and anabolic activities of chondrocytes are tightly regulated by the biological (matrix components and fragments, growth factors, cytokines) (117) and biomechanical (physical stress, osmotic/hydrostatic

pressure, piezoelectric forces) environment (131). The cell membrane of chondrocytes is integrated with a variety of receptors, ion channels and organelles (i.e., cilium) that perceive biomechanical stimuli and transduce them into intracellular signals (145-147). The metabolic outcome of such mechano-transduction depend on the magnitude, duration and rate of mechanical stimuli (131). In addition, as cartilage is an avascular connective tissue, chondrocytes are adapted to anaerobic metabolism and can survive with limited oxygen supply (1 – 10% of normal arterial oxygen tension) (148-150), while maintaining metabolic flexibility toward aerobic energy production (144, 151).

1.3.3 Microstructure

1.3.3.1 Zones

Depending on the shape and alignment of chondrocytes and collagen network, articular cartilage can be divided into three horizontal zones (115-117) (**Figure 1.8**). They are, from articular surface downward, the superficial zone (SZ) or tangential zone, middle zone (MZ) or transitional zone, and deep zone (DZ) or radial zone. SZ accounts for about 10 – 20% of full cartilage thickness. In the SZ, spindle-shaped elongated chondrocytes are embedded in the tightly packed, horizontally arranged collagen network that is roughly parallel to the articular surface. The SZ has relatively higher collagen and lower proteoglycan content compared to the MZ and DZ. The MZ represents approximately 40 – 60% of cartilage thickness. Collagen fibrils in the MZ are obliquely orientated and are occupied by randomly distributed, relatively large, and sphere-like chondrocytes. The DZ has collagen fibrils that are aligned perpendicular to the articular surface and are the largest in diameter. It also has the greatest amount of proteoglycan among the three zones. Chondrocytes in the DZ are mostly grouped in columns that are vertically orientated.

The DZ of articular cartilage is connected to the underlying subchondral bone through a thin and irregular layer of a specialised type of tissue – calcified cartilage, which functions as an anchor and is important for the transformation of stress between hyaline cartilage and subchondral bone (152, 153) (**Figure 1.8**). The histologically defined basophilic line separating the DZ and calcified cartilage is called the tidemark. Chondrocytes in this area are scarce in number and are hypertrophic (117).

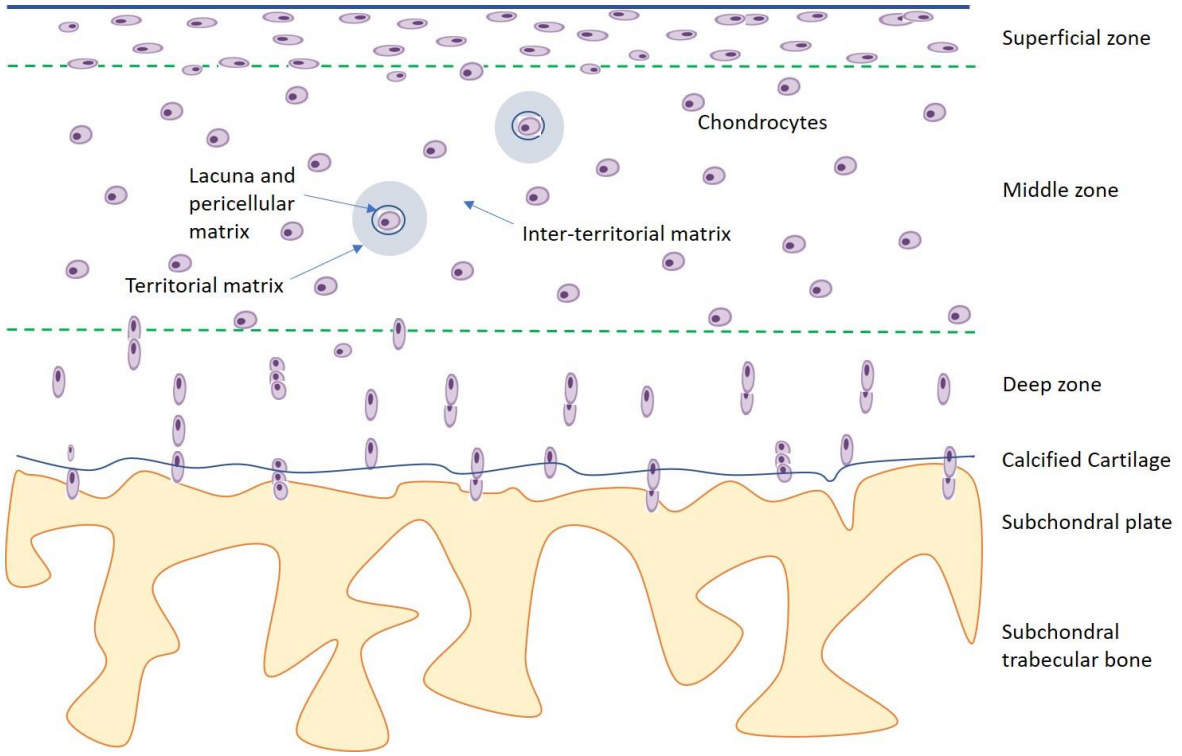

Figure 1.8. Osteochondral unit, showing zones and territories of cartilage extracellular matrix, and compartments of subchondral bone. Depending on the shape and alignment of chondrocytes and collagen network, articular cartilage can be horizontally divided into superficial, middle, and deep zones. According to the relative location and proximity to chondrocytes, the extracellular matrix of cartilage can be subdivided into pericellular matrix, territorial matrix and inter-territorial matrix. Calcified cartilage anchors articular cartilage to the subchondral bone, which can be divided into different compartments: subchondral plate and subchondral trabecular bone. Articular cartilage, calcified cartilage, and subchondral bone form a structural and functional unit called osteochondral unit. Figure was created using Microsoft PowerPoint.

1.3.3.2 Territories

According to the relative location and proximity to chondrocytes, the ECM of cartilage can be subdivided into different territories (**Figure 1.8**). Chondrocytes are situated in a microenvironment named lacunae, in which they are immediately surrounded by a thin layer of pericellular matrix (PCM) separating them from other chondrocytes and the rest of the ECM. The chondrocyte(s) and its PCM constitute a functional unit termed as chondron (125, 154). The PCM has a unique composition as it is rich in Col VI, Col IX, aggrecan monomers and

small aggregates, and other proteoglycans such as biglycan, decorin, and perlecan (124). In normal cartilage, these macromolecules assemble to build a meshwork anchoring and connecting chondrocytes to the outer ECM, putting cell-matrix communications and cell activities under control (125). The PCM also functions as a passage and a repository for extracellular regulators (e.g., cytokines and growth factors), newly synthesised matrix molecules and degraded fragments (116, 155). Biochemical changes in the PCM can be perceived by chondrocytes to initiate cellular reactions. Moreover, the PCM is where biomechanical stimuli such as cartilage deformation and osmotic changes are transduced into intracellular signals through the interactions between chondrocytes and the PCM framework (125, 131, 133, 156).

The territorial matrix (TM) is located around chondrons and is thicker than the PCM. It contains dense and thin collagen fibres to form a basket-like structure, protecting chondrocytes from hazardous mechanical stress (116). The rest of the ECM filling the spaces between territorial matrices is called inter-territorial matrix (ITM). The arrangement of collagen fibres in the ITM follows the zonal features described in the above section and the ITM contributes largely to the overall biomechanical property of cartilage (157).

1.3.4 Biomechanics

The primary function of cartilage is to provide a smooth gliding surface to allow frictionless articulation, and to absorb and distribute stress during joint movement when it is exposed to a combination of shear (tearing), tensile (stretching), and compressive (pressing) forces. The mechanical properties of cartilage supporting these functions are determined by the composition, arrangement and molecular characteristics of the ECM (116). The collagen fibrils, especially within the SZ where they are aligned parallel to the articular surface, are stretched but only to a limited extent as their elongation is restricted by the intra- and inter-molecular crosslinks (114, 158). This provides cartilage with its resistance against shear and tensile stress. In the meantime, the vertical compression is resisted and absorbed by the viscoelastic nature of cartilage, which is attributed to aggrecans, especially in the MZ and DZ where the content is higher. The viscoelasticity of cartilage consists of two aspects, one is the mutual repulsion among negatively charged GAG molecules; the other is the hydrostatic and osmotic pressure

generated by water flow (115, 157). As mentioned previously, aggrecans are responsible for maintaining a certain osmotic pressure in cartilage by attraction of water. Upon application of load on the surface, cartilage is deformed and the trapped water is squeezed out at a low speed due to limited permeability of cartilage, generating an increased interstitial and hydrostatic pressure against the applied stress (159).

1.4 CARTILAGE-BONE CROSSTALK

1.4.1 Osteochondral unit

Bone at the end of long bone covered by articular cartilage is named subchondral bone. It can be further separated into two compartments: subchondral plate, which is composed of Haversian systems and is biologically comparable to cortical bone, and subchondral trabecular bone, which spreads out from the bottom of subchondral plate and connects with deeper epiphyseal trabeculae (**Figure 1.8**) (160, 161). Articular cartilage, calcified cartilage, and subchondral bone form a structural and functional bio-composite termed as the osteochondral unit (**Figure 1.8**) (113). It is where communications between cartilage/joint cavity and bone/bone marrow happen and plays a critical role in mechanical and biological homeostasis of joint.

1.4.2 Cartilage-bone interactions

1.4.2.1 Biomechanical relationship

Subchondral bone provides a mechanical support and protection for cartilage, absorbing and distributing mechanical forces, transforming shear stress into compressive and tensile stress (113, 153, 161-163). On the other hand, articular cartilage also protects subchondral bone in that it lubricates joint movement, prevents direct bone-on-bone contact, and distributes load avoiding concentrated focal stress (115, 164). Changes in the biomechanical properties of either of these two tissues will inevitably affect the transmission and transformation of load

to the other, which can be perceived by chondrocytes and osteocytes to initiate adaptive activities respectively (165-167).

1.4.2.2 Biochemical communication

There is also a biochemical communication between cartilage and subchondral bone through the osteochondral unit. Supply of nutrients and regulatory factors from the bottom of articular cartilage was thought to be ceased in adulthood as osteochondral ossification stops, and calcified cartilage and subchondral bone plate were traditionally considered impenetrable (114, 168, 169). However, cumulating evidence show that the transport between cartilage and subchondral bone exists in normal, ageing, and diseased joints, through direct cartilage-bone contact (170), vascular channels (171-174), microcracks (163, 175, 176), and actually permeable calcified cartilage (168). In fact, regulatory factors produced by bone cells may be crucial for chondrocyte physiology in normal conditions, as the coculture of cartilage explants with the underlying subchondral bone greatly improved chondrocyte survival, compared to cartilage cultured alone (177).

1.5 OSTEOPOROSIS

OP is a systemic bone disease characterised by reduced bone mass and deteriorated architecture, eventually leading to fragility and fracture.

1.5.1 Epidemiology and risk factors

Age is a primary risk factor for OP. The prevalence of OP increases from 2% at the age of 50 years to 25% at the age of 80 years in women (178). According to the National Health Services (NHS) of the United Kingdom (https://www.nhs.uk/conditions/osteoporosis/), more than three million British citizens have OP and about half million of them suffer a fragility fracture each year. It is estimated that in the United States (US) about 10 million people over 50-years of age are affected by OP, of whom about 1.5 million would suffer fragility fracture each year (179, 180). Females generally have higher risk of fragility fractures than their male

counterparts. A study in England and Wales reported that about half of women and a fifth of men at 50 years of age will suffer a fracture related to OP in the remaining lifetime (181). The economic burden imposed by OP is huge across the world. In 2010, OP-related fractures costed over 37 billion Euros in 27 European countries (182). It is projected that there will be 3 million fractures annually and the medical expenditures for osteoporotic fractures will amount to 25.3 billion dollars per year by 2025 in the US (183, 184).

1.5.2 Pathophysiology

The nature of OP is the imbalance between bone resorption and formation, with the former overweighing the latter leading to loss of bone mass and structural integrity. According to the aetiology, OP can be classified into primary and secondary categories. Primary OP includes menopause related type I OP in female and age-related type II OP in both male and female (also known as the senile OP) (185-188). Secondary OP is attributed to specific medical or physical conditions such as glucocorticoid overuse, hyperthyroidism, smoking, Vitamin D deficiency and immobilisation (188-190). This section will focus on the primary OP. Of note, whether or not the imbalance between bone resorption and formation and its related bone loss will eventually lead to OP is also dependent on the peak bone mass achieved in adulthood (191), i.e., the more bone one has at the baseline, the more tolerant he or she is to the bone loss in later life. Peak bone mass is reached around 30 years of age, and is influenced by various genetic and non-genetic factors in different individuals (192).

1.5.2.1 Type I primary OP

Age-related bone loss is a chronic procedure that commences around the age of 30 years in both male and female (193). However, in female, during the first 5-8 years of menopause, the loss of bone is greatly accelerated due to the acute drop in oestrogen level, but returns to the ageing-driven slow phase afterwards (185, 187, 194, 195).

At physiological level, oestrogen has an overall anti-remodelling effect. It suppresses osteoclastogenesis by downregulating RANKL and upregulating OPG in the osteoblast lineage, stromal cells, monocytes and lymphocytes, a process mediated by oestrogen receptor (ER) (185, 187, 196). Production of other cytokines by these cells such as M-CSF, interleukin-1 (IL-

1), IL-6, and tumour necrosis factor-α (TNF-α) which are stimuli of osteoclastogenesis is also inhibited by oestrogen (197-199). In addition, oestrogen directly inhibits the differentiation of osteoclast precursors through the ER-mediated interference with the signalling cascade of RANK (187, 196, 200, 201). Moreover, oestrogen promotes apoptosis of mature osteoclasts directly through the Fas ligand pathway, or indirectly through the regulation of transforming growth factor β (TGF-β) production in osteoblasts (202-204). Except for the effects on osteoclasts, oestrogen compatibly suppresses osteoblastogenesis to maintain the restrained rate of remodelling (205-208). In the meantime, apoptosis of osteoblasts and osteocytes is inhibited by oestrogen (194, 207-210). This action is likely to be mediated by the survival signalling pathway – Src/Shc/ERK and its downstream transcription factors such as Elk-1, CCAAT enhancer binding protei-β, and c-Jun/c-Fos (210, 211).

Oestrogen deficiency during menopause leads to a global increase in bone remodelling events with an overproduction of both osteoclasts and osteoblasts, meaning that both bone resorption and formation activities are boosted (185, 212, 213). This is due to relaxation of the restraint on osteoclastogenesis and osteoblastogenesis. Accelerated apoptosis of osteocytes which releases remodelling initiating signals may also contribute (195, 214). However, as apoptosis of osteoclasts is inhibited while that of osteoblasts is promoted, the lifespan of osteoclasts is much longer than that of osteoblasts (215, 216). This phenomenon results in the unbalanced remodelling cycle – the inadequate bone formation cannot keep up with the aggressive bone resorption, eventually leading to systemic loss of bone mass.

1.5.2.2 Type II primary OP

Age-related factors that contribute to bone loss include those associated with chronic decrease of sex hormones in both male and female, in contrast to the abrupt reduction during menopause in female, and those associated with ageing *per se*.

The general mechanisms of bone loss related to hormonal deficiency have been discussed in the previous section. Androgen also has a biological influence on bone remodelling mainly through regulation of bone formation (217), but is less important compared to oestrogen. In fact, BMD and fracture risk in men are predominantly associated with the circulating level of oestradiol (from aromatisation of testosterone) rather than testosterone (216, 218).

Ageing itself is characterised by the shortening of chromosomic telomere, mitochondrial dysfunction, cumulation of reactive oxygen species (ROS) and excess oxidative stress, leading to the disrupted cell proliferation, damage of macromolecules and dysregulation of intracellular signalling pathways (219-221). Oxidative stress can lead to apoptosis of osteoblasts and osteocytes through DNA damages as in numerous other cell types (222-226). Also, retention of the anti-oxidative forkhead box O (FOXO) transcription factors in the osteoblast nucleus competes for the binding of β-catenin, disrupting the canonical Wnt signalling pathway that is important for normal osteoblast formation and activities (227). Consequently, ageing of the skeletal system is associated with both reduced number and compromised function of osteoblasts. In addition, apoptosis of osteocytes is accompanied by increased production of signals (e.g., RANKL) that stimulate osteoclast differentiation and activity (228), further worsening the imbalanced bone turnover.

Due to the fact that trabecular bone possesses a relatively large surface available for remodelling events, bone loss at early phases before the age of 65 years, including the period of menopause, is largely from trabecular bone(229). However, with progression of bone loss, endocortical and intracortical surfaces are gradually exposed and enlarged, becoming the predominant sites for remodelling (216, 230). As cortical bone accounts for larger proportion (~80%) of total bone volume in mature skeleton, intracortical remodelling is responsible for over 70% of bone loss after the age of 50 (44). Later phases of bone loss are therefore associated with further thinning of individual trabeculae, trabecularisation of the inner cortical wall, and increased intracortical porosity (44, 216, 230). This is why vertebral fractures, which are mainly due to collapse of trabecular bone, are more common in people <65 years of age while non-vertebral fractures, which are due to fragile cortical bone, represent a relatively larger proportion in the older population (207, 231).

1.5.3 Signs and symptoms

Loss of bone mass by itself is symptomless, until fragility fracture happens. Fragility fractures are defined as those caused by low-energy trauma, such as falling from the standing height (232). They are most common at locations such as vertebrae, proximal femur, proximal humerus, and distal radius. Fracture of limbs leads to acute pain, deformity, and immobility,

while compressive fractures of vertebrae are often painless and are found incidentally by radiography. Though various surgical procedures are available, fragility fractures in the elderly are associated with serious reduction in mobility and life quality, multiorgan complications, and excessively high mortality (181, 233-235).

1.5.4 Imaging of OP

Fracture can be diagnosed on plain or digital X-ray (**Figure 1.1**). Evaluation of bone quality for clinical or research purposes is typically carried out using dual-energy X-ray absorptiometry (DXA) due to its low radiation, cost-effectiveness and wide accessibility with good reproducibility (236). By calibration against a standard phantom with known density of calcium hydroxyapatite, DXA provides an *in vivo* measurement of bone mineral content (BMC) and areal, two-dimensional bone mineral density (BMD) (237). Areal BMD measured by DXA correlates with and explains about 60-70% of bone strength (238). Limitations of DXA include that the two-dimensional measurement is greatly affected by the volumetric size of the target bone, and that in the elderly people it is subjected to the influence of degenerative changes such as bone spurs (239).

In contrast to DXA, quantitative computed tomography (QCT) can be used to generate volumetric measurement of BMD. It is able to precisely define a three-dimensional region of interest, therefore averaging out the effect of skeletal size and avoiding inclusion of unwanted bony structures (239). It also allows investigation of cortical and trabecular bone separately, and provides additional parameters of bone quality such as bone volume fraction and cortical thickness (240, 241). However, the use of QCT is limited by its higher radiation and cost, more complex acquisition and analysis procedure, and that currently there is not a standard reference range for the evaluation of OP (238, 239).

1.5.5 Diagnosis

Occurrence of a fragility fracture by itself is adequate for the diagnosis of OP (242, 243). However, diagnosis of OP solely based on fracture inevitably excludes people who are at risk and who are more likely to benefit from available treatments (244). The World Health Organisation (WHO) recommended a standardised criterion according to the measurement

of BMD at the lumbar spine, femoral neck, or total hip area using DXA (245). The outcome can be reported as a comparison to the standard deviation of sex-matched young healthy population (T-score) or sex- and age-matched healthy population (Z-score). A T-score above -1.0 indicates normal range of BMD while less than -2.5 is diagnostic of OP. Osteopenia is indicated by a T-score lying between -1.0 and -2.5. The T-score correlates well with fracture risk (246). The definition of OP by DXA derived BMD is widely adopted for clinical and research purposes. However, this definition has been criticised for the difficulties in the generalisation to non-Caucasian populations, and for not being able to incorporate other identified risk factors for a more sensitive prediction of fractures (232, 244, 247). In 2008, WHO developed the Fracture Risk Assessment Tool (FRAX) for the individualised estimation of 10-year probability of fragility fractures, based on established risk factors such as low body mass index (BMI), smoking, alcoholism, glucocorticoid use and previous fracture (247, 248). This new tool can now be used clinically in combination with BMD measurements for a more comprehensive evaluation of fracture risks and assist in decision-making of intervention (242, 249, 250). Serum or urinary biochemical markers of bone turnover such as CTX-I can be useful for general assessment of response to therapies in clinical or observational studies (251). A few studies claimed their value in predicting fractures (252). But their diagnostic value for OP is still limited (253).

1.5.6 Treatment

The aim of therapies for OP is to reduce fracture risks by improving bone quality and preventing falling. When fractures happen, efforts shall be made to relieve symptoms, prevent sequelae, and preserve physical functions.

1.5.6.1 Non-pharmacological approaches

Lifestyle managements build the primary non-pharmacological care for OP (250). Reducing smoking and alcohol intake removes adverse effects of these risk factors on bone metabolism. Individualised exercise programmes improve muscle strength and motion balance, therefore help reduce frequency of falls. Various exercises have also been reported to be beneficial for the BMD of spine and hip (254, 255). A sufficient protein supply is important for the general health of musculoskeletal system. Supplementation of calcium and Vitamin D through dietary

or supplements are generally recommended, to maintain normal daily intake and serum levels (256, 257).

1.5.6.2 Pharmacological approaches

Pharmaceutical therapies include those targeting bone resorption and those promoting bone formation (188, 254). They aim to maintain and/or improve BMD and thus lower the risk of fractures. Selection and administration of drugs depend on gender, types (causes) of OP, and comorbidities. Before and during therapies, calcium and Vitamin D deficiencies should be corrected and contradictions should be carefully evaluated.

1.5.6.2.1 Antiresorptive agents

Bisphosphonates are analogues of pyrophosphate. They have a high binding affinity for bone minerals and can be endocytosed by osteoclasts during the remodelling cycle. They disrupt intracellular signalling of osteoclasts by interfering with the GTPases' functions, resulting in decreased resorptive capabilities (258). Bisphosphonates can be administered either orally or intravenously. There are four subtypes of Bisphosphonates that are currently prescribed: alendronate, risedronate, zolendronic acid and ibandronate. The former three have been proven effective for reducing fracture risks in vertebrae, hip and non-vertebral sites, while ibandronate is not yet fully determined for hip and non-vertebral fractures (250).

Denosumab is a monoclonal antibody to RANKL. Through competitive binding to RANKL, denosumab imitates the actions of OPG and reduces RANK-RANKL interactions leading to reduced osteoclast differentiation and activation and increased apoptosis (259). In contrast to bisphosphonates, denosumab efficiently lowers the number of osteoclasts (260). Subcutaneous administration of denosumab is capable of decreasing vertebral, non-vertebral and hip fracture incidence in postmenopausal women (261).

Raloxifene is a selective oestrogen receptor modulator (SERM) that is used for postmenopausal OP in women, to counteract the plunged oestrogen level and inhibit bone resorption. It has been shown to reduce vertebral fracture risk but not for hip and non-vertebral fractures (262). Hormone replacement therapies (HRT) utilising various

formulations of oestrogen to target the reduced hormone level are also available. However, usage of them is restricted due to risks of tumour and cardiovascular side effects (263, 264).

When classic antiresorptive options have been exhausted or excluded due to, for example, contradictions, some surrogates such as calcitonin (265) and strontium ranelate (266, 267) are available but are not recommended as first-line candidates (242, 243, 253). It is worth noting that strontium ranelate may have dual effects on bone metabolism – promoting bone formation and inhibiting resorption simultaneously, though the exact mechanism is not fully understood (268, 269).

1.5.6.2.2 Anabolic agents

Parathyroid hormone (PTH) regulates bone remodelling as one of its mechanisms to maintain systemic calcium homeostasis. Continuously elevated serum PTH promotes catabolic bone activities while intermittently administered PTH exerts anabolic effects (270). The anabolic effects of intermittent PTH can be attributed to the modulation of Wnt signalling pathways leading to stimulated proliferation of osteoblast precursors and/or inhibited osteoblast apoptosis (271). Intermittent subcutaneous injection of teriparatide, a recombinant human PTH1-34, has been shown to lower the incidence of vertebral and non-vertebral fractures (272).

1.6 OSTEOARTHRITIS

1.6.1 Epidemiology and risk factors

Prevalence and incidence of OA reported in the literature depend on the joint studied (hip, knee, hand, etc), population selected (country origin, ethnicity, age, gender, etc), and the definition of OA adopted (symptomatic, radiologic, etc) (273-275). About 1 in 5 adults over 45 years age have knee OA and around 1 in 9 have hip OA in England according to Versus Arthritis (https://www.versusarthritis.org/public-health-bulletins/osteoarthritis/). Approximately 10-12% of the adult Americans have symptomatic OA (276), while radiologic OA has been reported in ~60%, 33% and 5% of adults over 65 years of age in north America and Europe for

hand, knee, and hip, respectively (277). OA imposes a huge burden on the affected individuals and on the society and economy. OA is one of the leading causes of disability accounting for 3.9% of years lived with disability worldwide in 2015 (278). In high-income countries the cost of medical care for OA has been reported to represent 1-2.5% of gross domestic product (276).

Age and gender are well-known systemic risk factors for OA. Prevalence and incidence of symptomatic OA increase by more than 10 folds from 30 to over 80 years of age (279, 280). The effects of age on OA development are attributable to alternations at systemic, organ, tissue and cellular levels, which include, but are not limited to, lifestyle changes, muscle and ligament weakness, ECM degeneration and cell senescence (274, 281, 282). With the increase in the ageing population and expected lifespan, the world is likely to witness a further growth of OA prevalence and incidence. Females are not only more prone to the development of OA, but are also associated with greater severity of the disease (283, 284). The gender related disparities are likely to be due to the hormonal differences and variations as the incidence of OA in females are significantly increased at the time of menopause (275, 284-286). OA is also associated with ethnic and genetic factors (285, 287, 288). For example, The Beijing Osteoarthritis Study (289) reported that the Chinese elderly has a significantly lower prevalence of hip OA than the American whites; knee OA in African-American females is more prevalent than in white females (290). A few independent susceptibility genetic loci have been suggested to be related to hand, hip, or knee OA (291-294).

OA is also associated with a number of risk factors that are related to joint biomechanics including joint trauma, joint malalignment, joint shape, occupation, physical activities, and obesity (280). For example, people with previous anterior cruciate ligament injury or meniscal tears have a risk of OA 2.5 times higher than those without such history (295); varus or valgus alignment of knee is correlated with OA progression on the medial or lateral tibial plateau, respectively (296, 297). All these factors can contribute to the development of OA by altering the pattern and magnitude of mechanical stress imposed on cartilage and bone (298-300), thereby interrupting normal remodelling mechanism of these tissues. They may also be related to OA through mechanisms that are irrelevant to joint biomechanics, such as the inflammation induced by adipokines in obesity (301-305) or by hemarthrosis in acute intra-articular injury (306-308).

1.6.2 Pathophysiology

Historically, OA was considered a disease of synovial joint affecting cartilage, subchondral bone and synovium. But recent evidence also suggest a role for systemic factors such as inflammation and metabolic syndrome in the pathophysiology of OA. Based on the initiating factors OA can be stratified into primary and secondary subtypes. Secondary OA is attributable to a specific triggering event or disease such as joint trauma (e.g., meniscus or ligament injury, intra-articular fracture), anatomical abnormalities (e.g., congenital dysplasia, malalignment, unequal leg length), inflammatory arthropathy and metabolic syndromes (309). Primary OA, in contrast, is mainly affected by intrinsic factors such as genetic predisposal, hormonal deficiencies, and ageing (285). All these contributing factors of OA, through various pathways, may converge and end up with common similar pathological processes affecting all components of a joint as a whole (278, 310-313). Of these processes, cartilage degradation, subchondral bone remodelling, and low-grade synovial inflammation are considered the hallmarks of OA.

1.6.2.1 Cartilage in OA

Cartilage is capable of remodelling itself through chondrocytes mediated degradation and synthesis of matrix macromolecules. However, unlike bone, this process in adult cartilage is extremely slow; complete turnover of proteoglycans and collagen takes decades or more in normal conditions (150, 314). The remodelling is under the delicate regulation by growth factors such as TGF-β, bone morphogenic proteins (BMPs), and insulin-like growth factors (IGF) (117). In the development of OA, however, the homeostasis is disrupted and cartilage turnover is accelerated. Both synthetic and proteolytic activities are elevated (315, 316), with the latter overweighing the former (150).

Depletion of proteoglycans, indicated by reduced cationic staining in the superficial zone of cartilage, is one of the earliest event in OA cartilage degradation (317). This is accompanied by also the dissociation of collagen network and subsequently an initial swelling and thickening of cartilage (113). It is not certain yet whether proteoglycan or collagen is the first to be affected in OA, but some researchers suggested that collagen breaks down only after proteoglycans are lost, indicating a protective role of proteoglycans (318-320). Progressive

loss of aggrecan and collagen leads to fibrillation of cartilage beginning at the articular surfaces, followed by thinning of cartilage with loss of matrix and development of fissures into middle and deep zones. Along with these changes there is also the re-initiation of chondrocyte proliferation symbolised by cell cluster formation, which, together with focally increased synthetic activities, may reflect an early attempt to repair (321, 322). However, with disease development eventually full-thickness cartilage will be lost and subchondral bone will be exposed (323).

Proteolytic degradation of aggrecan and collagen are mediated by aggrecanases and collagenases which belong to two subfamilies of metalloproteinases, namely matrix metalloproteinases (MMPs) and a disintegrin and metalloproteinase with thrombospondin motifs (ADAMTS) (318). Fibrillar collagens are fairly stable – their degradation can only be initiated by collagenases including MMP1, 8, 13 and 14 (318). Cleavage of intact Col II by collagenases is located at the Gly794-Leu795 site of α chains, producing two fragments that are 1/4 and 3/4 of molecular length (117, 118, 324). These fragments then disassemble from their triple helix structure (denature) spontaneously at physiological temperature and are subjected to further enzymatic degradation by gelatinases (MMP2 and MMP9) and other proteinases (118, 325). A few ADAMTS family members, including ADAMTS1, 4, 5, 8, 9, and 15, are capable of degrading aggrecan *in vitro* and are named 'aggecanases' (318, 326). They cut the aggrecan core protein at the Glu373- Ala374 site within the IGD and four other sites between the G2 and G3 domains (**Figure 1.7**) (327, 328). These processes cause the detachment of GAG-rich regions and their subsequent loss from cartilage matrix. Numerous studies have identified altered expression profile of the above enzymes in OA in both humans and animal models, implicating their distinct roles in the unbalanced cartilage metabolism (329-337).

The shift of cartilage metabolism can be a result of multiple conditions including unfavorable mechanical stress, local or systemic inflammation, and senescence of chondrocytes and matrix macromolecules.

Metabolic response of chondrocytes to the biomechanical environment depends on the pattern and magnitude of strain. Physiological and dynamic loading of cartilage enhances anabolic activities of chondrocytes and inhibit catabolism and inflammation (338-340).

However, in the context of acute or chronic injurious loading, such as those seen in joint trauma and deformities, a series of hazardous consequences can be observed. They include direct damage to chondrocytes leading to apoptosis or necrosis, and activation of catabolic and proinflammatory pathways with increased expression of proteinases, cytokines and other inflammatory mediators (131, 150, 341). These outcomes are mediated by the interactions between chondrocytes and the PCM. As discussed in **Section 1.3.3.2**, PCM serves as a reservoir for various biological signals and is responsible for mechano-transduction due to its unique biochemical composition and biomechanical properties. Chondrocytes, through its surface mechano-sensitive primary cilia (342) and receptors (e.g., integrins (343) and the transient receptor potential cation channel subfamily V member 4 (TRPV4) (145)), transform extracellular stimuli into intracellular signals and promote the production of catabolic factors. It is worth noting that the alternations in chondrocyte metabolism upon injurious loading persist even when the loading is set back to normal, indicating a sustained phenotype change of chondrocytes (113, 131).

One of the catabolic factors released in response to abnormal mechanical stress is the serine proteinase high temperature requirement A1 (HTRA1) (343-346). Elevated expression of HTRA1 has been identified in human OA cartilage and in animal OA models induced by joint destabilisation (346-348). Substrates of HTRA1 include those highly expressed in the PCM, such as decorin, fibronectin and Col VI (318). Disruption of PCM is an early event in OA and leads to exposure of chondrocyte surface receptors (e.g., integrins (343), syndecans (349), discoindin domain receptor 2 (DDR2) (350)) to their ligands. These are components and degradation products of territorial and inter-territorial matrix which are not accessible in normal conditions. Activation of these receptors further enhances the production of cytokines, aggrecanases and collagenases, forming a positive feedback loop leading to progressive degradation of cartilage (310, 351).

Chondrocytes are both sources and targets of many cytokines, the level of which are elevated in OA cartilage, synovium, and synovial fluid (310, 332, 352-354). Of these cytokines, IL-1β and TNF-α are probably the most extensively studied. They are expressed by both chondrocytes and synoviocytes. They can stimulate the expression of themselves and other cytokines and inflammatory mediators such as IL-6, -17, -18, oncostatin M, chemokines, nitric

oxide and prostaglandin E2 (PGE2) in an autocrine and paracrine manner (150, 301, 313, 355-357). Many of these factors function in a synergistic way to promote catabolic activities of chondrocytes and induce production of various proteinases including MMPs and ADAMTS, leading to degradation of cartilage matrix (313, 351). The degradation products may act back on cell surface receptors as mentioned in the previous paragraph. They may also activate innate immune mechanisms involving the complement pathways, toll-like receptors, and receptor for advanced glycation end-products (RAGE) (301, 358, 359), further amplifying local inflammation and matrix catabolism. All the above processes reflect the existence and importance of an inflammatory environment in the pathogenesis and progression of OA (360). Indeed, synovitis, represented by mononuclear cell infiltration and joint effusion, is detectable by magnetic resonance imaging (MRI), ultrasound, arthroscopy and histology in up to 75%-90% of OA patients at both early and late stages (320, 351, 359, 361). Though at a lower grade compared to rheumatoid arthritis, presence of synovitis in OA is associated with more severe symptoms and tissue destruction (301).

Ageing is one of the major risk factors for OA but the exact link between ageing and OA is to be elucidated. Unlike other cell types, mature chondrocytes exhibit limited mitotic activities so their senescence is largely due to extrinsic stress rather than intrinsic mechanisms (i.e., shortening of chromosomic telomeres as a result of repeated replication) (362). With advancing age, chondrocytes are subjected to the effects of chronic low grade systemic inflammatory stress (termed as 'inflammaging') in addition to local inflammation discussed above (281, 363). Inflammaging is characterized by abrupted adaptive and innate immunity, impaired autophagy, cumulation of inflammasomes, metabolic syndromes and excessive oxidative stress (281, 364). These conditions, together with repeated mechanical loading and injuries, potentiate the senescence of chondrocytes (362, 363). Senescent chondrocytes are associated with increased apoptosis, dampened metabolic capacities, as well as reduced sensitivity to biochemical (i.e., growth factors) and mechanical stimuli (362, 365). They also develop a hypertrophic phenotype characterized by abnormal secretome (senescence associated secretory phenotype (SASP)) with greater production of pro-inflammatory cytokines and degradative proteinases (364, 366). In the meantime, cartilage matrix also exhibits age-related degenerations over time, including reduced water content, accumulation of advanced glycation end products (AGEs), decreased size and integrity of aggrecan

aggregates, and increased crosslinking of collagen fibers (364). These changes compromise the mechanical properties of cartilage, further contributing to the degradative status of chondrocytes.

It should be noted that the above-mentioned mechanisms (ageing, mechanical stress, inflammation) of cartilage degradation in OA are not independent from each other but are intrinsically linked. However, for now there is not a consensus on a sequential or causative relationship between them (150). It is likely that one or more mechanism(s) are more important than others in a specific type of OA but once initiated, all other mechanisms will be involved to form a vicious feedback loop amplifying the effects and eventually leading to the disease.

1.6.2.2 Subchondral bone in OA

Although cartilage degradation has been the focus of OA research since the beginning and was believed to be the primary pathological alternation in OA (367), increasingly more evidence point to a critical role of subchondral bone. Subchondral bone sclerosis, characterised by increased radio-opacity on X-ray, is an established feature of OA (368, 369). Initially, Radin and colleagues suggested that thickened and therefore stiffened subchondral bone with less shock-absorbing capability increases the mechanical stress borne by cartilage and is responsible for its degradation (370, 371). This view has been supported by human radiographic studies showing that subchondral sclerosis occurs months before and predicts the thinning of cartilage represented by joint space narrowing (368, 372-374). It is also supported by animal models showing that thickened subchondral plate is present when histopathological cartilage changes are not obvious yet (375-379). However, the situation is not that simple and several aspects of Radin's hypothesis has been challenged.

First, human *ex vivo* studies combining structural and mechanical examinations showed that subchondral trabecular bone in early OA, characterised by cartilage with macroscopically identifiable fibrillation, was actually less stiff than normal at the apparent level despite its sclerotic structure (denser, thicker, and more plate-like trabeculae) (380, 381). This was attributable to a significant decrease (up to 60%) in the elastic modulus of bone at the tissue material level, which the authors speculated was a result of compromised mineralisation.

Second, human *in vivo* studies showed that radiographic early OA of the knee (K-L grade ≤2) is associated with a reduction rather than an increase in subchondral and/or subarticular bone density (382, 383). This is consistent with the findings that an increase in joint bone remodelling measured by scintigraphy precedes and predicts the progression of radiographically detectable structural changes in both subchondral bone and cartilage (384-386). These observations are also in line with the increase in urinary biomarkers of bone resorption in progressive OA patients (387). Furthermore, family members bearing a mutation leading to high bone mass did not develop OA, indicating that the process of subchondral bone remodelling may be more important than subchondral sclerosis itself in causing joint deterioration (161, 388).

Third, recent studies of different animal models challenged Radin's theory. Thinning of subchondral plate and/or trabecular bone is generally observed at early stage after OA induction. Cartilage groove and anterior cruciate ligament transection (ACLT) induced canine OA models both showed increased subchondral bone remodelling, which was accompanied by cartilage degeneration and thinning of subchondral plate and/or trabecular bone in the first 20 weeks (389-391). This was followed by sclerotic subchondral changes much later at 54 months when full-thickness cartilage erosion developed (392, 393). Similar findings have also been reported in other animal models (377, 394-404). In some of these models, blocking the elevated early bone remodelling following OA induction has shown a chondro-protective effect (396, 405). Moreover, it seems that the rate of subchondral bone remodelling, i.e., the speed of subchondral thickening, is more important than the thickness itself in OA pathogenesis. This is supported by a comparison of two spontaneous OA models. The guinea pig strain with thicker subchondral plate at the beginning but smaller increase in plate thickness displayed less cartilage damage compared to the strain with thinner plate but greater increase in thickness (406). In addition, increased bone resorption and deterioration of subchondral bone architecture induced by oestrogen depletion not only lead to the development of OA (407-411), but also aggravate the severity of OA in models created by other methods such as meniscectomy (411-414). These effects of oestrogen depletion can be counteracted by anti-resorptive treatments (407, 409, 415-417). Lastly, a manually stiffened subchondral bone in sheep joint did not trigger development of OA in a period of 5 years (161, 418), suggesting, again, that subchondral sclerosis alone is not necessarily leading to OA.

Altogether, the role subchondral bone plays in OA is rather complicated and cannot be simply explained by subchondral sclerosis and stiffening. Based on the above and other evidence, currently, an emerging theory is that the increased subchondral bone remodelling in OA may be a biphasic process toward resorption at early stage and formation at late stage (161, 167, 419, 420). This is supported by the identification of two phenotypes of osteoblasts in OA. Massicotte et al reported that osteoblasts collected from subchondral bone of OA knees can be classified into two subgroups differentiated by the production of PGE2 and IL-6 (421). The study for the first time introduced the concepts of low and high osteoblasts, corresponding to the expression level of the two specific cytokines. Interestingly, the same research group later reported that low osteoblasts are characterised by significantly higher level of RANKL expression and markedly reduced OPG/RANKL ratio compared to normal and high osteoblasts (55, 422, 423). Expectedly, low osteoblasts exhibited greater capability of inducing osteoclastogenesis and are therefore suggested to promote bone resorption in contrast to high osteoblasts which seem to favour bone formation (422). The authors assumed that the different osteoblast phenotypes are responsible for the stagewise differences in subchondral bone remodelling in OA (422, 424).

Questions remain, however, about the initiating factor(s) for the abnormal remodelling. Candidate suspects include the alternations in the biomechanical loading caused by, for example, joint injuries, and the cumulation of microcracks in the subchondral region which are associated osteocyte apoptosis, release of remodelling signals (e.g., RANKL) and subsequent targeted repair (113, 310, 425).

The morphological/microarchitectural changes (thickness, volume, etc) are only one aspect of subchondral bone remodelling in OA. Another feature exists with bone tissue mineralisation and composition. Hip and knee subchondral bone specimens collected from end-stage OA patients showed decreased mineralisation and calcium to collagen ratio at tissue level, as measured by a variety of techniques (426-430). This is reflected by a reduced bone stiffness also at tissue level (431). The decreased mineralisation is likely to be caused by rapid bone remodelling that leaves insufficient time for the secondary mineralisation of newly synthesised osteoid (432), compromised biochemistry of Col I (increased hydroxylation,

presence of homotrimers) (433-436), and a phenotype change of osteoblasts with compromised ability to deposit minerals (421, 435, 437-439).

Subchondral bone remodelling in OA is also associated with presence of pathological features including subchondral bone attrition (SBA), bone marrow lesions (BML) and cysts. SBA describes depression or flattening of the contour of subchondral surface. It can be observed by MRI at early stage of OA and reflects an altered pattern of mechanical loading (440-442). Appearance of SBA is associated with knee pain (440) and is able to predict later focal changes in the overlying cartilage (162). BML is also associated with joint pain and a number of OA characteristics including joint pain, loss of cartilage, SBA, subchondral sclerosis and cysts (443-454). It is represented by abnormal hyperintensity on T2-weighted or proton density-weighted MRI images (167, 443). Histological studies suggested that BMLs are likely to be a result of microdamage and the attempt to repair in the region (113, 446, 455). Bone cysts, shown as rounded fluid phase on MRI (456, 457) or focal radiolucency on X-ray (458), seem to develop within the pre-existing BMLs (449, 456). They are more common at advanced stage of OA when the overlying cartilage is severely damaged or depleted and are a good predictor of the need for joint arthroplasty (451, 458, 459).

1.6.2.3 Subchondral bone – cartilage crosstalk in OA

The disrupted interactions between articular cartilage and subchondral bone are among the key factors in the development of OA (**Figure 1.9**). From a biomechanical aspect (**Figure 1.9A**), deleterious tissue remodelling of cartilage, as a result of the ageing process or acute or cumulated joint injuries, will compromise its mechanical properties and impact the distribution of load to subchondral bone, increasing stress and initiating adaptive structural modifications in the latter. On the other hand, abnormal remodelling and alternations in the contour, architecture and mineralization of subchondral bone will increase the stress borne by cartilage and contribute to its degradation.

From a biological aspect, cellular and molecular communications between subchondral bone and cartilage through the osteochondral interface via microcracks and vascular channels increase in OA (**Figure 1.9B, C**). A characteristic of inflamed and hypertrophic chondrocytes is the production of factors that promote chemotaxis and differentiation of the precursors of

osteoclasts and endothelial cells, such as vascular endothelial growth factor (VEGF), IL1-β, TNF-α and RANKL (460, 461). Local resorption of subchondral plate and calcified cartilage by osteoclasts undermines the integrity of the osteochondral junction and creates channels connecting the marrow space and deep layers of articular cartilage (**Figure 1.9B**). These channels and adjacent marrow spaces are subsequently infiltrated by mesenchymal tissues expressing VEGF, nerve growth factor (NGF) and platelet derived growth factor (PDGF) which are then vascularised through angiogenesis (460, 462). The newly formed blood vessels function as a 'highway' that further facilitates the bi-directional transport of molecules between cartilage and subchondral regions (**Figure 1.9C**). Except for the factors mentioned above that originate from cartilage and act on bone cells, various molecules such as TGF-β, IGF-1 and hepatocyte growth factors (HGF) are derived from subchondral bone and can travel to cartilage and regulate the metabolic activities of chondrocytes (461, 463). In the meantime, the vascular invasion into calcified cartilage is associated with new bone formation and advancement of tidemark, contributing to the thinning of articular cartilage and thickening of subchondral plate (113, 460). The above processes seem to recapitulate the features of endochondral ossification which is seen during skeletal development. In addition, vascular channels penetrating the osteochondral junction are often innervated by sensory and sympathetic nerves which are suspected to be responsible for the generation of joint pain in OA (462, 464).

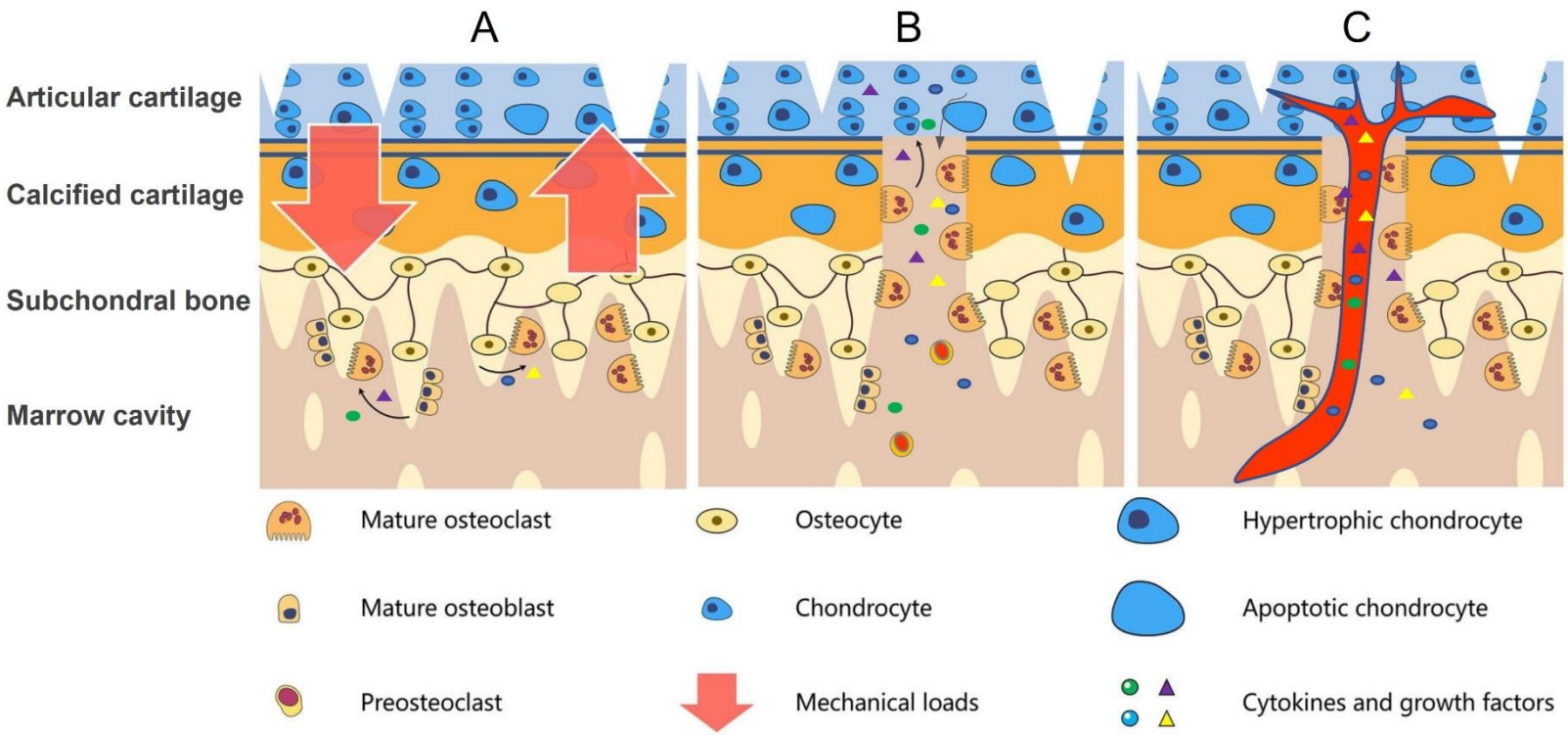

Figure 1.9. Crosstalk between cartilage and subchondral bone in OA. (A) Biomechanical crosstalk between articular cartilage and subchondral bone: the changes in mechanical properties of either tissue will affect the load transmission to the other, which is perceived by cells in each tissue to initiate adaptive remodelling. (B) Local resorption of subchondral plate and calcified cartilage by osteoclasts: progenitors of osteoclasts are attracted by inflammatory factors and differentiate into mature osteoclasts, which then create channels connecting the marrow space and deep layers of articular cartilage through bone resorption. (C) Vascular invasion at the osteochondral unit: the channels created by osteoclasts are subsequently infiltrated by mesenchymal tissues expressing VEGF, NGF and PDGF which are then vascularised through angiogenesis. The newly formed blood vessels function as a 'highway' that further facilitates the transport of molecules between cartilage and subchondral bone. Figure is adapted from (461) with modifications.

1.6.3 Signs and symptoms

Joint pain is the most predominant symptom of OA and the leading cause for patients' presentation at clinics (465). Pain often becomes worse when the joint is moved or in weight-bearing, and is relieved after the joint rests. There is also stiffness of the affected joint. It is most apparent in the morning but usually lasts for a shorter period of time (less than half an hour) (466). Physical examination of the affected joint may display tenderness, pain and crepitus along with restricted range of joint motion. Severity of these symptoms can be evaluated using a number of validated measures including the Western Ontario and McMaster Universities OA index (WOMAC) (467). Joint deformities and bony enlargement may develop, for example, valgus or varus malalignment of knees, and Heberden's or Bouchard's nodes on the fingers. Another feature of OA is the asymmetry – the occurrence or severity of OA in one joint is not necessarily matched by the contralateral joint (466). In addition, OA often presents as a mono-arthritis in contrast to the polyarthritis such as RA. Eventually OA will lead to disability with loss of joint function and reduced daily activity.

1.6.4 Imaging of OA

Plain X-ray or digital X-ray is the most widely used imaging tool to identify structural changes in the suspected joint and is currently the gold standard for diagnosis of OA (468). Typical radiographic signs include joint space narrowing (JSN) due to thinning of articular cartilage, formation of osteophytes at the joint margin, and sclerosis of subchondral bone (**Figure 1.1D**). These changes can be qualitatively evaluated using systems such as the classic Kellgren and Lawrence (K-L) grading (469). The K-L grade ranges from 0 to 4 to indicate increasing severity of OA from normal (no radiographic features of OA) to end-stage (marked JSN, large osteophytes, severe subchondral bone sclerosis and apparent bony deformity) on an anteroposterior weight bearing X-ray (470). A K-L grade ≥2 (presence of osteophytes possible JSN) is typically required for radiographic diagnosis of OA (471, 472).

Though not routinely used for clinical diagnosis of OA, MRI has the advantage that it allows three-dimensional assessment of all joint components in greater details, which is especially relevant in detection of early OA (473). MRI is more sensitive in terms of cartilage morphology as cartilage volume and localized cartilage damage can be measured (474). Enhanced MRI

scanning with more advanced techniques can also be used to detect changes in the biochemical composition of cartilage (GAG depletion, collagen orientation, water content), which are present at very early stage of OA (474, 475). In addition, features that cannot be detected with traditional radiography, such as meniscal and ligamental degeneration and injury, synovitis, SBA and BMLs, can be visualized by MRI (470). These advantages, plus the non-radiological nature, make MRI a good candidate for the research of OA progression and treatment efficacy (473).

1.6.5 Diagnosis

Various guidelines have been produced by clinical societies for diagnosis of OA in different joints (471, 476-478). In general, diagnosis is based on patient-reported symptoms, physical examinations, and radiographic inspections. It is worth mentioning that people who demonstrate radiographic joint changes (radiographic OA) may be asymptomatic (274), while those who meet both radiographic and clinical criteria are often classified as symptomatic OA (273). Another key element of these diagnostic guidelines is the differential diagnosis between OA and other diseases such as joint infection, rheumatoid arthritis, avascular necrosis, and gout. In this regard, in addition to a detailed acquirement of medical history, blood tests for biomarkers such as uric acid, rheumatoid factor, erythrocyte sedimentation rate, and C-reactive protein may be needed to exclude other joint diseases like rheumatoid arthritis and gout. A number of OA specific diagnostic biochemical markers (C-terminal telopeptide of Col II (CTX-II), for example) are currently under investigation, but to date none of them have been proven to be clinically useful (479, 480).

1.6.6 Treatment

A number of clinical and research committees have been updating their recommendations for the treatment of OA every few years (481-490). However, both pharmacological and non-pharmacological approaches are still palliative, restricted to symptom relief and functional preservation. Many of these therapeutic approaches have been controversial and inconsistent between guidelines as conflicting results were generated due to varying size and quality of clinical trials. No disease modifying OA drugs are available to halt structural damage, slow down, or reverse the progression of OA.

1.6.6.1 Non-pharmacological approaches

Weight management, and land-based (e.g., Tai Chi, Yoga) or aquatic exercises help relieve joint load and restore joint stability. Many studies have provided evidence for their effectiveness on reducing pain and improving joint function (491-494). They are therefore recommended as key treatment by most guidelines for non-pharmacological management of OA (486, 495). Patient education is another basic strategy in most cases (496). In addition, biomechanical protections (knee braces or sleeves, foot orthoses), walking aids (canes or crutches), psychosocial intervention and physical therapies (acupuncture, thermal therapy, electrotherapy, ultrasound) can be conditionally exploited (485, 486). Selection of these approaches need be tailored to individuals and the specific joint affected (481).

At end-stage of OA with severely deteriorated joint structure and function, and when symptomatic improvement is far from being satisfactory from treatments, joint replacement is the nly solution to restore life quality (497, 498). Despite varied magnitude of benefit (499, 500) and risks of revisions (501, 502) and complications (503-505), total knee arthroplasty (TKA) and total hip arthroplasty (THA) are recommended as more 'cost-effective' for late OA by the Osteoarthritis Research Society International (OARSI) (483).

1.6.6.2 Pharmacological approaches

Non-steroidal anti-inflammatory drugs (NSAIDs), either oral or topical, is considered the top-ranked choice for the control of pain in OA due to a favourable trade-off between efficacy and cardiovascular and gastrointestinal side effects (278, 485). Paracetamol has also been widely used for pain relief in OA, but is no longer recommended by the most recent OARSI guideline (485). The use of other pain killers such as topical capsaicin, duloxetine and opioids has been complicated and controversial over the recent years in various guidelines due to inconsistent data. Intra-articular injection of corticosteroids and hyaluronan may provide short- to mid-term pain relief and are only conditionally recommended (486). Important components of cartilage ECM, chondroitin and glucosamine, prepared either at pharmaceutical or dietary grade, are widely perceived by patients as efficacious. However, they are now recommended against in most conditions due to inconsistent results and potential investigator bias (481, 486, 506-508). Again, selection of pharmaceutical

approaches need to be individualised according to patient expectations, comorbidities, severity and location of OA (487).

1.6.6.3 Disease modifying OA drugs

Disease modifying OA drugs (DMOADs) are a special group of OA drugs that are expected to directly target the mechanisms and/or processes in OA pathogenesis, i.e., cartilage degradation, subchondral bone remodelling, and inflammation (509-512). The US Food and Drug Administration and the European Medicine Agency demand that DMOADs should be able to provide both joint structural modifications and symptom improvement (513). However, of the many potential DMOADs under investigation (e.g., MMP or aggrecanase inhibitors, anti-bone resorption drugs, and cytokine antagonists), none has been approved by the regulatory committees for routine OA treatment. Review of different types of DMOADs can be found in (509, 513, 514)

Development of DMOADs is challenged by several issues. First, there is no consensus on what measures progression of OA and what marks the response to treatments. Biomarkers (biochemical, radiographical, and clinical) currently used as clinical end-point lack of specificity and/or sensitivity (513, 515, 516). Second, for clinical trials, the sampling criteria usually generates a group of subjects in which OA is already at its advanced stage, when treatments may be too late for effective intervention (511). Thirdly, preclinical models of OA do not closely reflect the characteristics of the human disease, imposing difficulties on translational research (517).

1.7 RELATIONSHIP BETWEEN OSTEOPOROSIS AND OSTEOARTHRITIS

1.7.1 An inverse relationship

OP and OA are historically thought to be inversely correlated as these two diseases rarely coexist in the same patients (518-521). It was reported by surgeons decades ago that femoral heads resected from fractured hips often had no obvious cartilage degradation while those

taken from OA hips seemed to have well preserved bone (519, 521-524). More importantly, numerous cross-sectional and longitudinal studies have shown that, in general, incidence and/or progression of OA in the hand, hip, and/or knee are associated with higher systemic BMD (518, 525-532). For example, the MOST study showed that higher BMD of femoral neck measured at baseline is related to an increased risk of knee OA incidence and JSN in a 30 months' follow-up study (531). In the Chingford study, patients with OA of the hand, spine, and/or knee had a significantly higher BMD at the spine and/or hip (518). In contrast, OP defined by BMD at the lumbar spine or the occurrence of a vertebral osteoporotic fracture is associated with significantly lower risk of OA and/or its progression (533, 534). Some researchers therefore suggested that OA protects against the development of OP and fragility fracture (522, 535-537).

Interpretation of the above clinical or population-based research needs careful considerations. The joint of interest (interphalangeal joints, hip, knee, spine, etc), the site of BMD measurement (spine, hip, distal arm, etc), the definition of OA and its progression (osteophyte, JSN, K-L grade, etc), the reference population, the subtype and stage of disease, the timeframe and endpoint of study would all likely to influence the findings of these studies (519, 538-540). Also, a technical limitation is that the accuracy of measurement of BMD in patients/joints with OA may be compromised by the presence of sclerosis and osteophytes (541). Furthermore, conflicting results have been reported – the higher systemic BMD in patients with knee or hip OA seemed unable to prevent fractures and sometimes even increase the risk of fracture at various skeletal sites (542-545). The postural instability, muscle biomechanics, and the associated risk of falls have been proposed to be responsible for these observations (541).

1.7.2 A possible connection

As discussed in **Section 1.6.2.2**, both human and numerous animal studies have revealed a phenomenon that at early stages of OA there is increased subchondral remodelling toward bone resorption. In addition, accelerated loss of subchondral bone induced by oestrogen depletion led to the development of OA (407-411), and pre-existing OP aggravated the severity of OA surgically induced in animal models (411-414). These data suggest that there

is a possible overlap between the pathophysiology of the two diseases (419), despite the circumstantial results generated from clinical and populational studies mentioned above. This overlap, in addition to the intimate crosstalk between subchondral bone and cartilage in both physiological and pathological conditions, provides the rationale for the use of anti-OP drugs as DMOADs with the expectation that they can retard the development of OA through modulation of subchondral bone remodelling.

In many animal OA models, including those induced by surgeries, oestrogen deficiency, and monosodium iodoacetate, common anti-OP therapies, such as bisphosphonates (396, 405, 546-552), calcitonin (416, 553-556), PTH (415, 557, 558), oestrogen replacement (407, 559), and strontium ranelate (560, 561), have been shown to reduce subchondral bone pathology and protect against cartilage degradation and/or OA symptoms. However, the mechanisms underlying the beneficial effects are sometimes unclear. Some of these reagents, such as hormones, strontium ranelate and calcitonin may have dual effects on both chondrocytes and bone cells (419, 561-563). Results generated from clinical trials have been controversial and currently there is no solid evidence of efficacy of these drugs for OA (for reviews, refer to (419, 463, 514, 562, 564, 565)). Currently, there is no bone-targeting DMOAD that has been approved by any regulatory committees. The timing of the most effective interference and the selection of a subgroup of patients that are most likely to benefit from these treatments may be the bottleneck of future studies and trials (419, 424, 562, 564).

1.8 HYPOTHESIS AND AIMS

Articular cartilage and subchondral bone are specialised tissues that function as one complementary unit in maintaining joint physiology. In OA, marked pathological alternations have been observed in both of these tissues and they may form a vicious feedback loop, promoting the development of OA in a synergistic manner (161). As reviewed above in this chapter, for subchondral bone, increased remodelling seems to be a biphasic process toward resorption at early but formation at late stage of OA development. This phenomenon has promoted the idea that anti-OP drugs, which either inhibit bone resorption or improve bone formation, may have the potential as DMOADs able to halt the disease progression at early

stage. However, results generated from pre-clinical and clinical trials revealed a lack of understanding of the overlap between the pathophysiology of OP and OA.

Study of the overlap must be built on a comprehensive knowledge of the differences and/or similarities in bone and cartilage between OP and OA. This is a complex topic and a number of considerations need to be taken. First, both OP and OA are skeletal conditions associated with systemic factors (ageing, hormonal changes, metabolic syndrome, inflammation, etc) but OP is reflected by systemic bone loss while OA is mainly represented by changes in the articular joints (subchondral bone, cartilage, synovium, etc) (368, 384, 424). Previous studies contrasting OP and OA most of the time focused on macroscopic features of vertebrae and proximal femur using clinical imaging, while those looking at microscopic features of bone in OP and OA were often separate studies focused on vertebrae/ilium/femoral neck and subchondral bone, respectively. Data for a direct comparison of microscopic features at the comparable relevant site, i.e., subchondral bone, are more appropriate and may help better understand the relationship between the two diseases and provide insights into the pathological process of OA.

Second, bone and cartilage must be studied concurrently due to the close interactions between them under both physiological and pathological conditions. Subchondral bone properties in OA joint are heterogeneously distributed in relation to the local status of cartilage degeneration (420, 426, 566-572). Such spatial variation should be accounted for as it provides an acceptable reference for the evaluation of temporal/stagewise changes in OA, especially when longitudinal samples are not available (329, 420, 426, 450, 568). Third, the investigation should involve all aspects of tissue properties and the associations between them, including but not limited to, matrix composition, cellular biology, microarchitecture, and biomechanics of both cartilage and bone. Moreover, whenever applicable, differentiation should be made between subareas, i.e., subchondral plate and trabecular bone, and zones and territories of cartilage, as they are biologically and mechanically distinct and may respond differently in the disease process (160, 161).

A study of subchondral bone and cartilage in human hip OP and OA covering the above-mentioned criteria was the aim of this PhD project. The overall hypothesis is that a comprehensive investigation of subchondral bone microarchitecture and mineralisation and

cartilage degeneration in OP and OA, based on an optimised sampling procedure and stagewise comparisons, will provide important new information regarding the commonalities and differences between the two diseases and help better understand the pathological process of OA.

Specifically, the objectives of this PhD project were to:

1. Develop and validate a standardised osteochondral sample collection and evaluation procedure that accurately reflects the regional differences in the stage of cartilage degeneration in hip OA.

2. Compare subchondral bone microarchitecture and mineralisation in OP with those at different stages of cartilage degradation in OA, in both subchondral plate and trabecular bone.

3. Examine the relationships between subchondral bone microarchitecture and mineralisation in OP and OA, in both subchondral plate and trabecular bone.

4. Compare the overall and zonal expression of cartilage matrix degradative proteinases in OP with it at different stages of OA.

5. Investigate the associations between subchondral bone properties and expression of cartilage matrix degradative proteinases in OP and OA.

Chapter 2

General methods

2.1 RESEARCH ETHICS

The use of human tissue in this project was approved by the Health Research Authority, UK (17/WS/0217). Written consent for tissue collection was obtained from patients prior to surgery at the Southmead Hospital, Bristol, UK.

2.2 TERMINOLOGY

Throughout the thesis, 'site' refers to anatomical locations, i.e., superior, anterior, posterior, medial, lateral, inferior. 'Region' refers to macro- or microscopically graded areas according to local severity of cartilage degeneration. 'Compartment' is used to describe structures of subchondral bone – subchondral plate or subchondral trabecular bone. 'Zone' is used specifically for horizontal divisions of cartilage matrix, i.e., superficial, middle, and deep zones.

2.3 PATIENT SELECTION AND FEMORAL HEAD COLLECTION

Thirty-one femoral heads were collected from patients undergoing total hip arthroplasty (THA) for hip OA (17 male and 14 female, mean age 69.03 ± 9.84 years) (**Table 2.1**). Clinical diagnosis of OA was based on guidelines produced by the American College of Rheumatology (477) incorporating clinical symptoms and radiographic features (joint space narrowing and osteophytes, etc) (**Figure 1.1D**). Patients with known history of hip trauma, infection, avascular necrosis and rheumatoid arthritis were excluded. Seven femoral heads were collected from patients undergoing hip arthroplasty for osteoporotic fracture of the femoral neck (4 male and 3 female, mean age 69.71 ± 5.94 years) (**Table 2.1**). Clinical diagnosis of OP was based on established clinical guidelines by American College of Physicians and American College of Endocrinology (242, 243), i.e., presence of low-energy fracture (falling from standing height) of hip in the elderly population (**Figure 1.1C**). Patients with secondary OP due

to prolonged use of corticosteroids, or on medications that affect bone metabolism were excluded. Inclusion criteria also involved a macroscopic inspection of specimens, which will be detailed in the next section. Femoral heads were soaked in ice-cold phosphate buffered saline (PBS) and transported to the lab, where they were processed within 3 hours post excision.

2.4 THE NEW MACROSCOPIC GRADING SYSTEM

A new macroscopic grading system (**Table 2.2**) was developed based on our observations in this study to visually evaluate severity of cartilage degeneration and guide osteochondral tissue collection. The grading is presented with the Roman numerals ranging from I to V, with higher grade indicating more severe degeneration. Detailed description and discussion of this new system will be presented in Chapter 3.

Except for the clinical criteria of femoral head selection described above, for OP group, femoral heads were included in the study only when their articular surface was normal or comparatively normal (macroscopic Grade I). OA femoral heads that were at end-stage of OA showing complete loss of cartilage and bone exposure (macroscopic Grade V) across the entire articular surface were excluded.

Table 2.1. List of participants.

OP				OA			
Sample ID	Gender	Age	Side	Sample ID	Gender	Age	Side
HF1	Female	71	Right	HOA5†	Female	82	Right
HF2	Female	71	Left	HOA7†	Female	63	Right
HF3	Female	70	Left	HOA8†	Female	70	Left
HF4	Male	60	Left	HOA9†	Female	82	Right
HF5	Male	65	Right	HOA10†	Male	58	Right
HF6	Male	79	Left	HOA11†	Female	75	Right
HF8	Male	72	Left	HOA14†	Female	74	Left
				HOA15†	Female	80	Left
				HOA25†	Male	83	Left
				HOA31†	Male	65	Right
				HOA32†	Male	82	Right
				HOA33†	Female	55	Left
				HOA34†	Male	74	Right
				HOA37†	Male	64	Right
				HOA41†	Male	44	Right
				HOA40‡	Female	77	Right
				HOA42‡	Male	64	Right
				HOA43‡	Male	70	Left
				HOA44‡	Female	72	Right
				HOA46‡	Female	71	Left
				HOA48‡	Female	69	Right
				HOA49‡	Male	77	Left
				HOA50‡	Male	82	Right
				HOA51‡	Male	75	Right
				HOA52‡	Male	55	Right
				HOA53‡	Female	56	Right
				HOA54‡	Male	59	Left
				HOA55‡	Female	59	Right
				HOA56‡	Male	72	Right
				HOA57‡	Male	64	Left
				HOA58‡	Male	67	Right

OP, osteoporosis group, mean age 69.71 ± 5.94 years. OA, osteoarthritis group, mean age 69.03 ± 9.84 years. †, the optimisation cohort of OA group, mean age 70.07 ± 11.69 years. ‡, the main study cohort of OA group, mean age 68.1 ± 8.00 years. HF, hip fracture. HOA, hip OA.

Table 2.2. The new macroscopic grading system for evaluation of cartilage degeneration.

Macroscopic Grade	Feature	Description
Grade I	Normal or comparatively normal	White, or slightly grey; surface intact, smooth, no visible irregularity or fibrillation; elastic, no thinning or softening.
Grade II	Surface irregularity	Grey or pink; surface intact but with roughening, peeling and/or small fibrils; thinning, softening or swelling.
Grade III	Matrix destruction	Yellow, grey, or 'bloody'; surface destructed, soft, fluffy, with severe fibrillation, cracks and fissures; obvious thinning compared to adjacent intact area.
Grade IV	Cartilage erosion	Dark grey or yellow; surface can be smooth, roughened, or fluffy; cartilage almost worn off, with only a thin layer (<1mm) left; immediately adjacent to areas of exposed bone.
Grade V	Bone exposure	Cartilage completely worn off, with only subchondral bone left and exposed.

2.5 OSTEOCHONDRAL PLUG EXTRACTION AND ASSIGNMENT

A steel hollow punch with 4mm inner diameter was used to extract osteochondral plugs that had subchondral bone 8-10mm in length. The whole procedure was carried out in a ventilation hood under sterile condition.

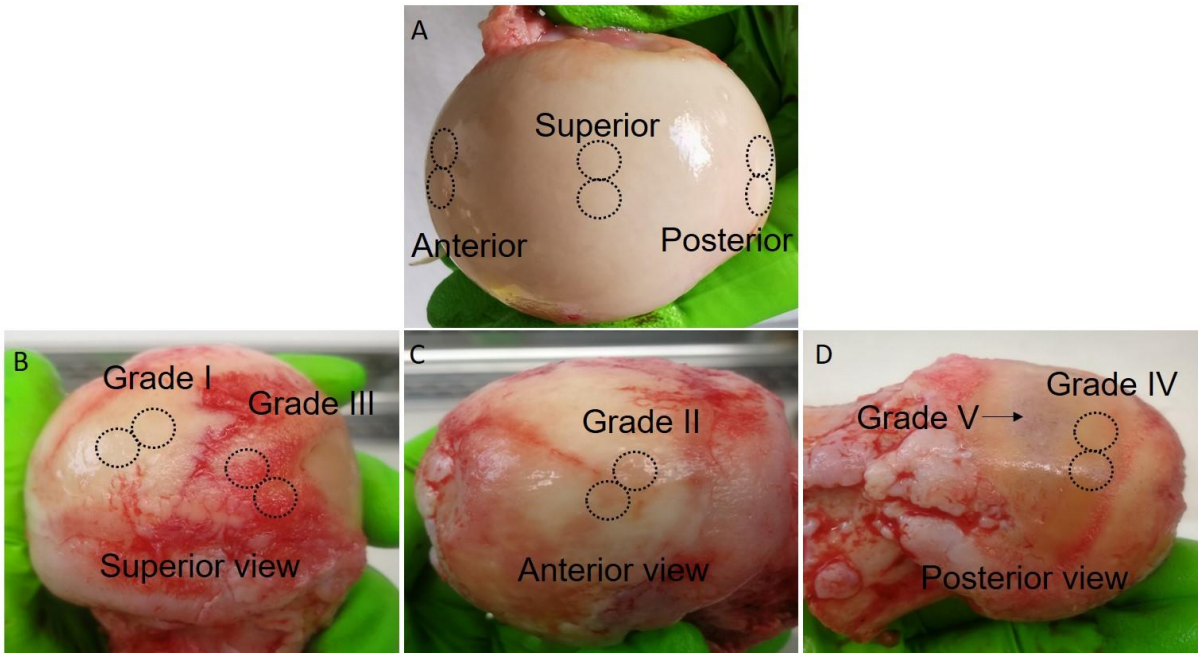

Figure 2.1. Macroscopic grading and osteochondral plug collection. Articular surfaces were regionally graded according to the new macroscopic grading system. For the OP femoral heads (A), two immediately adjacent Grade I osteochondral plugs were collected from anterior, superior, and posterior sites. For the OA femoral heads (B, C and D), adjacent osteochondral plugs were collected from each of the macroscopically graded regions (Grade I to Grade IV) depending on availability. (B), (C) and (D) show the same femoral head viewed from different angles. A Grade V region is indicated in (D) (black arrow).

For the OP femoral heads, two immediately adjacent plugs (21 pairs) were collected from each of the three anatomical sites: anterior, posterior, and superior (**Figure 2.1A**). One set was used for the histology (Chapter 3) and immunohistochemistry (IHC) studies (Chapter 6); the other set was used for the micro-computed tomography (microCT) study (Chapter 4 and 5).

The OA femoral heads consisted of two separate cohorts: the optimisation cohort (N=15, 7 male and 8 female, mean age 70.07 ± 11.69 years) which represents a collection at early phase of the study, and the main study cohort (N=16, 10 male and 6 female, mean age 68.1 ± 8.00 years) (**Table 2.1**). For both cohorts, the articular surface of each femoral head was divided and graded on a regional basis from macroscopic Grade I to Grade V (**Figure 2.1B-D**).

For the optimisation cohort, plugs were extracted from each of the macroscopically graded regions (Grade I to Grade IV only) depending on availability. These plugs were used for the histology study (N=37) and various optimisation purposes. For the main study cohort, two immediately adjacent plugs (52 pairs) were collected from each of the macroscopically graded regions (Grade I to Grade IV only) depending on availability (**Figure 2.1B-D)**. One set was assigned to the histology and IHC studies; the other set was used for the microCT study. In small regions where only one plug was available, priority was given to microCT (N=4 plugs). In larger regions, additionally available plugs (N=12) were collected and used for histology study only. These procedures yielded 101 OA plugs (37+52+12) designated for the histology study (Chapter 3); 56 OA plugs (52+4) assigned to the microCT study (Chapter 4 and 5); and 52 OA plugs, which are immediately adjacent and paired to the 52 microCT plugs, intended for the IHC study (Chapter 6).

Note that Grade V regions were only used for demonstration of grading in Chapter 3 and were not included in any analysis in this project because (i), the integrity of subchondral plate was often breached and trabecular bone was frequently accompanied by cysts when articular cartilage was completely eroded (153, 459), making these regions not suitable for the study of bone microarchitecture; (ii), these regions were not applicable for the IHC study of proteinases in cartilage as there was not cartilage left. In addition, lateral and marginal areas where were occupied by osteophytes, medial areas surrounding the fovea, and inferior areas where fibrillar tissue and oedema-like cartilage were present were excluded from OA plug collection procedure (**Figure 2.2**).

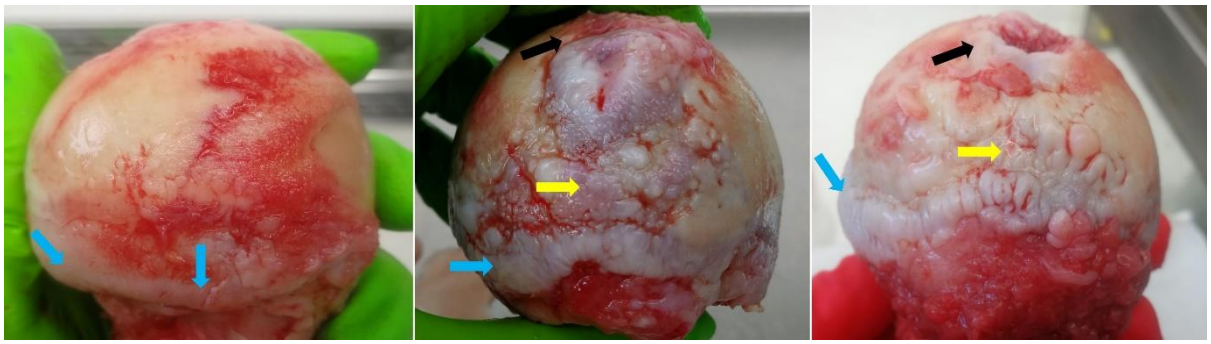

Figure 2.2. Excluded areas that were not suitable for the study. Lateral and marginal areas occupied by osteophytes (blue arrows), medial areas surrounding the fovea (black arrows), and inferior areas where fibrillar tissue and oedema-like cartilage were present (yellow arrows).

2.6 HISTOLOGICAL PROCESSING AND SECTIONING

2.6.1 Undecalcified tissue histology

Plugs assigned to the histology and IHC studies were processed for paraffin embedding without decalcification. The standard histological processing method was optimised to produce a protocol for sectioning undecalcified osteochondral tissue. First, the subchondral bone of osteochondral plugs was carefully trimmed by a surgical bone cutter to about 1mm in length without damaging articular cartilage. Plugs were immediately fixed in formalin for 24 hours, and then processed for paraffin embedding with a 15 hours' protocol (8 hours in ethanol for dehydration, 3 hours in Xyline to clear ethanol, and 4 hours for paraffin infiltration). This processing protocol has been tested to provide sufficient paraffin penetration, facilitating later microtome sectioning.

Tissue sectioning was performed using a RM2235 microtome (Leica Biosystems, UK). Microtome blades (N35, Feather, Japan) designed for hard tissue sectioning were chosen. Paraffin blocks were first trimmed to the desired level, and were cooled in ice-cold water before and during sectioning to moisturise the cutting surface and solidify paraffin to provide stronger support. The osteochondral plug was placed with its long axis parallel to the blade, so the blade region cutting cartilage was not damaged or blunted by bone. The clearance

angle was set to 4°, and section thickness was 7µm. The harvested osteochondral sections were floated on a 40°C water bath to be flattened.

With the optimised embedding and cutting protocols, sections of desired quality can be obtained without decalcification. However, there were still about 20% sections associated with visible lesions and cracks. Therefore, random sections from an osteochondral plug, rather than serial sections, were picked up and mounted onto SuperFrost Plus microscope slides (2-4 sections per slide) (VWR, UK). Slides were then vertically incubated at 40°C for 2-3 days, and stored in a cool, dry and dark place for later use.

2.6.2 Decalcified tissue histology

Plugs assigned to the microCT study were snap-frozen upon extraction and stored at -80°C until scanning. We did not have a microCT device available on-site, so frozen plugs were transported to the collaborating lab (Skeletal.AI Laboratory) at the University of Sheffield. Plugs were thawed at room temperature before scanning. Re-evaluation of macroscopic grading for each plug was performed at this stage, to evaluate intra-observer reproducibility. After microCT scanning (see **Section 2.10**), they were re-frozen and transported back to Bristol. These plugs were then processed for paraffin embedding with decalcification because the initial plan included histomorphometry and IHC on subchondral bone of these samples. Briefly, plugs were thawed again, fixed in formalin for 24 hours without trimming of subchondral bone, and decalcified with ethylenediaminetetraacetic acid (EDTA) based reagent (RDF Mild Decalcifier, CellPath, UK) for 3-4 weeks. Completion of decalcification was determined by disappearance of precipitates in the solution and physical probing of bone. Then plugs were then embedded in paraffin and sectioned as in the previous section.

2.7 HISTOLOGICAL STAINING

Hematoxylin – Eosin (H&E) and Safranin O – Fast Green staining were carried out for evaluation of tissue histological quality and severity of cartilage degeneration. Sections from one plug (the standard) were used as quality control in each batch of staining to ensure staining consistency.

For better adherence of tissue sections, slides were first incubated at 58°C for 60 minutes to melt and remove excess paraffin, then gradually cooled back to room temperature. This was followed by dewaxing and rehydration starting from three washes (10 minutes each) with the Clearene Solvent (Leica Biosystems, UK), followed by three changes of graded ethanol solution (100%, 75%, 50%; 5 minutes each), and 10 minutes' dipping in distilled water.

For H&E staining, slides were left in Harris Hematoxylin (Leica Biosystems, UK) for 15 minutes, followed by a rinse with running tap water for 15 minutes (the 'bluing' step). Then slides were stained with Eosin (Leica Biosystems, UK) for 1 minute, and washed with distilled water (2 x 5 minutes). Finally, slides were dehydrated in absolute ethanol for 2 x 1 minute and mounted with coverslip using the Clearium Mounting Media (Leica Biosystems, UK).

For Safranin O – Fast Green staining, slides were first incubated with Hematoxylin and washed with tap water as above. Slides were then stained with Fast Green (Sigma Aldrich, UK) solution (0.05% in deionized water) for 5 minutes and quickly dipped in 1% acetic acid for 15 seconds. This was followed by a 5 minutes' soaking in Safranin O (Sigma Aldrich, UK) solution (0.06% in deionized water). Finally, slides were directly washed and dehydrated in absolute ethanol for 2 x 1 minutes before mounting with coverslip.

Slides were viewed and photographed with DM5500 microscope and digital camera (Leica Microsystems, UK).

2.8 MODIFICATION OF THE OARSI MICROSCOPIC GRADING SYSTEM

For histopathological evaluation of cartilage degeneration, the OARSI microscopic grading system (323) was modified as detailed in **Table 2.3**. As with the original system, the grading is presented with the Arabic numerals. Grade 0 indicates normal cartilage while higher grades indicate increasing severity of degeneration. Both general grading (from 0 to 6) and advanced grading (with 0.5 subgrades from 0.0 to 6.5) can be selected depending on the requirement of different research. Rationales for modification, and detailed description and discussion of this grading system are included in Chapter 3.

Table 2.3 The modified OARSI microscopic grading system used for evaluation of cartilage degeneration.

<table>
<tr><th rowspan="2">General Grading</th><th rowspan="2">Advanced Grading</th><th colspan="5">Matrix Structure</th><th colspan="2">Chondrocyte Biology</th><th rowspan="2">Proteoglycan Depletion</th></tr>
<tr><th>Surface</th><th>Fibrillation</th><th>Fissure</th><th>Matrix Loss</th><th>Others</th><th>Proliferation & Cluster[C]</th><th>Others</th></tr>
<tr><td>0</td><td>0.0</td><td>Intact and smooth.</td><td>N/A</td><td>N/A</td><td>N/A</td><td>N/A</td><td>(-)</td><td>N/A</td><td>SZ only</td></tr>
<tr><td rowspan="2">1</td><td>1.0</td><td>Intact but irregular.</td><td>Superficial, usually appears as irregularity or small fibrils on the cartilage surface.</td><td>N/A</td><td>N/A</td><td rowspan="4">Oedema, matrix hypertrophy or atrophy [B].</td><td>(-) to (+)</td><td>N/A</td><td>SZ only</td></tr>
<tr><td>1.5</td><td>Intact but irregular.</td><td>As above, with superficial microcracks.</td><td>N/A</td><td>N/A</td><td>(-) to (+)</td><td rowspan="5">Cell death (empty lacunae, membrane ‘ghost’, fragmented nuclei), cell hypertrophy (increased size and chondron staining), disrupted alignment of cells.</td><td>SZ only</td></tr>
<tr><td rowspan="2">2</td><td>2.0</td><td>SZ[A] exposed.</td><td>Discontinuity and/or microcracks into and confined to SZ.</td><td>N/A</td><td>Superficial abrasion, floating matrix ‘flakes’, ‘fibrils’.</td><td>(+)</td><td>SZ to Upper 1/3 MZ</td></tr>
<tr><td>2.5</td><td>SZ exposed.</td><td>Discontinuity and/or microcracks through SZ.</td><td>N/A</td><td>As above, deeper and through SZ.</td><td>(+)</td><td>Upper 1/3 MZ</td></tr>
<tr><td rowspan="2">3</td><td>3.0</td><td>Upper 1/3 of MZ exposed.</td><td>N/A</td><td>Simple, confined to upper 1/3 MZ.</td><td>Deep spallation along the fissures, with major loss of SZ.</td><td rowspan="3">N/A</td><td>(+) to (++)</td><td>Upper 1/3 MZ or lower</td></tr>
<tr><td>3.5</td><td>Lower 2/3 of MZ exposed.</td><td>N/A</td><td>Branched, or simple but reaches lower 2/3 MZ.</td><td>Deep spallation along fissures, with complete loss of SZ and partial loss of MZ.</td><td>(++)</td><td>Lower 2/3 MZ to DZ</td></tr>
<tr><td rowspan="2">4</td><td>4.0</td><td>MZ-DZ junction exposed.</td><td>N/A</td><td>Down to MZ-DZ junction.</td><td>Erosion/excavation down to MZ-DZ junction, with partial loss of MZ.</td><td>(++)</td><td>DZ</td></tr>
<tr><td>4.5</td><td>DZ exposed, only a thin layer of cartilage attached to SB.</td><td>N/A</td><td>Down to lower DZ. Or no fissure presents, just jigsaw-like surface.</td><td>Erosion/excavation down to lower DZ, with complete loss of MZ.</td><td>(-) to (++)[C]</td><td>DZ</td></tr>
<tr><td>5</td><td>5.0
5.5</td><td colspan="8">Subchondral bone exposed, with (5.5) or without (5) reparative tissue.</td></tr>
<tr><td>6</td><td>6.0
6.5</td><td colspan="8">Marginal (6) or central (6.5) osteophyte observed.</td></tr>
<tr><td colspan="10">(A) Superficial zone (SZ), middle zone (MZ) and deep zone (DZ) are grossly divided according to the shape and alignment of chondrocytes, occupying approximately 10-20%, 50-60% and 30-40% of cartilage full depth, respectively. (B) For small and localised sample, matrix hypertrophy or atrophy is difficult to identify on histology sections. Overall macroscopic inspection during the sampling procedure needs to be considered. (C) Chondrocyte cluster is defined by the number of cells in the same lacunae: (-) < 4; 4 ≤ (+) < 10; (++) ≥ 10. At Grade 4.5, clusters may not be observed due to cartilage loss.

For cartilage changes in OA, the Generalised Grade 1 and Grade 2 (Advanced Grade 1.0-2.5) are considered as early degeneration; Generalised Grade 3 and 4 (Advanced Grade 3.0-4.5) are considered as advanced degeneration; Generalised Grade 5 and 6 (Advanced Grade 5.0-6.5) are considered as end-stage degeneration.</td></tr>
</table>

2.9 MICROSCOPIC GRADING

Microscopic grading was performed on Safranin O – Fast Green stained sections using the modified OARSI grading system. Scoring was carried out for both undecalcified and decalcified samples. Slide labels exhibiting sample origins and macroscopic grades were covered to ensure that the process was implemented in a blinded manner. Three examiners were involved to evaluate inter-observer variability. Re-scoring with at least 8 weeks' interval was employed to check for intra-observer variability.

2.10 MICROCT SCANNING AND IMAGE ANALYSIS

Frozen plugs were transported to University of Sheffield for microCT scanning. The scanning was carried out with the Skyscan 1172 (Skyscan, Belgium). Plugs were thawed, wrapped in clingfilm to keep moisture, and placed into the scanning chamber at upright standing position. Images were obtained with a 50 KeV and 179 µA X-ray source. An isotropic voxel size of 4.87µm was acquired, with 1180ms integration time and 180° rotation. A 0.5mm aluminium filter was chosen for reducing beam-hardening artifacts. Three-dimensional reconstruction was carried out using the NRecon software (1.6.9.4, Skyscan, Belgium) which yielded a stack of 938 consecutive cross-sections for each plug with a slice thickness of one pixel (4.87µm). Reconstructed datasets saved in .BMP format were then imported into the CT Analyzer software (CTAn, 1.17.7.2, Skyscan, Belgium) for image processing and analysis as described in details in Chapter 4 and 5. The scanned plugs were re-frozen and transported back to Bristol, decalcified, processed and sectioned as described in **Section 2.6.2**.

2.11 IHC FOR MMP13 AND ADAMTS4

Originally, it was planned to carry out IHC on the same plugs scanned by microCT to study cartilage degradation and bone remodelling associated biomarkers. However, the two cycles of freezing-thawing, together with a lengthy decalcification period, brought detrimental effects on cell and tissue morphology and immunogenicity in both cartilage and bone. The resultant tissue sections were fine for histopathological evaluation, but not good enough for IHC staining. Therefore, the immediately adjacent plugs, which were processed without freezing and decalcification (see **Section 2.6.1**), were used for the IHC study. Since the

subchondral bone was trimmed, only targets in cartilage (ADAMTS4 and MMP13) were studied.

Slides were immersed in the Clearene Solvent to remove paraffin, followed by graded ethanol solutions and distilled water to rehydrate. Then heat-induced antigen retrieval was carried out by incubating slides with citrate buffer (10mM sodium citrate and 0.05% Tween® 20 in distilled water, PH=6) at 95°C for 10 minutes. This was followed by PBS wash and treatment with hydrogen peroxide solution (3% in distilled water) for 10 minutes at room temperature to quench endogenous peroxidase activities. Next, the blocking buffer (10% normal goat serum (ab7481, Abcam, UK) in PBS with 0.3% Triton® X-100) was applied to tissue sections for 1 hour at room temperature to prevent non-specific antibody binding. Polyclonal rabbit primary antibodies (IgG) against the C-terminal of human ADAMTS4 and the hinge region of human MMP13 (ab84792 and ab39012, Lot No. GR3281410-2 and GR3327965-1, Abcam, UK) were diluted with the blocking buffer at 1:200 and 1:300, respectively. They were then applied to tissue sections for overnight incubation at 4°C. One extra slide from each osteochondral plug was incubated with the blocking buffer only, as negative antibody control. Non-immune rabbit IgG (ab37415, Abcam, UK), prepared in the same way as primary antibodies, was also utilised as negative antibody control on a selection of slides as a part of the optimisation procedure, which generated negligible background. A paraffin embedded human benign prostate tissue (a generous gift from Professor Claire Perks, University of Bristol) was employed as negative tissue control for MMP13 (https://www.proteinatlas.org/ (573, 574)).

The next day, sections were thoroughly washed with PBS and treated with biotinylated goat anti-rabbit secondary antibody (ready-to-use, ab64256, Abcam, UK) for 30 minutes. After rinsing with PBS for 3 x 5 minutes, streptavidin-horseradish peroxidase (HRP) conjugate (ready-to-use, ab64269, Abcam, UK) was applied for 10 minutes to bind secondary antibody, followed by another round of PBS wash. Chromogenic detection was then carried out with 3, 3'-diaminobenzidine (DAB) chromogen and substrate (1:50 dilution, ab64238, Abcam, UK) which produced brown precipitates in chondrocytes expressing ADAMTS4 and MMP13 upon enzymatic reaction catalysed by HRP. Reaction was closely monitored under a light microscope and was stopped by PBS rinse when optimal staining was achieved. Finally, sections were counter-stained with hematoxylin which labelled cell nucleus purple to create

contrast and facilitate cell counting. Slides were washed in running tap water for 15 minutes, air-dried and mounted with the resinous Clearium Mounting Media, ready for microscopic inspection and imaging.

2.12 MEASUREMENT OF MMP13 AND ADAMTS4 EXPRESSION

The number of chondrocytes positively and negatively stained with MMP13 or ADAMTS4 was counted manually. A region of interest (ROI) was selected for each tissue section. The overall expression of MMP13 and ADAMT4 was expressed as percentage of positively stained cells through the full-thickness of cartilage in the ROI. The zonal expression was defined as percentage of positive cells in the superficial zone, middle zone, and deep zone, respectively, which were differentiated according to characteristic chondrocyte morphology and alignment as described in **Section 1.3.3.1**.

2.13 STATISTICAL ANALYSIS

Data are presented as mean $\pm$ standard deviation (SD) unless otherwise indicated. Assumptions of statistical tests were carefully evaluated. Normal distribution of data was inspected by Shapiro-Wilk test. Homogeneity of variance was checked by Brown-Forsythe test. Then comparisons between groups and associations between various parameters were investigated using appropriate tests as detailly explained in each of the following chapters. Statistical significance was indicated by two-tailed P value less than 0.05. GraphPad Prism (8.3.0, GraphPad Software, USA) and IBM SPSS (26.0, IBM Corp., USA) were used for statistical analysis and graphing.

Chapter 3

Standardisation of osteochondral tissue collection and evaluation of cartilage degeneration

3.1 INTRODUCTION

Collection of samples that cover and accurately reflect different stages of cartilage degeneration is a fundamental step in this PhD project. It relies on a combination of both macroscopic and microscopic evaluation of cartilage pathology, in which macroscopic assessment directs tissue extraction and determines the range and diversity of samples, while microscopic assessment determines the severity/stage of histopathology for each sample.

The 'Collins system' was one of the earliest grading scheme to evaluate chondro-pathology for clinical and research purposes. It was based on description of macroscopic features of cartilage surface, lesions and bony alternations on human patella (575, 576). The grading was related to the uptake of $^{35}SO_4$ by chondrocytes (576) and suggested that OA is not simply a result of 'wear and tear' but is associated with biological and cellular reactions (323). In 1971, Mankin et al (577) developed the first microscopic grading system for osteoarthritic cartilage, which is widely known as the 'Mankin score' or the 'Histologic/Histochemical Grading System (HHGS)'. It scores osteochondral pathology on a 14-point scale based on four parameters, namely matrix structure, cell morphology, GAG content, and tidemark integrity. The system has been widely adopted on samples from both human subjects and animal models for decades. It has been through numerous rounds of modifications by different studies and for various research purposes (578). Although it is still a popular option in OA research, the Mankin system has been criticised for its lack of sensitivity to early disease and its questionable validity and reproducibility (578-580). Currently there are also grading systems available for specific purposes such as cartilage repair (e.g., International Cartilage Repair Society (ICRS) score (581-583)) and tissue engineering (e.g., the Bern score (584)), but they are generally more specialised and have a narrow application (580).

To overcome the disadvantages of the Mankin system, in 2006 the Osteoarthritis Research Society International developed a new microscopic grading scheme, known as the OARSI system (323). It was original designed for human OA but has been generalised for various large and small animal models (585-587). The scheme consists of two components, grading and staging. The grading element evaluates the vertical development of pathology and is designated to be an indicator of the process and severity of OA progression, while the staging component examines the horizontal extension of the affected area (323, 578). The grading ranges from 0 to 6 to reflect more severe focal degradation, with optional inclusion of 0.5 subgrades, while the staging ranges from 0 to 4 to represent wider articular surfaces being affected. In a series of studies comparing the HHGS with OARSI scores, the latter performed well with good reproducibility and minimal variability, and appeared to be more 'beginner-friendly' (578, 579, 588, 589). Since then, the OARSI system, especially the grading element, has gained increasing attention and become widely adopted by OA researchers.

However, the original OARSI scoring scheme was aimed at evaluation of cross-sections of entire joint surfaces, e.g., a plain through the medial femoral condyle from one edge to the other, so that both grading and staging can be implemented (323, 588). When applying just the grading component to regionally collected samples with relatively small dimensions as in the current study, grading may be somewhat difficult and inconsistent because adjacent areas are not available for referencing. Grading of this type of samples should highlight changes in the vertical direction, and relies heavily on a clear, comprehensive, and stratified description of each assessment criterion, i.e., the structural, cellular, and biochemical features seen in the process of cartilage degradation. Regional sample collection and evaluation are common for studies using human joint specimens, but to date no grading method specialised for these purposes has been reported. The variability of grading may hinder the comparison of results between different studies. The limitations of the OARSI grading protocol in the evaluation of small samples, in addition to our own experience with samples from femoral heads with OA, provided the impetus to develop a modified OARSI microscopic grading scheme.

Moreover, as mentioned earlier, macroscopic evaluation is also important for regionalised investigations as it provides a first-line screening and determines the range and diversity of sample collection. It should be used in combination with microscopic examinations to enable

more accurate representation of different stages of disease progression in mechanistic or observational studies of, for example, gene expression profile, biomarkers, and subchondral bone changes. However, macroscopic grading methods have been rather diverse, vague, and inconsistent between studies in the literature (590-596).

Accordingly, the overall aim of this chapter is to develop a standardised protocol for collection of osteochondral plugs that accurately represent various stages of cartilage degradation, based on a combination of reliable macroscopic and microscopic evaluations. The specific aims of this chapter are:

(i), Develop a new macroscopic grading system for regionalised assessment of cartilage degradation on the articular surface of hip joint.

(ii), Develop a modified version of the OARSI microscopic grading scheme to make it suitable for evaluation of regionally collected osteochondral samples with limited dimensions.

(iii), Evaluate the reproducibility and reliability of the above grading systems.

(iv), determine the associations between the two grading systems to validate their usage in regionalised sample collection.

3.2 MATERIALS AND METHODS

3.2.1 Patient selection and femoral head collection

All OP (N=7) and OA (N=31) femoral heads, including both the optimisation and the main study cohorts, were included in the histology study (see **Section 2.3** and **2.5**).

3.2.2 Standardisation of osteochondral plug collection

The study aimed to collect osteochondral samples in a regionalised manner to represent different stages and severity of cartilage degradation. The study also planned to look at a broad spectrum of pathophysiological changes in OA including cell biology, matrix

biochemistry, and bone biological and structural properties. Therefore, though only a few aspects were finally included in this current PhD project, at the beginning we aimed to establish a sample collection procedure that is able to consistently generate adequate and standardised samples for a variety of research techniques and purposes. Hence, collection of samples needed to fulfil the following criteria. First, the physical dimensions of the sample should be relatively small to allow precise representation of the regional features, and allow multiple collections from the same region wherever possible to yield more samples. Second, the dimensions of samples should be large enough to include adequate amount of tissue for investigation, especially for subchondral bone microarchitecture. Third, the sample extraction process should be precise and neat, producing minimum damage to tissue and cells.

We tested three different instruments: a hand-driven osteochondral tissue harvester with 8mm diameter (Platts & Nisbett, UK), a diamond coring trephine with 6mm diameter (Tacklife, China), and a steel hollow punch with 4mm diameter (SPC, China). Finally, the hollow punch was chosen as it best fulfilled the criteria set above.

3.2.3 Chondrocyte viability and confocal microscopic imaging

Chondrocyte viability assay was carried out with live/dead staining using two fluorescent dyes (Invitrogen, Thermo Fisher Scientific, USA), 5-chloromethylfluorescein diacetate (CMFDA, C2925) and propidium iodide (PI, P3566). CMFDA crosses cytomembrane freely, and once truncated by intracellular esterase, it is trapped in live cells and stains them green (excitation wavelength 488nm). In contrast, PI is impermeant to cytomembrane of live cells due to positive charge. Once cells are dead, PI enters the cell, combines with nucleic contents and stains it red (excitation wavelength 543nm) (177).

Osteochondral plugs collected by either 8mm osteochondral tissue harvester or 4mm hollow punch were incubated with 10uM CMFDA and 5uM PI in PBS for 30 min at 37°C. Then they were washed with PBS for 5 x 1minutes, followed by 20 minutes' fixation in formalin. Eventually plugs were washed in PBS and subjected to confocal microscope imaging.

Fluorescent images were acquired by confocal laser scanning microscopy (SP5, Leica Microsystems, UK). With laser excitation of CMFDA and PI, fluorescence emissions (498-

540nm and 576-700nm, respectively) were detected and captured by a fitted objective through corresponding channels. The focal plane was first placed on cartilage surface at the edge of samples, and then moved downward with a 9.9um interval to a depth of about 80-100um, where penetration of laser met its limit. Eventually 8-10 consecutive two-dimensional images were acquired and reconstructed into a three-dimensional stack by the Volocity software (v6.3, PerkinElmer, USA).

3.2.4 The new macroscopic grading system

A new macroscopic grading system (**Table 2.2**) was designed for this study to visually evaluate cartilage degeneration and guide osteochondral tissue collection. The system aims to incorporate a wide spectrum of features observed on hip femoral articular surface with OA and OP. It includes visual inspection of cartilage colour, surface integrity and fibrillation, appearance and depth of fissure, and thickness. It also involves physical probing of surface smoothness/roughness, overall elasticity/softness, and thickness under pressure. According to these features, cartilage degradation is divided into five categories with ascending severity: normal or comparatively normal, surface irregularity, matrix destruction, cartilage erosion, and bone exposure. These categories are represented by Roman numerals from I to V, to differentiate from microscopic grading using Arabic numerals. It should be noted that 'normal' and 'comparatively normal' cannot be differentiated by eyes, at least in the group of elderly subjects recruited in this study; therefore, they are combined as Grade I. A template with a series of typical examples of grading is provided in **Figure 2.1** and **Figure 3.1**. Osteochondral plugs collected from the femoral head shown in **Figure 2.1B-C** according to the macroscopic grading system are shown in **Figure 3.2**.

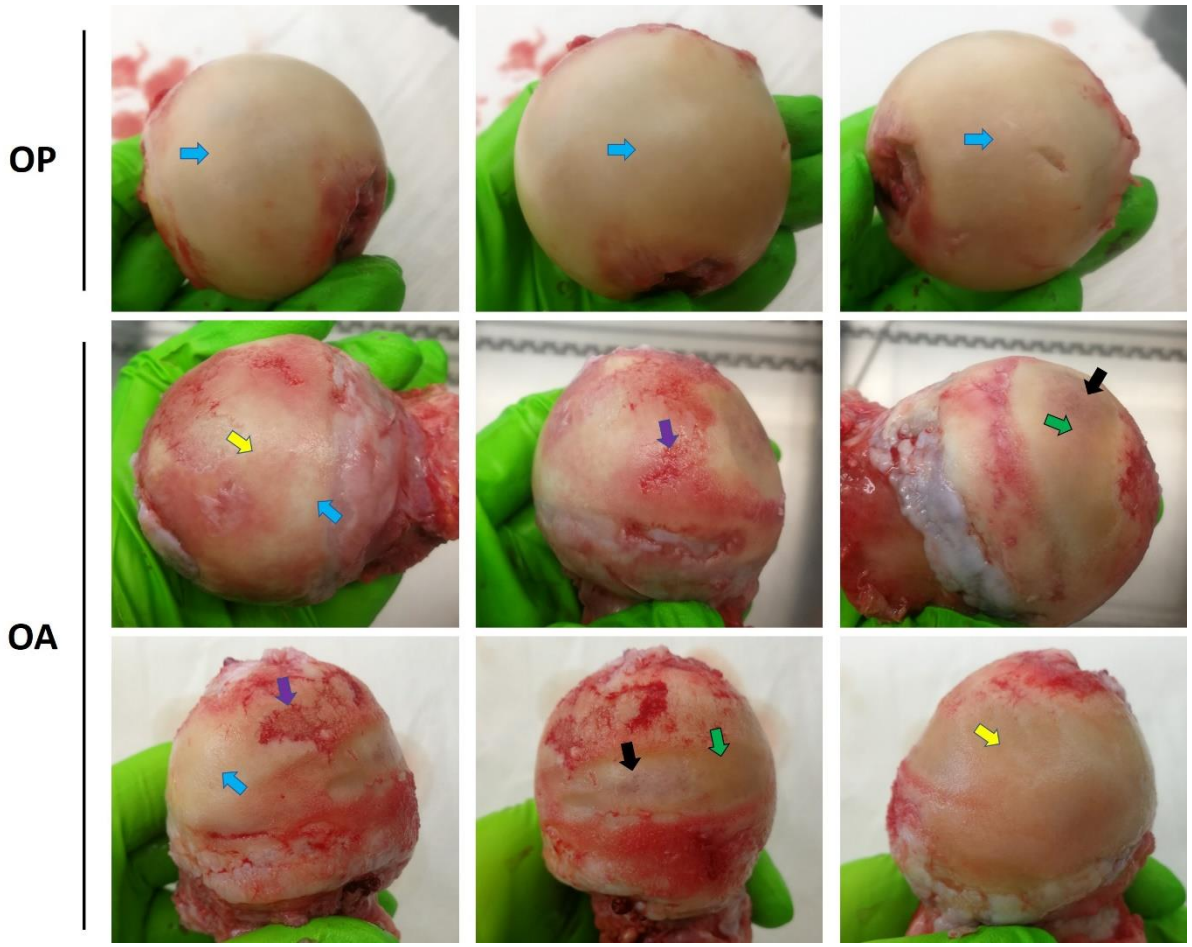

Figure 3.1. Macroscopic grading of articular surfaces. At Grade I (blue arrows), articular surface is slightly grey but smooth, intact, with no superficial fibrillation. At Grade II (yellow arrows), cartilage appears to be grey or slightly pink, with observable superficial roughening, pilling or fibrillation. At Grade III (purple arrows), cartilage becomes soft and fluffy, with obvious fissure development and thinning. Grade IV (green arrows) is characterised by a thin layer of cartilage remnant with a smooth or slightly roughened surface. Grade IV is often adjacent to Grade V areas (black arrows) where cartilage is completely worn off and subchondral bone is exposed. Each row shows the same femoral head viewed from anterior, superior and posterior angles.

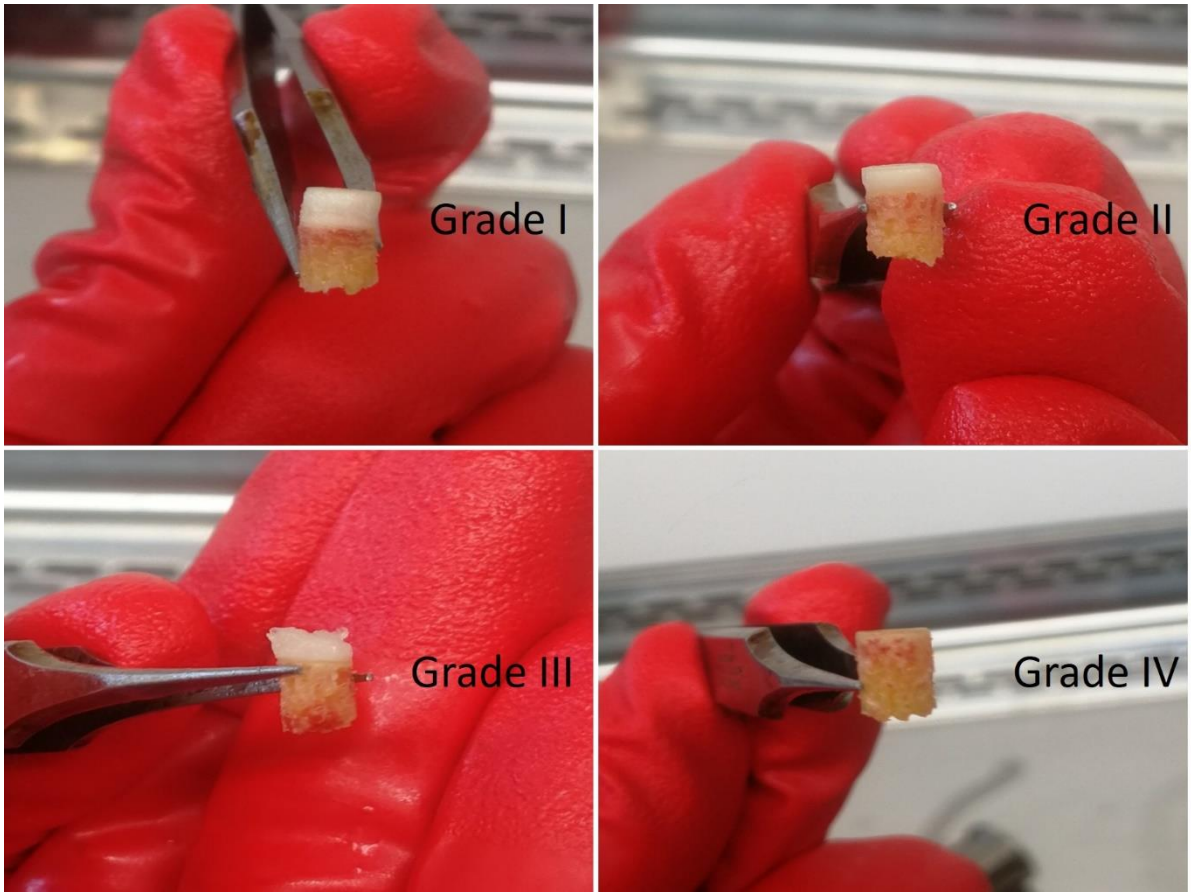

Figure 3.2. Osteochondral plugs collected according to the new macroscopic grading system. The articular surfaces are intact at Grade I and Grade II. At Grade II, there are observable superficial fibrillations, though they cannot be identified on the images. At Grade III, there are obvious fissure development, and the cartilage becomes soft and fluffy. At Grade IV, there is just a thin layer of cartilage left.

3.2.5 Osteochondral plug extraction

After macroscopic grading, osteochondral plugs with 4mm diameter were extracted in a regionalised manner as described in **Section 2.5**. Briefly, for OP group, in which articular surfaces were macroscopic Grade I, plugs (N=21) were collected from superior, posterior and anterior sites. For OA group, plugs (N=101) were collected from regions with different macroscopic grades (Grade I to IV) depending on availability. A few Grade V plugs were collected for the purpose of demonstration of grading only and were not included in analysis as explained in **Section 2.5**.

3.2.6 Histological processing, sectioning, and staining

Shaving cartilage from subchondral bone and processing it for paraffin embedding are commonly adopted procedures for cartilage histology and IHC. However, the deepest portion closest to tidemark and subchondral bone may be lost or destroyed by blades. More importantly, when cartilage is at its advanced stage of degeneration and becomes soft and fluffy, and when just a thin layer is left (Grade III, and especially Grade IV), shaving may completely smash the sample. This is not an option in this study as we aimed to cover a wide range of cartilage degradation as well as provide a detailed zonal differentiation.

To maintain the integrity of full-thickness articular cartilage, osteochondral samples can be utilised with decalcification. However, fast decalcification using strong acids may compromise nuclear staining, tissue morphology and antigenicity of molecular targets, while mild decalcification using EDTA based reagents is a lengthy procedure that takes weeks and is associated with significant loss of matrix contents which will affect histological and immunochemical examinations (581). Frozen and resin embedded sections are also options for osteochondral tissue. Frozen sections were tested in this study but resulted in unsatisfying quality. Resin embedding was not tested, as preliminary studies by other student in our group showed that resin infiltration was associated with false positive IHC staining.

Therefore, a protocol for histological processing and sectioning of undecalcified osteochondral tissue was developed for this study. It allowed preservation of the true full-thickness cartilage with excellent quality. The optimised protocol has been explained in detail

in **Section 2.6.1**. This optimised protocol was used to obtain tissue sections with 7µm thickness which were stained with H&E for evaluation of histological quality, and with Safranin O – Fast green for microscopic grading of cartilage degradation (see **Section 2.7**).

3.2.7 Modification of the OARSI Microscopic grading system

The modified OARSI microscopic grading system is presented in **Table 2.3**. The grading system was designed to suit regionalised collection of samples with relatively small volume/dimensions, by emphasizing and defining the characteristic changes in each zone of cartilage in different grades. Modifications were also made according to features that were observed in this study on proximal femoral articular surfaces which were not accounted for by the original OARSI grading system. For example, when fissures developed into the MZ (even just simple unbranched ones), 'delamination' of the SZ had already began and there was major or complete loss of the SZ due to shear forces. Typical features of the SZ could not be identified at the articular surface; instead, only residuals of the SZ matrix could be observed, accompanied by obvious thinning of cartilage. Moreover, before cartilage is entirely eroded from subchondral bone, there was always a stage when a thin layer of cartilage was present which had smooth or slightly roughened surface (macroscopic Grade IV, **Figure 3.1**, **Figure 3.2**). Microscopically, the surface is jigsaw-like without fissures or clefts. This type of cartilage often has typical features of the DZ in terms of both thickness and chondrocyte morphology, indicating that at this stage the MZ has been mostly or completely lost.

Presentation of the grading system has been optimised for easier learning and usage by researchers with limited experience on cartilage histopathology. Evaluation criteria were formulated into columns consisting of three main parameters (matrix structure, chondrocyte biology and proteoglycan depletion) and eight sub-parameters. Grading was stratified into rows with descriptions and positive or negative observations of each sub-parameter. By doing so, characteristic changes in the vertical direction (i.e., in each zone of cartilage) in different grades were highlighted and clearly differentiated. A semi-quantitative definition of cell clusters was provided, as well as a classification of early (Grade 1.0 to 2.5), advanced (Grade 3.0 to 4.5), and end-stage disease (Grade 5.0 to 6.0). The scoring was also simplified, by

downgrading the importance of features (such as oedema, cartilage hypertrophy, and chondrocyte death) that are difficult to assess by inexperienced observers, subjected to the influences of artefacts, or need referencing to the adjacent tissue areas (578, 597).

3.2.8 Microscopic grading

Microscopic grading was performed on Safranin O – Fast Green stained sections. To evaluate and validate the modified OARSI grading method, and to see if it is 'beginner-friendly', except for the leading researcher who designed the grading system (Y Li), two other examiners, Y Liem and H Ahmed were invited in the study. Y Liem is a PhD candidate working in an unrelated OA PhD project who has knowledge of OA but no experience of histology; H Ahmed was a medical student who did not have experience in either OA or cartilage histology. They were briefly trained on cartilage histology and pathology, introduced to the grading method, and practised on about 50 slides.

The three examiners, blinded to sample origins and macroscopic grades, scored slides independently. Scoring was carried out using the advanced grading with subgrade of 0.5. For each osteochondral plug, two to three slides were included. Y Li and Y Liem scored all 308 slides while H Ahmed scored 195 random slides. Re-evaluation was carried out by Y Li and Y Liem on a random subset of slides (N=100) with 8-week's interval. Final microscopic grade for each plug was obtained by averaging and rounding scores between the first readings by Y Li and Y Liem.

3.2.9 Statistical analysis

Reliability and reproducibility of microscopic grading was evaluated using intraclass correlation coefficients (ICCs) and limits of agreement (LOA) according to an established protocol (578). ICCs were calculated using two-way random effects analysis of variance aiming at absolute agreement. For the LOA, firstly, the mean and standard deviation of the differences between two scores of the same slide (first and second scores from the same observer, or scores from two observers) were calculated. Then the LOA was constructed by adding and subtracting 1.96*standard deviation to and from the mean (598, 599). The LOA indicates the range within which 95% of measurement errors are expected to locate. Intra-

observer ICCs and LOAs were investigated between the first and second scores of Y Li and Y Liem. Inter-observer ICCs and LOAs were investigated between the first scores of Y Li, Y Liem, and H Ahmed. Reproducibility of macroscopic grading was evaluated using ICC based on the first and second scores of Y Li. The correlation between macro- and microscopic grading was assessed using Spearman's Rank Order test.

3.3 RESULTS

3.3.1 Selection of tools for tissue extraction

In general, the osteochondral tissue harvester and the diamond coring trephine caused significant damage to the edges of collected samples, and also damaged tissues around the sample, causing an unacceptable waste. The damage can be clearly seen under confocal microscope, showing disrupted tissue morphology and excessive cell death (**Figure 3.3A**). In contrast, the hollow punch produced a neat cut of tissue (**Figure 3.2**) and limited cell death in a thin belt at the edge (**Figure 3.3B**). Therefore, in the end the 4mm hollow punch was chosen for tissue collection.

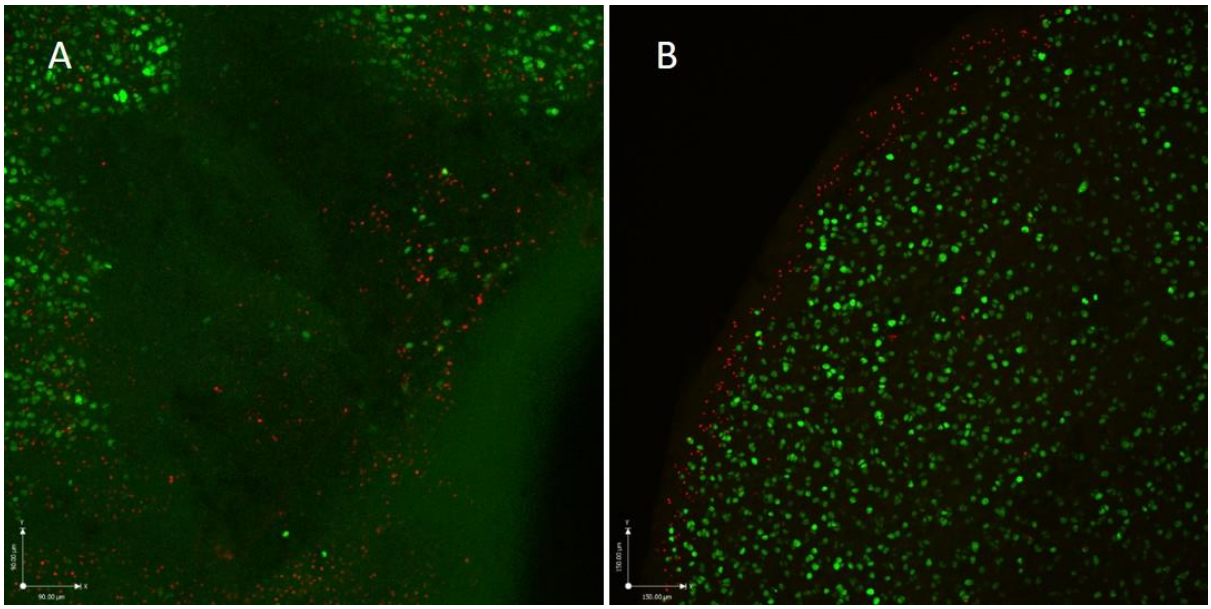

Figure 3.3. Tissue morphology and chondrocyte viability of osteochondral plugs extracted by different tools. (A) The hand-driven osteochondral tissue harvester with 8mm diameter. (B) The steel hollow punch with 4mm diameter. Red indicates dead cells stained with propidium iodide (PI), and green indicates live cells stained with 5-chloromethylfluorescein diacetate (CMFDA).

3.3.2 Quality of histology

As expected, there was various degree of cracking of subchondral bone on the undecalcified tissue sections. However, the histological quality was excellent throughout the full-thickness of cartilage with or without degradation (**Figure 3.4**). The folding of tissue sections, as with traditional histology methods, cannot be completely avoided; however, it was minimal and did not affect histological examination. No severe cutting lesions were observed. Spindle-like cells in the SZ (**Figure 3.4E**, **F**), isogenous chondrocyte groups (cell clusters) near fissures (**Figure 3.4G**, **H**), and column-like cells in the DZ can be easily and clearly identified (**Figure 3.4K**). Interestingly, cell and tissue morphology in areas closest to the tidemark were still excellent even when the adjacent subchondral bone is shattered (**Figure 3.4I**, **K**, **L**). Moreover, attachment of subchondral bone did not affect the sectioning of cartilage even in the worst scenario where most cartilage was eroded and there was just a thinner layer left (**Figure 3.5**). The undecalcified histology protocol was further tested the on the osteophyte tissue which,

again, displayed excellent quality of fibrocartilage and hypertrophic chondrocytes (**Figure 3.6**). The above observations on undecalcified osteochondral tissue were clearly contrasted by frozen sections on which significant lesions, loss of cells, excessive crumpling and folding, and distortion of matrix were present (**Figure 3.7**).

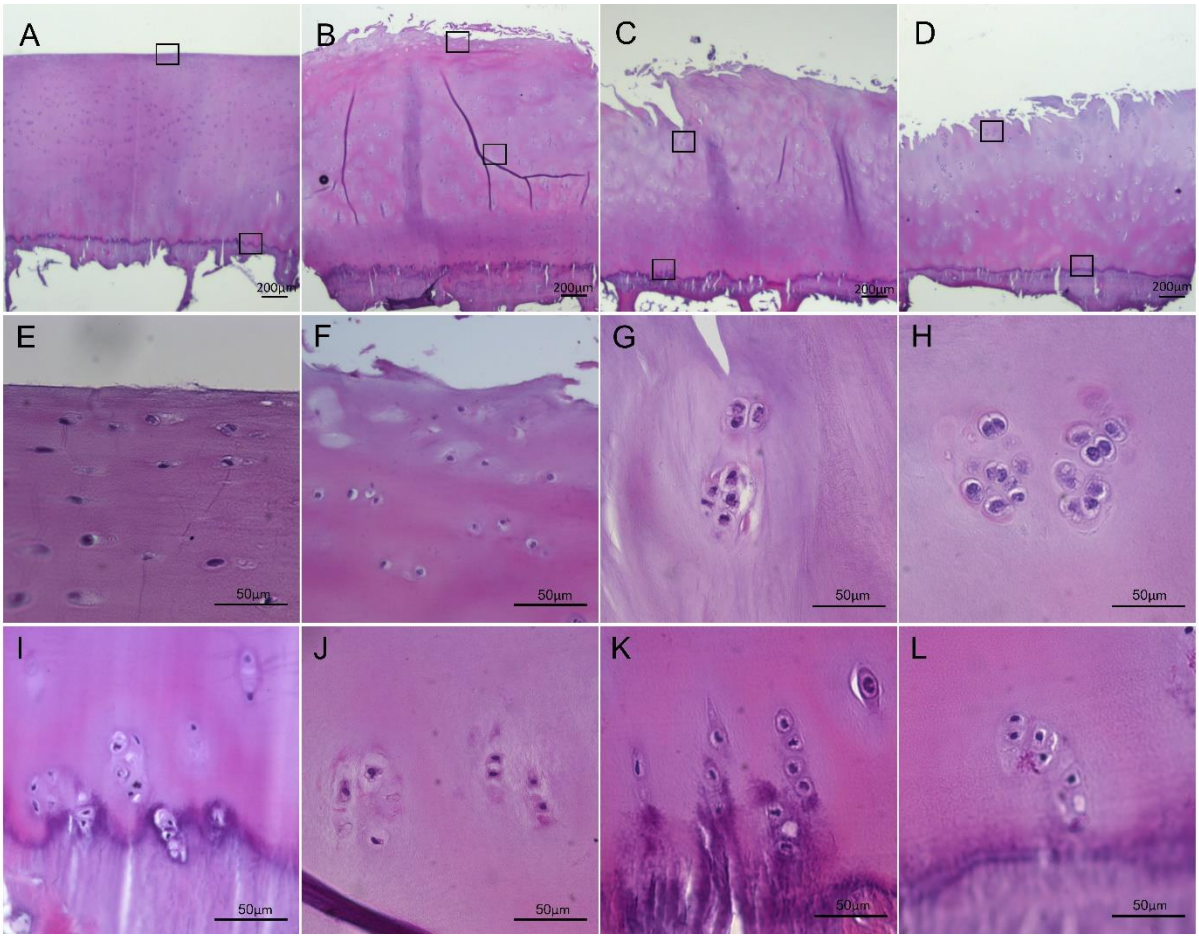

Figure 3.4. Hematoxylin and eosin staining of undecalcified osteochondral tissue sections. Full-thickness cartilage sections with (B, C, and D) and without (A) degradation are displayed at 25x magnification. Squares in the top panel indicate areas within the superficial, middle, or deep zones that are shown at 400x magnification in the subjacent images from E to L. Chondrocyte and matrix histology were excellent across the full-depth of cartilage, even in the deepest area near the cracked subchondral bone. Folding artefacts are minimal and no obvious sectioning lesions were observed.

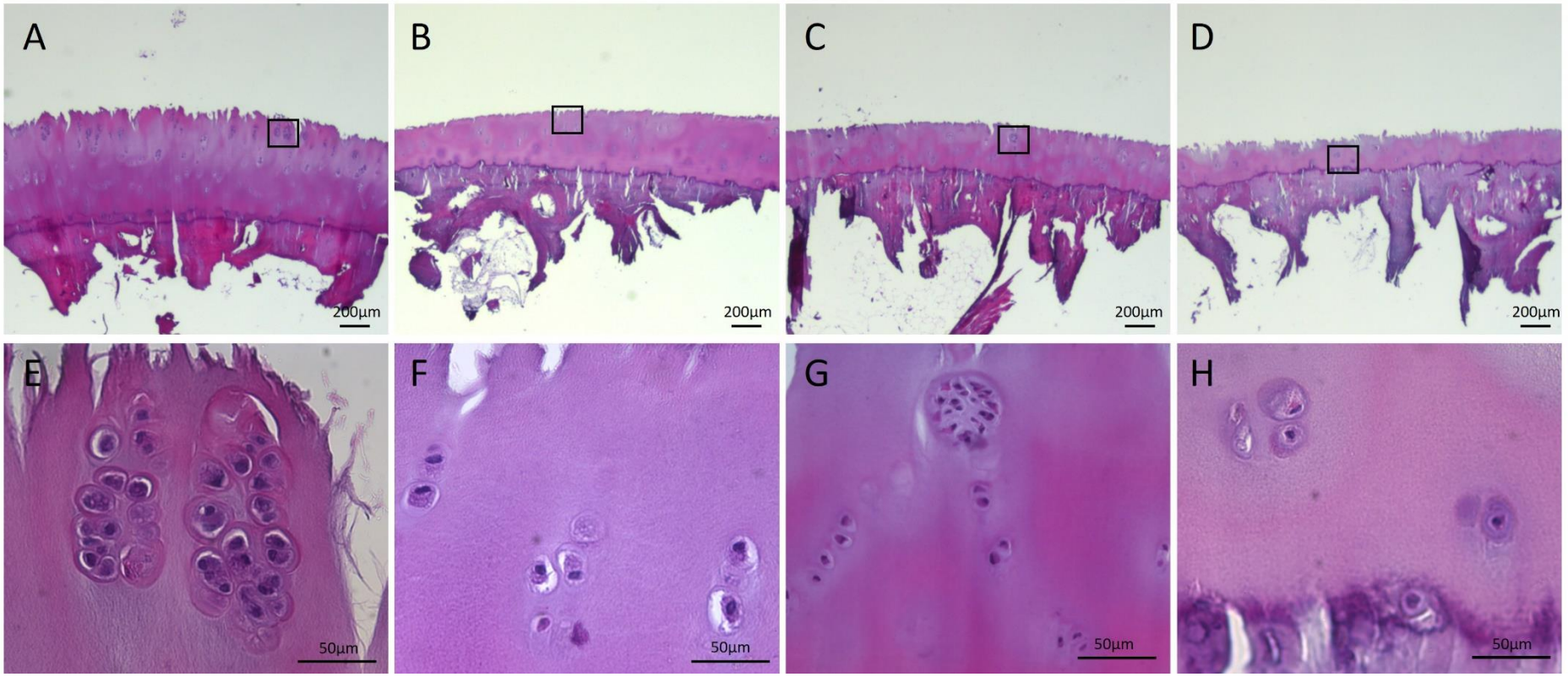

Figure 3.5. Hematoxylin and eosin staining of undecalcified osteochondral tissue sections with severe cartilage erosion. Samples in which most cartilage is eroded and there is just a thin layer left are displayed in A to D (25x magnification). Squares indicate areas that are shown at 400x magnification in the subjacent images (E to H). The quality of chondrocyte staining and general matrix histology were excellent, with no obvious artefacts within cartilage. Jigsaw-like surfaces can be observed on these sections.

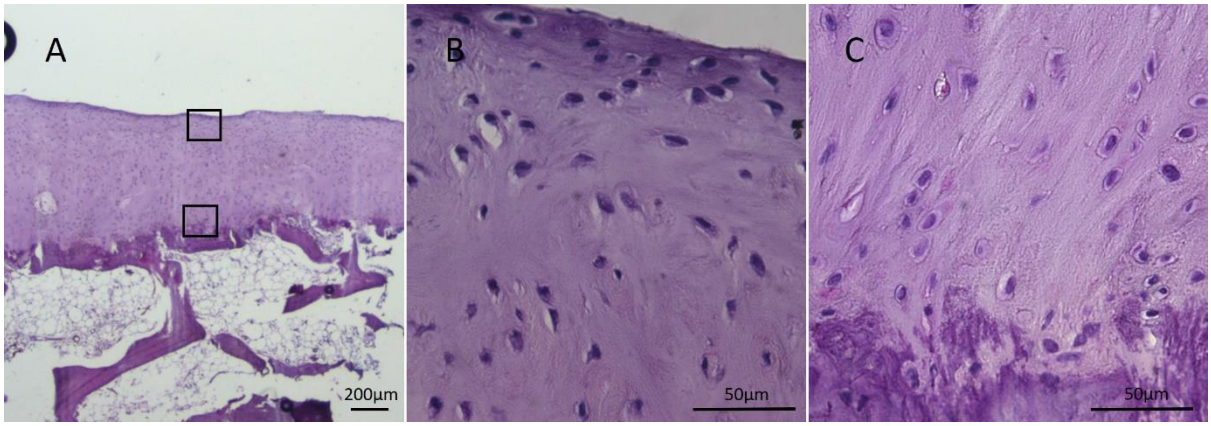

Figure 3.6. Hematoxylin and eosin staining of undecalcified osteophyte tissue section. The figure show that full-thickness fibrocartilage on osteophyte can be sectioned with excellent histology quality. 25x magnification in A, and 400x in B and C.

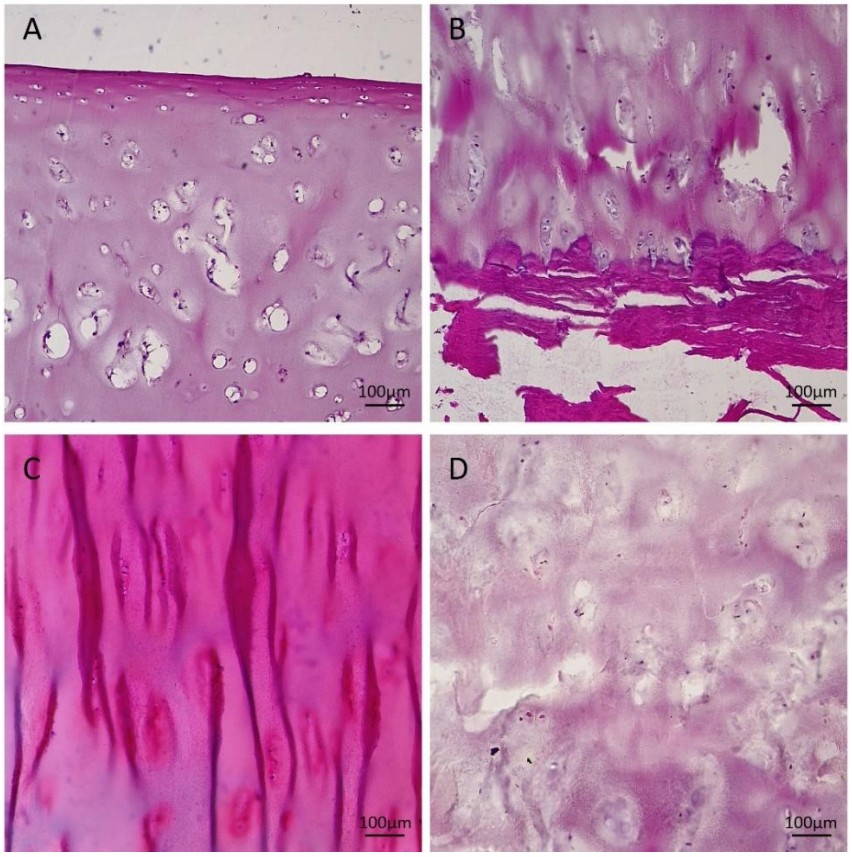

Figure 3.7. Hematoxylin and eosin staining of undecalcified frozen osteochondral tissue section. Significant artefacts were observed on frozen sections, including cutting lesions leading to loss of cells (A) and damage of matrix (B), excessive folding of tissue section (C), and distortion of matrix (D). Original magnification 100x.

3.3.3 Microscopic grading

The samples collected in this study covered all stages of cartilage degradation as assessed by the modified OARSI grading method. A series of representative sections are provided here which can be used as a template for grading.

In Grade 0 (**Figure 3.8**), GAG loss was restricted to the SZ only. The cell arrangement and morphology were normal. The articular surface was smooth and intact; no superficial fibrillation was observed.

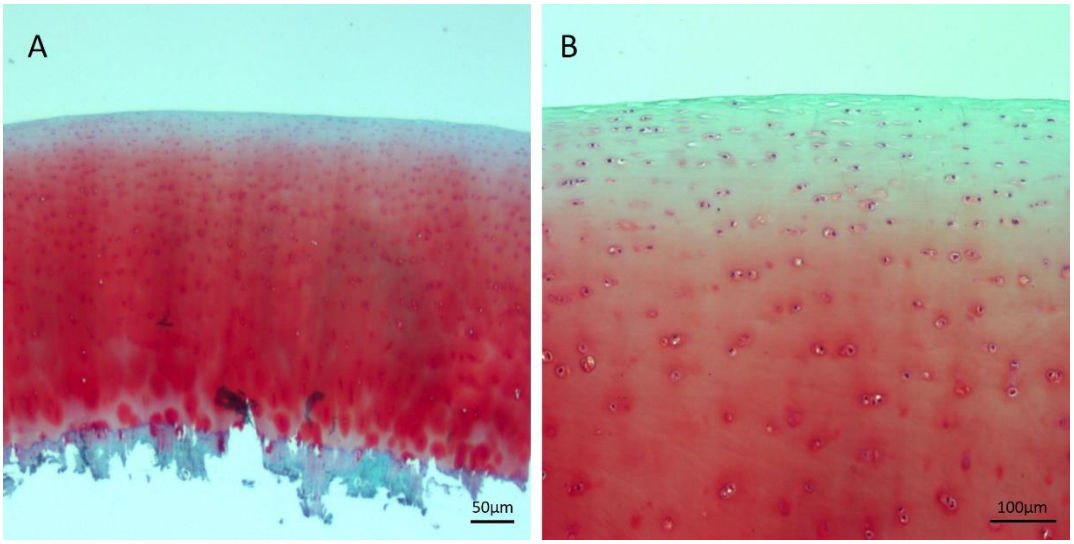

Figure 3.8. Microscopic Grade 0. Articular surface is intact and smooth. No significant loss of proteoglycans can be observed. Chondrocyte morphology and arrangement are normal. Original magnification 25x (A) and 100x (B).

The overall trend of changes in cartilage from Grade 1.0 to 4.5 is presented at lower magnification in **Figure 3.9**, showing vertical progression of degradation and obvious thinning. The higher magnification images (**Figure 3.10**) provide a detailed account of the microscopic features observed in these grades. Superficial fibrillation was observed in Grade 1.0 and 1.5, with the latter being more severe (**Figure 3.9A, B, Figure 3.10A, B**). Increased staining of

chondron was also present, indicating elevated local biosynthesis by chondrocytes. Floating fragments which reflect the loss of matrix can be observed in Grade 2.0 and 2.5 (**Figure 3.9C, D, Figure 3.10C, D**). The loss was within the upper SZ in Grade 2.0 and through the SZ at Grade 2.5. Moreover, depletion of proteoglycan developed into the MZ in Grade 2.0 and 2.5. In Grade 3.0, the SZ was almost entirely eroded and there was a simple unbranched fissure down to the upper 1/3 of MZ (**Figure 3.9E, Figure 3.10E**). In Grade 3.5, branched fissures down to the lower 2/3 of MZ were observed (**Figure 3.9F, Figure 3.10F**). In addition, large chondrocyte clusters containing more than 10 cells appeared around the fissures, and proteoglycan was lost in the lower MZ in Grade 3.0 and 3.5. In Grade 4.0, the MZ was completely degraded, with the interface between MZ and DZ becoming the articular surface (**Figure 3.9G, Figure 3.10G**). In Grade 4.5, upper half of the DZ was eroded and there was just a thin layer of cartilage left (**Figure 3.9H, Figure 3.10H**). The surface was jigsaw-like without fissures, and typical cell clusters were no longer visible (**Figure 3.10H**). Surprisingly, proteoglycans seemed to be relatively well preserved in the DZ in Grade 4.0 and 4.5, despite that the remaining cartilage was extremely thin.

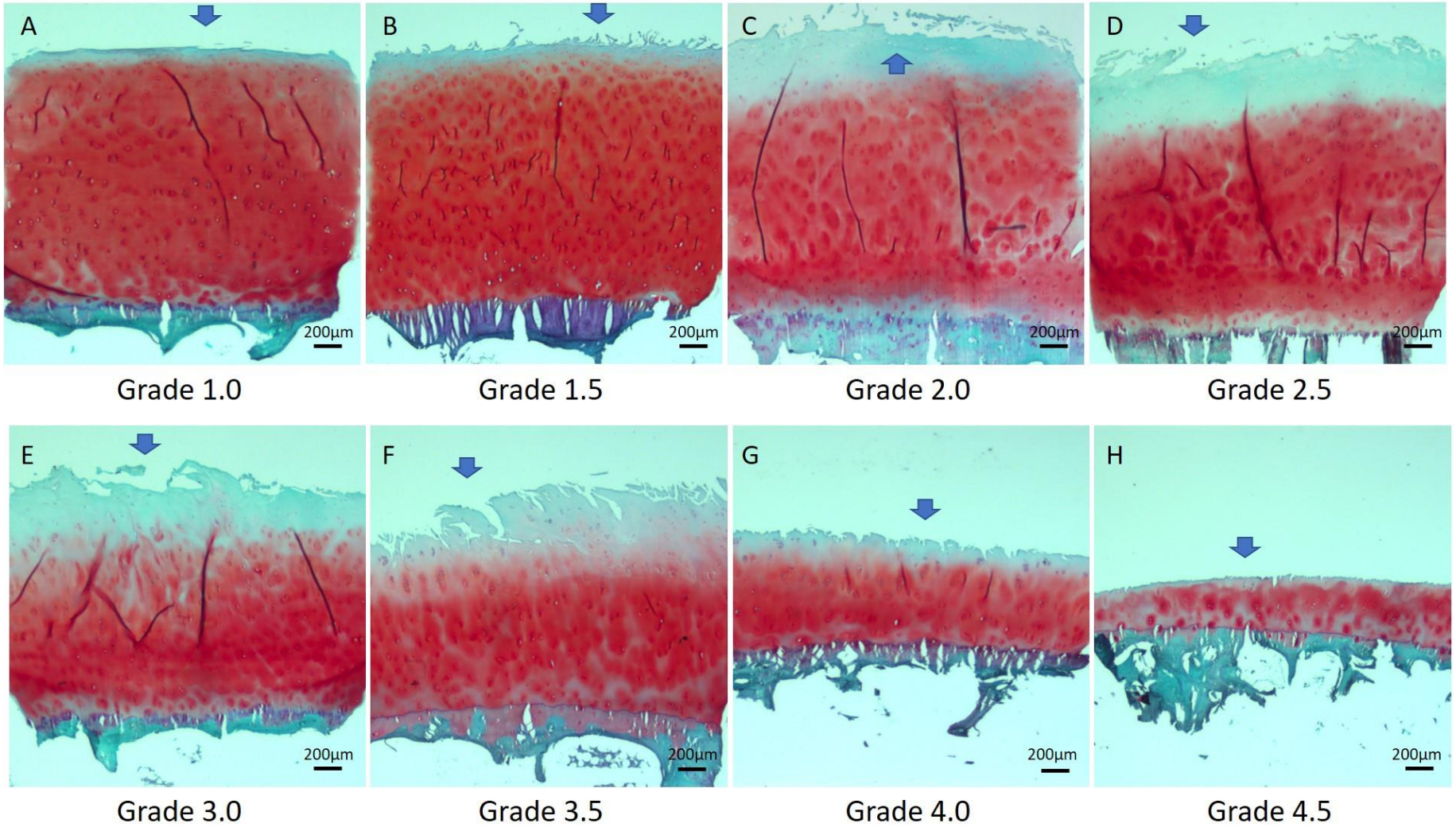

Figure 3.9. Images of microscopic Grade 1.0 to 4.5 at lower magnification. Images show the overall trend of changes in cartilage thickness and structure from Grade 1.0 to 4.5. Arrows point to areas shown at higher magnification in Figure 3.10. original magnification 25x.

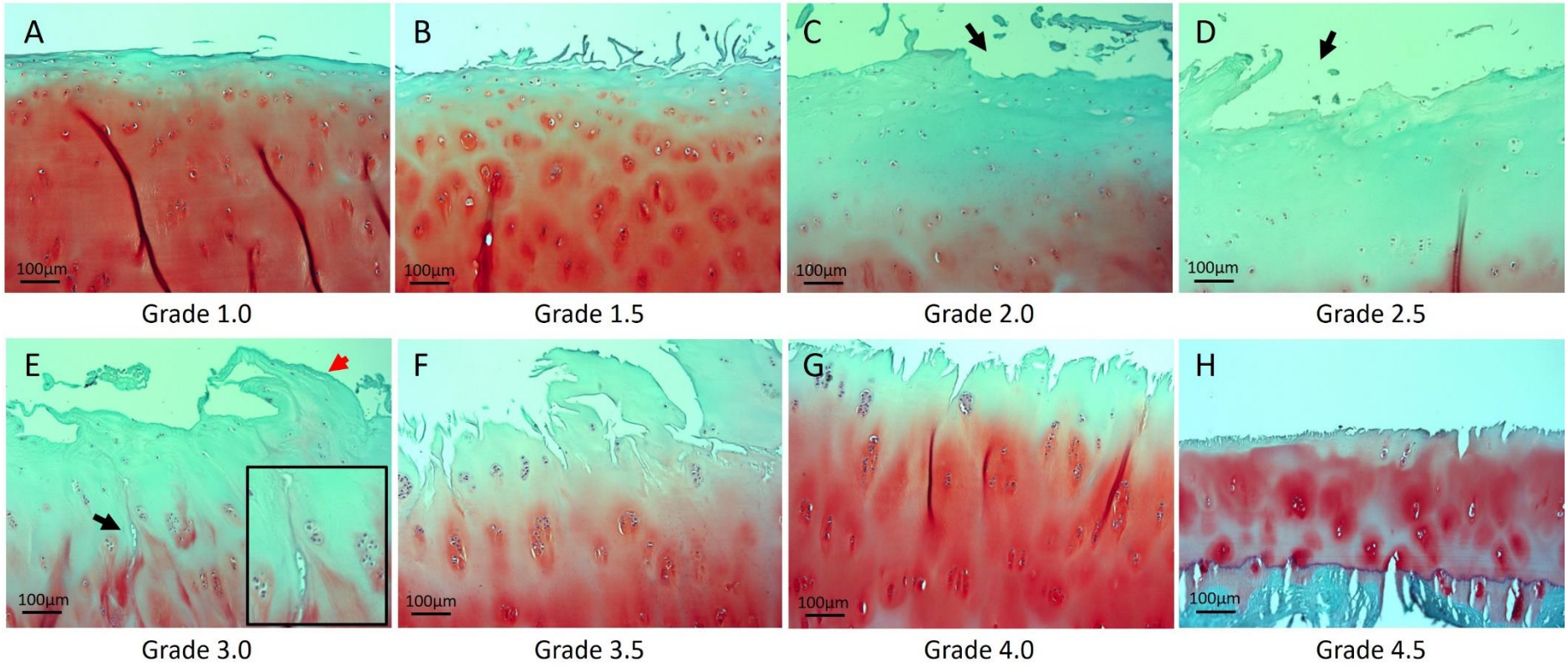

Figure 3.10. Higher magnification of microscopic Grade 1.0 to 4.5. Superficial fibrillation and increased chondron staining can be observed at Grade 1.0 (A) and 1.5 (B), with the latter being more obvious. Loss of matrix can be seen at Grade 2.0 (C) and 2.5 (D). The loss of matrix (black arrows) is within the upper superficial zone at Grade 2.0, and though the superficial zone at Grade 2.5. In Grade 3.0 (E), the superficial zone is eroded with only remnant fragments left (red arrow). A simple unbranched fissure extends to upper 1/3 of middle zone (black arrow with zoom-in view). Branched fissures reaching lower middle zone are characteristic of Grade 3.5 (F). Large chondrocyte clusters with more than ten cells occur around fissures in Grade 3.0 and 3.5 samples. With progression of cartilage erosion, the middle zone can hardly be observed at Grade 4.0 (G), and almost 50% of the deep zone is lost at Grade 4.5 (H). The articular surface becomes jigsaw-like. Classic chondrocyte clusters were not observed at Grade 4.5. Original magnification 100x.

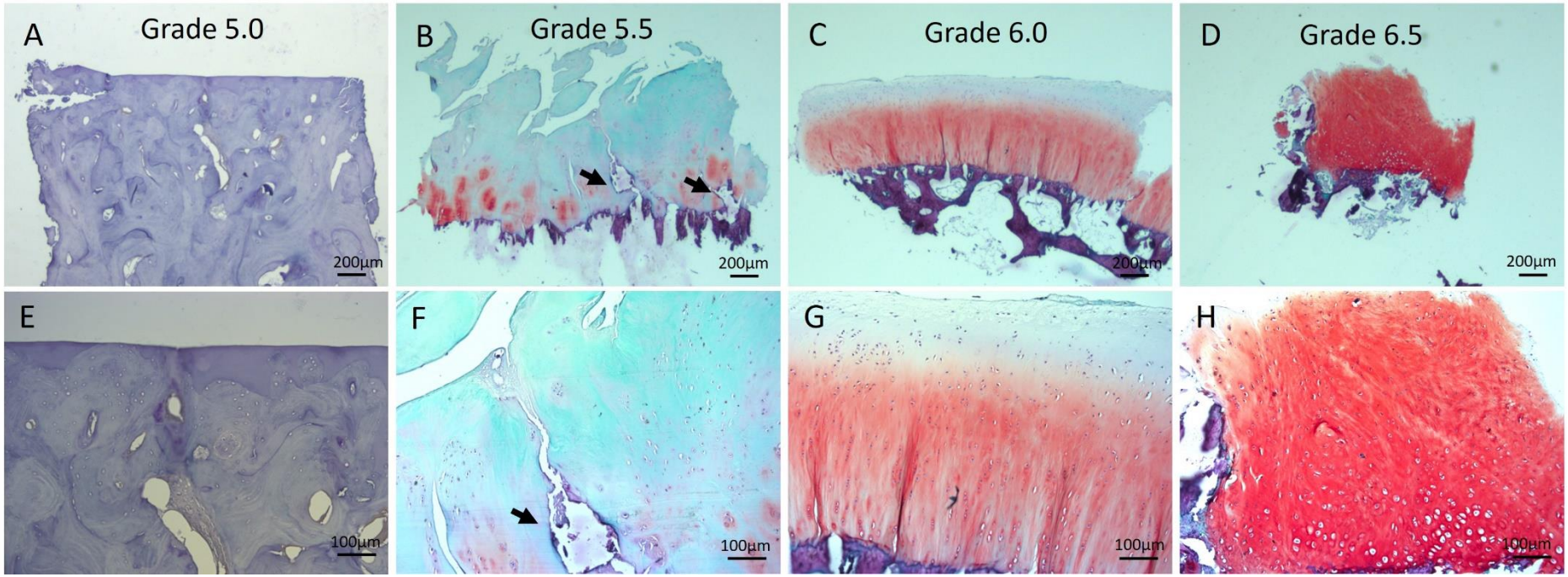

Figure 3.11. Microscopic Grade 5.0 to 6.5. Ordinary hyaline cartilage tissue was completely worn off at Grade 5.0 (A, E) and subchondral bone becomes the articular surface. Reparative cartilaginous tissue can be seen around bone microcracks (black arrows) at Grade 5.5 (B, F). Marginal and central osteophytes with fibrocartilage and hypertrophic chondrocytes can be seen in Grade 6.0 (C, G) and 6.5 (D, H), respectively. A-D, magnification 25x, E-H 100x. Note that A and E were decalcified because sectioning of bone when there is no cartilage left is not possible without decalcification.

Images of typical Grade 5.0 to 6.5 samples are shown in **Figure 3.11**. Ordinary cartilage tissue was completely worn off in Grade 5.0. The subchondral bone became the articular surface. There was reparative cartilaginous tissue growing around bone microcracks in Grade 5.5. Marginal and central osteophytes with fibrocartilage and hypertrophic chondrocytes can be seen in Grade 6.0 and 6.5, respectively. Note that Grade 5.0 to 6.5 samples were used only for demonstration of grading and were not included in the following analysis.

3.3.4 Reproducibility of macroscopic and microscopic grading

For microscopic grading, the ICCs and LOAs are given in **Table 3.1**. The inter-observer ICC between two PhD students Y Li and Y Liem was 0.946, which is 'excellent' as statistically defined (>0.900) by Koo (600) and meets the recommendations for observer performance in the evaluation of articular cartilage histopathology (>0.900) (578). The inter-observer ICCs for the medical student were lower, at 0.833 with Y Li and 0.869 with Y Liem, respectively, falling in the range of 'good' (600). The intra-observer ICCs were 0.950 for Y Li and 0.945 for Y Liem, again, meeting the requirements suggested by other investigators (578).

The means of intra-observer errors (differences between first and second readings) were negligible for Y Li (-0.086) and Y Liem (-0.015) compared to the 0.5 point scoring increment, showing no obvious systemic bias for both scorers. The intra-observer LOAs were between -0.939 and 0.768 for Y Li and between -0.975 and 0.940 for Y Liem, showing that 95% of errors were less than 1 point, similar to the results reported by experts in cartilage histopathology (578). Similarly, the inter-observer LOA (-0.955 to 0.965) and mean (0.005) of errors between Y Li and Y Liem were also excellent. However, the inter-observer differences for H Ahmed were greater (0.437 compared to Y Li and 0.384 compared to Y Liem, respectively), and the LOAs were wider (within 1.5 points).

The intra-observer (Y Li) ICC for macroscopic grading was 0.934 (95% confidence interval 0.887 – 0.961).

Table 3.1. Reproducibility of microscopic grading.

	Intraclass correlation coefficient		
	Y Li	Y Liem	H Ahmed
Y Li	0.950 (0.926, 0.966)	0.946 (0.933, 0.957)	0.833 (0.640, 0.909)
Y. Liem		0.945 (0.919, 0.963)	0.869 (0.710, 0.929)
	Limits of agreement		
	Y Li	Y Liem	H Ahmed
Y Li	-0.086 (-0.939, 0.768)	0.005 (-0.955, 0.965)	0.437 (-0.947, 1.821)
Y Liem		-0.015 (-0.975, 0.940)	0.384 (-0.854, 1.622)

Microscopic grading of slides was carried out twice by Y Li and Y Liem, and once by H Ahmed, to evaluate the intra- and inter-observer reproducibility. Intraclass correlation coefficients (ICCs) are given together with 95% confidence intervals. Limits of agreement (LOAs) are presented as the mean of the differences between two scores of the same slide (first and second scores from same observer, or scores from two observers), plus and minus 1.96*standard deviation.

3.3.5 Association between macro- and microscopic grading

The associations between microscopic and macroscopic gradings of samples are shown in **Figure 3.12**. The figure shows that the new macroscopic grading system reflects well the differences in cartilage histopathology assessed by the modified microscopic grading system. A significant and strong positive correlation was found between macro- and microscopic grading as shown by the Spearman's Rank Order test ($P<0.001$, correlation coefficient 0.936).

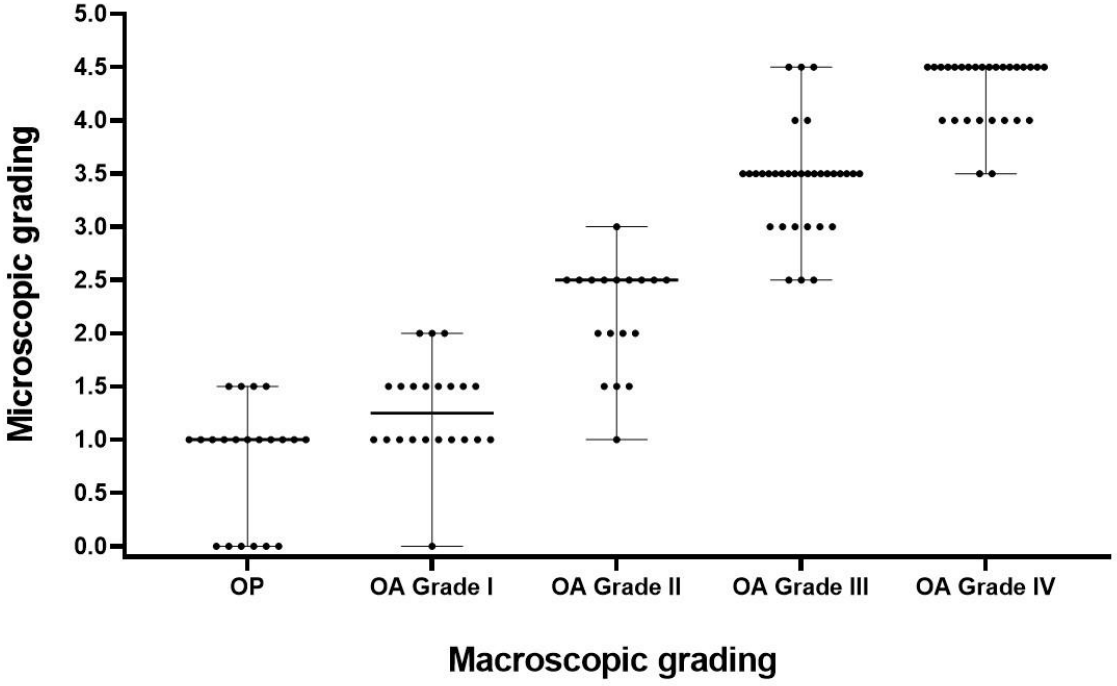

Figure 3.12. Association between the macro- and microscopic grading. The microscopic grading of each plug is plotted against its microscopic grading in OP and OA groups. Lines indicate median values and bars indicate min and max values.

3.4 DISCUSSION

In this chapter, we standardised a tissue collection procedure that covered and differentiated between samples at different stages of cartilage degradation in femoral heads with OA and OP. The procedure was based on a combination of reliable macro- and microscopic evaluations of cartilage pathology.

Competent histological preparation of tissue is the basis of accurate assessment of cartilage histopathology and is critical for immunohistochemical studies. The optimised histological processing and sectioning protocols developed here can be used to generate true full-thickness cartilage sections of high quality. This protocol helped avoid shaving of cartilage from subchondral bone which could cause loss and damage of the deepest area, thus maintaining the integrity of cartilage irrespective of the severity of degradation. This study has shown for the first time that even without decalcification, sectioning of osteochondral tissue without affecting cartilage histological quality is possible. Decalcification is a time-

consuming and laborious procedure and could compromise cell and matrix morphology and antigenicity (601, 602). It is also associated with significant depletion of proteoglycans by up to 70% (581). This is most obvious in cartilage with advanced degeneration. In this study, at Grade 4.0/4.5 when there was just a thin layer of the DZ left, the loss of Safranin O staining was significantly less compared to studies that utilised decalcification (323, 603). Such artefact could potentially jeopardise the evaluation of cartilage histopathology (578) as almost all scoring systems involve safranin O staining as a key parameter. The usage of the undecalcified osteochondral tissue sections for IHC study of collagenases and aggrecanases is presented in Chapter 6.

Histopathological evaluation of cartilage is a powerful tool in OA research as it provides a semi-quantitative measurement of disease severity and progression, which can be used to investigate disease mechanisms and assess effects of treatments. Currently, a number of scoring methods are available, of which the OARSI system is probably the most widely used. It has the advantage of being sensitive to early OA and has been proved to be a reliable replacement of the HHGS scheme (578, 579, 588). However, when applied to regionally collected samples, such as cartilage discs or osteochondral plugs/blocks with relatively small volume, significant inter-study variability has been observed (603, 604). To overcome this limitation of the OARSI grading module, in this project we modified the original scheme and developed a comprehensive template (from **Figure 3.8** to **Figure 3.11**) for grading cartilage degradation. In this template, important pathological features of OA in terms of cartilage surface and matrix structure, chondrocyte biology, and proteoglycan content can be clearly identified and differentiated between different grades with or without 0.5 sub-score. This is likely to be due to a clear description and stratification of changes in the vertical direction, i.e., extent of proteoglycan depletion, depth of fissures, and cartilage erosion from SZ to DZ. However, it should be noted that though examples of Grade 5.0 to 6.5 have been given, this modified grading system focused more on cartilage changes and was not optimised for a detailed evaluation of subchondral bone denudation when cartilage is completely lost.

Before any quantitative scoring scheme of OA histopathology can be adopted, its reproducibility should be investigated. For this purpose, three scorers were recruited in this study to evaluate the inter- and intra-observer ICCs and LOAs. Of these scorers, Y Li is a PhD

candidate who is familiar with both OA and cartilage histopathology, Y Liem is a PhD candidate who works with OA soluble biomarkers but has no experience with cartilage histopathology, while H Ahmed is an intercalating medical student who has no experience in OA research. It was shown that the inter-observer reliability was 'excellent' (ICC above 0.90) between Y Li and Y Liem, and was 'good' (above 0.800) for H Ahmed, according to the recommended criteria for general medical research (600) and criteria specific for OA histopathology (578). The intra-observer reliability was also 'excellent', for both Y Li and Y Liem. The ICCs and LOAs turned out to be as good as or even better than many other investigations of histopathological grading published in the literature (578, 579, 588, 589). These results suggest that the modified microscopic grading system reported here can be reproducibly adopted, and appears to be easy to learn and can be used by researchers with limited experience.

The new macroscopic grading method developed in this study also exhibited outstanding reliability, with an intra-observer ICC over 0.900. This is fairly good for a macroscopic evaluation mainly based on visual assessment, and better than the values reported for other macroscopic grading systems (596, 605). More importantly, the sensitivity of the new macroscopic grading for evaluation of cartilage pathology has been confirmed by the microscopic grading, as shown by the scatter plot and the close correlation between the two systems with a Spearman's correlation coefficient of 0.936. This data has important implications. First, the mutual validation between the two grading schemes proved that they are both reliable tools for the evaluation of cartilage degradation. Second, the tissue collection procedure adopted in this study generated a group of samples representing different stages of cartilage degradation, allowing the study to investigate subchondral bone and immunohistochemical features according to the disease severity in the following chapters. Future studies may carry out further validation against other existing macro- and microscopic grading methods or biochemical and mechanical properties of cartilage, to provide independent data on the application of these new grading systems for investigation of cartilage degradation.

In this study, to make clear contrast to samples with OA, we limited the selection of OP specimens to those with normal or comparatively normal (macroscopic Grade I) articular surfaces. However, microscopically, majority of OP samples exhibited features of early

cartilage degeneration (Grade 1.0 and 1.5) (**Figure 3.12**). These were treated as acceptable age-related changes. Therefore, no further differentiation within the OP group were made. As for the OA group, for simplicity and due to limited sample size, the advanced grading with 0.5 subgrades was generalised to Grade 1, 2, 3, and 4 based on **Table 2.3**. OA samples were then grouped according to the generalised microscopic grading for comparisons in the following chapters.

3.5 SUMMARY

In this chapter, results of experiments performed to develop a new macroscopic grading scheme for the initial examination of cartilage conditions on femoral heads collected from OA and OP patients were presented. Also, the OARSI microscopic grading system was optimised, to make it suitable for the histopathological evaluation of regionally collected samples with relatively small dimensions. Based on the reproducible and accurate assessment of cartilage degradation using the two grading schemes, we standardised a tissue extraction protocol that was able to collect osteochondral samples precisely representing various stages of cartilage degradation in OA and OP.

Chapter 4

Subchondral bone microarchitecture in hip OP and OA: a regional and compartmental comparison

4.1 INTRODUCTION

Clinical studies investigating the relationship between OP and OA are generally based on comparisons of BMD at systemic (femoral neck or vertebrae) or whole-joint levels using traditional measurements such as DXA. Though in general they show that OA is associated with higher bone density while patients with OP have lower risk of OA, careful interpretation of these results is needed to avoid bias in terms of study design and technical limitations, as discussed in **Section 1.7.1**. More importantly, these studies did not provide much information regarding the pathological mechanisms contrasting the two diseases because (i), changes at microscopic levels which can reflect the pattern of bone remodelling were not examined, and (ii), subchondral bone, which is the most significantly affected area in OA, was not targeted.

There have been a few studies comparing microscopic properties of subchondral bone between OP and OA using femoral heads excised during THA surgeries for femoral neck fracture and hip OA (606-609). Typically, these studies collected subchondral bone samples from a fixed anatomical site (superior) assuming that the loading pattern of hip joint is universal across the population. Also, they only included end-stage OA samples that displayed severe or complete cartilage erosion at the site; a detailed histopathological evaluation of cartilage degeneration was missing. Inevitably and expectably, they came to the conclusion that subchondral bone is subjected to opposite pathological processes in OP and OA (606-609).

However, numerous studies on knee OA specimens have revealed a spatial coupling between pathology of subchondral bone and cartilage – microarchitecture of subchondral bone is heterogeneously distributed within the joint and varied with local degeneration severity of the overlying cartilage (381, 450, 567-572, 610). This is easy to understand as cartilage and

subchondral bone act in a complementary manner in the transmission of load and there is a mutual biomechanical adaption between them (165, 166). Failure of one tissue will inevitably lead to failure of the other. Also, degradation of cartilage and remodelling of subchondral bone are accompanied with biochemical signals, including growth factors, cytokines and proteinases, that can communicate across the osteochondral unit, therefore synergising biological activities in the two neighbouring tissues (611). Considering that progression of OA is associated with worsening cartilage damage and that eventually cartilage will be completely depleted from the entire articulating surface (323), the cartilage-dependent spatial variation of subchondral bone can be used as an indication of temporal changes at various stages of OA (420, 426, 567, 568, 604). This is especially important for studies based on human subjects since longitudinal sample collection is not possible.

Surprisingly, a detailed regional variation of subchondral bone microarchitecture in relation to local cartilage degeneration has not been reported before for hip OA. A few studies that attempted to investigate the heterogeneity of hip OA subchondral bone microarchitecture often used a small number of samples and had a limited scope. For example, Ryan and co-workers explored the distribution of subchondral bone microarchitecture in six OA femoral heads as a function of the anatomical location but not the status of the overlying cartilage (612). Chappard et al reported the disparities in subchondral bone microarchitecture between regions covered and not covered by cartilage, but they did not carry out a histological evaluation and only looked at trabecular bone (426). Using histomorphometry, Jensen et al studied only the two-dimensional area fraction of subchondral trabecular bone with regard to the condition of the overlying cartilage (420).

Histomorphometry, based on methacrylate embedding and sectioning of tissue, is a classic experimental method to study bone biology. A major advantage is that it allows inspection of bone structure and ongoing remodelling at the same time, with the latter being evaluated by a set of specialised indices such as osteoid surface and eroded surface representing focal bone formation and resorption, respectively (97). However, a number of advanced morphometric parameters of bone, which are among the determinants of biomechanical properties, cannot be studied with histomorphometry due to its two-dimensional nature. MicroCT, by contrast,

provides a gold standard for three-dimensional measurement of bone microarchitecture in small animal models and biopsied human samples (613).

Therefore, based on histopathological evaluation of local cartilage degradation and microCT scanning, the aims and objectives of the experiments in this chapter are to:

(i), Explore the regional variations of subchondral bone microarchitecture, including both pate and trabecular bone, in hip OA in relation to degeneration stages of the overlying cartilage.

(ii), Compare subchondral bone microarchitecture in OP with that in different stages of OA.

4.2 MATERIALS AND METHODS

4.2.1 Patient selection

As plugs extracted from the optimisation OA cohort were exhausted by various testing procedures and the histology study, only the main study cohort together with seven OP specimens, were included in the microCT studies (see **Section 2.5**).

4.2.2 Macroscopic evaluation and osteochondral plugs extraction

Osteochondral plugs with 4mm diameter were extracted from OP and OA femoral heads using a steel hollow punch as described in **Section 2.5**. Briefly, for OP group, plugs (N=21) were collected from three anatomical sites: superior, posterior and anterior. For OA group, plugs (N=56) were collected from different macroscopically graded regions on each femoral head (Grade I to Grade IV). Grade V plugs were not included as explained previously. The subchondral bone of plugs was preserved with a length of 8-10mm. Plugs were snap-frozen and stored at -80 °C until scanning.

4.2.3 Micro CT scanning

Plugs were transported to the University of Sheffield for MicroCT scanning. Settings of scan can be found in **Section 2.10**. Reconstructed image datasets were then imported into the CT Analyzer software (CTAn) for processing and analysis.

4.2.4 MicroCT Image processing

A global threshold of greyscale CT value (60-255) was used for binarization of images to differentiate between bone and soft tissues including marrow and cartilage (**Figure 4.1C, D**). Noises and isolated particles were removed by the Despeckle function of the CTAn. A primary cylindrical region of interest (ROI) with 3.0mm diameter and 4.0mm depth was selected in the centre of plugs to exclude potentially cracked edge caused by punching during tissue extraction (**Figure 4.1A**, **B**).

This preliminary ROI was then segmented into ROIs of subchondral plate and trabecular bone using a custom developed semi-automated method with the aid of CTAn. Specifically, the 'narrowing points' where trabeculae started to stretch out from the bottom of subchondral plate were manually identified and lined up (**Figure 4.1B**). The drawing was repeated on every 3-5 slices depending on the variation. The lines between slices were automatically interpolated. The dataset above this line was further contoured by the Shrink-Wrap function of CTAn to remove redundant image areas, marrow space and cartilage, creating the subchondral plate ROI (**Figure 4.1C, E, G**). The dataset beneath this line constituted the trabecular ROI, with redundant image areas removed by Shrink-Wrap (**Figure 4.1D, F, H**). The resulted ROIs were visually checked on each dataset to ensure close representation of the subchondral bone compartments. To evaluate the reliability of the ROI selection and segmentation protocol, the above procedure, from selection of the preliminary ROI to generation of the compartmental ROIs, was repeated with 8 weeks' interval on all datasets. Three-dimensional images were created by the Amira software (2020.1, Thermo Scientific, USA).

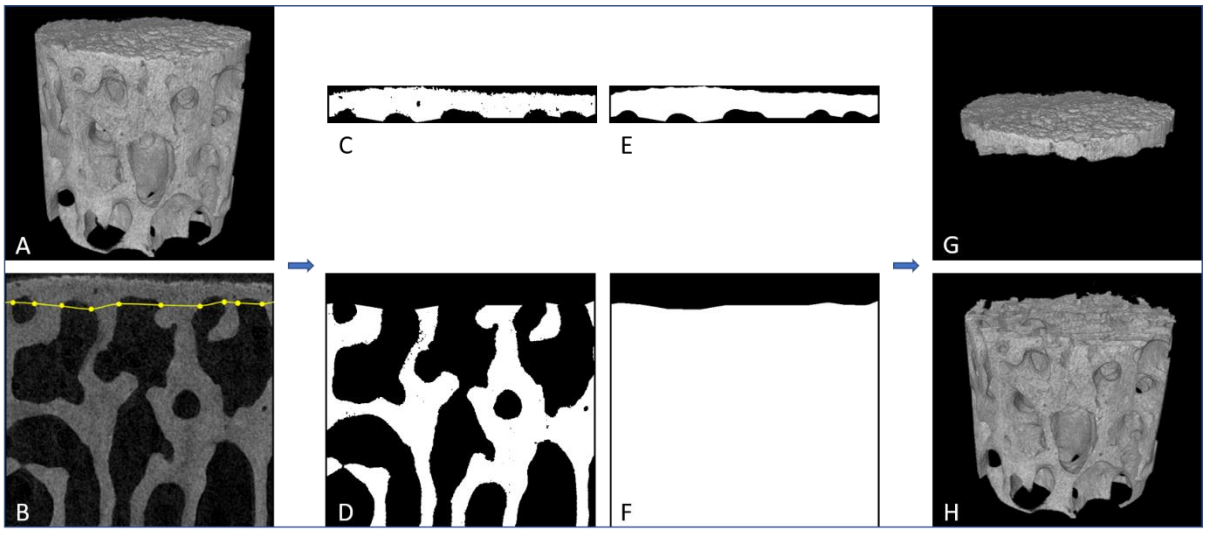

Figure 4.1. Selection of regions of interest on microCT image dataset. A primary cylindrical ROI (A) with 3.0mm diameter and 4.0mm depth was selected in the centre of plugs. In the cylindrical primary ROI, the 'narrowing points' where trabeculae start to stretch out from the bottom of subchondral plate were manually identified and lined up (B). The dataset above this line (C) was further contoured by the Shrink-Wrap function of the CT Analyser software to create the subchondral plate ROI (E and G). The dataset beneath the line (D) constituted the trabecular bone ROI (F and H).

4.2.5 Microarchitecture analysis

Microarchitecture of subchondral plate and trabecular bone were analysed automatically within the corresponding ROIs using CTAn. Algorithm of measurements was described in the Skyscan handbook and summarised by an established guideline (613). For trabecular bone, bone volume fraction (volume of bone tissue divided by total volume of ROI including bone and marrow space, BV/TV) and specific bone surface (bone surface/bone volume, BS/BV) were calculated based on the volumetric marching cubes model. Trabecular thickness (Tb.Th), trabecular separation (Tb.Sp), and trabecular number (Tb.N) were calculated based on the sphere-fitting method. Structural model index (SMI) was measured based on dilation of the three-dimensional voxel model. It ranges from 0 to 3 to describe the shape of trabeculae, with 0 indicating pure rod while 3 indicating ideal plate model. However, it may become a negative value in the situation of high BV/TV. The connectivity of trabecular bone was estimated by connectivity density (Conn.Dn), which was measured as the Euler number per tissue volume.

For subchondral plate, plate thickness (Pl.Th) was calculated by applying the sphere-fitting method to the contour of subchondral plate ROI. Total porosity (Pl.Po) was calculated as volume of pores per volume of the plate ROI**.**

4.2.6 Histology and microscopic grading

After microCT scanning, without trimming of subchondral bone, plugs were decalcified and processed for paraffin embedding and sectioning, as described in **Section 2.6.2**. The osteochondral plugs scanned by microCT had been through multiple freezing-thawing circles and lengthy decalcifying procedure. However, the histological quality of the tissue sections remained sufficiently good for histopathological evaluation. Duplicated slides from each plug were stained with safranin O – fast green as in **Section 2.7**. Microscopic severity of cartilage degradation was scored using the modified OARSI grading system. For this batch of samples, only two examiners (Y Li and Y Liem) were involved. Blinded to sample origins and macroscopic grades, they scored all slides independently using advanced grading with 0.5 subgrades. Final microscopic grade for each plug was obtained by averaging and rounding scores between the two examiners.

4.2.7 Statistical analysis

Since osteochondral plugs were collected based on the condition of the overlying cartilage and the research aimed to investigate how cartilage degeneration was related to changes in subchondral bone, independence of samples was assumed in this study. Comparisons of microarchitectural parameters were first made between microscopic grades within OA group to verify the variations in relation to the severity of cartilage degeneration, using one-way ANOVA (followed by Bonferroni test) for parametric data and Kruskal-Wallis (K-W) test (followed by Dunn's test) for non-parametric data, respectively. These tests were then repeated to include the OP group and compare OP with different microscopic grades of OA.

4.3 RESULTS

4.3.1 Compartmental segmentation

Reliability of the protocol for segmentation between subchondral plate and trabecular bone on microCT datasets was evaluated by repeating the contouring (lining) procedure and comparing between the initial and repeated measurements of subchondral plate thickness and trabecular bone volume fraction. The calculated ICC was 0.971 for BV/TV and 0.949 for Pl.Th, respectively, indicating excellent consistency of the compartmental ROI segmentation.

4.3.2 Microscopic evaluation

The inter-observer ICC for microscopic grading of this batch of samples was 0.967, as good as the value reported in Chapter 3, indicating excellent agreement between the two observers. As discussed in Chapter 3, in the following comparisons of bone microarchitecture, for simplicity and due to limited sample size, the advanced grading of OA plugs was generalised to Grade 1, 2, 3, and 4 according to **Table 2.3**. In addition, the advanced grading of OP plugs ranged from 0 – 1.5, and 1 – 1.5 were treated as acceptable age-related minor degeneration. Therefore, the data from the OP group were pooled without further differentiation.

4.3.3 Microarchitecture of subchondral trabecular bone

Representative three-dimensional microCT images of samples from OP and each OA grade and the corresponding safranin O stained tissue sections are shown in **Figure 4.2**. Microarchitectural parameters of subchondral trabecular bone and results of analysis of variance are summarised in **Table 4.1**. Between-group comparisons are depicted in **Figure 4.3** to **Figure 4.5**. Overall, a significant regional variation of subchondral bone microarchitecture in relation to the degree of cartilage degradation in OA group was found, except for Tb.Sp. Data for the OP group were generally similar to early OA but different from advanced OA.

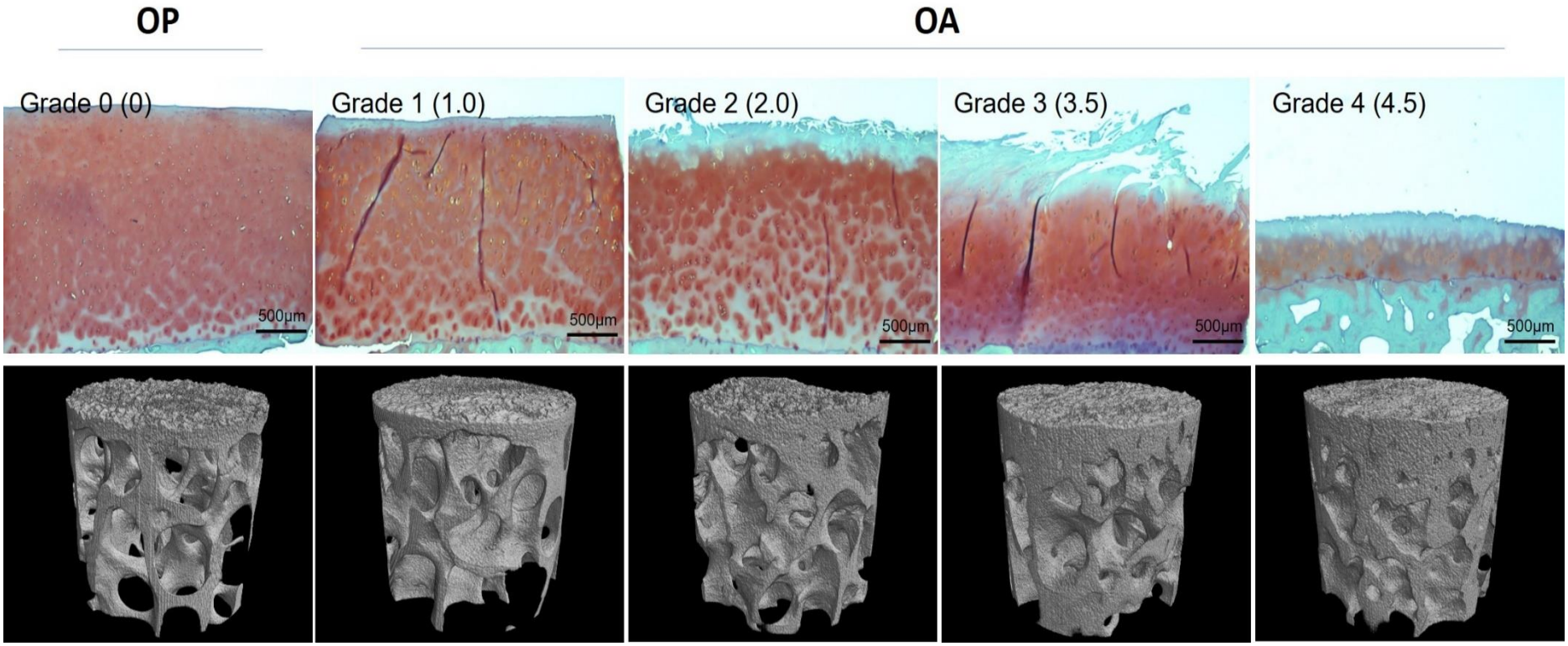

Figure 4.2. Representative tissues sections stained with safranin O, and the corresponding three-dimensional microCT images of OP and OA samples. Both generalised grading and advanced grading (values in bracket) are given.

Table 4.1. Analysis of variance of subchondral trabecular bone microarchitecture in relation to severity of cartilage degeneration in OA and OP.

	OP (N=21)	OA Grade 1 (N=14)	OA Grade 2 (N=12)	OA Grade 3 (N=14)	OA Grade 4 (N=16)	P Value (OA Grades only)	P Value (OP and OA Grades)
BV/TV (%)	25.64±6.24	22.04±8.81	27.32±7.19	35.93±7.95	39.06±10	<0.001	<0.001
BS/BV (mm-1)	20.64±3.46	23.34±4.00	21.93±3.23	17.97±2.25	17.40±3.41	<0.001	<0.001
Tb.Th (mm)	0.18±0.03	0.16±0.03	0.17±0.03	0.20±0.03	0.22±0.04	<0.001	<0.001
Tb.N (mm^{-1})	1.40±0.27	1.37±0.45	1.64±0.41	1.75±0.29	1.81±0.28	0.009	<0.001
Tb.Sp (mm)	0.55±0.08	0.58±0.13	0.50±0.12	0.50±0.10	0.46±0.08	0.052	0.024
SMI (-)	1.31±0.22	1.27±0.42	1.13±0.37	0.37±0.79	0.05±1.32	<0.001	<0.001
Conn.Dn (mm^{-3})	2.25±1.28	2.42±1.33	3.73±1.89	4.26±1.90	5.93±2.49	<0.001	<0.001

Values are presented as mean ± SD. One-way ANOVA was used for parametric data and Kruskal-Wallis test was used for non-parametric data (SMI and Conn.Dn). Analysis was first made between OA Grades to examine the variations in relation to the severity of OA. Then the tests were repeated to include the OP group to compare OP with different OA Grades.

4.3.3.1 Basic volumetric parameters

There was a significant increase in BV/TV with the increasing severity of cartilage degradation in OA (ANOVA, P<0.001) (**Table 4.1**). BV/TV at OA Grade 1 was significantly lower than at Grade 3 and 4 (Bonferroni test, both P<0.001), while that at Grade 2 was significantly lower than at Grade 4 (Bonferroni test, P<0.05) (**Figure 4.3A**). When the OP group was included in the analysis, it was shown that OP had a BV/TV similar to OA Grade 1 and 2, but significantly lower than OA Grade 3 and 4 (Bonferroni test, P<0.05, P<0.001, respectively) (**Figure 4.3A**).

BS/BV demonstrated an inverse trend in OA against that seen for BV/TV. BS/BV reduced as cartilage damages became more evident (ANOVA, P<0.001) (**Table 4.1**). The values for OA Grade 1 and 2 were significantly higher than for OA Grade 3 and 4 (Bonferroni test, Grade 1 *vs* Grade 3: P<0.001; Grade 1 *vs* Grade 4: P<0.001; Grade 2 *vs* Grade 3: P<0.05; Grade 2 *vs*

Grade 4: P<0.05) (**Figure 4.3B**). BS/BV of the OP group was higher than advanced OA and but was statistically significant for Grade 4 only (Bonferroni test, P<0.05) (**Figure 4.3B**).

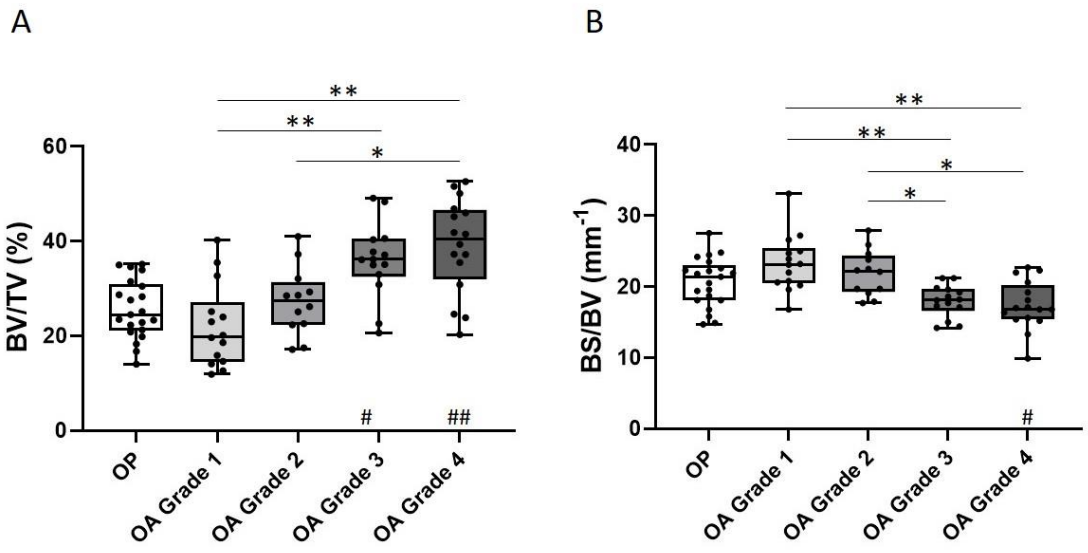

Figure 4.3. Comparisons of basic volumetric parameters of subchondral trabecular bone in relation to severity of OA cartilage degeneration. The boxplot shows the median, the interquartile range (IQR), and individual values. Statistical significance is indicated by * or # for multiple comparisons between OA Grades, and between OP and OA Grades, respectively, according to post-hoc tests. *P < 0.05; **P < 0.001; the same for #.

4.3.3.2 Basic morphological parameters

Both Tb.Th and Tb.N exhibited an increasing trend in the OA group toward more severe cartilage degradation (ANOVA, P<0.001 and P<0.05, respectively) (**Table 4.1**). Specifically, trabecular bone with Grade 1 degeneration of the overlying cartilage had significantly thinner trabeculae compared with Grade 3 and Grade 4 (Bonferroni test, P<0.001 and P<0.05, respectively). Meanwhile, OA Grade 2 had significantly thinner subchondral trabecular bone compared to Grade 4 only (Bonferroni test, P<0.05) (**Figure 4.4A**). The number of trabeculae in OA Grade 1 was significantly greater than in Grade 3 and Grade 4 (Bonferroni test, both P<0.05), but there was not statistically significant difference between Grade 2 and advanced OA (Grade 3 and Grade 4) (**Figure 4.4B**). In contrast to Tb.Th and Tb.N, there was a decreasing

trend in Tb.Sp toward greater local OA severity, though the trend was not statistically significant (ANOVA, P=0.052) (**Table 4.1**). No significant difference in Tb.Sp was found between different OA Grades (Bonferroni test, P>0.05 for all pairs) (**Figure 4.4C**).

When the OA groups were compared with OP, Bonferroni post-hoc tests showed that Tb.Th and Tb.N were not statistically different between OP and early OA (Grade 1 and 2). However, the value of Tb.Th in OP was significantly lower compared with OA Grade 4 (Bonferroni test, P<0.05), and the value of Tb.N in OP was significantly smaller compared with both OA Grade 3 and Grade 4 (Bonferroni test, both P<0.05) (**Figure 4.4A, B**). By contrast, Tb.Sp was not significantly different between OP and all OA grades (Bonferroni test, P>0.05 for OP *vs* OA Grade 1, 2, 3, and 4) (**Figure 4.4C**).

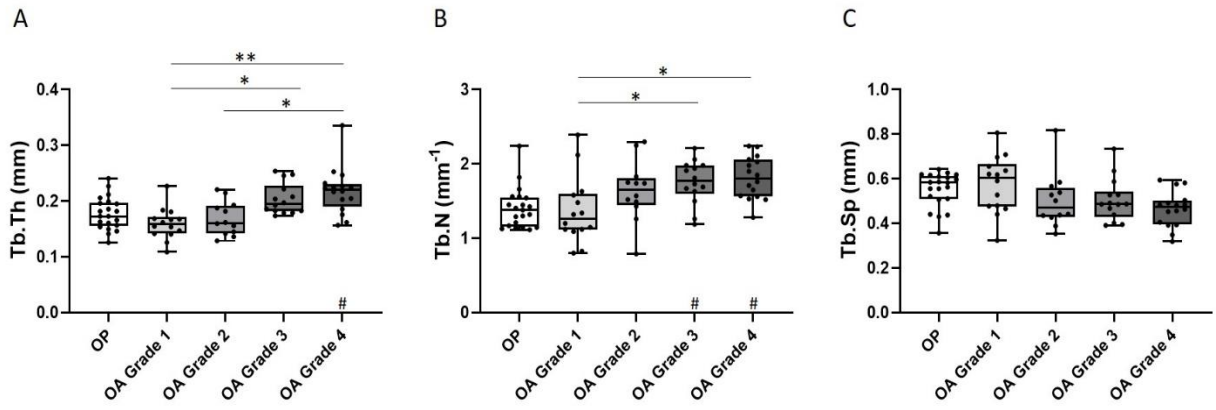

Figure 4.4. Comparisons of basic morphological parameters of subchondral trabecular bone in relation to severity of OA cartilage degeneration. The boxplot shows the median, the interquartile range (IQR), and individual values. Statistical significance is indicated by * or # for multiple comparisons between OA Grades, and between OP and OA Grades, respectively, according to post-hoc tests. *P < 0.05; **P < 0.001; the same for #.

4.3.3.3 Advanced morphological parameters

With regional progression of disease, subchondral trabeculae became more plate-like in OA, as shown by a decreasing SMI (K-W test, P<0.001) (**Table 4.1**). The values for OA Grade 1 and Grade 2 were both significantly greater than that for OA Grade 4 (Dunn's test, P<0.001 and

P<0.05, respectively), while only in Grade 1 SMI was higher than in Grade 3 (Dunn's test, P<0.05) (**Figure 4.5A**). Subchondral trabeculae in OP were more rod-like at a level similar to OA Grade 1 and 2, and was significantly different from OA Grade 3 and 4 (Dunn's test, both P<0.001) (**Figure 4.5A**).

The subchondral trabeculae in advanced OA were better connected compared with those in early OA, with a significant increase in Conn.Dn toward worse degeneration of the overlying cartilage (K-W test, P<0.001) (**Table 4.1**). However, the pairwise comparison within OA group was statistically significant only between Grade 1 and Grade 4 (Dunn's test, P<0.001) (**Figure 4.5B**). In line with most of the above-mentioned parameters, Conn.Dn in the OP group was similar to that in OA Grade 1 and 2, but was significantly lower compared with that in OA Grade 3 and 4 (Dunn's test, P<0.05 and P<0.001, respectively) (**Figure 4.5B**).

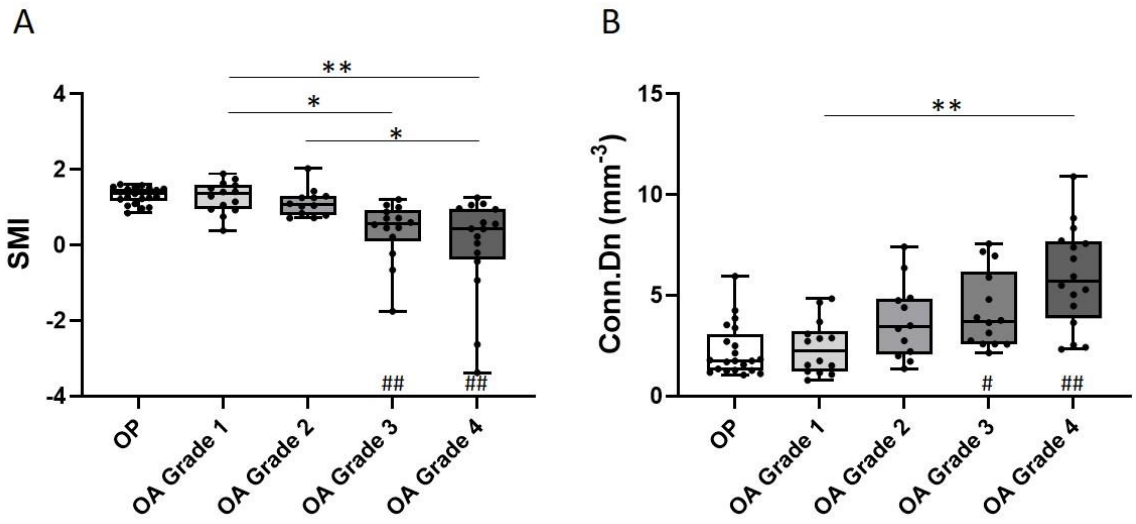

Figure 4.5. Comparisons of advanced morphological parameters of subchondral trabecular bone in relation to severity of OA cartilage degeneration. The boxplot shows the median, the interquartile range (IQR), and individual values. Statistical significance is indicated by * or # for multiple comparisons between OA Grades, and between OP and OA Grades, respectively, according to post-hoc tests. *P < 0.05; **P < 0.001; the same for #.

4.3.4 Microarchitecture of subchondral plate

Data for the microarchitectural parameters of subchondral plate and results of comparisons are summarised in **Table 4.2**. Subchondral bone plate became thicker with the progression of cartilage degeneration in OA, and the trend was statistically significant (ANOVA, P<0.001). Post-hoc comparisons showed that Pl.Th in OA Grade 1 was significantly lower compared to advanced OA (Bonferroni test, P<0.05 for both Grade 3 and 4), while the difference between Grade 2 and advanced OA (Grade 3 and 4) was not statistically significant (**Figure 4.6A**). In addition, the OP group had a significantly thinner subchondral plate compared to OA Grade 2, Grade 3 and Grade 4 (Bonferroni test, P<0.05, P< 0.001, P<0.001, respectively) (**Figure 4.6A**). In contrast, no obvious pattern was seen for the porosity of subchondral plate in OA (ANOVA, P=0.974) (**Table 4.2**). Statistical comparisons did not reveal any significant difference for Pl.Po between different OA grades or between OP and OA grades (Bonferroni test, P>0.05 for all pairwise comparisons) (**Figure 4.6B**).

Table 4.2. Analysis of variance of subchondral plate microarchitecture in relation to severity of cartilage degeneration in OA and OP.

	OP (N=21)	OA Grade 1 (N=14)	OA Grade 2 (N=12)	OA Grade 3 (N=14)	OA Grade 4 (N=16)	P Value (OA Grades only)	P Value (OP and OA Grades)
Pl.Th (mm)	0.26±0.04	0.29±0.06	0.33±0.06	0.39±0.09	0.42±0.11	<0.001	<0.001
Pl.Po (%)	9.75±3.11	8.72±2.20	8.57±2.43	8.79±2.32	8.41±2.65	0.974	0.554

Values are presented as mean ± SD. One-way ANOVA was used as the data are parametric. Analysis was first made between OA Grades to examine the variations in relation to the severity of OA. Then the tests were repeated to include the OP group to compare OP with different OA Grades.

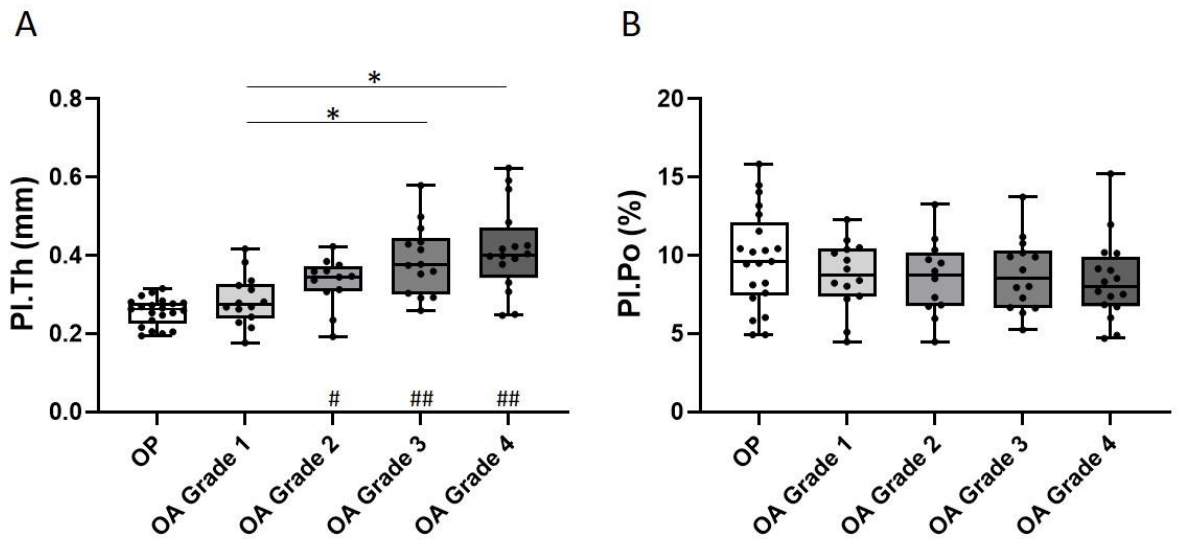

Figure 4.6. Comparisons of microarchitecture of subchondral plate in relation to severity of OA cartilage degeneration. The boxplot shows the median, the interquartile range (IQR), and individual values. Statistical significance is indicated by * or # for multiple comparisons between OA Grades, and between OP and OA Grades, respectively, according to post-hoc tests. *P < 0.05; **P < 0.001; the same for #.

4.4 DISCUSSION

Segmentation between cortical and trabecular bone on microCT-derived images has been reported and standardised mostly for vertebrae and diaphysis of long bone (614-616), which are enclosed environment easier to delineate using automated algorithm. For subchondral bone in both human specimens and animal joints, contouring methods to separate subchondral plate from trabecular bone varied among different studies and have generally been subjective and vague (378, 617). No standardised protocol is available. Based on a custom designed contouring method, Wen et al reported a porosity of subchondral plate in human tibia up to 70%, which is somewhat unreasonable and does not meet the general definition of compact bone (45, 618). This may be due to that part of the marrow space beneath subchondral plate was unnecessarily included and interpreted as intra-plate pores. The semi-automated protocol developed for the current study overcame this issue by combining manual delineation with a built-in algorithm of the CTAn (the shrink-wrap function)

which can remove redundant image spaces automatically. Segmentation between subchondral plate and trabecular bone using this protocol was accurate (**Figure 4.1**) and exhibited good reproducibility in this study.

The experiments in this chapter are the first to comprehensively investigate the regional variations of subchondral bone three-dimensional microarchitecture as a function of local cartilage degeneration in hip OA. Also, this study is the first to compare the microarchitecture of subchondral bone in OP with those in OA across various stages of cartilage degeneration. The results show that majority of the parameters tested for OA subchondral plate and trabecular bone varied with the condition of the overlying cartilage. These parameters in OP were similar to regions with early but different from regions with advanced cartilage degeneration in OA.

As in tibial plateaus affected by OA (566-568, 570, 610), volumetrically denser trabecular bone, represented by higher BV/TV, and thicker subchondral plate were present in regions with more severe cartilage degeneration but not where cartilage is still relatively preserved in OA femoral head. This is consistent with the findings that late-stage OA is associated with increased bone formation outweighing resorption, leading to subchondral sclerosis (161, 619). The changes in BV/TV of trabecular bone can be explained by the variations in three basic parameters (Th.Th, Tb.N and Tb.Sp) describing the morphological features of trabeculae. Unlike BV/TV, data for the latter parameters have been more complicated and inconsistent in the literature. Using histomorphometry, Bobinac et al reported that increased bone volume fraction in regions with severe cartilage degradation in knee OA was caused by thicker trabeculae that are less in number and closer to each other (568). Using microCT based three-dimensional measurements, one recent study showed that only increased Tb.N was accountable for the hypervolume of subchondral trabecular bone seen with more severe cartilage degradation in knee OA (570), whereas another study showed that thicker, closer and increased number of trabeculae were all responsible (567). Data presented in this chapter revealed a different pattern – Tb.Th and Tb.N increased significantly with the microscopic grading of cartilage in hip OA but the decrease in Tb.Sp was non-significant. The contradictory results are possibly due to the locations of extracted samples, cartilage grading variabilities, measuring techniques and settings, and varying sample sizes across different studies.

Except for basic trabecular morphology, mechanical properties of trabecular bone are also related to the shape and connectivity of trabeculae. Plate-shaped and well-connected trabecular network provides stronger support than rod-like perforated trabeculae (**Figure 1.5**) (49, 620). Progression of OA has been reported to be accompanied by a decrease in SMI and an increase in Conn.Dn in subchondral bone of both human and animal models (377, 378, 381). Moreover, these two parameters correlate significantly (negatively and positively, respectively) with the severity of focal cartilage degradation in OA knees, (49, 567, 570). Such correlations have been confirmed in hip OA by data presented in this chapter, indicating an architecturally strengthened subchondral trabecular bone at late stage of OA.

During progression of OA, elevated subchondral bone remodelling is associated with increased vascular invasion and microcracks at osteochondral junction, which together lead to increased porosity of subchondral plate (166, 463). This has been well documented in both spontaneous and induced animal models (378, 389, 391, 394). *In vivo* study of plate porosity in human is technically not possible and results generated from *ex vivo* studies have been scarce and conflicting. Chu and co-workers reported that there was not a significant difference between OA and healthy control (621) while Wen et al found more porous subchondral plate beneath severely damaged cartilage (617). Data presented here, however, are in agreement with a previous study of OA knees (450), showing no correlation between cartilage degradation and total porosity of subchondral plate. Future studies may utilise more advanced imaging techniques to differentiate between open (penetrating vascular channels and cracks) and closed porosity (intra-plate pores and canals).

Overall, the changes in subchondral plate and trabecular bone microarchitecture in advanced OA, which outweigh the effects of decreased mineralisation (see Chapter 5), point to a stiffened structure with dampened capability of absorbing and dispatching stress. This corresponds and coexists with the degradation and compromised mechanical properties of the overlying cartilage, reflecting an abnormal and disrupted mutual adaption between the two tissues under disease condition. However, a cause-effect relationship between subchondral sclerosis and severe cartilage damage cannot be established in this study, as they presented concurrently.

For trabecular and cortical bone microarchitecture in OP, studies were almost exclusively restricted to femoral neck, vertebrae and ilium. In these locations, cortical bone becomes increasingly thinner and more porous (618, 622). Lower BV/TV, thinner, lesser and widely spaced trabeculae compared with control were also found, despite some extent of variation between genders and at different phases of disease (618, 623-626). In addition, trabeculae become more rod-shaped and less well connected in OP, the same as in normal ageing process, rendering bone less capable of coping with mechanical stress and potentiating risk of bone failure (618, 626, 627). However, data specific for the changes in subchondral bone microarchitecture in OP are rare.

In terms of comparison between OP and OA, subchondral trabecular samples collected from a fixed site (superior) of femoral heads without accounting for cartilage degeneration exhibited denser, thicker, more plate-like and better connected trabeculae in OA than in OP, while the data for Tb.N and Tb.Sp have been inconsistent between studies (607-609). By grouping OA samples according to cartilage histopathological grading, the present project additionally demonstrated how subchondral bone properties at different stages of cartilage degeneration are related to those in OP. It was shown that at Grade 1 and Grade 2 of OA, all architectural parameters of subchondral trabecular bone were not significantly different from those in OP, indicating that in these regions there may exist unbalanced bone remodelling toward resorption. This imbalance was reversed in Grade 3 and Grade 4 toward bone formation and sclerosis, as discussed above. It is worth noting that the difference in Pl.Th between OP and OA was already significant from OA Grade 2, which supports the view that in non-traumatic type of OA the changes in subchondral plate are faster than and precede those in trabecular bone, and interact more closely with cartilage degeneration (165, 376, 628-630). In any case, the presence of osteoporosis-like subchondral bone beneath cartilage with relatively less degenerative changes does not support that subchondral sclerosis is responsible for the initiation and early changes of OA.

Based on the quantitatively and morphologically similar subchondral plate and trabecular bone structure, it may be reasonable to speculate that the unbalanced remodelling favouring resorption in subchondral bone at early stage of cartilage degeneration in OA is as severe as in the subchondral bone of OP patients, and probably has the similar pattern. This hypothesis

can be directly tested by comparing cell biology and remodelling status between OP and different stages of OA. Indeed, differing phenotypes of subchondral osteoblasts (i.e., high and low osteoblasts) have already been identified between OA patients (see **Section 1.6.2.2**) (421-423), as well as between sclerotic and non-sclerotic regions of the same OA joint (631-633). These phenotypic changes may reflect the temporal alternations in osteoblast cell biology across the process of OA (422, 424). In addition, histomorphometry studies have revealed that the remodelling status in OA subchondral bone, measured by relative bone formation and resorption surfaces, also displayed stagewise variations as reflected by the heterogeneity in relation to local severity of cartilage degeneration (420). Thus, it may be useful to combine the approaches used in these studies and incorporate subchondral bone in OP to investigate the similarities and differences in cell biology and remodelling status between OP and different stages of OA. By doing so, the mechanism of subchondral bone remodelling that leads to excessive resorption at the early phase of OA can be better understood, and therefore the use of anti-OP drugs as DMOADs can be further supported and guided.

4.5 SUMMARY

In this chapter the heterogeneity of three-dimensional subchondral bone microarchitecture in relation to the local severity of cartilage degeneration has been reported for hip OA. It was shown that characteristic features of subchondral sclerosis, including thicker subchondral plate, volumetrically denser trabecular bone, and thicker, plate-like and well-connected trabeculae, were associated with advanced degradation of the overlying cartilage. In addition, subchondral bone in OP was compared with those in OA across various stages of cartilage degeneration. It was shown that subchondral plate and trabecular bone in OA samples with early cartilage damage were as porous as those in OP samples. These data provide evidence at microscopic level that at early stage of OA there is unbalanced subchondral bone remodelling toward resorption, probably in a similar pattern as in OP. The imbalanced remodelling appears to be reversed toward formation leading to subchondral sclerosis in advanced OA.

Chapter 5

Subchondral bone mineral densities in hip OP and OA and their associations with microarchitecture

5.1 INTRODUCTION

Mineralisation is another aspect of bone remodelling in addition to microarchitecture. As discussed in **Section 1.2.4**, degree of mineralisation is the primary determinant of bone mechanical properties at tissue/material level (the elastic modulus/stiffness/hardness of bone tissue itself) (380, 431, 634, 635). A combination of the degree of mineralisation, the quantity of bone present, and the characteristics of bone morphology together explains the biomechanical properties of bone at apparent level (the elastic modulus or strength of an entire bone specimen) (380, 591).

There are two terms that are frequently used to describe the status of bone mineralisation – bone mineral density (BMD) and tissue mineral density (TMD). The former is an analogue to apparent density, that is, mineral content divided by total volume of bone specimen including bone tissue itself and marrow space; the latter, on the other hand, is comparable to material density, i.e., mineral content divided by volume of bone tissue only, excluding the interspersing vacuous spaces (45, 636). Accordingly, TMD is a direct measurement of the degree of matrix mineralisation in bone tissue (566, 636), whereas BMD is a parameter combining the effects of matrix mineralisation and quantity of bone in a defined region of interest (572, 591).

BMD and TMD can be directly calculated for biopsied bone specimens based on gravimetric principles, or can be indirectly measured by radiographic techniques based on resorption of radiation by minerals (637). In clinical practice and clinical research, BMD is most frequently measured by DXA and QCT, the pros and cons of which have been discussed in **Section 1.5.4**. It is worth pointing out that though DXA and QCT are non-invasive and have the advantage of

in vivo investigation in human joints, they are neither capable of deriving TMD and accurate microarchitectural parameters due to the two-dimensional nature (DXA) and inadequate spatial resolution (200-500μm for QCT) (240, 241, 572, 638), nor able to allow assessment of the local conditions of cartilage. In contrast, microCT can be used for measurement of both BMD and TMD, and can benefit from *ex vivo* studies which enable histological evaluation of tissue.

Subchondral bone specimens collected from end-stage OA joints generally exhibited decreased mineralisation despite its sclerotic structure. Based on biochemical analysis, Mansell and Bailey showed that subchondral trabecular bone in OA femoral head had increased collagen synthesis but reduced calcium to collagen ratio, indicating that there was elevated bone formation but the newly deposited osteoid was under-mineralised (430). Using gravimetric methods, Grynpas et al reported that subchondral bone in OA is associated with lower material density compared to aged and young controls (429). In addition, the tissue-level stiffness of OA subchondral bone is lower than normal (639). Likely explanations for the compromised mineralisation in OA subchondral bone have been discussed in **Section 1.6.2.2**, including elevated remodelling rate and phenotype changes in osteoblasts and collagen molecules. However, the above-mentioned studies only looked at end-stage samples and did not account for the status of cartilage degradation. The effects of cartilage degradation on the mineralisation of the underlying subchondral bone in OA had been investigated by just one study to date on the tibial plateau of knee joint (566).

OP was traditionally considered as a disease with 'too little bone' but 'what there is, is normal', meaning that bone is only inferior in quantity but the material properties and chemical compositions may be unaffected (640, 641). However, at ultrastructural level, it was shown that trabeculae in osteoporotic iliac bone are heterogeneously mineralised, with presence of both hyper- and hypo-mineralised laminar packets (19, 635, 642). There is also altered biochemical properties of hydroxyapatite and organic components such as collagen fibres (107). Though normal ageing of human skeleton has been suggested to result in elevated mean degree of mineralisation despite a moderate decrease in bone quantity (634), the mean degree of matrix mineralisation in OP has been inconsistently reported across the literature (107, 229, 635, 643, 644).

Comparison of subchondral bone mineralisation between OP and OA has seldomly been reported. Only a few studies on this topic have been identified (426, 427, 609), but as with microarchitecture as discussed in the previous chapter, these studies included only end-stage samples from fixed site(s) and neglected the influence of the overlying cartilage.

Moreover, it has been hypothesised that bone mineralisation and microarchitecture have a mutually adaptive relationship in the biomechanical response – mineralisation and tissue elastic modulus are optimised against the thickness, shape, and/or connectivity of cortical and trabecular bone, and *vice versa*, to maintain the apparent elastic modulus at a competent level (634, 645). Changes in any of these parameters will be followed by adjustments in the others. This process is likely to be under the control of osteoblast and osteocyte mediated mechano-transduction and subsequent bone remodelling (645), but may be jeopardised in diseases with abnormal bone metabolism such as OA and OP (427, 566, 608).

Therefore, the aims and objectives of this chapter are to:

(i), Explore the regional variations of subchondral bone mineralisation, including both subchondral plate and trabecular bone, in hip OA in relation to degeneration stages of the overlying cartilage.

(ii), Compare subchondral bone mineralisation in OP with that in different stages of OA.

(iii), Investigate the relationships between subchondral bone microarchitecture and mineralisation in OP and OA, and make comparisons as appropriate.

5.2 MATERIALS AND METHODS

Patient selection, macroscopic evaluation and osteochondral plugs extraction, microCT scanning and image processing, microarchitectural analysis, and histology and microscopic grading are as described in **Section 4.2** in Chapter 4.

5.2.1 Mineral density analysis

Two calcium hydroxyapatite phantoms of known mineral density (0.25 and 0.75 g/cm^3) were scanned and reconstructed under the same conditions as the osteochondral plugs. The X-ray attenuation coefficient values of these phantoms were recorded and a linear calibration equation was used to calculate the mineral density of the samples.

On microCT images, the apparent density, or volumetric bone mineral density (BMD), was defined as mineral density over the total volume of the defined ROI, including bone and marrow space (613). It was measured for trabecular bone only. The material density, or tissue mineral density (TMD), was measured as mineral density over the volume of bone only (613). TMD reflects the mean degree of bone matrix mineralisation (566, 646) and was measured for both subchondral plate and trabecular bone. For measurement of TMD, one-voxel thick surface layer was removed from the bone surface to correct for partial volume effect.

5.2.2 Statistical analysis

Comparisons of mineral densities (all parametric) were first made between microscopic grades within OA group to verify the regional variations in relation to the severity of cartilage degeneration, using one-way ANOVA, followed by Bonferroni post-hoc tests for pairwise comparisons. These tests were then repeated to include OP group and compare OP with different microscopic grades of OA. Comparisons of TMD between subchondral plate and trabecular bone were carried out by Paired Student T-test, matching the two compartments for each osteochondral plug. The associations between microarchitectural and mineral parameters were investigated using linear regression. Slopes of regression lines were compared using general linear model.

5.3 RESULTS

5.3.1 Comparisons of mineral densities

Representative three-dimensional microCT images of samples from OP and OA are shown in **Figure 5.1**, with coloured densitometric map to indicate the level of mineralisation in

subchondral plate and trabecular bone. Measurements of mineral densities and results of analysis of variance are summarised in **Table 5.1**.

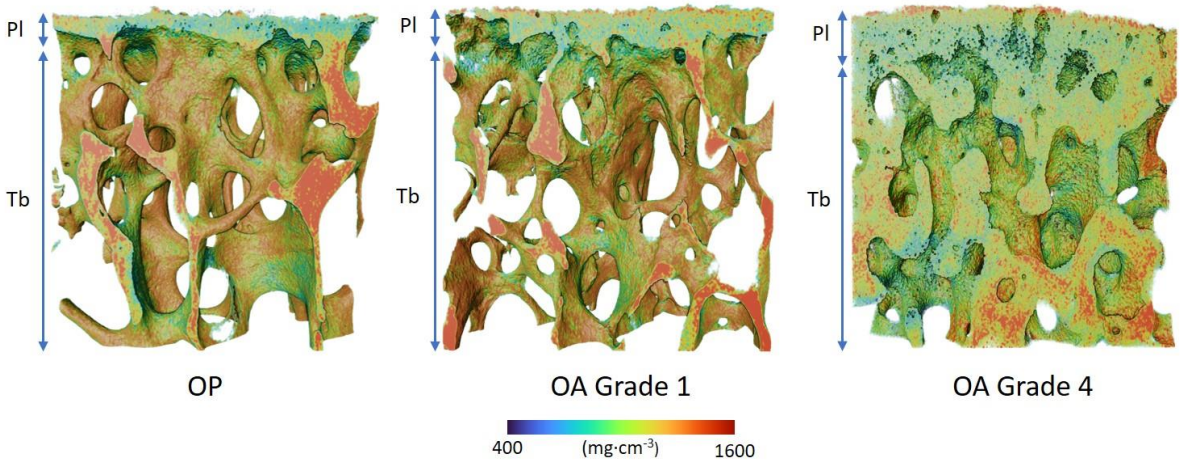

Figure 5.1. Three-dimensional densitometric map of subchondral bone in OP and OA. Red indicates higher level of mineralisation while blue indicates lower level of mineralisation. It is shown that trabeculae in OP and OA Grade 1 are more mineralized than in OA Grade 4. Also, the mineralization of trabecular bone is higher than subchondral plate in OP, OA Grade 1, and OA Grade 2. Tb: trabecular bone. Pl: subchondral plate.

Table 5.1. Analysis of variance of subchondral bone mineral densities in relation to severity of cartilage degeneration in OA and OP.

	OP (N=21)	OA Grade 1 (N=14)	OA Grade 2 (N=12)	OA Grade 3 (N=14)	OA Grade 4 (N=16)	P Value (OA Grades only)	P Value (OP and OA Grades)
Tb.TMD (g/cm^3)	1.41±0.06	1.45±0.11	1.39±0.07	1.27±0.07	1.24±0.09	<0.001	<0.001
Pl.TMD (g/cm^3)	1.22±0.07	1.20±0.09	1.17±0.07	1.17±0.07	1.15±0.07	0.300	0.032
BMD (g/cm^3)	0.27±0.10	0.20±0.14	0.31±0.11	0.42±0.10	0.44±0.14	<0.001	<0.001

Values are presented as mean ± SD. Using one-way ANOVA, analysis was first made between OA Grades to examine the variations in relation to the severity of OA. Then the tests were repeated to include the OP group to compare OP with different OA Grades.

5.3.1.1 Tissue mineral density

5.3.1.1.1 Subchondral plate

The status of the overlying cartilage did not have a statistically significant effect on the TMD of subchondral plate in the OA group (ANOVA, P=0.300) (**Table 5.1**), and there was no significant difference in subchondral plate TMD between different OA grades (**Figure 5.2A**). The TMD of subchondral plate in OP was similar to that in different grades of OA except Grade 4, which was significantly lower (Bonferroni test, P<0.05) (**Figure 5.2A**).

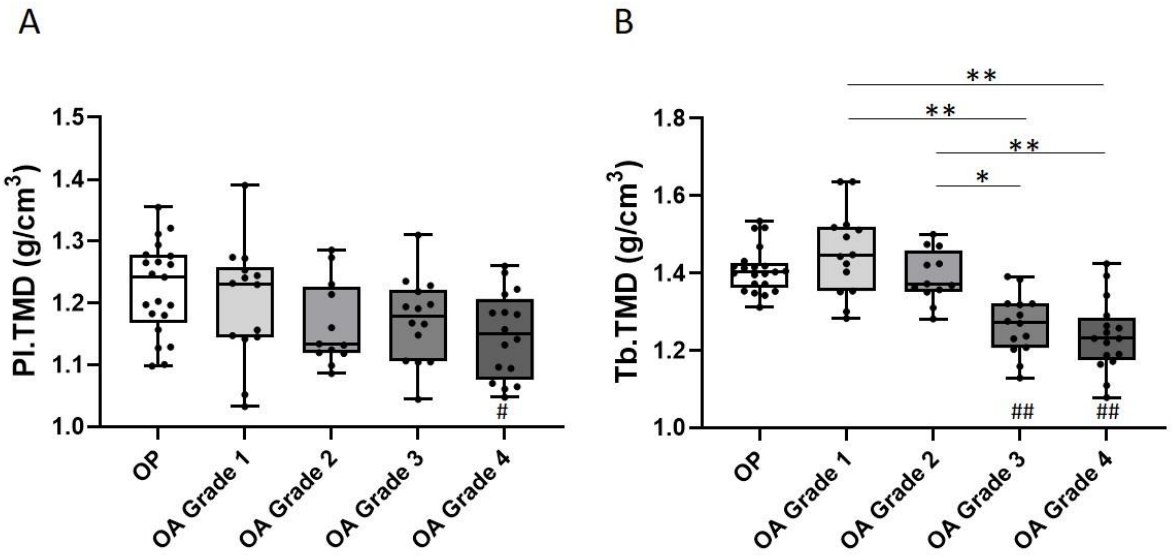

Figure 5.2. Comparisons of TMD in subchondral plate and trabecular bone in relation to severity of OA cartilage degeneration. The boxplot shows the median, the interquartile range (IQR), and individual values. Statistical significance is indicated by * or # for multiple comparisons between OA Grades, and between OP and OA Grades, respectively, according to post-hoc tests. *P < 0.05; **P < 0.001; the same for #.

5.3.1.1.2 Trabecular bone

A statistically significant decreasing trend was seen for the TMD of trabecular bone toward worsening cartilage degradation in the OA group (ANOVA, P<0.001) (**Table 5.1**). Both Grade 1 and Grade 2 OA trabecular samples displayed significantly better mineralisation compared

to OA Grade 3 and 4 (Bonferroni test, Grade 1 *vs* Grade 3: P<0.001; Grade 1 *vs* Grade 4: P<0.001; Grade 2 *vs* Grade 3: P<0.05; Grade 2 *vs* Grade 4: P<0.001) (**Figure 5.1**, **Figure 5.2B**). Trabecular bone in OA Grade 3 and Grade 4 was also significantly hypo-mineralised in contrast to that in OP (Bonferroni test, both P<0.001), while no significant difference in the TMD was detected between OP and early OA (Grade 1 and 2) (**Figure 5.1**, **Figure 5.2B**).

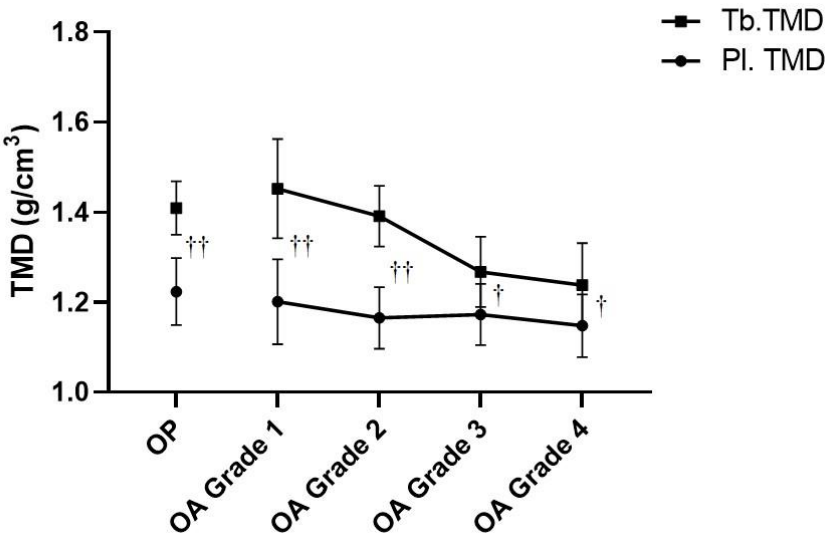

Figure 5.3. Compartmental comparisons of TMD between subchondral plate and trabecular bone in OA and OP. Graphs show mean ± SD. † indicates comparisons between subchondral plate and trabecular bone using Paired Student T-test. †P < 0.05; ††P < 0.001.

5.3.1.1.3 Compartmental comparison

The comparisons of mean mineralisation between subchondral plate and trabecular bone are illustrated in **Figure 5.1** and **Figure 5.3**. It was shown that the TMD of subchondral plate was significantly lower than that of trabecular bone in all conditions (OP, OA Grade 1, 2, 3, and 4). The compartmental difference was larger in OP, and OA Grade 1 and Grade 2 (+15%, +21%, +19%, Paired T-test, P<0.001, respectively), and smaller in OA Grade 3 and 4 (+8%, +8%, Paired T-test, P=0.005 and 0.007, respectively).

5.3.1.2 Bone mineral density

BMD was measured only for trabecular bone. Cartilage degradation in OA had a significant influence on the BMD of the underlying subchondral trabecular bone as shown by one-way ANOVA (P<0.001) (**Table 5.1**). Increased BMD was observed for higher OA scores. In specific, trabecular bone in OA Grade 4 was significantly denser as compared to both OA Grade 1 and Grade 2 (Bonferroni test, both P<0.001), whereas that in OA Grade 3 was statistically denser only compared to OA Grade 1 (Bonferroni test, P<0.001) (**Figure 5.4**). When the BMD of subchondral trabecular bone in OP was compared to OA Grades, statistically significant difference was found between OP and OA Grade 3 and 4 (Bonferroni test, P<0.05 and P<0.001, respectively), but not between OP and OA Grade 1 and 2 (**Figure 5.4**).

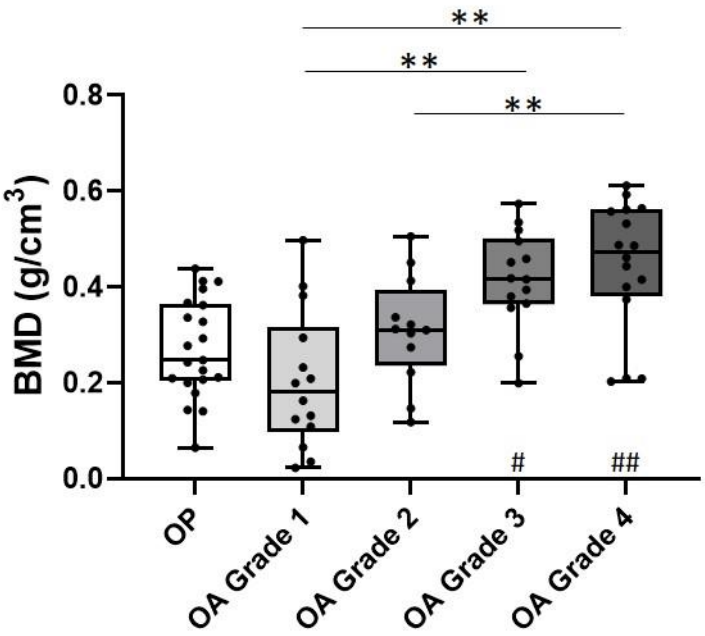

Figure 5.4. Comparisons of BMD in subchondral trabecular bone in relation to severity of OA cartilage degeneration. The boxplot shows the median, the interquartile range (IQR), and individual values. Statistical significance is indicated by * or # for multiple comparisons between OA Grades, and between OP and OA Grades, respectively, according to post-hoc tests. *P < 0.05; **P < 0.001; the same for #.

5.3.2 Associations between microarchitectural and mineral properties

5.3.2.1 Bone volume fraction, material density, and apparent density

BV/TV and TMD are the most important determinants of mechanical properties of trabecular bone. They are the determinants of apparent density (BMD) which explains up to 85% of apparent bone strength. The results of the linear regression analyses among BV/TV, TMD and BMD are summarized in

Table 5.2 and depicted in **Figure 5.5**.

Table 5.2. Results of linear regression between BV/TV, material density (TMD), and apparent density (BMD) of trabecular bone in OP and OA group, and in each Grade of OA group.

	BV/TV *vs* TMD			BV/TV *vs* BMD			TMD *vs* BMD		
	P value	R^2	Slope (95% CI)	P value	R^2	Slope (95% CI)	P value	R^2	Slope (95% CI)
OP Group (N=21)	<0.001	0.81	-0.009 (-0.011, -0.007)	<0.001	0.98	0.016 (0.015, 0.018)	<0.001	0.81	-1.563 (-1.931, -1.195)
OA Group (N=58)	<0.001	0.85	-0.011 (-0.012, -0.009)	<0.001	0.96	0.014 (0.013, 0.015)	<0.001	0.81	-1.125 (-1.274, -0.976)
OA Grade 1 (N=14)	<0.001	0.84	-0.011 (-0.015, -0.008)	<0.001	0.97	0.016 (0.014, 0.018)	<0.001	0.85	-1.204 (-1.523, -0.885)
OA Grade 2 (N=12)	<0.001	0.72	-0.008 (-0.011, -0.004)	<0.001	0.95	0.015 (0.013, 0.018)	<0.001	0.78	-1.484 (-2.041, -0.928)
OA Grade 3 (N=14)	<0.001	0.65	-0.008 (-0.012, -0.004)	<0.001	0.93	0.013 (0.010, 0.015)	0.003	0.53	-0.965 (-1.541, -0.389)

OA Grade 4 (N=16)	<0.001	0.76	-0.008 (-0.011, -0.006)	<0.001	0.94	0.013 (0.011, 0.015)	<0.001	0.65	-1.180 (-1.674, -0.686)

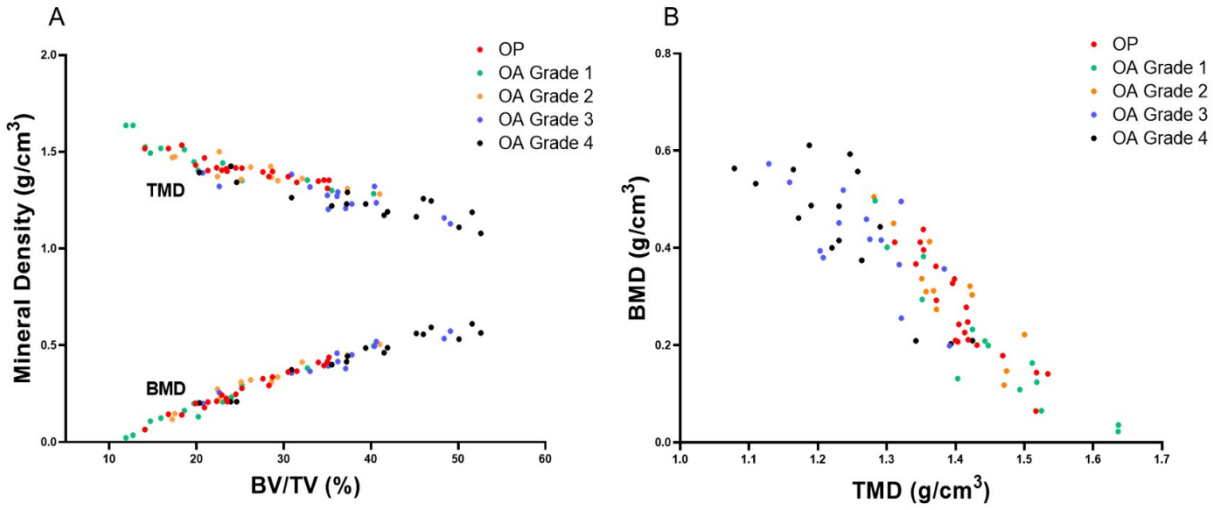

Figure 5.5. Associations between BV/TV, material density (TMD), and apparent density (BMD) of trabecular bone in OP and OA, and in each Grade of OA group. (A) Associations between BV/TV and TMD, and between BV/TV and BMD. (B) Associations between BMD and TMD

In both OP and OA groups, the variation in BV/TV of trabecular bone was positively associated with that in BMD (OP: R^2=0.98, P<0.001; OA: R^2=0.96, P<0.001), but was inversely associated with the change in TMD (OP: R^2=0.81, P<0.001; OA: R^2=0.85, P<0.001) (

Table 5.2, **Figure 5.5A**). Moreover, TMD was inversely correlated with BMD in both groups (OP: R^2=0.81, P<0.001; OA: R^2=0.81, P<0.001) (

Table 5.2, **Figure 5.5B**). In addition, the general linear model, which incorporated an interaction term as independent variable, showed that the slopes of regression lines were not significantly different between OP and OA for BV/TV *versus* TMD (P=0.327), BV/TV *versus* BMD (P=0.077), and TMD *versus* BMD (P=0.085).

For the OA group, when samples were analysed separately according to the degree of cartilage degeneration, the above-mentioned trends remained the same, i.e., at each grade of OA, the increase in BMD of trabecular bone was accompanied by a significant rise in BV/TV but a significant reduction in TMD (

Table 5.2, **Figure 5.5**). Furthermore, the severity of cartilage degeneration did not influence the relationships between each pair of the three parameters, as shown by the non-significant difference in regression slopes among OA grades (P=0.661 for BV/TV *versus* TMD, P=0.115 for BV/TV *versus* BMD, and P=0.638 for TMD *versus* BMD). Similarly, there was no statistically significant difference in the slopes of these correlations between OP and different grades of OA (P=0.647 for BV/TV *versus* TMD, P=0.055 for BV/TV *versus* BMD, and P=0.399 for TMD *versus* BMD).

5.3.2.2 Mineralisation and other microarchitectural parameters

The associations between mean mineralisation of bone matrix (TMD) and microarchitectural parameters in subchondral plate and trabecular bone in OP and OA were explored by lineal regression. Only the microarchitectural parameters that showed a variation in relation to the severity of cartilage degeneration were included. Results were summarised in **Table 5.3**.

Table 5.3. Results of linear regressions between microarchitecture and mineralisation of subchondral bone in OA and OP.

		Subchondral plate	Subchondral trabecular bone					
		Pl.Th	BV/TV	BS/BV	Tb.Th	Tb.N	SMI	Conn.Dn
OP	P	ns	<0.001	0.010	0.029	<0.001	0.044	ns
	R^2	/	0.82	0.30	0.23	0.48	0.20	/
	Slope	/	-0.009	0.009	-0.973	-0.150	0.120	/
OA	P	<0.001	<0.001	<0.001	<0.001	<0.001	<0.001	<0.001
	R^2	0.20	0.85	0.69	0.57	0.48	0.62	0.44
	Slope	-0.352	-0.011	0.025	-2.328	-0.222	0.100	-0.036
Slope difference	P	/	ns	0.002	0.036	ns	ns	/

Associations between microarchitectural parameters and mineralisation (TMD) of subchondral plate and trabecular bone in OP and OA were investigated using linear regression. Slopes of regression lines were compared using general linear model.

For subchondral plate, plate thickness was significantly associated with the status of mineralisation only in OA ($P<0.001$). On the contrary, five of the six microarchitectural parameters of trabecular bone showed statistically significant correlation with TMD in both OP and OA. In specific, except for BV/TV which has been described in the previous section, Tb.Th (OP: $R^2=0.23$, $P=0.029$; OA: $R^2=0.57$, $P<0.001$) and Tb.N (OP: $R^2=0.48$, $P<0.001$; OA: $R^2=0.48$, $P<0.001$) were negatively associated with TMD. On the other hand, BS/BV (OP: $R^2=0.30$, $P=0.010$; OA: $R^2=0.69$, $P<0.001$) and SMI (OP: $R^2=0.20$, $P=0.044$; OA: $R^2=0.62$, $P<0.001$) were positively associated with TMD. The directions of these correlations were the same in the OP and OA groups. The regression slopes were not significantly different between OP and OA for Tb.N *versus* TMD ($P=0.322$), and SMI *versus* TMD ($P=0.700$). However, for BS/BV and Tb.Th, the disease conditions had a significant effects on their relationships with mineralisation, as shown by the statistically significant difference between regression gradients in OP and OA ($P=0.002$ for BS/BV and $P=0.036$ for Tb.Th, respectively). Moreover, in OA, the increase in subchondral trabecular connectivity was accompanied by a significant decrease in mineralisation ($R2=0.44$, $P<0.001$). Such a relationship was not seen in the OP group.

5.4 DISUCUSSION

In this chapter, material density (TMD), which reflects the level of bone matrix mineralisation, and apparent density (BMD), which represents the combinatory effects of mineralisation and structure, were investigated in the subchondral plate and subchondral trabecular bone in OA and OP. To our knowledge, this is the first study looking to explore the relationship between subchondral bone mineral properties and degeneration of the overlying cartilage in human hip joints. In general, it was found that TMD and BMD of trabecular bone, but not TMD of subchondral plate, had a significant regional variation in OA in relation to the severity of

cartilage degradation. Meanwhile, these parameters in OP were similar to regions with early but different from regions with advanced cartilage degeneration in OA. Secondly, this chapter reports the results of novel experiments for a compartmental comparison of TMD between subchondral plate and trabecular bone, showing that trabecular bone is more mineralized than subchondral plate in both OP and OA, and this compartmental difference varied with severity of cartilage degeneration. The data also showed that the relationships among bone volume fraction, material density, and apparent density were similar in OP and in different stages of cartilage degradation in OA, which has not been reported previously.

A number of earlier studies using tissue samples from fixed site(s) regardless of the status of the overlying cartilage showed that the matrix mineralization of subchondral trabecular bone, measured by material density or TMD, decreased in OA compared to healthy and OP (427, 430, 609). More recently it was shown that trabecular bone was more hypo-mineralized in regions with complete cartilage loss compared to those still covered by cartilage in OA specimens (426, 566). Our results are generally consistent with these studies but additionally showed that the decrease in TMD of subchondral trabecular bone in hip OA was stagewise in terms of cartilage degeneration and was already significant before the exposure of subchondral bone, thus providing new evidence that subchondral bone mineralization and cartilage degradation are intrinsically related in OA.

The matrix mineralization of trabeculae in OP had been shown to be decreased (647), increased (644), or unchanged (427) compared to control by different studies. The conflicting results are likely to be due to the site of tissue sampling (vertebrae, ilium, femur, etc.) and the stage of disease (menopause-related rapid or age-driven slow phase of bone turnover) (229, 645). The current study has been limited to the subchondral bone of hip joint with established OP and OA. The recruited female subjects were more than eight years post menopause and were therefore likely to be at the slow phase of bone turnover comparable to the male subjects (185, 187). The data show that the mineralization of subchondral trabecular bone in OP was similar compared to regions with early cartilage degradation (Grade 1 and Grade 2) in OA, but significantly higher compared to regions with advanced cartilage degradation (Grade 3 and Grade 4). This regionalized observation may partly explain why the tissue hardness of trabeculae, measured by nanoindentation, was found to be

different between OP and OA by one study (431) but similar by another study (609), as they both collected samples from a fixed anatomical site without examining the conditions of the overlying cartilage.

In contrast to trabecular bone, there were subtle variations in the TMD of subchondral plate in relation to local severity of cartilage degradation. This is in line with Aspden et al who showed that there was no site-related variation in the material density of subchondral plate, without accounting for the condition of the overlying cartilage (428). In another study (427) they also reported values for trabecular bone but a comparison with subchondral plate was missing. Our study provided new data showing that the TMD of the subchondral plate was significantly lower than that of trabecular bone in OA, and this compartmental difference varied significantly between regions with varying severity of cartilage degradation. The compartmental difference of TMD in hip OA supports the findings by Cox et al (566) who showed decreased subchondral trabecular bone mineralization toward articular surface in knee OA. Our results additionally indicate that such depth-related difference is not OA-specific, but also exists in OP. Interestingly, a very recent publication reported that this phenomenon was observed in disease-free femoral head as well, using a two-dimensional imaging technique (648). However, Cox et al reported that the cartilage degradation related regional difference of subchondral bone TMD in OA was larger toward articular surface, whereas the regional difference of subchondral plate TMD in our study was not statistically significant. Taken together, our results support the concept that subchondral plate and trabecular bone are biologically and mechanically distinct (153, 166), and provide further evidence for the view that they respond differently during the progression of OA (160, 161).

Our regionalized investigation of subchondral bone in this chapter and Chapter 4 indicates that before a comparatively normal region progresses to end-stage OA with eroded cartilage and subchondral sclerosis, there is a period when subchondral bone is osteoporosis-like in terms of both microarchitecture and matrix mineralization, for both subchondral plate and trabecular compartment (**Figure 5.1**). This provides further support for the hypothesis presented in Chapter 4 that the unbalanced remodelling favouring resorption in subchondral bone at early stage of OA may have the similar pattern with that in the subchondral bone of OP. Collectively these results also support the hypothesis that subchondral bone remodelling

in OA is a biphasic process with a transition from favouring resorption and mineral preservation at early stage to favouring formation and demineralisation at late stage (161, 562). We would suggest that this transition is caused by increased shear stress concentrated at the intervening area between sclerotic and porotic regions, i.e., a steep stiffness gradient. The elevated mechanical stress perceived by osteocytes and osteoblasts in this area may trigger the phenotype change described by previous studies (421, 436, 649), switching osteoblasts from pro-resorption to pro-formation status. In the meantime, production of collagen homotrimers and changes in mineralization-related proteins in these abnormal osteoblasts lead to disrupted mineral deposition and consequently hypo-mineralization (436, 438, 632, 650). This theory parallels the hypothesis that the elevated shear stress, rather than compressive stress, is the cause of cartilage deformation and degradation (113, 161). Further research on local subchondral bone mechanical properties and cell phenotyping, using the same regionalised tissue sampling procedure as in this study, is needed to validate this theory.

The biomechanical properties of bone are characterized by a series of parameters at both microstructural and tissue material levels. Of these parameters, BV/TV and TMD are considered the most important for trabecular bone (427, 608, 651). They are the determinants of apparent density/BMD (BMD=BV/TV*TMD) (572, 591, 652) which explains up to 85% of apparent bone strength if measured volumetrically (622, 653, 654). The rest is attributable to other architectural parameters such as SMI and Conn.Dn (108).

Our study showed that there was an inverse correlation between BV/TV and TMD and between BMD and TMD of trabecular bone in OA, and a positive correlation between BV/TV and BMD. Together they indicate that in OA the decreased matrix mineralization can be over-compensated by the increased bone volume and lead to increased apparent density. This is consistent with a previous study showing that decreased mineralization in OA trabecular bone only compromised but did not completely abolish the increase in bone strength with rising apparent density (427, 519). The result is also consistent with the report that a 4-6% decrease in TMD in sclerotic bone samples was responsible for only a 4-9% increase in BV/TV, much less than the actual change (69%) in BV/TV (566). Another interesting observation from our study is that the pattern of the mutual correlations among BMD, BV/TV and TMD in OA remained the same when analysed separately by the microscopic grades. This finding was

unexpected as the feature of bone remodelling at varying stages and regions of OA was expected to be different, as discussed above and in several previous studies (420, 649). Also, a study reported that there was no statistically significant correlation between BV/TV and TMD in end-stage OA subchondral trabecular bone with cysts and no cartilage coverage (459). A possible explanation for our finding is that the mineralization of bone is affected by a complex mechanism involving not just remodelling rate, but also remodelling balance and mineralization kinetics (19).

We have also shown that the correlations among BV/TV, TMD and BMD discussed above also exist in the OP group in a similar pattern. These correlations suggest that loss of trabecular bone in OP is associated with, but not compensated by the increased mineral content, leading to a lower apparent density. This is consistent with the findings that the decreased trabecular bone apparent density in OP was accompanied by stronger trabeculae (643). The increasing TMD in OP trabecular bone can be a result of active response of osteocytes and osteoblasts to counteract the decreasing apparent stiffness caused by the reducing bone volume (634, 645). It can also be a non-specific phenomenon as the trabeculae surviving resorption were composed of inner, older, and thus better mineralized laminae due to complete secondary mineralisation (634).

Apart from trabecular volume fraction, mineralisation is also correlated with other architectural parameters (i.e., Pl.Th, BS/BV, Tb.Th, Tb.N, SMI and Conn.Dn) associated with cartilage degradation in OA in both subchondral plate and trabecular bone. Together they indicate that there is still a mutual adaption between mineralisation and bone morphology in response to local biomechanical environment in the disease process. However, presence of other bone pathology such as cysts, which were not sampled in the current study, may disrupt these relationships and de-couple mineralisation from bone morphology (459). Analysis specific for each OA grade was not performed for these parameters due to the relatively weak correlations and limited sample size in this study. As for OP, the above mentioned correlations are generally weaker (BS/BV, Tb.Th, Tb.N, and SMI) or insignificant (Pl.Th and Conn.Dn) compared to those in OA. This may be caused by significant loss of bone, leaving not enough tissue for bone cells to make compatible adjustments at architectural and morphological levels.

5.5 SUMMARY

Similar to most microarchitectural parameters, the TMD of subchondral trabecular bone varies with the severity of histopathology of the overlying cartilage in OA, showing decreased mineralisation toward more sever cartilage degradation. However, the decrease in mineralisation can be over-compensated by the increase in bone volume, resulting in higher apparent density (BMD) in advanced OA. Mineral properties of subchondral plate and trabecular bone in early OA are similar with those in OP, supporting the theory raised in Chapter 4 that subchondral bone remodelling at early stage of OA is likely to have the similar pattern with subchondral bone remodelling in OP. It is also shown in this chapter that mineralisation of subchondral trabecular bone is better than subchondral plate in both OP and OA, providing further evidence that the two compartments are distinct structures and may respond differently in disease conditions. Moreover, the similar associations among TMD, BMD and BV/TV of subchondral trabecular bone in OP and various stages of OA point to a complex mechanism in the adaptive relationship between bone mineralisation and microarchitecture.

Chapter 6

Expression of cartilage degradative proteinases in hip OP and OA and its associations with subchondral bone properties

6.1 INTRODUCTION

In the previous chapters, it has been shown that microarchitecture and mineralization of subchondral plate and trabecular bone in OA are closely associated with the local severity of cartilage degradation. Cartilage degradation in OA, represented by the loss of matrix macromolecules, especially proteoglycans and type II collagens, is attributable to the proteolytic activities of aggrecanases and collagenases. However, it is not clear yet to what extent these enzymes contribute to cartilage degradation at different stages of OA and how their expression by chondrocytes may be related to the structural and mineral properties of subchondral bone.

Depletion of aggrecans from cartilage is caused by enzymatic cleavage within the IGD of aggrecan core protein, allowing the GAG-rich regions to detach from the hyaluronan anchor and freely leave the matrix (655). Cleavage of the IGD can be fulfilled by both MMPs (in particular stromelysin, MMP3 (325, 336)) and aggrecanases (see **Section 1.6.2.1**). However, the GAG-containing large aggrecan fragments released into synovial fluid of OA are mainly the N-terminal neoepitope ARGSV, a product of the aggrecanase mediated proteolysis of the IGD (656, 657). It has therefore been suggested that aggrecanases, especially ADAMTS4 and ADAMTS5 which have the highest catalytic activities, are responsible for the pathological degradation of proteoglycans in OA whereas MMPs are more constructive, mainly implicated in the non-destructive processing (326, 658). The relative importance of ADAMTS4 and ADAMTS5 in the pathophysiology of OA is still debated and seems to vary between species (326, 328). ADAMTS5, rather than ADAMTS4, has been implicated in the cartilage aggrecanolysis in mouse models of OA (659-661). ADAMTS4 seems to be more important in porcine and equine (662, 663) while both ADAMTS4 and ADAMTS5 have been found

responsible for cartilage breakdown in bovine and canine models (335, 664). In human OA cartilage, elevated levels of both ADAMTS4 and ADAMTS5 mRNA have been reported, with ADAMTS4 showing a larger degree of increased expression (355). ADAMTS4 is likely to be more important as it only presents in disease conditions while ADAMTS5 is constitutively expressed by normal cartilage (665, 666) and seems not fully functional in OA synovial fluid (667).

Depletion of aggrecan from cartilage is followed by destruction of the fibrillar network. Of the collagenases found in joint tissues, MMP13 is a marker for hypertrophic chondrocyte (668), and is highly potent for degradation of type II collagen while MMP1 and MMP8 predominantly act on type III and type I collagen respectively (325, 669). MMP13 has therefore been considered the primary collagenase involved in the cartilage pathology in OA (313, 318, 330, 670). MMP13 can hardly be detected in normal adult cartilage (336, 356, 671), but both mRNA and active proteins are expressed in human OA (332, 334, 336). Specific inhibition of MMP13 activity is able to significantly reduce collagen degradation in human OA cartilage (324). The role of MMP13 in OA is also supported by data from animal models. Expression of MMP13 was upregulated in both spontaneous and induced models of OA and associated with cartilage degradation (664, 672-674). In addition, conditional expression of MMP13 in articular cartilage led to the development of OA in mice (675), while both MMP13 inhibitors and the knockout of gene encoding MMP13 greatly attenuated the severity of OA in surgically induced OA models (676, 677).

Expression of the above-mentioned enzymes by chondrocytes may be interrelated with the biomechanics and biology of subchondral bone. On the one hand, the mechanical properties of subchondral bone determine the nature and magnitude of mechanical stress endured by the overlying cartilage and *vice versa*. The elevated mechanical stress that is seen in OA can be transduced by chondrocytes and osteocytes and osteoblasts into intra-cellular signals disrupting normal cell metabolism and matrix remodelling in the two neighbouring tissues. On the other hand, phenotypically shifted chondrocytes and bone cells in OA may exert regulatory effects on each other. It has been shown by *in vitro* studies that osteoblasts derived from OA joints were capable of inducing GAG release from normal cartilage and increasing expression of MMPs and ADAMTSs by normal chondrocytes (678-680). Meanwhile,

chondrocytes from OA cartilage were able to upregulate expression of genes involved in bone remodelling by normal osteoblasts (679, 681). These effects are likely to be mediated by biochemical factors (e.g., cytokines and growth factors) which can travel through the osteochondral junction in OA joints via increased vascular channels.

Microarchitecture and mineralisation not only reflect the remodelling activities of bone cells, but also are the determinants of bone mechanical properties. Therefore, a comprehensive investigation of how these parameters are associated with the expression and distribution of cartilage degradative enzymes in OA may provide crucial information regarding how cartilage destruction and subchondral bone remodelling are synergised in the disease process. Many previous studies have investigated the changes either in subchondral bone properties or in expression of cartilage proteinases in human OA samples and animal models, but only a few animal studies have examined the two aspects simultaneously (405, 682-684). To our knowledge, study of the latter kind has not been reported for human subjects, and there have been no studies in which chondrocyte expression of degradative enzymes is directly related to the microarchitecture and mineralisation of subchondral bone through various stages of OA in either human joints or animal models.

A phenotypic change of chondrocytes with increased production of cartilage degradative enzymes may also be a result of the normal ageing process (i.e., cell and matrix senescence), or can be caused by local or systemic inflammation. Ageing and inflammation are both associated with pathogenesis of OP (199). More importantly, increased bone remodelling in OP is systemic, meaning that it will also affect subchondral bone and therefore is likely to have an impact on the overlying articular cartilage. The relationship between cartilage expression of degradative proteinases and subchondral bone properties in OP has never been studied previously. An investigation of this relationship and comparison with OA may provide information on the interactions between subchondral bone and articular cartilage in the two most common musculoskeletal conditions.

The aims of this chapter are to:

(i), Carry out a detailed investigation on the expression of degradative enzymes by chondrocytes and their distribution in human OA and OP articular cartilage using IHC. MMP13 and ADAMTS4 were selected to represent the enzymes responsible for the destruction of the major ECM components, Col II and aggrecan, respectively.

(ii), Examine how their expression and distribution may differ with regard to the different stages of cartilage degradation.

(iii), Determine the associations of MMP13 and ADAMTS4 expression by chondrocytes with subchondral bone microarchitecture and mineralisation in OA and OP.

6.2 MATERIALS AND METHODS

6.2.1 Patient selection

The IHC study data reported in this chapter was obtained from 16 OA (the main study cohort) and 7 OP femoral heads (see **Section 2.5**).

6.2.2 Macroscopic evaluation and osteochondral plugs extraction

Ideally the IHC study should have been carried out on the same plugs scanned by microCT. However, freezing-thawing cycles together with a lengthy decalcification process had significant detrimental effects on the histological quality and immunogenicity of both cartilage and bone. Tissue sections resulted from these plugs were competent for histological staining and histopathological evaluation (**Figure 4.2**) but could not withstand more atrocious IHC procedures such as antigen retrieval, hydrogen peroxide incubation and rigorous washing steps.

Therefore, as described in **Section 2.5**, a second set of plugs, which were immediately adjacent to the plugs collected for the microCT study within the same macroscopically graded regions, were used in the IHC study. They consisted of 21 OP plugs and 52 OA plugs

(macroscopic Grade I to Grade IV). These plugs have also been included in the histology study in Chapter 3.

6.2.3 Histological processing and microscopic grading

Plugs were fixed in formalin immediately after extraction and were processed for paraffin embedding without decalcification as described in **Section 2.6.1**. Microscopic grades of these plugs were determined as a part of the histology study in Chapter 3 using the modified OARSI grading. At last, two OA plugs were excluded from the IHC study because the microscopic grading of them did not match that of the paired microCT plugs.

6.2.4 Detection of MMP13 and ADAMTS4 in cartilage by IHC

Expression of MMP13 and ADAMTS4 by chondrocytes was detected by IHC staining. The protocol has been described in detail in **Section 2.11**. Briefly, after dewaxing and rehydration, duplicated slides were subjected to heat induced antigen retrieval and quenching of endogenous peroxidase activity. Sections were then blocked by 10% normal goat serum before over-night incubation with rabbit primary IgG against MMP13 (1:300) and ADAMTS4 (1:200). Negative controls including blank diluent, non-immune rabbit IgG, and tissue known not to express one of the target proteins (MMP13) were utilised to check for specificity of staining (**Figure 6.1**). Goat anti-rabbit secondary antibody and HRP conjugates were then applied to sections. Finally, colour was developed with DAB chromogen and substrate.

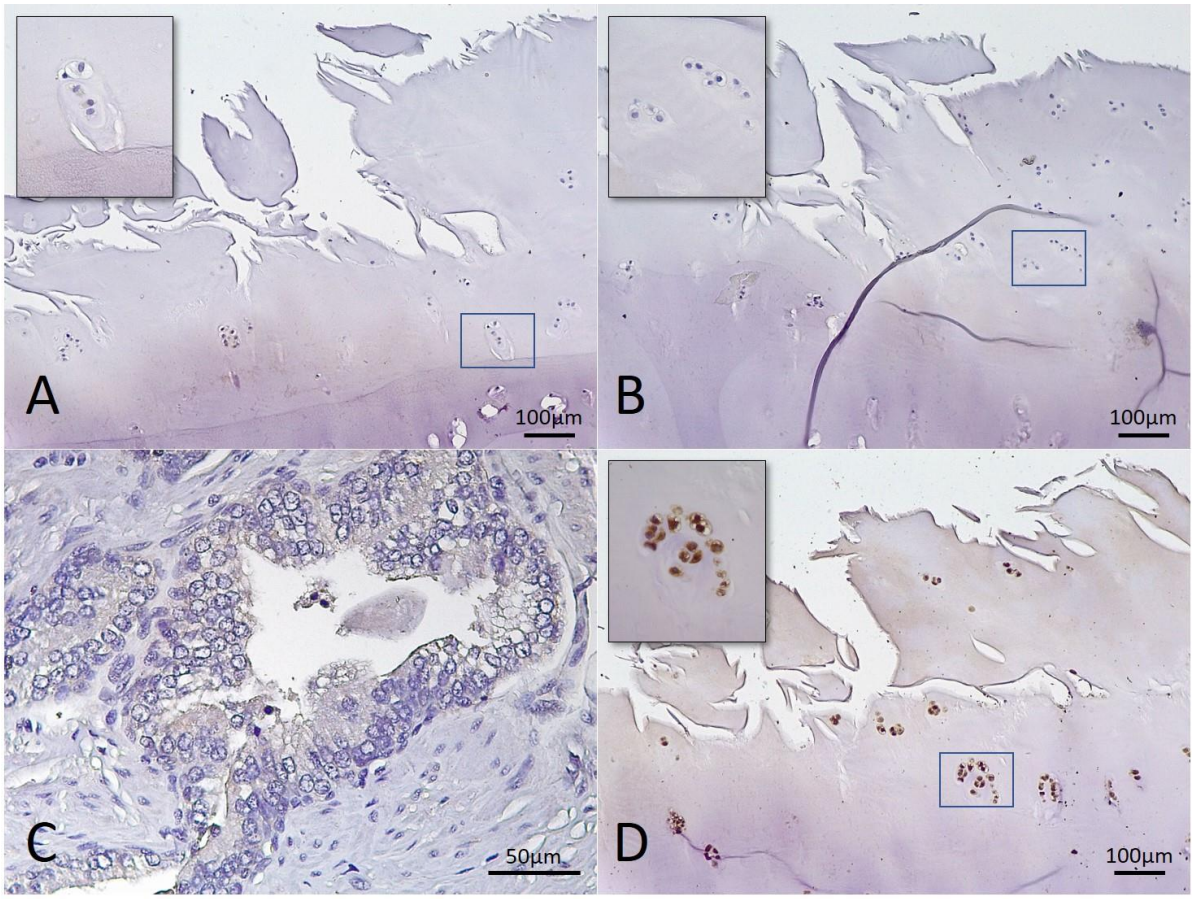

Figure 6.1. Specificity of staining. Tissue sections were incubated with blank diluent (A) and non-immune rabbit IgG (B) as negative antibody control. Benign prostate tissue section (C) was utilised as negative tissue control for MMP13. OA cartilage stained with MMP13 antibody is shown in (D). Negligible background was observed in controls and specific staining can be seen in chondrocytes. Original magnification 100x in (A), (B) and (D), and 400x in (C). Squares indicate areas shown with 400x magnification.

6.2.5 Measurement of MMP13 and ADAMTS4 expression

Stained slides were observed under a light microscope at 100x magnification. A region of interest (ROI) was selected in the middle of cartilage sections, with a width of 2mm as indicated by the red square in **Figure 6.2**. The number of chondrocytes positively and negatively stained with MMP13 or ADAMTS4 was counted manually within the ROI. The overall expression of MMP13 and ADAMT4 was expressed as percentage of positively stained cells through the full-thickness of cartilage in the ROI. The zonal expression was defined as percentage of positive cells in the superficial zone (SZ), middle zone (MZ), and deep zone (DZ),

respectively, which were differentiated according to characteristic chondrocyte morphology and alignment described in **Section 1.3.3.1** (**Figure 6.2**). Availability of zones varied with severity of cartilage degradation, i.e., SZ was lost and therefore not counted for OA Grade 3, and both SZ and MZ were not counted for OA Grade 4 (see **Table 2.3**). The counting was first carried out on all stained tissue sections, and then repeated with at least 8-weeks' interval on randomly selected 50 sections to evaluate intra-observer variability. The ICCs for the percentage of positively stained cells were 0.906, 0.975, 0.943, and 0.954 for the SZ, MZ, DZ, and full-thickness of cartilage respectively.

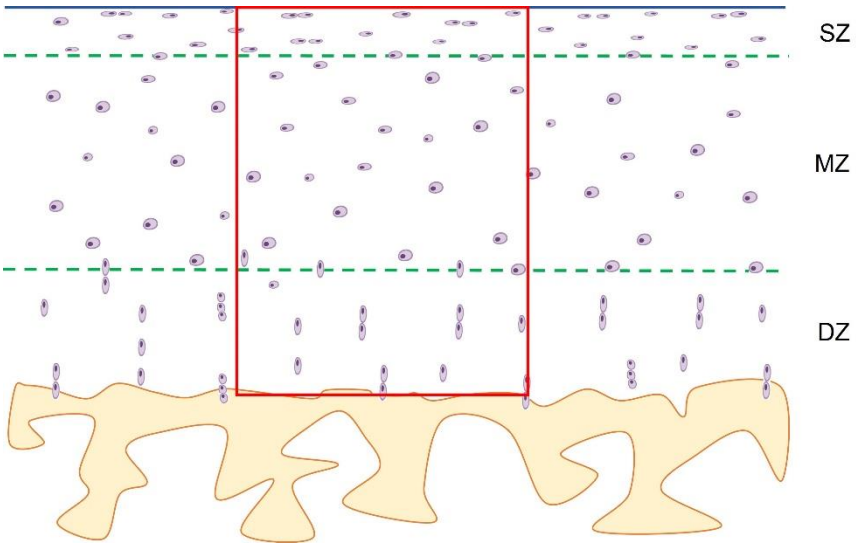

Figure 6.2. Region of interest for measurement of expression of MMP13 and ADAMTS4.

6.2.6 Statistical analysis

Unpaired Student T-test and one-way ANOVA with Bonferroni's post-hoc test were used for parametric data; Mann-Whitney U test and Kruskal-Wallis (K-W) test with Dunn' post-hoc test were used for non-parametric data. Inter-group comparisons of proteinases' expression were first made between different microscopic grades in the OA group to investigate the variations related to severity of cartilage degradation. Tests were then repeated to incorporate the OP group to compare OP with different grades of OA. Intra-group comparisons were made

between SZ, MZ and DZ for OP and each grade of OA. The associations between expression of proteinases and subchondral bone properties in OP and OA were determined using Pearson's correlation for parametric data and Spearman's correlation for non-parametric data.

6.3 RESULTS

6.3.1 Expression of ADAMTS4

Overall and zonal expressions of ADAMTS4, represented by percentage of positively stained chondrocytes in full-depth and each zone of cartilage respectively, are summarised in **Table 6.1**. Results of intra- and inter-group comparisons are depicted in **Figure 6.3** and **Figure 6.4** for overall and zonal expression respectively. Representative images of staining are given in **Figure 6.5**.

Table 6.1. Overall and zonal expression of ADAMTS4.

	OP (N=21)	OA Grade 1 (N=13)	OA Grade 2 (N=10)	OA Grade 3 (N=12)	OA Grade 4 (N=15)
ADAMTS4					
Overall	21.12±9.48	61.59±6.06	62.37±10.02	51.96±10.97	53.86±13.84
SZ	53.90±17.34	88.48±5.59	92.07±6.26	/	/
MZ	15.17±12.96	82.82±7.68	78.97±11.26	92.00±7.76	/
DZ	3.93±3.11	13.38±7.48	18.71±11.52	10.48±5.46	53.86±13.84

Data are presented as percentage (mean ± SD) of positively stained chondrocytes. SZ, superficial zone; MZ, middle zone; DZ, deep zone.

6.3.1.1 Overall expression of ADAMTS4

Within OA group, one-way ANOVA showed that there was a statistically significant variation in the overall expression of ADAMTS4 in relation to local severity of cartilage degradation

(P=0.044). OA Grade 1 and Grade 2 had higher expression (61.59% and 62.37%, respectively) as compared to Grade 3 and 4 (51.96% and 53.86%, respectively) (**Table 6.1**). However, Bonferroni post-hoc test did not reveal any statistically significant pair-wise differences (**Figure 6.3**). When the OP group was incorporated in the analysis, overall expression of ADAMTS4 was significantly higher in all OA grades compared with OP, in which around 21.12% chondrocytes were synthesising ADAMTS4 (Bonferroni test, P<0.001 for all comparisons) (**Figure 6.3**).

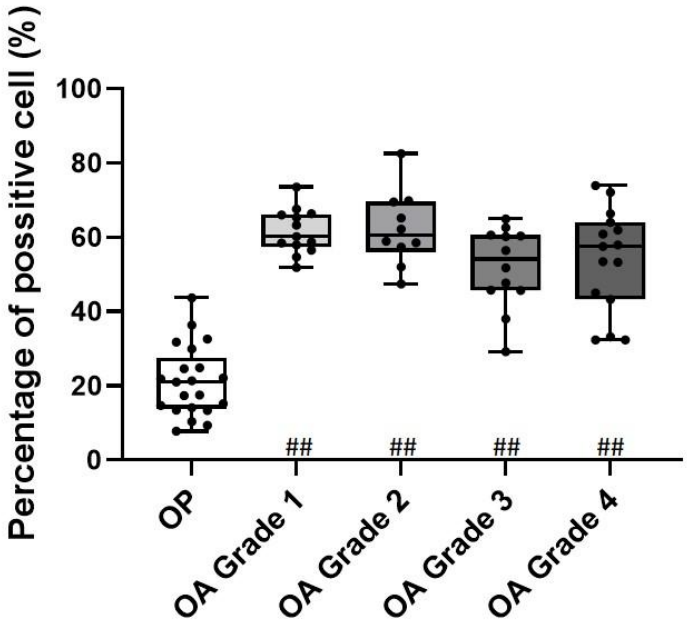

Figure 6.3. Comparisons of overall expression of ADAMTS4 in relation to severity of OA cartilage degeneration. The boxplot shows the median, the interquartile range (IQR), and individual values. Statistical significance is indicated by * or # for multiple comparisons between OA Grades, and between OP and OA Grades, respectively, according to post-hoc tests. *P < 0.05; **P < 0.001; the same for #.

6.3.1.2 Zonal expression of ADAMTS4

6.3.1.2.1 Intra-group comparisons

Significant zonal variations were found in OP and all OA grades. In general, the expression of ADAMTS4 by chondrocytes was higher in the upper zone(s) (**Table 6.1**, **Figure 6.4A**, **Figure 6.5**). Specifically, in the SZ of OP group, about 53.90% of chondrocytes expressed ADMATS4 and the value was significantly lower in MZ (15.17%) and DZ (3.93%) (K-W test, $P<0.001$; Dunn's test, $P<0.001$ for SZ *vs* MZ and SZ *vs* DZ, and $P<0.05$ for MZ *vs* DZ). In OA Grade 1, around 88.48% of chondrocytes expressed ADAMTS4 in the SZ and around 82.82% and 13.38% in the MZ and DZ, respectively (ANOVA, $P<0.001$). The differences were statistically significant between SZ and DZ and between MZ and DZ (Bonferroni test, both $P<0.001$), but not between SZ and MZ (Bonferroni test, $P>0.05$). As for OA Grade 2, expression of ADAMTS4 was highest in the SZ (92.07%), followed by about 78.97% in MZ and 18.71% in DZ (ANOVA, $P<0.001$; Bonferroni test, $P<0.001$ for SZ *vs* DZ and MZ *vs* DZ, and $P<0.05$ for SZ *vs* MZ). The SZ in OA Grade 3 samples was completely eroded so was not counted. The MZ in Grade 3 had about 92.00% of chondrocytes expressing ADAMTS4, which was significantly higher than the percentage expression in the DZ (10.48%) (Mann-Whitney U test, $P<0.001$). Zonal comparisons were not made for OA Grade 4 as only DZ was left, in which about 53.86% chondrocytes were producing ADAMTS4.

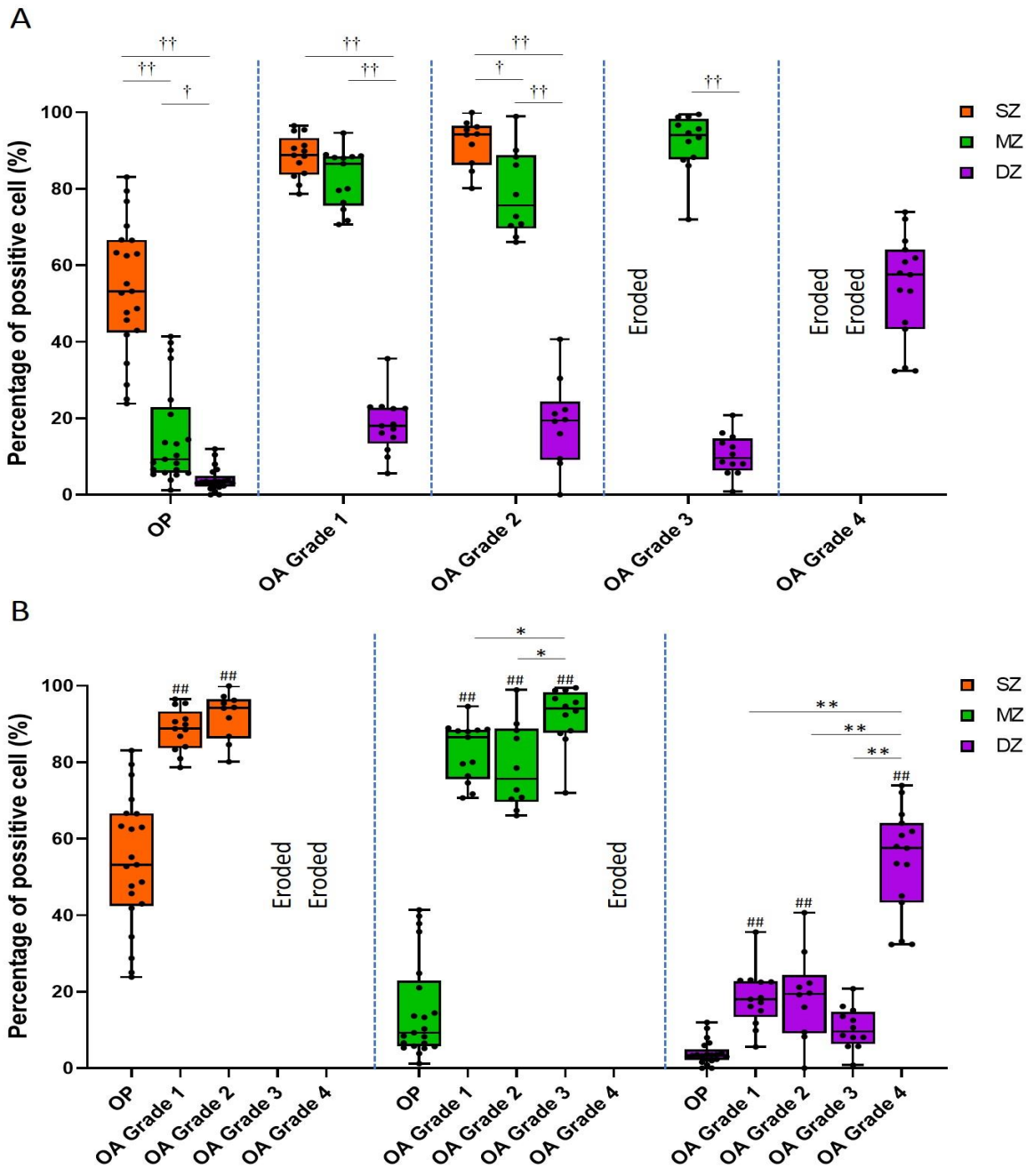

Figure 6.4. Zonal expression of ADAMTS4 in OP and different stages of OA. (A) intra-group comparisons between the superficial zone (SZ), middle zone (MZ), and deep zone (DZ) in OP and each OA Grade. Statistical significance is indicated by †. (B) inter-group comparisons between OA Grades (statistical significance indicated by *) and between OP and OA Grades (statistical significance is indicated by #) in each zone. The boxplot shows the median, the interquartile range (IQR), and individual values. †P < 0.05; ††P < 0.001; the same for * and #.

6.3.1.2.2 Inter-group comparisons

For the SZ, there was no statistically significant difference in the expression of ADAMTS4 between OA Grade 1 and Grade 2 (unpaired Student T test, P=0.162), but both Grade 1 and Grade 2 had significantly higher percentage of positively stained cells compared to OP (Bonferroni test, both P<0.001) (**Figure 6.4B**). In the MZ of OA group, a significant regional variation with regard to local severity of cartilage degradation was detected (ANOVA, P<0.05) (**Figure 6.4B**). Specifically, OA Grade 3 had significantly more chondrocytes expressing ADAMTS4 than both Grade 1 and Grade 2 in the MZ (Bonferroni test, both P<0.05). When OP group was included in the analysis, it was shown that all OA Grades had significantly higher percentage of ADAMTS4-expressing chondrocytes than OP in the MZ (Bonferroni test, all P<0.001). In the OA group, with loss of cartilage progressing into the DZ (Grade 4), the remaining chondrocytes appeared to be significantly more active in producing ADAMTS4 than those in the DZ of OA Grade 1, 2 and 3 (ANOVA, P<0.001; Bonferroni test, P<0.001 for Grade 4 *vs* Grade 1, 2, and 3) (**Figure 6.4B**). However, before cartilage matrix in DZ was affected, i.e., in OA Grade 1, 2, and 3, the expression of ADAMTS4 by chondrocytes in the DZ was not significantly different (Bonferroni test, P>0.05 for each pair of comparison). The ADAMTS4 production in the DZ of OP group was significantly lower compared to that in the DZ of OA at various stages of cartilage degradation (Bonferroni test, P<0.001 for OP *vs* Grade 1, 2, and 4) except Grade 3 (Bonferroni test, P>0.05).

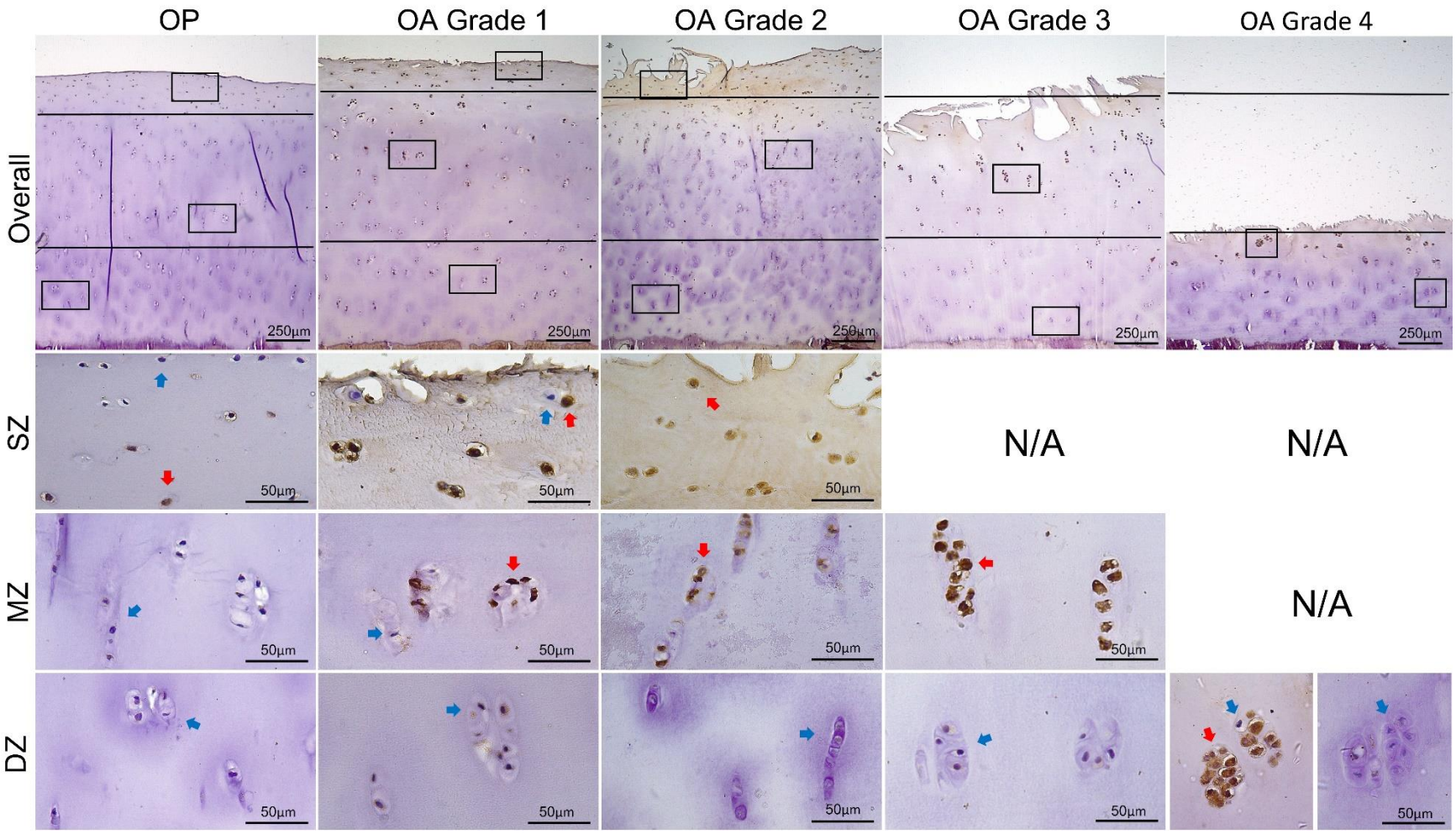

Figure 6.5. Representative images of IHC staining with ADAMTS4 in OP and different stages of OA. The overall expression through full-thickness of cartilage is presented in the first row at 40x magnification. Lines indicate separation of superficial (SZ), middle (MZ) and deep (DZ) zones and squares indicate areas shown at higher magnification (400x) in the subjacent rows. Blue and red arrows point to typical negatively and positively stained cells, respectively.

6.3.2 Expression of MMP13

Overall and zonal expressions of MMP13 are summarised in **Table 6.2**. Results of intra- and inter-group comparisons are illustrated in **Figure 6.6** (overall expression) and **Figure 6.7** (zonal expression). Typical examples of IHC staining for MMP13 are presented in **Figure 6.8**.

Table 6.2. Overall and zonal expression of MMP13.

	OP (N=21)	OA Grade 1 (N=13)	OA Grade 2 (N=10)	OA Grade 3 (N=12)	OA Grade 4 (N=15)
MMP13					
Overall	22.76±10.57	61.22±8.29	61.53±11.82	54.55±8.99	53.17±12.37
SZ	56.39±19.62	88.64±7.33	91.73±4.64	/	/
MZ	19.25±16.11	83.59±10.35	80.22±11.82	92.52±6.34	/
DZ	4.45±3.58	17.90±8.67	17.87±12.55	11.07±6.26	53.17±12.37

Data are presented as percentage (mean ± SD) of positively stained chondrocytes. SZ, superficial zone; MZ, middle zone; DZ, deep zone.

6.3.2.1 Overall expression of MMP13

OA Grade 1 and Grade 2 samples had 61.22% and 61.53% chondrocytes producing MMP13 across the full-depth of cartilage while Grade 3 and 4 had about 54.55% and 53.17%, respectively (**Table 6.2**). There was no statistically significant variation in the overall expression of MMP13 within OA group in relation to local severity of cartilage degradation, as shown by one-way ANOVA (P=0.104) and Bonferroni post-hoc tests (**Figure 6.6**). When the OP group (22.76% positive cells) was included in the analysis, overall expression of MMP13 was significantly higher in all OA grades compared to OP (Bonferroni test, all P<0.001) (**Figure 6.6**).

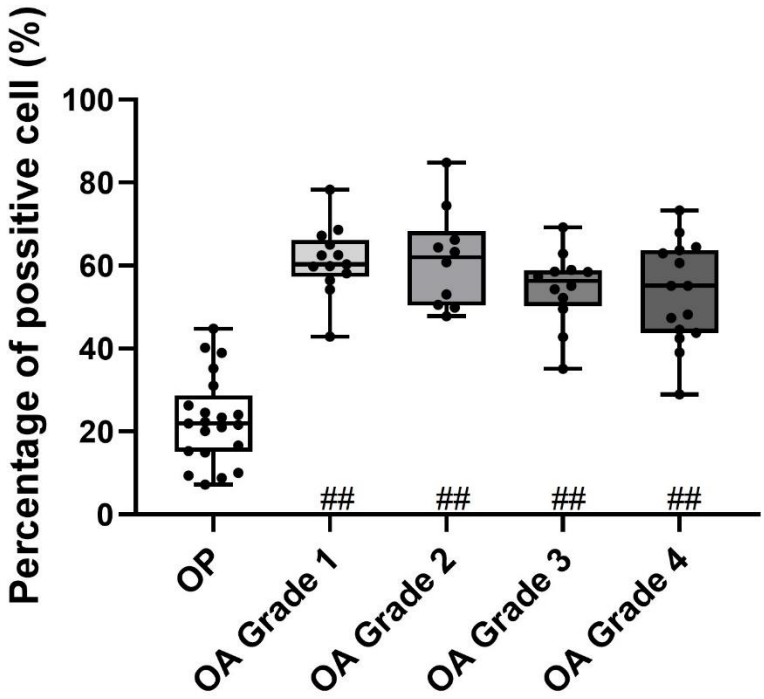

Figure 6.6. Comparisons of overall expression of MMP13 in relation to severity of OA cartilage degeneration. The boxplot shows the median, the interquartile range (IQR), and individual values. Statistical significance is indicated by * or # for multiple comparisons between OA Grades, and between OP and OA Grades, respectively, according to post-hoc tests. *P < 0.05; **P < 0.001; the same for #.

6.3.2.2 Zonal expression of MMP13

6.3.2.2.1 Intra-group comparisons

In general, there were more chondrocytes expressing MMP13 in the upper zone(s) in OP and all OA groups (**Table 6.2**, **Figure 6.7A**, **Figure 6.8**). In the OP group, about 56.39% of chondrocytes expressed MMP13 in the SZ, and 19.25% and 4.45% in the MZ and DZ respectively. The Differences between the three zones in OP were statistically significant (K-W test, P<0.001; Dunn's test, P<0.001 for SZ *vs* MZ and SZ *vs* DZ, and P<0.05 for MZ *vs* DZ). In contrast, over 80% of chondrocytes appeared to be producing MMP13 in the SZ (88.64%) and MZ (83.59%) in OA Grade 1, which were both significantly higher than the percentage expression in the DZ (17.90%) (ANOVA, P<0.001; Bonferroni test, P<0.001 for SZ *vs* DZ and MZ *vs* DZ). Similarly, in OA Grade 2, about 91.73% and 80.22% of chondrocytes expressed MMP13 in the SZ and MZ, respectively, and only about 17.87% in the DZ. The zonal differences were

statistically significant between SZ and DZ and between MZ and DZ (ANOVA, $P<0.001$; Bonferroni test, both $P<0.001$), but not between SZ and MZ. As for OA Grade 3, when the SZ was depleted, 92.52% of cells in the MZ were expressing MMP13, whereas majority of cells in the DZ were still inactive (only 11.07% cells were positively stained) (Mann-Whitney U test, $P<0.001$ for MZ *vs* DZ). Again, zonal comparisons were not made for OA Grade 4, in which about 53.17% chondrocytes produced MMP13.

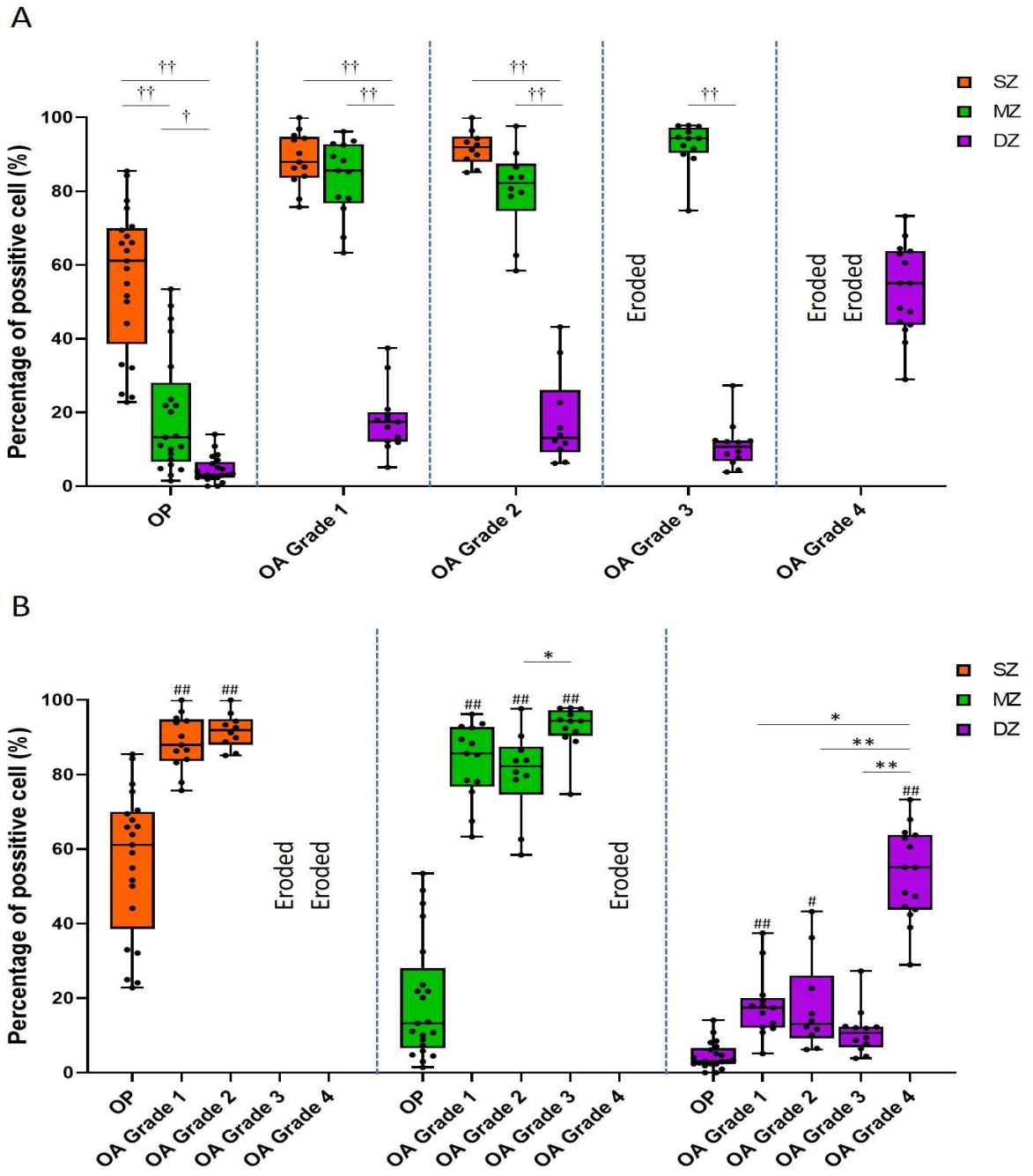

Figure 6.7. Zonal expression of MMP13 in OP and different stages of OA. (A) intra-group comparisons between the superficial zone (SZ), middle zone (MZ), and deep zone (DZ) in OP and each OA Grade. Statistical significance is indicated by †. (B) inter-group comparisons between OA Grades (statistical significance indicated by *) and between OP and OA Grades (statistical significance is indicated by #) in each zone. The boxplot shows the median, the interquartile range (IQR), and individual values. †P < 0.05; ††P < 0.001; the same for * and #.

6.3.2.2.2 Inter-group comparisons

For comparisons between different stages of OA (**Figure 6.7B**), it was shown that there was no significant difference between OA Grade 1 and Grade 2 in the expression of MMP13 in the SZ (unpaired Student T test, P=0.258). However, the expression in MZ was significant higher at OA Grade 3 compared to Grade 2 (ANOVA, P<0.05; Bonferroni test, P<0.05 for Grade 2 *vs* Grade 3, P>0.05 for Grade 1 *vs* Grade 2 and Grade 1 *vs* Grade 3). As for DZ, MMP13 production was significantly higher in OA Grade 4 compared to Grade 1, 2 and 3 (K-W test, P<0.001; Dunn' test, P<0.05 for Grade 1 *vs* Grade 4, and P<0.001 for Grade 2 and Grade 3 *vs* Grade 4).

For comparisons between OP and OA Grades (**Figure 6.7B**), in the SZ, the percentage of MMP13-producing chondrocytes in OP was significantly lower than those in OA Grade 1 and Grade 2 (Bonferroni test, both P<0.001). Similarly, in the MZ, OP group had significantly less chondrocytes expressing MMP13 compared to OA Grade 1, 2 and 3 (Bonferroni test, all P<0.001). As for the DZ, statistically significant differences were found between OP and OA Grade 1, 2, and 4 (Dunn' test, P<0.001 for OP *vs* Grade 1 and Grade 4, and P<0.05 for OP *vs* Grade 2), but not between OP and OA Grade 3 (Dunn' test, P>0.05).

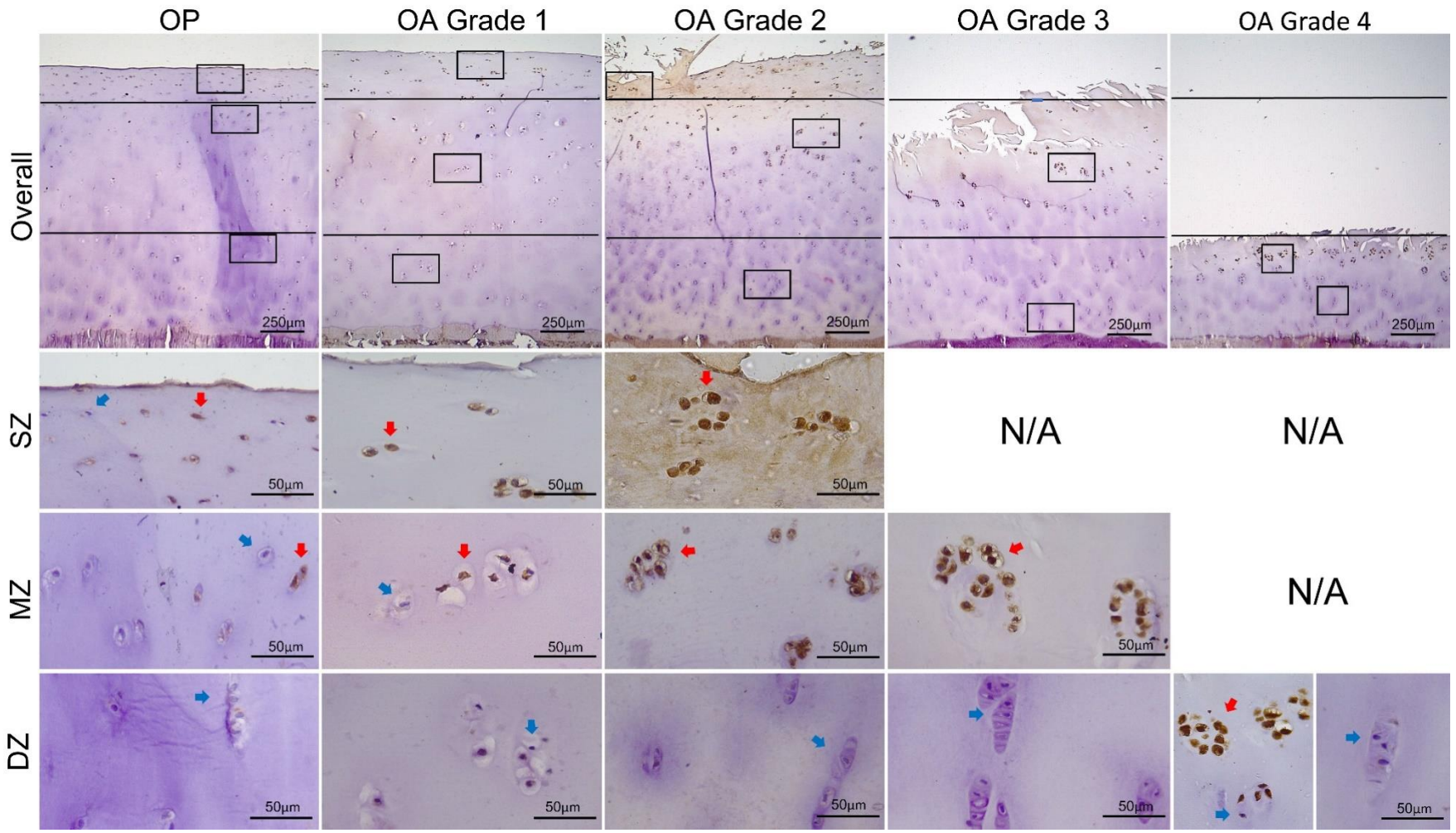

Figure 6.8. Representative images of IHC staining with MMP13 in OP and different stages of OA. The overall expression through full-thickness of cartilage is presented in the first row at 40x magnification. Lines indicate separation of superficial (SZ), middle (MZ) and deep (DZ) zones and squares indicate areas shown at higher magnification (400x) in the subjacent rows. Blue and red arrows point to typical negatively and positively stained cells, respectively.

6.3.3 Correlations between enzyme expression and subchondral bone properties

Results of correlations between the expression of ADAMTS4 and MMP13 by chondrocytes and the microarchitectural and mineral properties of subchondral bone are summarised in **Table 6.3** and **Table 6.4**.

For the OP group, no statistically significant associations were found, for either ADAMTS4 or MMP13. For the OA group, a few subchondral bone parameters were found to be significantly associated with either zonal or overall expression of the two enzymes, but the correlations were generally weak with a P value of just below 0.05 and correlation coefficients around 0.3. In specific, the overall expression of ADAMTS4 in OA cartilage was significantly and negatively associated with BV/TV, Tb.Th, and BMD, and positively with TMD of the subchondral trabecular bone (P=0.049, 0.03, 0.03, and 0.02, Pearson' correlation coefficient=-0.28, -0.30, -0.30 and 0.33, respectively). The expression of MMP13 in the DZ of cartilage was significantly associated with BV/TV, Tb.Th, and Tb.TMD (P=0.049, 0.03, 0.02, Spearman's correlation coefficient=0.28, 0.31 and -0.34, respectively). The overall expression of MMP13 in full-thickness OA cartilage was associated with Conn.Dn and BMD of the subchondral trabecular bone (P=0.03 and 0.046, Pearson' correlation coefficient=-0.31 and -0.28, respectively).

Table 6.3. Correlations between the expression of ADAMTS4 by chondrocytes and subchondral bone microarchitecture and mineral densities.

ADAMTS4	OP				OA			
	SZ	MZ	DZ	Overall	SZ	MZ	DZ	Overall
BV/TV	0.74 (-0.08)	0.09 (-0.38)	0.99 (0.003)	0.45 (-0.18)	0.24 (0.25)	0.20 (0.22)	0.12 (0.22)	0.049* (-0.28)
Tb.Th	0.72 (-0.08)	0.98 (0.01)	0.09 (0.38)	0.64 (0.11)	0.35 (0.21)	0.06 (0.32)	0.10 (0.24)	0.03* (-0.30)
Tb.N	0.92 (0.02)	0.30 (-0.28)	0.41 (-0.26)	0.23 (-0.27)	0.51 (0.14)	0.57 (0.10)	0.36 (0.13)	0.22 (-0.18)
BS/BV	0.52 (0.15)	0.65 (0.11)	0.18 (-0.31)	0.93 (-0.02)	0.50 (-0.15)	0.05 (-0.33)	0.15 (-0.21)	0.06 (0.26)
SMI	0.30 (0.24)	0.22 (0.28)	0.13 (0.34)	0.41 (0.19)	0.78 (0.06)	0.16 (-0.24)	0.15 (-0.21)	0.44 (0.11)
Conn.Dn	0.80 (-0.06)	0.15 (-0.33)	0.50 (-0.16)	0.30 (-0.24)	0.05 (0.41)	0.52 (0.11)	0.19 (0.19)	0.14 (-0.21)
Pl.Th	0.33 (0.22)	0.58 (-0.13)	0.73 (0.08)	0.63 (0.11)	0.28 (0.24)	0.17 (0.24)	0.18 (0.19)	0.67 (-0.06)
BMD	0.87 (-0.04)	0.08 (-0.39)	0.87 (-0.04)	0.57 (-0.13)	0.20 (0.28)	0.19 (0.23)	0.18 (0.19)	0.03* (-0.30)
Tb.TMD	0.91 (0.03)	0.11 (0.36)	0.96 (0.01)	0.57 (0.13)	0.25 (-0.25)	0.21 (-0.22)	0.08 (-0.25)	0.02* (0.33)
Pl.TMD	0.74 (-0.08)	0.78 (-0.06)	0.93 (-0.072	0.84 (0.05)	0.31 (-0.22)	0.82 (-0.04)	0.05 (-0.28)	0.41 (-0.12)

Associations between chondrocyte expression of ADAMTS4 and subchondral bone properties were determined using Pearson's correlation or Spearman's correlation (underlined). Data shown are P values (correlation coefficients). Statistically significant results are indicated by *.

Table 6.4. Correlations between the expression of MMP13 by chondrocytes and subchondral bone microarchitecture and mineral densities

MMP13	OP				OA			
	SZ	MZ	DZ	Overall	SZ	MZ	DZ	Overall
BV/TV	0.53 (-0.14)	0.19 (-0.30)	0.88 (0.04)	0.40 (-0.19)	0.06 (0.40)	0.17 (0.24)	0.049* (0.28)	0.12 (-0.22)
Tb.Th	0.86 (-0.04)	0.56 (-0.13)	0.76 (0.07)	0.94 (0.02)	0.78 (0.06)	0.55 (0.10)	0.03* (0.31)	0.14 (-0.21)
Tb.N	0.68 (-0.09)	0.20 (-0.29)	0.92 (0.02)	0.39 (-0.20)	0.10 (0.21)	0.17 (0.24)	0.55 (0.09)	0.14 (-0.21)
BS/BV	0.54 (0.14)	0.36 (0.21)	0.99 (-0.00)	0.71 (0.08)	0.54 (-0.14)	0.37 (-0.16)	0.06 (-0.27)	0.14 (0.21)
SMI	0.14 (0.34)	0.61 (0.12)	0.11 (0.36)	0.28 (0.25)	0.05 (-0.22)	0.30 (-0.31)	0.09 (-0.24)	0.99 (-0.00)
Conn.Dn	0.87 (-0.04)	0.27 (-0.25)	0.35 (-0.22)	0.47 (-0.17)	0.12 (0.33)	0.86 (0.03)	0.11 (0.23)	0.03* (-0.31)
Pl.Th	0.95 (-0.01)	0.16 (-0.32)	0.27 (-0.25)	0.60 (-0.12)	0.93 (-0.02)	0.87 (0.03)	0.37 (0.13)	0.20 (-0.18)
BMD	0.66 (-0.10)	0.31 (-0.23)	0.88 (0.03)	0.56 (-0.14)	0.07 (0.39)	0.17 (0.24)	0.10 (0.24)	0.046* (-0.28)
Tb.TMD	0.59 (0.13)	0.21 (0.29)	0.45 (0.17)	0.34 (0.22)	0.06 (-0.40)	0.06 (-0.32)	0.02* (-0.34)	0.12 (0.22)
Pl.TMD	0.40 (-0.19)	0.78 (-0.07)	0.52 (0.15)	0.94 (-0.02)	0.47 (0.16)	0.96 (0.01)	0.51 (-0.10)	0.67 (0.06)

Associations between chondrocyte expression of ADAMTS4 and subchondral bone properties were investigated using Pearson's correlation or Spearman's correlation (underlined). Data presented are P values (correlation coefficients). Statistically significant results are indicated by *.

6.4 DISCUSSION

In this chapter, we carried out a detailed investigation of the expression of MMP13 and ADAMTS4 by chondrocytes in OA and OP cartilage. We showed that chondrocytes expressing these enzymes are mainly located in the upper zone(s) of cartilage regardless of the stage of degradation. It was also shown that the zonal expression of MMP13 and ADAMTS4 in OA, rather than their overall expression, exhibited a significant variation with the severity of cartilage degradation. We have also shown for the first time that the associations between subchondral bone properties and expression of the two main enzymes responsible for cartilage ECM degradation by chondrocytes were not statistically significant in OP, and were generally weak or not significant in OA.

Since the cloning of MMP13 in early 90s (685), numerous studies have been dedicated to exploring its role in OA. The team led by Martel-Pelletier was among the earliest to report the localisation of MMP13 expressing chondrocytes in both human and animal OA cartilage (686, 687). Consistent with results presented in this study, they showed that the overall immunoreactivity through full-thickness of human OA cartilage was not significantly different between non-fibrillated and fibrillated regions. They also reported that the increased production of MMP13 in OA mainly came from chondrocytes in the DZ and lower MZ and thus they suggested that biological factors diffused from subchondral bone may be, at least partly, responsible for the phenotypic changes of chondrocytes in OA. However, this contrasts with data presented here as well as a number of other previous studies which showed that MMP13 production was mainly located in the upper zone(s) (332, 666, 688, 689), irrespective of whether the sample had early or advanced cartilage degradation. In addition, the steep drop in the percentage of positive cells from MZ to DZ in OA Grade 1, 2, and 3 in this study corresponds to the strikingly sharp transition shown by Wu et al (688) between areas displaying extensive staining and those with limited staining. This may indicate a very slow progression of the phenotypic change in the OA chondrocyte population (688), which will be further discussed later. Animal studies further added to the complexity, with those showing MMP13 expression mainly in SZ (675, 682, 683), DZ (687), or across the entire specimen (664, 684).

Compared with MMP13, the localisation of ADAMTS4 production in OA cartilage is more consistent in the literature. Chondrocytes expressing ADAMTS4 are predominantly located in the upper zone(s) of articular cartilage in both patients (666, 689, 690) and animal models (664), as was shown by the present study. This is in line with the universal observation that the loss of proteoglycans is most significant at and near the articular surface across various stages of OA, as demonstrated by the reduced cationic (toluidine blue or safranin O) staining. It is also worth noting that the zonal distribution of ADAMTS4 production was similar with that of MMP13 (**Figure 6.4** and **Figure 6.7**), supporting the contention that these two enzymes are co-expressed by the same group of chondrocytes in OA (689), a group termed as the 'degradative chondrocytes' (689, 690). Such co-expression can be further verified either by staining the consecutive tissue sections, or by double antibody labelling. However, this is beyond the scope of the current study.

The findings that both ADAMTS4 and MMP13 are produced by chondrocytes located in the upper zone(s) are supportive of the concept that cellular alternations in OA cartilage, including proliferation and hypertrophic differentiation, starts from articular surface (323, 688). With matrix degradation advancing toward subchondral bone and with increasing severity of cartilage damage, it was expected that chondrocytes in the deeper layers of cartilage would become affected and exhibit the degradative phenotype (688-690), starting to express proteinases (e.g., collagenases and aggrecanases) and matrix components (e.g., Col X) that are not seen in healthy adult cartilage (668, 691). However, the data presented in this chapter show that chondrocytes in the DZ, which were not expressing MMP13 and ADAMTS4 in OA Grade 1 and Grade 2, were still 'clean' of staining (negative for production of the enzymes) when matrix loss progressed into the MZ (Grade 3). More surprisingly, even when matrix degradation developed into the DZ (Grade 4) and there was just a thin layer of cartilage left, almost half of the surviving chondrocytes, located mainly in the lower DZ next to subchondral bone, were still negatively stained and displayed relatively normal morphology. In Grade 3 and Grade 4, chondrocytes expressing MMP13 and ADAMTS4 increased in the MZ and DZ respectively, but the positively stained cells were located almost exclusively in clusters near the surface and fissures (**Figure 6.5** and **Figure 6.8**). These observations explain why the overall expression of the enzymes did not vary significantly between OA grades and may have important implications.

First, a theoretical model of cartilage degradation in the process of OA can be suggested. Initially, degradation of the ECM is driven largely by the proteolysis of macromolecules, as a result of the phenotypic change of chondrocytes in the upper zones with increased production of cytokines, collagenase(s) and aggrecanase(s). Once the ECM is compromised, cartilage loses its unique elastic and frictionless properties and becomes more susceptible to mechanical destruction. The mechanical wear of the cartilage with inferior quality advances toward deeper layers quickly, while the shift of chondrocyte phenotype may be a much more gradual process that takes years (688). At a certain stage of progression (likely to be between Grade 2 and Grade 3), the direct damaging effects of mechanical forces may outrun that of biochemical disruption and reach the deeper layers of cartilage before subjacent chondrocytes develop a degradative phenotype. Then at the late- to end-stage of OA (Grade 4 to Grade 5), erosion of the last portion of cartilage leading to the exposure of subchondral bone may be largely or purely mechanical rather than biological. Earlier studies have pointed out long time ago that OA is not simply a consequence of 'wear and tear' but a disease resulting from both biological and biomechanical reactions with the former being more important (278, 305, 323, 351, 360, 692). The model presented here is consistent with these previous studies but additionally suggests that the relative contribution and importance of biological factors and mechanical disruptions to cartilage degradation and matrix loss may vary at different stages of the disease.

Second, it seems that biochemical factors (e.g., growth factors and cytokines) that induce chondrocyte dysfunction are mainly produced by chondrocytes in the upper zones to act in an autocrine or paracrine manner, and/or from the synovium rather than from subchondral bone and marrow. If this was not the case then the chondrocytes in the DZ, which are closest to subchondral bone and are subjected to vascular invasion, should be affected at least at some point in the degradation process. Another possibility is that chondrocytes in the DZ may function as an intermediate of subchondral bone derived signals rather than a direct effector that produces enzymes to degrade the ECM.

In the articular cartilage of OP patients which exhibited none or minor microscopic degenerative changes, there were also chondrocytes producing MMP13 and ADAMTS4, although the percentage was significantly less compared to OA in terms of both overall and

zonal distribution. This is natural since both chondrocytes and matrix macromolecules are subjected to a series of age-related changes. Senescence of chondrocytes is associated with an abnormal secretory phenotype characterised by increased production of cytokines, growth factors, and MMPs (362). In the meantime, accumulation of advanced glycation end products (AGEs) has an impact on the size and crosslinking of collagen fibres and aggrecan molecules, compromising the mechanical properties of ECM and rendering it susceptible to the effects of mechanical stress, which in turn further adds to the senescent phenotype of chondrocytes (281, 364). These events could be amplified in OP patients whose subchondral bone is subjected to accelerated and imbalanced remodelling, and whose skeletal system is exposed to a chronic inflammatory environment that may be responsible for such remodelling (199).

The findings that the level of MMP13 and ADAMTS4 expression in OP is significantly lower than OA are consistent with previous descriptive studies (689, 690) and explain the comparatively normal cartilage histology of OP samples. However, the current study additionally reported a more heterogeneous frequency of expression of these enzymes in OP cartilage compared with OA, especially in SZ in which the percentage of MMP13 and ADAMTS4 positive cells ranged from 20% to 80%. Such heterogeneity was also shown by Wu et al in aged but healthy knee joint (688). Based on this, and that the patterns of type II collagen cleavage and MMP13 expression were similar (e.g., more prominent in the upper zone(s)) between aged healthy and OA cartilage, Wu et al suggested that age-related changes in cartilage to some extent reflect the degenerative events at early stage of OA. Similarly, based on the data presented here, it is reasonable to suggest that at least some of the joints affected by OP may represent a pre-initiation or early stage of OA. Later in life, accumulation of degradative chondrocytes and their products, as a result of ageing, inflammation and/or subchondral bone remodelling, may reach a threshold that triggers an irreversible amplifying cascade leading to the progressive degradation of ECM seen in OA. In addition, it is worth noting that the distribution of ADAMTS4 production seemed to overlap with MMP13 in OP, indicating a co-expression of the two enzymes by ‘degradative chondrocytes’ which is also seen in OA as mentioned earlier. The above hypothesis is consistent with the existence of a subgroup of patients who suffered osteoporotic fracture and OA simultaneously (592).

Subchondral bone is important for the maintenance of cartilage physiology in normal joint, and contributes to cartilage pathology in disease conditions such as OA. It fulfils such roles by affecting the distribution of load in the overlying cartilage and through the cellular and biochemical crosstalk via osteochondral junction. However, in this study, a statistically significant correlation between cartilage enzyme expression (overall and zonal) and subchondral bone microarchitectural and mineral properties was only observed for a few of the parameters investigated and the associations were rather weak with P values between 0.02 and 0.05 and correlation coefficients just around 0.3. This was unexpected since both the zonal expression of MMP13 and ADAMTS4 by chondrocytes and the microarchitecture and mineralisation of subchondral bone exhibited significant variations in relation to the degree of cartilage damage (modified OARSI grading). One possible explanation for this finding may be that the efficiency of adaption in response to various mechanical or biological stimulus is markedly different between cartilage and bone (103, 113, 165). Bone remodelling is a rapid process, the duration of a typical remodelling cycle takes 3-6 months from osteoclast activation to the finish of bone formation by osteoblasts (82). On the contrary, turnover of cartilage matrix components, especially aggrecan and Col II, takes decades in normal conditions, reflecting the limited capacity of chondrocytes to modify its surrounding matrix (314). Though metabolic activities of chondrocytes are elevated in OA, it is still relatively slow and the phenotype transition may take years (165, 688). Therefore, the pathological changes in subchondral bone and chondrocytes are likely to be at different paces throughout OA, despite the fact that they both contribute to cartilage degradation. This is complementary to the cartilage degradation model suggested above: the increased mechanical stress borne by cartilage, as a result of the rapidly deteriorating subchondral bone properties and increasing shear forces, may outrun the biochemical degradation at some point and erodes cartilage quickly before chondrocytes in the deeper areas can respond.

The same principles may also apply for the observation of non-significant correlations between cartilage enzyme expression and subchondral bone microarchitectural and mineral properties in joints affected by OP. Although there is abnormal remodelling in subchondral bone, the number of degradative chondrocytes and the level of MMP13 and ADAMTS4 production in cartilage have not yet reached a threshold needed for the initiation of degradation cascade leading to OA. This may be due to the fact that, except for the influence

of subchondral bone, chondrocyte biology is affected also by many other genetic and environmental factors which have a chronic and cumulative impact.

6.5 SUMMARY

In this chapter, it was shown that the chondrocytes expressing MMP13 and ADMATS4 were mainly located in the upper zone(s) of cartilage regardless of the stage of degradation in OA and OP. The zonal expression of MMP13 and ADAMTS4 in OA varied with the severity of cartilage degradation, but the overall expression across the full-thickness of cartilage did not. The expression in OP was significantly lower in all zones compared to various stages of OA, but exhibited greater heterogeneity in the SZ. The associations between subchondral bone properties and expression of the two main enzymes responsible for cartilage degradation by chondrocytes were generally weak or not statistically significant in OA and OP. Based on these data, a theoretical model of cartilage degradation in OA can be suggested, that is, biochemical influences are more important for the ECM degradation at the initiation and early stage of OA, but the mechanical wear outruns biochemical effects and is responsible for the loss of cartilage at later stages.

Chapter 7

Final discussion

OA and OP are two of the most common musculoskeletal disorders associated with ageing. OP is characterised by systemic imbalanced bone remodelling toward excessive resorption, leading to bone loss and impaired mechanical properties and subsequent fragility. In contrast, resulting from both systemic and local factors, OA affects diarthrodial joints and involves pathological changes in all components of a joint, including cartilage degradation, subchondral bone remodelling, and synovial inflammation.

The relationship between OP and OA has been debated for decades. Clinical studies showed that patients with OA of the knee, hip, spine, or fingers generally have higher systemic BMD measured at the femoral neck or lumbar vertebrae, while the majority of patients who suffered osteoporotic fractures seemed to be free of joint damage (**Section 1.7.1**). In addition, subchondral bone sclerosis, represented by the increased radiographic intensity, is a hallmark of the joints affected by OA. These data are supportive of an inverse relationship between the two diseases. In contrast, there is also evidence indicating some similar features in the pathophysiology of OP and OA. Increased remodelling (384) and decreased BMD (382) have been identified in peri-articular bone at early stages of OA in human joints. Elevated level of urinary biomarkers of bone resorption has been found in patients showing OA progression (387). Moreover, numerous animal studies have revealed increased subchondral bone resorption after OA induction, and that accelerated loss of subchondral bone can lead to the development, or aggravate the progression, of OA (**Section 1.6.2.2**). The possible overlap between OP and OA promoted the use of anti-OP drugs as DMOADs, but to date they demonstrated limited and inconsistent evidence of efficacy for treating human OA and therefore have not been approved by any regulatory agencies.

A comprehensive investigation of the differences and similarities between OP and OA is needed, to better understand the associations between the two diseases and provide greater insights into the pathological process of OA. Such investigation should focus on the

osteochondral unit where direct relevant comparisons can be made. It should include features of both subchondral bone and cartilage, as well as the associations between them. It ought to be as detailed and comprehensive as possible, involving all aspects of tissue biology and making differentiations between sub-structures. A study of subchondral bone and cartilage in human hip OP and OA covering the above-mentioned criteria was the aim of this PhD project.

7.1 GENERAL DISCUSSION

Longitudinal tissue collection is not possible from human subjects due to obvious ethical restrictions. Therefore, variations in relation to different stages of local cartilage degradation may provide an acceptable reference for the temporal changes in OA. Accordingly, in Chapter 3, we first standardised a tissue collection procedure in order to provide osteochondral samples that cover and represent various stages of cartilage degradation in hip OA and OP. This procedure was built on the combination of a new macroscopic grading system and a modified version of the OARSI microscopic grading scheme for the evaluation of cartilage pathology. The macroscopic grading, based on a more detailed description of visually detectable changes on the articular surfaces of hip joint, guided the regionalised tissue extraction and ensured the range and diversity of samples. The original OARSI microscopic grading was optimised to overcome its innate disadvantage (i.e., not suitable for assessment of regionally extracted samples with relatively small volume) and to incorporate a number of new features that were observed on hip specimens. Based on the depth-specific and stratified characterisation, changes in cartilage matrix structure, cellular morphology and biochemical features can be clearly identified and differentiated and scored using the modified microscopic grading. Both the macro- and microscopic gradings appeared to be highly reproducible, as reflected by the excellent inter- and/or intra-observer agreement. More importantly, the two grading systems correlated very well with each other implying that they are both reliable tools for the assessment of cartilage pathology, and that the tissue collection procedure was precise in the generation of samples to represent different stages of cartilage degradation in this study.

The collected osteochondral plugs were scanned by microCT to examine the properties of subchondral bone in OP and in different stages of OA. In Chapter 4 and Chapter 5, we first verified the heterogeneity of subchondral bone properties in hip OA as a function of the severity of degradation of the overlying cartilage. The data showed that the microarchitecture of subchondral plate (Pl.Th) and subchondral trabecular bone (BV/TV, BS/BV, Tb.Th, Tb.N, SMI and Conn.Dn) varied significantly depending on the stage of cartilage degradation, changing toward sclerosis (thicker subchondral plate and volumetrically denser trabecular bone with thicker, plate-like and well-connected trabeculae) in more advanced disease. In addition, the data showed that the changes in the mineralisation (TMD) of subchondral trabecular bone was also significantly influenced by the status of cartilage, with hypo-mineralisation seen in sclerotic samples. Such heterogeneity supports the validity of using cartilage degradation as an indication of the process of OA development.

The next question to address was what the subchondral bone was like at early stage of OA as compared to OP? It was shown that the subchondral plate and trabecular bone underneath the cartilage with early degenerative changes in hip OA were similar to those in OP. Such similarity applies to a wide variety of parameters commonly used to describe the quantity and quality of bone, including volumetric, morphological, and mineral properties. These observations argue against Radin's original theory that subchondral sclerosis is responsible for the initiation of OA, and support the increasingly popular hypothesis that subchondral bone remodelling in OA is a biphasic process with a transition from favouring resorption at early stage to favouring formation at late stage. This transition is also accompanied by the altered capacity of bone to deposit minerals. Previous studies have reported the existence of different phenotypes of osteoblasts in OA joints, which could explain the varying behaviours of subchondral bone in the process of OA (421, 422, 632). Based on the data presented here, it is reasonable to further suggest that the pattern of subchondral bone remodelling toward resorption at early stage of OA may be similar to that in OP in terms of bone cells phenotype (e.g., expression profile) and remodelling status (e.g., osteoid surfaces and eroded surfaces). It is necessary to further compare these features in OP with different stages of OA, to provide information regarding the mechanism of early subchondral bone changes in OA and how it can be more specifically targeted for treatment of OA.

Although microarchitecture and mineralisation of subchondral trabecular bone changed in opposite directions with the increasing degree of cartilage degeneration in OA, they were intrinsically correlated and the overall effects pointed to a stiffened structure as indicated by the increase in BMD, which is a key predictor of bone strength at apparent level. This phenomenon implied that in OA the decreased matrix mineralization can be over-compensated by the increase in bone volume. Indeed, the hypo-mineralisation and increased bone formation in OA may not simply be a result of mechano-adaption in response to each other but are mainly consequences of the disease (i.e., disrupted joint mechanics and dysregulated remodelling activities) (566). The inverse correlation between BV/TV and TMD and between TMD and BMD, and the positive correlation between BV/TV and BMD were also found in subchondral trabecular bone affected by OP. Since OP is characterised by the progressive loss of bone, overall effects of these correlations seemed to point to an opposite direction compared to OA – the preservation of matrix mineralisation could not keep up with bone resorption, leading to the decreased BMD and subsequent compromised mechanical properties.

It was expected that the relationships among BV/TV, TMD and BMD were different between OP and OA in terms of the gradients of change, especially for samples with advanced cartilage degradation because the remodelling patterns were supposed to be distinct. However, this was not the case as shown by the similar regression slopes between different groups. These findings suggest a more complex mechanism affecting the relationship between structural and mineral properties of bone in the disease conditions, which may involve the combinatory effects of remodelling rate, remodelling balance, and mineralization kinetics.

Since subchondral bone microarchitecture and mineralisation were closely associated with the severity of cartilage degradation, in Chapter 6 we investigated how these properties of subchondral bone may affect the expression of enzymes by chondrocytes that are responsible for cartilage degradation. As in previous chapters, we first examined the zonal (percentage of positive cells in SZ, MZ and DZ) and overall expression (percentage of positive cells in full-thickness of cartilage) of MMP13 and ADAMTS4 by chondrocytes in OA as a function of the modified OARSI grading. It was shown that zonal expression rather than overall expression varied in different stages of OA. A characteristic distribution of the degradative chondrocytes

was also found – they were mainly located in the upper zone(s) and the DZ was less affected even when all other zones were eroded. Based on these data we suggested a novel model of cartilage degradation in OA, in which biological disruption of the ECM is more important in the initiation and early stages, while mechanical wear of the compromised tissue is faster than phenotypic change of chondrocytes and is critical in advanced stages.

The degradative chondrocytes characterised by the expression of MMP13 and ADAMTS4 in OA were also found in OP samples, probably as a result of ageing, inflammation, and/or remodelling of the subchondral bone. The percentage of these cells in OP was significantly lower compared to OA, but exhibited a wider variation. This may indicate that some of the OP samples were at the pre-initiation or early stage of OA. Further accumulation of the degradative chondrocytes and increased production of proteinases may finally reach a threshold that triggers an irreversible and amplifying cascade leading to the progressive degradation of ECM.

The correlations between expression of degradative enzymes by chondrocytes and subchondral bone properties in OA were statistically significant for just a few parameters examined, and the correlations were generally weak. For the OP group, these correlations were not statistically significant. These findings may reflect the markedly different capacity and efficiency of bone cells and chondrocytes to adapt to the dynamic biological and biomechanical environment. The pathological changes in subchondral bone and chondrocytes are likely to proceed at different rates throughout the process of OA. The rapidly deteriorating properties of subchondral bone may accelerate the mechanical wear of the ECM and erode cartilage before chondrocytes in the DZ adopt a degradative phenotype, further supporting the degradation model suggested above.

7.2 STRENGTH, LIMITATIONS, AND FUTURE STUDIES

Previous clinical studies contrasting the changes in bone in OP and OA were generally based on radiographic imaging techniques which were subjected to a variety of technical limitations and could only provide estimation of BMD at systemic level. The current study focused on the

comparison of subchondral bone between the two diseases, and benefited from the higher resolution of microCT which allowed accurate assessment of bone microarchitecture and matrix mineralisation, as well as differentiation between subchondral plate and trabecular bone. More importantly, based on the regionalised tissue collection protocol and combined macro- and microscopic evaluation of cartilage pathology, this study was able to compare subchondral bone changes in OP with those in different stages of cartilage degradation in OA, which has not been reported in the literature before. Compared to previous studies which collected samples from fixed anatomical site(s) of femoral heads without considering the effects of cartilage, the current study provided data that can be used as a reference for the stagewise changes in subchondral bone in the pathological process of OA. Future studies should include samples collected from young and age-matched healthy subjects (cadaveric specimens) to provide baseline information for subchondral bone microarchitecture and mineralisation.

This study developed a new approach for histological processing and sectioning of osteochondral tissue. Compared to traditional processing protocol, the new method skipped the lengthy and labour-consuming decalcification procedure and permitted preservation of full-thickness cartilage without sacrificing the deepest areas. Tissue sections resulted from the new processing approach displayed excellent quality for both histological and immunohistochemical studies on cartilage. However, decalcification is still an indispensable step if subchondral bone is the among the main targets of research. In this study we planned to carry out IHC on both cartilage and subchondral bone on the same osteochondral samples scanned by microCT. This goal was not achieved as those samples had to go through multiple freeze-thaw cycles during which the quality of tissue was compromised. This technical limitation shall be addressed in future studies.

In the current study we showed that subchondral bone at an early stage of cartilage degradation had features in common with those in OP, in terms of both microarchitecture and matrix mineralisation. However, it should be noted that desktop microCT is associated with beam-hardening effects and can only measure the mean degree of mineralisation of bone tissue (TMD). As a result, the heterogeneity of mineralisation at the lamellar level (bone mineral density distribution (BMDD)) was overlooked. BMDD is a more comprehensive

assessment of bone mineralisation status and is significantly altered in various musculoskeletal conditions including OP but has rarely been investigated in OA (19). Therefore, techniques such as quantitative backscatter scanning electron microscopy and calibrated monochromatic synchrotron microCT imaging can be used in the future to confirm the similarity and/or differences of subchondral bone mineralisation in OP and different stages of OA. This, together with cell phenotyping and histomorphometry studies, will provide a more detailed understanding of subchondral bone remodelling in the pathological process of OA.

BMD is determined by BV/TV and TMD and is an indicator of trabecular bone strength. BMD varied significantly between regions with early and advanced cartilage degradation in OA specimens. These data may indicate a steep stiffness gradient between porotic and sclerotic regions of subchondral bone, which we suggest may be the cause of the phenotypic changes of bone cells that are responsible for the transition of remodelling balance from resorption to formation. Further studies using mechanical tests to determine the elastic modulus and ultimate strength of subchondral bone in these regions are needed to verify our hypothesis.

Calculation of the percentage of chondrocytes stained positive for target proteins is a semi-quantitative measurement of the level of expression. Polymerase chain reaction (PCR) and western blot, which can be used to directly measure the quantity of mRNA and protein respectively, may be utilised in the future to examine the relationship between subchondral bone properties and expression of proteinases. In addition, although chondrocytes in the DZ were not producing ADAMTS4 and MMP13, they may still be abnormal and may function as a mediator of biochemical signals originated from subchondral bone as discussed in Chapter 6. Further study of other biomarkers of chondrocyte hypertrophy is needed, such as RANKL, Col X and VEGF. Identification of different phenotypes of chondrocytes in different zones may help understand the role of subchondral bone derived factors in OA.

Another limitation of our study is the assumption of independence of samples in data analysis, when multiple plugs were sampled from the same specimen. We made this assumption because the plug collection was based on the condition of the overlying cartilage, and the histopathological evaluation confirmed that our sampling procedure well represented and differentiated between varying degrees of cartilage degradation. This assumption is

supported by the intra-specimen variation of bone parameters in relation to regional severity of cartilage degradation observed in this and other previous studies (420, 426, 566, 567).

Finally, the findings reported in this project should be confirmed by animal studies. To date a direct and longitudinal comparison of subchondral bone microarchitecture and mineralisation as a function of cartilage degradation between OP and OA animal models has not been reported in the literature. As an example, animals of the same species can be allocated into three groups: a control group, an OP group (induced by ovariectomy, orchiectomy or glucocorticoids etc), and an OA group (induced by joint destabilisation or joint overload etc). The temporal changes in both cartilage and subchondral bone shall be closely monitored using different techniques such as histology, IHC, PCR, biochemical analysis and microCT to investigate the similarities and differences between OP and OA.

7.3 CONCLUSION

This PhD project developed a new macroscopic grading system and modified the OARSI microscopic grading scheme for the evaluation of cartilage pathology in hip OA and OP. Development of these procedures allowed histopathological evaluation of regionally collected samples with relatively small dimensions and permitted collection of osteochondral samples representing various stages of cartilage degradation in a standardised manner. Using microCT, it was shown that the microarchitecture and mineralisation of subchondral bone varied significantly depending on the stage of cartilage degradation in OA, changing toward sclerosis and hypo-mineralisation in more advanced disease. Moreover, subchondral bone with early cartilage degradation in OA was similar to those in OP in terms of both microarchitecture and mineralisation. These findings indicate that subchondral bone remodelling in OA is a biphasic process and at an early stage it may have the similar pattern as in OP. Based on IHC studies, it was shown that chondrocytes expressing MMP13 and ADAMTS4 were located mainly in the upper zone(s) of cartilage in both OP and OA. The zonal expression of MMP13 and ADAMTS4 by chondrocytes in OA exhibited a significant variation with the severity of cartilage degradation. The expression was significantly lower in OP in all zones compared to various stages of OA, but exhibited greater heterogeneity in the SZ. The

correlations between expression of degradative enzymes by chondrocytes and subchondral bone properties in OA and OP were statistically significant for a few of the parameters examined, and the correlations were generally weak. Based on these data a novel model of cartilage degradation in OA can be proposed, in which biochemical disruption is more important in early stages while mechanical wear is critical in advanced stages.

Reference

1. Reznikov N, Bilton M, Lari L, Stevens MM, Kröger R. Fractal-like hierarchical organization of bone begins at the nanoscale. Science. 2018;360(6388).

2. Ren L, Yang P, Wang Z, Zhang J, Ding C, Shang P. Biomechanical and biophysical environment of bone from the macroscopic to the pericellular and molecular level. Journal of the Mechanical Behavior of Biomedical Materials. 2015;50:104-22.

3. Weiner S, Wagner HD. The material bone: structure-mechanical function relations. Annual Review of Materials Science. 1998;28(1):271-98.

4. Teti A. Bone development: overview of bone cells and signaling. Current Osteoporosis Reports. 2011;9(4):264-73.

5. Seeman E. Bone modeling and remodeling. Critical Reviews in Eukaryotic Gene Expression.2009;19(3).

6. Robling AG, Turner CH. Mechanical signaling for bone modeling and remodeling. Critical Reviews in Eukaryotic Gene Expression.2009;19(4).

7. Cohen Jr MM. The new bone biology: pathologic, molecular, and clinical correlates. American Journal of Medical Genetics Part A. 2006;140(23):2646-706.

8. Fratzl P, Gupta H, Paschalis E, Roschger P. Structure and mechanical quality of the collagen–mineral nano-composite in bone. Journal of Materials Chemistry. 2004;14(14):2115-23.

9. Olszta MJ, Cheng X, Jee SS, Kumar R, Kim Y-Y, Kaufman MJ, et al. Bone structure and formation: A new perspective. Materials Science and Engineering. 2007;58(3-5):77-116.

10. Garnero P. The role of collagen organization on the properties of bone. Calcified Tissue International. 2015;97(3):229-40.

11. Viguet-Carrin S, Garnero P, Delmas PD. The role of collagen in bone strength. Osteoporosis International. 2006;17(3):319-36.

12. Ruppel M, Miller L, Burr D. The effect of the microscopic and nanoscale structure on bone fragility. Osteoporosis International. 2008;19(9):1251-65.

13. Landis WJ, Hodgens KJ, Arena J, Song MJ, McEwen BF, technique. Structural relations between collagen and mineral in bone as determined by high voltage electron microscopic tomography. Microscopy Research and Technique. 1996;33(2):192-202.

14. Downey PA, Siegel MI. Bone biology and the clinical implications for osteoporosis. Physical Therapy. 2006;86(1):77-91.

15. Von Euw S, Chan-Chang T-H-C, Paquis C, Haye B, Pehau-Arnaudet G, Babonneau F, et al. Organization of bone mineral: the role of mineral–water interactions. Geosciences. 2018;8(12):466.

16. Lotsari A, Rajasekharan AK, Halvarsson M, Andersson M. Transformation of amorphous calcium phosphate to bone-like apatite. Nature communications. 2018;9(1):1-11.

17. Landi E, Celotti G, Logroscino G, Tampieri A. Carbonated hydroxyapatite as bone substitute. Journal of the European Ceramic Society. 2003;23(15):2931-7.

18. Ruffoni D, Fratzl P, Roschger P, Klaushofer K, Weinkamer R. The bone mineralization density distribution as a fingerprint of the mineralization process. Bone. 2007;40(5):1308-19.

19. Roschger P, Paschalis E, Fratzl P, Klaushofer K. Bone mineralization density distribution in health and disease. Bone. 2008;42(3):456-66.

20. Fuchs RK, Faillace ME, Allen MR, Phipps RJ, Miller LM, Burr DB. Bisphosphonates do not alter the rate of secondary mineralization. Bone. 2011;49(4):701-5.

21. Wang Y, Von Euw S, Fernandes FM, Cassaignon S, Selmane M, Laurent G, et al. Water-mediated structuring of bone apatite. Nature Materials. 2013;12(12):1144-53.

22. Gorski JP. Biomineralization of bone: a fresh view of the roles of non-collagenous proteins. Frontiers in Bioscience. 2011;16:2598.

23. Anderson HC. Matrix vesicles and calcification. Current Rheumatology Reports. 2003;5(3):222-6.

24. Morgan S, Poundarik AA, Vashishth D. Do non-collagenous proteins affect skeletal mechanical properties? Calcified Tissue International. 2015;97(3):281-91.

25. Licini C, Vitale-Brovarone C, Mattioli-Belmonte M. Collagen and non-collagenous proteins molecular crosstalk in the pathophysiology of osteoporosis. Cytokine & Growth Factor Reviews. 2019;49:59-69.

26. Yoder CH, Pasteris JD, Worcester KN, Schermerhorn DV. Structural water in carbonated hydroxylapatite and fluorapatite: confirmation by solid state 2 H NMR. Calcified Tissue International. 2012;90(1):60-7.

27. Nyman JS, Ni Q, Nicolella DP, Wang X. Measurements of mobile and bound water by nuclear magnetic resonance correlate with mechanical properties of bone. Bone, 2008;42(1):193-9.

28. Fernandez-Seara MA, Wehrli SL, Wehrli FW. Diffusion of exchangeable water in cortical bone studied by nuclear magnetic resonance. Biophysical Journal. 2002;82(1):522-9.

29. Nyman JS, Roy A, Shen X, Acuna RL, Tyler JH, Wang X. The influence of water removal on the strength and toughness of cortical bone. Journal of Biomechanics. 2006;39(5):931-8.

30. Burr DB. Bone morphology and organization. Basic and applied bone biology: Elsevier; 2019. p. 3-26.

31. Clarke B. Normal bone anatomy and physiology. Clinical Journal of the American Society of Nephrology. 2008;3(3):S131-9.

32. Brookes M, Revell WJ. Blood supply of bone: scientific aspects: Springer Science & Business Media; 2012.

33. Cowin SC. Bone poroelasticity. Journal of Biomechanics. 1999;32(3):217-38.

34. Mader KS, Schneider P, Müller R, Stampanoni M. A quantitative framework for the 3D characterization of the osteocyte lacunar system. Bone. 2013;57(1):142-54.

35. Lai X, Price C, Modla S, Thompson WR, Caplan J, Kirn-Safran CB, et al. The dependences of osteocyte network on bone compartment, age, and disease. Bone Research. 2015;3(1):1-11.

36. Peyrin F, Dong P, Pacureanu A, Langer M. Micro-and nano-CT for the study of bone ultrastructure. Current Osteoporosis Reports. 2014;12(4):465-74.

37. Burger EH, Klein - Nulend J. Mechanotransduction in bone — role of the lacunocanalicular network. Mechanotransduction in bone—role of the lacunocanalicular network. The FASEB Journal. 1999;13(9001):S101-S12.

38. Hemmatian H, Bakker AD, Klein-Nulend J, van Lenthe GH. Aging, osteocytes, and mechanotransduction. Current Osteoporosis Reports. 2017;15(5):401-11.

39. van Hove RP, Nolte PA, Vatsa A, Semeins CM, Salmon PL, Smit TH, et al. Osteocyte morphology in human tibiae of different bone pathologies with different bone mineral density—is there a role for mechanosensing? Bone. 2009;45(2):321-9.

40. Wang L, Wang Y, Han Y, Henderson SC, Majeska RJ, Weinbaum S, et al. In situ measurement of solute transport in the bone lacunar-canalicular system. Proceedings of the National Academy of Sciences. 2005;102(33):11911-6.

41. Cardoso L, Fritton SP, Gailani G, Benalla M, Cowin SC. Advances in assessment of bone porosity, permeability and interstitial fluid flow. Journal of Biomechanics. 2013;46(2):253-65.

42. Heřt J, Fiala P, Petrtýl M. Osteon orientation of the diaphysis of the long bones in man. Bone. 1994;15(3):269-77.

43. Seeman E, Delmas PD. Bone quality—the material and structural basis of bone strength and fragility. New England Journal of Medicine. 2006;354(21):2250-61.

44. Bala Y, Zebaze R, Seeman E. Role of cortical bone in bone fragility. Current Opinion in Rheumatology. 2015;27(4):406-13.

45. Zioupos P, Cook RB, Hutchinson JR. Some basic relationships between density values in cancellous and cortical bone. Journal of Biomechanics. 2008;41(9):1961-8.

46. Martin RB. Porosity and specific surface of bone. Critical Reviews in Biomedical Engineering. 1984;10(3):179-222.

47. Seeman E, Sciences M. Age-and menopause-related bone loss compromise cortical and trabecular microstructure. Journals of Gerontology Series A: Biomedical Sciences and Medical Sciences. 2013;68(10):1218-25.

48. Allen MR, Hock JM, Burr DB. Periosteum: biology, regulation, and response to osteoporosis therapies. Bone. 2004;35(5):1003-12.

49. Chen Y, Hu Y, Yu YE, Zhang X, Watts T, Zhou B, et al. Subchondral trabecular rod loss and plate thickening in the development of osteoarthritis. Journal of Bone and Mineral Research. 2018;33(2):316-27.

50. Aubin JEJRiE, Disorders M. Regulation of osteoblast formation and function. Reviews in Endocrine and Metabolic Disorders. 2001;2(1):81-94.

51. Lian JB, Stein GS, Javed A, Van Wijnen AJ, Stein JL, Montecino M, et al. Networks and hubs for the transcriptional control of osteoblastogenesis. Reviews in Endocrine and Metabolic Disorders. 2006;7(1):1-16.

52. Harada S-i, Rodan GA. Control of osteoblast function and regulation of bone mass. Nature. 2003;423(6937):349-55.

53. Baron R, Rawadi G. Targeting the Wnt/β-catenin pathway to regulate bone formation in the adult skeleton. Endocrinology. 2007;148(6):2635-43.

54. Baron R, Kneissel M. WNT signaling in bone homeostasis and disease: from human mutations to treatments. Nature Medicine. 2013;19(2):179-92.

55. Neve A, Corrado A, Cantatore FP. Osteoblast physiology in normal and pathological conditions. Cell and Tissue Research. 2011;343(2):289-302.

56. Golub EE, Boesze-Battaglia K. The role of alkaline phosphatase in mineralization. Current Opinion in Orthopaedics.2007;18(5):444-8.

57. Neve A, Corrado A, Cantatore FP. Osteocalcin: skeletal and extra‐skeletal effects. Journal of Cellular Physiology. 2013;228(6):1149-53.

58. Vanderschueren D, Gevers G, Raymaekers G, Devos P, Dequeker J. Sex-and age-related changes in bone and serum osteocalcin. Calcified Tissue International. 1990;46(3):179-82.

59. Tobiume H, Kanzaki S, Hida S, Ono T, Moriwake T, Yamauchi S, et al. Serum bone alkaline phosphatase isoenzyme levels in normal children and children with growth hormone (GH) deficiency: a potential marker for bone formation and response to GH therapy. The Journal of Clinical Endocrinology & Metabolism. 1997;82(7):2056-61.

60. Crockett JC, Rogers MJ, Coxon FP, Hocking LJ, Helfrich MH. Bone remodelling at a glance. Journal of Cell Science. 2011;124(7):991-8.

61. Bonewald LF. The amazing osteocyte. Journal of Bone and Mineral research,2011;26(2):229-38.

62. Rutkovskiy A, Stensløkken K-O, Vaage IJ. Osteoblast differentiation at a glance. Medical Science Monitor Basic Research. 2016;22:95.

63. Matic I, Matthews BG, Wang X, Dyment NA, Worthley DL, Rowe DW, et al. Quiescent bone lining cells are a major source of osteoblasts during adulthood. Stem Cells. 2016;34(12):2930-42.

64. Delaisse J-M, Andersen TL, Kristensen HB, Jensen PR, Andreasen CM, Søe K. Re-thinking the bone remodeling cycle mechanism and the origin of bone loss. Bone. 2020:115628.

65. Owen R, Reilly GC. In vitro models of bone remodelling and associated disorders. Frontiers in Bioengineering and Biotechnology. 2018;6:134.

66. Bellido T. Osteocyte-driven bone remodeling. Calcified Tissue International. 2014;94(1):25-34.

67. Plotkin LI, Manolagas SC, Bellido T. Transduction of cell survival signals by connexin-43 hemichannels. Journal of Biological Chemistry. 2002;277(10):8648-57.

68. Plotkin LI, Bellido T. Osteocytic signalling pathways as therapeutic targets for bone fragility. Nature Reviews Endocrinology. 2016;12(10):593.

69. Marotti G. The structure of bone tissue and the cellular control of their deposition. Ital J Anat Embryol. 1996;101:25-79.

70. Tate MK, Knothe U. An ex vivo model to study transport processes and fluid flow in loaded bone. Journal of Biomechanics. 2000;33(2):247-54.

71. Burger EH, Klein-Nulend J, Smit TH. Strain-derived canalicular fluid flow regulates osteoclast activity in a remodelling osteon—a proposal. Journal of Biomechanics. 2003;36(10):1453-9.

72. You J, Yellowley C, Donahue H, Zhang Y, Chen Q, Jacobs C. Substrate deformation levels associated with routine physical activity are less stimulatory to bone cells relative to loading-induced oscillatory fluid flow. Journal of Biomechanical Engineering. 2000;122(4):387-93.

73. Galli C, Passeri G, Macaluso G. Osteocytes and WNT: the mechanical control of bone formation. Journal of Dental Research. 2010;89(4):331-43.

74. Kennedy OD, Laudier DM, Majeska RJ, Sun HB, Schaffler MB. Osteocyte apoptosis is required for production of osteoclastogenic signals following bone fatigue in vivo. Bone. 2014;64:132-7.

75. Kennedy OD, Herman BC, Laudier DM, Majeska RJ, Sun HB, Schaffler MB. Activation of resorption in fatigue-loaded bone involves both apoptosis and active pro-osteoclastogenic signaling by distinct osteocyte populations. Bone. 2012;50(5):1115-22.

76. Boyle WJ, Simonet WS, Lacey DL. Osteoclast differentiation and activation. Nature. 2003;423(6937):337-42.

77. Sims NA, Gooi JH. Bone remodeling: Multiple cellular interactions required for coupling of bone formation and resorption. Seminars in Cell and Developmental Biology. 2008;19(5):444-451.

78. Yamaza T, Goto T, Kamiya T, Kobayashi Y, Sakai H, Tanaka T. Study of immunoelectron microscopic localization of cathepsin K in osteoclasts and other bone cells in the mouse femur. Bone. 1998;23(6):499-509.

79. Ljusberg J, Wang Y, Lång P, Norgård M, Dodds R, Hultenby K, et al. Proteolytic excision of a repressive loop domain in tartrate-resistant acid phosphatase by cathepsin K in osteoclasts. Journal of Biological Chemistry. 2005;280(31):28370-81.

80. Olsen BR, Reginato AM, Wang W. Bone development. Annual Review of Cell and Developmental Biology. 2000;16(1):191-220.

81. Berendsen AD, Olsen BR. Bone development. Bone. 2015;80:14-8.

82. Allen MR, Burr DB. Bone Growth, Modeling, and Remodeling. Basic and applied bone biology: Elsevier; 2019. p. 85-100.

83. Allen MR, Burr DB. Bone modeling and remodeling. Basic and applied bone biology: Elsevier; 2014. p. 75-90.

84. Kenkre J, Bassett J. The bone remodelling cycle. Annals of Clinical Biochemistry. 2018;55(3):308-27.

85. Matsuo K, Irie N. Osteoclast–osteoblast communication. Archives of Biochemistry and Biophysics. 2008;473(2):201-9.

86. Jilka RL. Biology of the basic multicellular unit and the pathophysiology of osteoporosis. Medical and Pediatric Oncology.2003;41(3):182-5.

87. Chen X, Wang Z, Duan N, Zhu G, Schwarz EM, Xie C. Osteoblast–osteoclast interactions. Connective Tissue Research. 2018;59(2):99-107.

88. Burgess TL, Qian Y-x, Kaufman S, Ring BD, Van G, Capparelli C, et al. The ligand for osteoprotegerin (OPGL) directly activates mature osteoclasts. The Journal of Cell Biology. 1999;145(3):527-38.

89. Yasuda H, Shima N, Nakagawa N, Mochizuki S-I, Yano K, Fujise N, et al. Identity of osteoclastogenesis inhibitory factor (OCIF) and osteoprotegerin (OPG): a mechanism by which OPG/OCIF inhibits osteoclastogenesis in vitro. Endocrinology. 1998;139(3):1329-37.

90. Simonet W, Lacey D, Dunstan C, Kelley M, Chang M-S, Lüthy R, et al. Osteoprotegerin: a novel secreted protein involved in the regulation of bone density. Cell. 1997;89(2):309-19.

91. Arai F, Miyamoto T, Ohneda O, Inada T, Sudo T, Brasel K, et al. Commitment and differentiation of osteoclast precursor cells by the sequential expression of c-Fms and

receptor activator of nuclear factor κB (RANK) receptors. The Journal of Experimental Medicine. 1999;190(12):1741-54.

92. Hauge EM, Qvesel D, Eriksen EF, Mosekilde L, Melsen F, Research M. Cancellous bone remodeling occurs in specialized compartments lined by cells expressing osteoblastic markers. Journal of Bone and Mineral Research. 2001;16(9):1575-82.

93. Kuo T-R, Chen C-H. Bone biomarker for the clinical assessment of osteoporosis: recent developments and future perspectives. Biomarker Research. 2017;5(1):1-9.

94. Parfitt AM. The coupling of bone formation to bone resorption: a critical analysis of the concept and of its relevance to the pathogenesis of osteoporosis. Metabolic Bone Disease and Related Research. 1982;4(1):1-6.

95. Martin TJ. Coupling factors: how many candidates can there be? Journal of Bone and Mineral Research. 2014;29(7):1519-21.

96. Compston JE, McClung MR, Leslie WD. Osteoporosis. Lancet. 2019;393(10169):364-76.

97. Dempster DW, Compston JE, Drezner MK, Glorieux FH, Kanis JA, Malluche H, et al. Standardized nomenclature, symbols, and units for bone histomorphometry: a 2012 update of the report of the ASBMR Histomorphometry Nomenclature Committee. Journal of Bone and Mineral Research. 2013;28(1):2-17.

98. Everts V, Delaisse J, Korper W, Jansen D, Tigchelaar ‐ Gutter W, Saftig P, et al. The bone lining cell: its role in cleaning Howship's lacunae and initiating bone formation. Journal of Bone and Mineral Research. 2002;17(1):77-90.

99. Mulari M, Qu Q, Härkönen P, Väänänen H. Osteoblast-like cells complete osteoclastic bone resorption and form new mineralized bone matrix in vitro. Calcified Tissue International. 2004;75(3):253-61.

100. Dempster DW. Tethering formation to resorption: reversal revisited. Journal of Bone and Mineral Research. 2017;32(7):1389-90.

101. Lassen NE, Andersen TL, Pløen GG, Søe K, Hauge EM, Harving S, et al. Coupling of bone resorption and formation in real time: new knowledge gained from human haversian BMUs. Journal of Bone and Mineral Research. 2017;32(7):1395-405.

102. Seeman E. Bone's material and structural strength. Current Opinion in Orthopaedics. 2007;18(5):494-8.

103. Goldring SR. Role of bone in osteoarthritis pathogenesis. Medical Clinics of North America. 2009;93(1):25-35.

104. Launey ME, Buehler MJ, Ritchie RO. On the mechanistic origins of toughness in bone. Annual Review of Materials Research. 2010;40:25-53.

105. Ritchie RO, Buehler MJ, Hansma P. Plasticity and toughness in bone. Physics Today. 2009;S003192280906030X

106. Turner C. Biomechanics of bone: determinants of skeletal fragility and bone quality. Osteoporosis International. 2002;13(2):97-104.

107. Faibish D, Ott SM, Boskey AL. Mineral changes in osteoporosis a review. Clinical Orthopaedics and Related Research. 2006;443:28.

108. Fonseca H, Moreira-Gonçalves D, Coriolano H-JA, Duarte JA. Bone quality: the determinants of bone strength and fragility. Sports Medicine. 2014;44(1):37-53.

109. Currey JD. The structure and mechanics of bone. Journal of Materials Science. 2012;47(1):41-54.

110. Sharir A, Barak MM, Shahar R. Whole bone mechanics and mechanical testing. The Veterinary Journal. 2008;177(1):8-17.

111. Hernandez CJ, van der Meulen MC, Research M. Understanding bone strength is not enough. Journal of Bone and Mineral Research. 2017;32(6):1157-62.

112. Felsenberg D, Boonen S. The bone quality framework: determinants of bone strength and their interrelationships, and implications for osteoporosis management. Clinical Therapeutics. 2005;27(1):1-11.

113. Goldring SR, Goldring MB. Changes in the osteochondral unit during osteoarthritis: structure, function and cartilage-bone crosstalk. Nature Reviews Rheumatology. 2016;12(11):632-44.

114. Brody LT. Knee osteoarthritis: Clinical connections to articular cartilage structure and function. Physical Therapy in Sport 2015;16(4):301-16.

115. Sophia Fox AJ, Bedi A, Rodeo SA. The basic science of articular cartilage: structure, composition, and function. Sports Health. 2009;1(6):461-8.

116. Buckwalter JA, Mankin HJ, Grodzinsky AJ. Articular cartilage and osteoarthritis. Instructional Course Lectures. 2005;54:465-80.

117. Martel-Pelletier J, Boileau C, Pelletier JP, Roughley PJ. Cartilage in normal and osteoarthritis conditions. Best Practice & Research in Clinical Rheumatology. 2008;22(2):351-84.

118. Charni-Ben Tabassi N, Garnero P. Monitoring cartilage turnover. Current Rheumatology Reports. 2007;9(1):16-24.

119. Nguyen LT, Sharma AR, Chakraborty C, Saibaba B, Ahn ME, Lee SS. Review of Prospects of Biological Fluid Biomarkers in Osteoarthritis. International Journal of Molecular Sciences. 2017;18(3).

120. Nelson F, Dahlberg L, Laverty S, Reiner A, Pidoux I, Ionescu M, et al. Evidence for altered synthesis of type II collagen in patients with osteoarthritis. The Journal of Clinical Investigation. 1998;102(12):2115-25.

121. Brewton R, Wright D, Mayne R. Structural and functional comparison of type IX collagen-proteoglycan from chicken cartilage and vitreous humor. Journal of Biological Chemistry. 1991;266(8):4752-7.

122. Eyre DR, Weis MA, Wu J-J. Articular cartilage collagen: an irreplaceable framework. European Cells & Materials. 2006;12(1):57-63.

123. Söder S, Hambach L, Lissner R, Kirchner T, Aigner T. Ultrastructural localization of type VI collagen in normal adult and osteoarthritic human articular cartilage. Osteoarthritis and Cartilage. 2002;10(6):464-70.

124. Wilusz RE, Sanchez-Adams J, Guilak F. The structure and function of the pericellular matrix of articular cartilage. Matrix Biology. 2014;39:25-32.

125. Zhang Z. Chondrons and the pericellular matrix of chondrocytes. Tissue Engineering Part B: Reviews.2015;21(3):267-77.

126. Hoyland JA, Thomas J, Donn R, Marriott A, Ayad S, Boot-Handford R, et al. Distribution of type X collagen mRNA in normal and osteoarthritic human cartilage. Bone and Mineral. 1991;15(2):151-63.

127. Boos N, Nerlich AG, Wiest I, von der Mark K, Ganz R, Aebi M. Immunohistochemical analysis of type X ‐ collagen expression in osteoarthritis of the hip joint. Journal of Orthopaedic Research. 1999;17(4):495-502.

128. Kiani C, Liwen C, Wu YJ, Albert JY, Burton BY. Structure and function of aggrecan. Cell Research. 2002;12(1):19-32.

129. Chandran PL, Horkay F. Aggrecan, an unusual polyelectrolyte: review of solution behavior and physiological implications. Acta Biomaterialia. 2012;8(1):3-12.

130. Lai WM, Hou J, Mow VC. A triphasic theory for the swelling and deformation behaviors of articular cartilage. Journal of Biomechanical Engineering. 1991; 113(3): 245-258.

131. Sanchez-Adams J, Leddy HA, McNulty AL, O'Conor CJ, Guilak F. The mechanobiology of articular cartilage: bearing the burden of osteoarthritis. Current Rheumatology Reports. 2014;16(10):451.

132. Wilusz RE, DeFrate LE, Guilak F. A biomechanical role for perlecan in the pericellular matrix of articular cartilage. Matrix Biology. 2012;31(6):320-7.

133. Vincent T, McLean C, Full L, Peston D, Saklatvala J. FGF-2 is bound to perlecan in the pericellular matrix of articular cartilage, where it acts as a chondrocyte mechanotransducer. Osteoarthritis and Cartilage. 2007;15(7):752-63.

134. Chang Z, Meer K, Rapraeger AC, Friedl A. Differential ability of heparan sulfate proteoglycans to assemble the fibroblast growth factor receptor complex in situ. The FASEB Journal. 2000;14(1):137-44.

135. Hedbom E, Heinegård D. Interaction of a 59-kDa connective tissue matrix protein with collagen I and collagen II. Journal of Biological Chemistry. 1989;264(12):6898-905.

136. Wiberg C, Klatt AR, Wagener R, Paulsson M, Bateman JF, Heinegård D, et al. Complexes of matrilin-1 and biglycan or decorin connect collagen VI microfibrils to both collagen II and aggrecan. Journal of Biological Chemistry. 2003;278(39):37698-704.

137. Halász K, Kassner A, Mörgelin M, Heinegård D. COMP acts as a catalyst in collagen fibrillogenesis. Journal of Biological Chemistry. 2007;282(43):31166-73.

138. Rosenberg K, Olsson H, Mörgelin M, Heinegård D. Cartilage oligomeric matrix protein shows high affinity zinc-dependent interaction with triple helical collagen. Journal of Biological Chemistry. 1998;273(32):20397-403.

139. Chen FH, Herndon ME, Patel N, Hecht JT, Tuan RS, Lawler J. Interaction of cartilage oligomeric matrix protein/thrombospondin 5 with aggrecan. Journal of Biological Chemistry. 2007;282(34):24591-8.

140. Burton-Wurster N, Lust G, Macleod JN. Cartilage fibronectin isoforms: In search of functions for a special populations of matrix glycoproteins. Matrix Biology. 1997;15(7):441-54.

141. Pulai JI, Chen H, Im H-J, Kumar S, Hanning C, Hegde PS, et al. NF-κB mediates the stimulation of cytokine and chemokine expression by human articular chondrocytes in response to fibronectin fragments. Journal of Immunology. 2005;174(9):5781-8.

142. Pitsillides AA, Beier F. Cartilage biology in osteoarthritis—lessons from developmental biology. Nature Reviews Rheumatology. 2011;7(11):654.

143. Hunziker EB, Lippuner K, Shintani N. How best to preserve and reveal the structural intricacies of cartilaginous tissue. Matrix Biology. 2014;39:33-43.

144. Mobasheri A, Rayman MP, Gualillo O, Sellam J, Van Der Kraan P, Fearon U. The role of metabolism in the pathogenesis of osteoarthritis. Nature Reviews Rheumatology. 2017;13(5):302-11.

145. O'Conor CJ, Leddy HA, Benefield HC, Liedtke WB, Guilak F. TRPV4-mediated mechanotransduction regulates the metabolic response of chondrocytes to dynamic loading. Proceedings of the National Academy of Sciences. 2014;111(4):1316-21.

146. Wann AK, Zuo N, Haycraft CJ, Jensen CG, Poole CA, McGlashan SR, et al. Primary cilia mediate mechanotransduction through control of ATP‐induced Ca2+ signaling in compressed chondrocytes. The FASEB Journal. 2012;26(4):1663-71.

147. Millward-Sadler S, Salter DM. Integrin-dependent signal cascades in chondrocyte mechanotransduction. Annals of Biomedical Engineering. 2004;32(3):435-46.

148. Pfander D, Gelse K. Hypoxia and osteoarthritis: how chondrocytes survive hypoxic environments. Current Opinion in Rheumatology. 2007;19(5):457-62.

149. Thoms BL, Dudek KA, Lafont JE, Murphy CL. Hypoxia promotes the production and inhibits the destruction of human articular cartilage. Arthritis & Rheumatism. 2013;65(5):1302-12.

150. Goldring MB, Marcu KB. Cartilage homeostasis in health and rheumatic diseases. Arthritis Research & Therapy. 2009;11(3):224.

151. Lane RS, Fu Y, Matsuzaki S, Kinter M, Humphries KM, Griffin TM, et al. Mitochondrial respiration and redox coupling in articular chondrocytes. Arthritis Research & Therapy. 2015;17(1):1-14.

152. Imhof H, Breitenseher M, Kainberger F, Rand T, Trattnig S. Importance of subchondral bone to articular cartilage in health and disease. Topics in Magnetic Resonance Imaging. 1999;10(3):180.

153. Madry H, van Dijk CN, Mueller-Gerbl M. The basic science of the subchondral bone. Knee Surgery, Sports Traumatology, Arthroscopy. 2010;18(4):419-33.

154. Poole CA. Articular cartilage chondrons: form, function and failure. The Journal of Anatomy. 1997;191(1):1-13.

155. Macri L, Silverstein D, Clark RA. Growth factor binding to the pericellular matrix and its importance in tissue engineering. Advanced Drug Delivery Reviews. 2007;59(13):1366-81.

156. Kanbe K, Yang X, Wei L, Sun C, Chen Q. Pericellular matrilins regulate activation of chondrocytes by cyclic load‐induced matrix deformation. Journal of Bone and Mineral Research. 2007;22(2):318-28.

157. Mow VC, Guo XE. Mechano-electrochemical properties of articular cartilage: their inhomogeneities and anisotropies. Annual Review of Biomedical Engineering. 2002;4(1):175-209.

158. Williamson AK, Chen AC, Masuda K, Thonar EJM, Sah RL. Tensile mechanical properties of bovine articular cartilage: variations with growth and relationships to collagen network components. Journal of Orthopaedic Research. 2003;21(5):872-80.

159. Mow VC, Kuei S, Lai WM, Armstrong CG. Biphasic creep and stress relaxation of articular cartilage in compression: theory and experiments. Journal of Biomechanical engineering. 1980;102(1):73-84.

160. Cucchiarini M, de Girolamo L, Filardo G, Oliveira JM, Orth P, Pape D, et al. Basic science of osteoarthritis. Journal of Experimental Orthopaedics. 2016;3(1):22.

161. Burr DB, Gallant MA. Bone remodelling in osteoarthritis. Nature Reviews Rheumatology. 2012;8(11):665-73.

162. Neogi T, Felson D, Niu J, Lynch J, Nevitt M, Guermazi A, et al. Cartilage loss occurs in the same subregions as subchondral bone attrition: a within‐knee subregion‐matched approach from the Multicenter Osteoarthritis Study. Arthritis Care & Research. 2009;61(11):1539-44.

163. Imhof H, Sulzbacher I, Grampp S, Czerny C, Youssefzadeh S, Kainberger F. Subchondral bone and cartilage disease - A rediscovered functional unit. Investigative Radiology. 2000;35(10):581-8.

164. Heinegard D, Saxne T. The role of the cartilage matrix in osteoarthritis. Nature Reviews Rheumatology. 2011;7(1):50-6.

165. Goldring SR. Alterations in periarticular bone and cross talk between subchondral bone and articular cartilage in osteoarthritis. Therapeutic Advances in Musculoskeletal Disease. 2012;4(4):249-58.

166. Li G, Yin J, Gao J, Cheng TS, Pavlos NJ, Zhang C, et al. Subchondral bone in osteoarthritis: insight into risk factors and microstructural changes. Arthritis Research & Therapy. 2013;15(6):223.

167. Zhu X, Chan YT, Yung PS, Tuan RS, Jiang Y. Subchondral bone remodeling: a therapeutic target for osteoarthritis. Frontiers in Cell and Developmental Biology. 2020;8.

168. Pan J, Zhou XZ, Li W, Novotny JE, Doty SB, Wang LY. In Situ Measurement of Transport between Subchondral Bone and Articular Cartilage. Journal of Orthopaedic Research. 2009;27(10):1347-52.

169. Huang Y, Chen C, Wang F, Chen G, Cheng S, Tang Z, et al. Observation of Solute Transport between Articular Cartilage and Subchondral Bone in Live Mice. Cartilage. 2020:1947603520951627.

170. Lyons TJ, McClure SF, Stoddart RW, McClure J. The normal human chondro-osseous junctional region: evidence for contact of uncalcified cartilage with subchondral bone and marrow spaces. BMC Musculoskeletal Disorders. 2006;7.

171. Lane LB, Villacin A, Bullough P. The vascularity and remodelling of subchondrial bone and calcified cartilage in adult human femoral and humeral heads. An age-and stress-related phenomenon. The Journal of Bone and Joint Surgery. 1977;59(3):272-8.

172. Clark JM. The structure of vascular channels in the subchondral plate. Journal of Anatomy. 1990;171:105.

173. Woods C, Greenwald A, Haynes D. Subchondral vascularity in the human femoral head. Annals of the Rheumatic Diseases. 1970;29(2):138.

174. Greenwald A, Haynes D. A pathway for nutrients from the medullary cavity to the articular cartilage of the human femoral head. The Journal of Bone and Joint Surgery. 1969;51(4):747-53.

175. Mori S, Harruff R, Burr DB. Microcracks in articular calcified cartilage of human femoral heads. Archives of Pathology & Laboratory Medicine. 1993;117(2):196-8.

176. Zarka M, Hay E, Ostertag A, Marty C, Chappard C, Oudet F, et al. Microcracks in subchondral bone plate is linked to less cartilage damage. Bone. 2019;123:1-7.

177. Amin AK, Huntley JS, Simpson AH, Hall AC. Chondrocyte survival in articular cartilage: the influence of subchondral bone in a bovine model. Journal of Bone and Joint Surgery. 2009;91(5):691-9.

178. Rabar S, Lau R, O'Flynn N, Li L, Barry P. Risk assessment of fragility fractures: summary of NICE guidance. The BMJ. 2012;345.

179. Clynes MA, Harvey NC, Curtis EM, Fuggle NR, Dennison EM, Cooper C. The epidemiology of osteoporosis. British Medical Bulletin. 2020;133(1):105.

180. Cooper C. Epidemiology of osteoporosis. Osteoporosis International. 1999;9:S2.

181. Van Staa T, Dennison E, Leufkens Ha, Cooper C. Epidemiology of fractures in England and Wales. Bone. 2001;29(6):517-22.

182. Hernlund E, Svedbom A, Ivergård M, Compston J, Cooper C, Stenmark J, et al. Osteoporosis in the European Union: medical management, epidemiology and economic burden. Archives of Osteoporosis. 2013;8(1):1-115.

183. Dempster DW. Osteoporosis and the burden of osteoporosis-related fractures. American Journal of Managed Care. 2011;17(6):S164.

184. Burge R, Dawson‐Hughes B, Solomon DH, Wong JB, King A, Tosteson A, et al. Incidence and economic burden of osteoporosis‐related fractures in the United States, 2005–2025. Journal of Bone and Mineral Research. 2007;22(3):465-75.

185. Feng X, McDonald JM. Disorders of bone remodeling. Review of Pathology: Mechanisms of Disease. 2011;6:121-45.

186. Pietschmann P, Rauner M, Sipos W, Kerschan-Schindl K. Osteoporosis: an age-related and gender-specific disease–a mini-review. Gerontology. 2009;55(1):3-12.

187. Lerner U. Bone remodeling in post-menopausal osteoporosis. Journal of Dental Research. 2006;85(7):584-95.

188. Sözen T, Özışık L, Başaran NÇ. An overview and management of osteoporosis. European Journal of Rheumatology. 2017;4(1):46.

189. Willson T, Nelson SD, Newbold J, Nelson RE, LaFleur J. The clinical epidemiology of male osteoporosis: a review of the recent literature. Clinical Epidemiology. 2015;7:65.

190. Mirza F, Canalis E. Secondary osteoporosis: pathophysiology and management. European Journal of Endocrinology. 2015;173(3):R131.

191. Bonjour J-P, Chevalley T, Ferrari S, Rizzoli R. The importance and relevance of peak bone mass in the prevalence of osteoporosis. Salud Publica de Mexico. 2009;51:s5-s17.

192. Mora S, Gilsanz V. Establishment of peak bone mass. Endocrinology and Metabolism Clinics. 2003;32(1):39-63.

193. Manolagas SC. From estrogen-centric to aging and oxidative stress: a revised perspective of the pathogenesis of osteoporosis. Endocrine Reviews. 2010;31(3):266-300.

194. Hendrickx G, Boudin E, Van Hul W. A look behind the scenes: the risk and pathogenesis of primary osteoporosis. Nature Reviews Rheumatology. 2015;11(8):462.

195. Khosla S, Melton III LJ, Riggs BL. The unitary model for estrogen deficiency and the pathogenesis of osteoporosis: is a revision needed? Journal of Bone and Mineral Research. 2011;26(3):441-51.

196. Khosla S. Pathogenesis of osteoporosis. Translational Endocrinology & Metabolism. 2010;1(1):55.

197. Eghbali-Fatourechi G, Khosla S, Sanyal A, Boyle WJ, Lacey DL, Riggs BL. Role of RANK ligand in mediating increased bone resorption in early postmenopausal women. The Journal of Clinical Investigation. 2003;111(8):1221-30.

198. Manolagas SC, Jilka RL. Bone marrow, cytokines, and bone remodeling—emerging insights into the pathophysiology of osteoporosis. New England Journal of Medicine. 1995;332(5):305-11.

199. Mundy GR. Osteoporosis and inflammation. Nutrition Reviews. 2007;65(3):S147-S51.

200. Shevde NK, Bendixen AC, Dienger KM, Pike JW. Estrogens suppress RANK ligand-induced osteoclast differentiation via a stromal cell independent mechanism involving c-Jun repression. Proceedings of the National Academy of Sciences. 2000;97(14):7829-34.

201. Srivastava S, Toraldo G, Weitzmann MN, Cenci S, Ross FP, Pacifici R. Estrogen decreases osteoclast formation by down-regulating receptor activator of NF-κB ligand (RANKL)-induced JNK activation. Journal of Biological Chemistry. 2001;276(12):8836-40.

202. Nakamura T, Imai Y, Matsumoto T, Sato S, Takeuchi K, Igarashi K, et al. Estrogen prevents bone loss via estrogen receptor α and induction of Fas ligand in osteoclasts. Cell. 2007;130(5):811-23.

203. Hughes DE, Dai A, Tiffee JC, Li HH, Mundy GR, Boyce BF. Estrogen promotes apoptosis of murine osteoclasts mediated by TGF–β. Nature Medicine. 1996;2(10):1132-6.

204. Kameda T, Mano H, Yuasa T, Mori Y, Miyazawa K, Shiokawa M, et al. Estrogen inhibits bone resorption by directly inducing apoptosis of the bone-resorbing osteoclasts. The Journal of Experimental Medicine. 1997;186(4):489-95.

205. Di Gregorio GB, Yamamoto M, Ali AA, Abe E, Roberson P, Manolagas SC, et al. Attenuation of the self-renewal of transit-amplifying osteoblast progenitors in the murine bone marrow by 17β-estradiol. The Journal of Clinical Investigation. 2001;107(7):803-12.

206. Jilka RL, Takahashi K, Munshi M, Williams DC, Roberson PK, Manolagas SC. Loss of estrogen upregulates osteoblastogenesis in the murine bone marrow. Evidence for autonomy from factors released during bone resorption. The Journal of Clinical Investigation. 1998;101(9):1942-50.

207. Manolagas SC, O'brien CA, Almeida M. The role of estrogen and androgen receptors in bone health and disease. Nature Reviews Endocrinology. 2013;9(12):699.

208. Almeida M, Martin‐Millan M, Ambrogini E, Bradsher III R, Han L, Chen XD, et al. Estrogens attenuate oxidative stress and the differentiation and apoptosis of osteoblasts by DNA‐binding‐independent actions of the ERα. Journal of Bone and Mineral Research. 2010;25(4):769-81.

209. Tomkinson A, Gevers E, Wit J, Reeve J, Noble B. The role of estrogen in the control of rat osteocyte apoptosis. Journal of Bone and Mineral Research. 1998;13(8):1243-50.

210. Kousteni S, Bellido T, Plotkin L, O'brien C, Bodenner D, Han L, et al. Nongenotropic, sex-nonspecific signaling through the estrogen or androgen receptors: dissociation from transcriptional activity. Cell. 2001;104(5):719-30.

211. Kousteni S, Han L, Chen J-R, Almeida M, Plotkin LI, Bellido T, et al. Kinase-mediated regulation of common transcription factors accounts for the bone-protective effects of sex steroids. The Journal of Clinical Investigation. 2003;111(11):1651-64.

212. Manolagas S, Kousteni S, Jilka R. Sex steroids and bone. Recent Progress in Hormone Research. 2002;57:385-410.

213. Garnero P, Sornay‐Rendu E, Chapuy MC, Delmas PD, research m. Increased bone turnover in late postmenopausal women is a major determinant of osteoporosis. Journal of Bone and Mineral Research. 1996;11(3):337-49.

214. Tomkinson A, Reeve J, Shaw R, Noble B, Metabolism. The death of osteocytes via apoptosis accompanies estrogen withdrawal in human bone. The Journal of Clinical Endocrinology & Metabolism. 1997;82(9):3128-35.

215. Manolagas SC. Birth and death of bone cells: basic regulatory mechanisms and implications for the pathogenesis and treatment of osteoporosis. Endocrine Reviews. 2000;21(2):115-37.

216. Seeman E. Pathogenesis of bone fragility in women and men. The Lancet. 2002;359(9320):1841-50.

217. Ferlin A, Selice R, Carraro U, Foresta C. Testicular function and bone metabolism—beyond testosterone. Nature Reviews Endocrinology. 2013;9(9):548.

218. Khosla S. Update in male osteoporosis. Journal of Clinical Endocrinology & Metabolism. 2010;95(1):3-10.

219. Finkel T, Holbrook NJ. Oxidants, oxidative stress and the biology of ageing. Nature. 2000;408(6809):239-47.

220. López-Otín C, Blasco MA, Partridge L, Serrano M, Kroemer G. The hallmarks of aging. Cell. 2013;153(6):1194-217.

221. Khosla S, Farr JN, Kirkland JL, Metabolism. Inhibiting cellular senescence: a new therapeutic paradigm for age-related osteoporosis. Journal of Clinical Endocrinology & Metabolism. 2018;103(4):1282-90.

222. Ambrogini E, Almeida M, Martin-Millan M, Paik J-H, DePinho RA, Han L, et al. FoxO-mediated defense against oxidative stress in osteoblasts is indispensable for skeletal homeostasis in mice. Cell Metabolism. 2010;11(2):136-46.

223. Hamada Y, Fujii H, Fukagawa M. Role of oxidative stress in diabetic bone disorder. Bone. 2009;45:S35-S8.

224. She C, Zhu L-q, Zhen Y-f, Wang X-d, Dong Q. Activation of AMPK protects against hydrogen peroxide-induced osteoblast apoptosis through autophagy induction and NADPH maintenance: new implications for osteonecrosis treatment? Cellular Signalling. 2014;26(1):1-8.

225. Kannan K, Jain SK. Oxidative stress and apoptosis. Pathophysiology. 2000;7(3):153-63.

226. Almeida M, Han L, Martin-Millan M, Plotkin LI, Stewart SA, Roberson PK, et al. Skeletal involution by age-associated oxidative stress and its acceleration by loss of sex steroids. Journal of Biological Chemistry. 2007;282(37):27285-97.

227. Almeida M, Han L, Martin-Millan M, O'Brien CA, Manolagas SC. Oxidative stress antagonizes Wnt signaling in osteoblast precursors by diverting β-catenin from T cell factor- to forkhead box O-mediated transcription. Journal of Biological Chemistry. 2007;282(37):27298-305.

228. Xiong J, O'Brien CA. Osteocyte RANKL: new insights into the control of bone remodeling. Journal of Bone and Mineral Research. 2012;27(3):499-505.

229. Osterhoff G, Morgan EF, Shefelbine SJ, Karim L, McNamara LM, Augat P. Bone mechanical properties and changes with osteoporosis. Injury-International Journal of the Care of the Injured. Injury. 2016;47:S11-S20.

230. Seeman E. Invited review: pathogenesis of osteoporosis. Journal of Applied Physiology. 2003;95(5):2142-51.

231. Zebaze RM, Ghasem-Zadeh A, Bohte A, Iuliano-Burns S, Mirams M, Price RI, et al. Intracortical remodelling and porosity in the distal radius and post-mortem femurs of women: a cross-sectional study. The Lancet. 2010;375(9727):1729-36.

232. Siris E, Adler R, Bilezikian J, Bolognese M, Dawson-Hughes B, Favus M, et al. The clinical diagnosis of osteoporosis: a position statement from the National Bone Health Alliance Working Group. Osteoporosis International. 2014;25(5):1439-43.

233. Sattui SE, Saag KG. Fracture mortality: associations with epidemiology and osteoporosis treatment. Nature Reviews Endocrinology. 2014;10(10):592.

234. Carpintero P, Caeiro JR, Carpintero R, Morales A, Silva S, Mesa M. Complications of hip fractures: a review. World Journal of Orthopedics. 2014;5(4):402.

235. Roche J, Wenn RT, Sahota O, Moran CG. Effect of comorbidities and postoperative complications on mortality after hip fracture in elderly people: prospective observational cohort study. The BMJ. 2005;331(7529):1374.

236. Blake GM, Fogelman I. The clinical role of dual energy X-ray absorptiometry. European Journal of Radiology. 2009;71(3):406-14.

237. Blake GM, Fogelman I. An update on dual-energy x-ray absorptiometry. Seminars in Nuclear Medicine. 2010;40(1):62-73.

238. Adams JE. Advances in bone imaging for osteoporosis. Nature Reviews Endocrinology. 2013;9(1):28-42.

239. Link TM. Osteoporosis imaging: state of the art and advanced imaging. Radiology. 2012;263(1):3-17.

240. Lespessailles E, Chappard C, Bonnet N, Benhamou CL. Imaging techniques for evaluating bone microarchitecture. Joint Bone Spine. 2006;73(3):254-61.

241. Ito M. Recent progress in bone imaging for osteoporosis research. Journal of Bone and Mineral Metabolism. 2011;29(2):131-40.

242. Qaseem A, Forciea MA, McLean RM, Denberg TD. Treatment of low bone density or osteoporosis to prevent fractures in men and women: a clinical practice guideline update from the American College of Physicians. Annals of Internal Medicine. 2017;166(11):818-39.

243. Camacho PM, Petak SM, Binkley N, Diab DL, Eldeiry LS, Farooki A, et al. American Association of Clinical Endocrinologists/American College of Endocrinology clinical practice guidelines for the diagnosis and treatment of postmenopausal osteoporosis—2020 update. Endocrine Practice. 2020;26:1-46.

244. Holroyd C, Cooper C, Dennison E. Epidemiology of osteoporosis. Best Practice & Research Clinical Endocrinology & Metabolism. 2008;22(5):671-85.

245. Kanis JA. Assessment of fracture risk and its application to screening for postmenopausal osteoporosis: synopsis of a WHO report. Osteoporosis International. 1994;4(6):368-81.

246. Johnell O, Kanis JA, Oden A, Johansson H, De Laet C, Delmas P, et al. Predictive value of BMD for hip and other fractures. Journal of Bone and Mineral Research. 2005;20(7):1185-94.

247. Kanis JA, Harvey NC, Johansson H, Liu E, Vandenput L, Lorentzon M, et al. A decade of FRAX: how has it changed the management of osteoporosis? Aging Clinical and Experimental Research. 2020;32(2):187-96.

248. Kanis J, McCloskey E, Johansson H, Oden A, Ström O, Borgström F. Development and use of FRAX® in osteoporosis. Osteoporosis International. 2010;21(2):407-13.

249. Kanis JA, Harvey NC, Cooper C, Johansson H, Odén A, McCloskey EV. A systematic review of intervention thresholds based on FRAX. Archives of Osteoporosis. 2016;11(1):1-48.

250. Compston J, Cooper A, Cooper C, Gittoes N, Gregson C, Harvey N, et al. UK clinical guideline for the prevention and treatment of osteoporosis. Archives of Osteoporosis. 2017;12(1):43.

251. Vasikaran S, Eastell R, Bruyere O, Foldes A, Garnero P, Griesmacher A, et al. Markers of bone turnover for the prediction of fracture risk and monitoring of osteoporosis treatment: a need for international reference standards. Osteoporosis International. 2011;22(2):391-420.

252. Garnero P, Sornay‐Rendu E, Claustrat B, Delmas PD. Biochemical markers of bone turnover, endogenous hormones and the risk of fractures in postmenopausal women: the OFELY study. Journal of Bone and Mineral Research. 2000;15(8):1526-36.

253. Camacho PM, Petak SM, Binkley N, Clarke BL, Harris ST, Hurley DL, et al. American Association Of Clinical Endocrinologists and American College of Endocrinology clinical practice guidelines for the diagnosis and treatment of postmenopausal osteoporosis—2016--executive summary. Endocrine Practice. 2016;22(9):1111-8.

254. Sandhu SK, Hampson G. The pathogenesis, diagnosis, investigation and management of osteoporosis. Journal of Clinical Pathology. 2011;64(12):1042-50.

255. Howe TE, Shea B, Dawson LJ, Downie F, Murray A, Ross C, et al. Exercise for preventing and treating osteoporosis in postmenopausal women. Cochrane Database of Dystematic Reviews. 2011(7).

256. Ross AC, Manson JE, Abrams SA, Aloia JF, Brannon PM, Clinton SK, et al. The 2011 report on dietary reference intakes for calcium and vitamin D from the Institute of Medicine: what clinicians need to know. The Journal of Clinical Endocrinology & Metabolism. 2011;96(1):53-8.

257. Rachner TD, Khosla S, Hofbauer LC. Osteoporosis: now and the future. The Lancet. 2011;377(9773):1276-87.

258. Russell RG. Bisphosphonates: the first 40 years. Bone. 2011;49(1):2-19.

259. Lacey DL, Boyle WJ, Simonet WS, Kostenuik PJ, Dougall WC, Sullivan JK, et al. Bench to bedside: elucidation of the OPG–RANK–RANKL pathway and the development of denosumab. Nature Reviews Drug Discovery.2012;11(5):401-19.

260. Baron R, Ferrari S, Russell RG. Denosumab and bisphosphonates: different mechanisms of action and effects. Bone. 2011;48(4):677-92.

261. Cummings SR, Martin JS, McClung MR, Siris ES, Eastell R, Reid IR, et al. Denosumab for prevention of fractures in postmenopausal women with osteoporosis. New England Journal of Medicine. 2009;361(8):756-65.

262. Drake MT, Clarke BL, Lewiecki EM. The pathophysiology and treatment of osteoporosis. Clinical Therapeutics. 2015;37(8):1837-50.

263. Writing Group for the Women's Health Initiative Investigators. Risks and benefits of estrogen plus progestin in healthy postmenopausal women: principal results from the Women's Health Initiative randomized controlled trial. JAMA. 2002;288(3):321-33.

264. McClung MR, Lewiecki EM, Cohen SB, Bolognese MA, Woodson GC, Moffett AH, et al. Denosumab in postmenopausal women with low bone mineral density. New England Journal of Medicine. 2006;354(8):821-31.

265. Chesnut III CH, Silverman S, Andriano K, Genant H, Gimona A, Harris S, et al. A randomized trial of nasal spray salmon calcitonin in postmenopausal women with established osteoporosis: the prevent recurrence of osteoporotic fractures study. The American Journal of Medicine. 2000;109(4):267-76.

266. Boivin G, Meunier P. The mineralization of bone tissue: a forgotten dimension in osteoporosis research. Osteoporosis International. 2003;14(3):19-24.

267. Curtis EM, Moon RJ, Dennison EM, Harvey NC, Cooper C. Recent advances in the pathogenesis and treatment of osteoporosis. Clinical Medicine. 2015;15(6):s92.

268. Marie PJ. Strontium ranelate: new insights into its dual mode of action. Bone. 2007;40(5):S5-S8.

269. Hamdy NA. Strontium ranelate improves bone microarchitecture in osteoporosis. Rheumatology. 2009;48(4):iv9-iv13.

270. Girotra M, Rubin MR, Bilezikian JP. The use of parathyroid hormone in the treatment of osteoporosis. Reviews in Endocrine and Metabolic Disorders. 2006;7(1):113-21.

271. Kraenzlin ME, Meier C. Parathyroid hormone analogues in the treatment of osteoporosis. Nature Reviews Endocrinology. 2011;7(11):647.

272. Neer RM, Arnaud CD, Zanchetta JR, Prince R, Gaich GA, Reginster J-Y, et al. Effect of parathyroid hormone (1-34) on fractures and bone mineral density in postmenopausal women with osteoporosis. New England Journal of Medicine. 2001;344(19):1434-41.

273. Pereira D, Peleteiro B, Araujo J, Branco J, Santos R, Ramos E, et al. The effect of osteoarthritis definition on prevalence and incidence estimates: a systematic review. Osteoarthritis and Cartilage. 2011;19(11):1270-85.

274. Zhang Y, Jordan JM. Epidemiology of osteoarthritis. Clinics in Geriatric Medicine. 2010;26(3):355-69.

275. Johnson VL, Hunter DJ, rheumatology rC. The epidemiology of osteoarthritis. Best Practice & Research Clinical Rheumatology. 2014;28(1):5-15.

276. Hunter DJ, Schofield D, Callander E. The individual and socioeconomic impact of osteoarthritis. Nature Reviews Rheumatology. 2014;10(7):437.

277. Martel-Pelletier J, Barr AJ, Cicuttini FM, Conaghan PG, Cooper C, Goldring MB, et al. Osteoarthritis. Nature Reviews Disease Primers. 2016;2.

278. Hunter DJ, Bierma-Zeinstra S. Osteoarthritis. Lancet. 2019;393(10182):1745-59.

279. Oliveria SA, Felson DT, Reed JI, Cirillo PA, Walker AM. Incidence of symptomatic hand, hip, and knee osteoarthritis among patients in a health maintenance organization. Arthritis & Rheumatism. 1995;38(8):1134-41.

280. Felson DT, Lawrence RC, Dieppe PA, Hirsch R, Helmick CG, Jordan JM, et al. Osteoarthritis: new insights. Part 1: the disease and its risk factors. Annals of Internal Medicine. 2000;133(8):635-46.

281. Mobasheri A, Matta C, Zákány R, Musumeci G. Chondrosenescence: definition, hallmarks and potential role in the pathogenesis of osteoarthritis. Maturitas. 2015;80(3):237-44.

282. Loeser RF. Age-related changes in the musculoskeletal system and the development of osteoarthritis. Clinics in Geriatric Medicine. 2010;26(3):371-86.

283. Jordan JM, Helmick CG, Renner JB, Luta G, Dragomir AD, Woodard J, et al. Prevalence of knee symptoms and radiographic and symptomatic knee osteoarthritis in African Americans and Caucasians: The Johnston County Osteoarthritis project. Journal of Rheumatology. The Journal of Rheumatology. 2007;34(1):172-80.

284. Srikanth VK, Fryer JL, Zhai G, Winzenberg TM, Hosmer D, Jones G, et al. A meta-analysis of sex differences prevalence, incidence and severity of osteoarthritis. Osteoarthritis and cartilage. 2005;13(9):769-81.

285. Herrero-Beaumont G, Roman-Blas JA, Castañeda S, Jimenez SA. Primary osteoarthritis no longer primary: three subsets with distinct etiological, clinical, and therapeutic characteristics. Seminars in Arthritis and Rheumatism. 2009;39(2):71-80).

286. Roman-Blas JA, Castañeda S, Largo R, Herrero-Beaumont G. Osteoarthritis associated with estrogen deficiency. Arthritis Research & Therapy. 2009;11(5):1-14.

287. Vina ER, Kwoh CK. Epidemiology of osteoarthritis: literature update. Current Opinion in Rheumatology. 2018;30(2):160-7.

288. Valdes AM, Spector TD. The contribution of genes to osteoarthritis. Medical Clinics of North America. 2009;93(1):45-66, x.

289. Nevitt MC, Xu L, Zhang Y, Lui LY, Yu W, Lane NE, et al. Very low prevalence of hip osteoarthritis among Chinese elderly in Beijing, China, compared with whites in the United States: the Beijing osteoarthritis study. Arthritis & Rheumatism. 2002;46(7):1773-9.

290. Anderson JJ, Felson DT. Factors associated with osteoarthritis of the knee in the first national Health and Nutrition Examination Survey (HANES I) evidence for an association with overweight, race, and physical demands of work. American Journal of Epidemiology. 1988;128(1):179-89.

291. Warner SC, Valdes AM. Genetic association studies in osteoarthritis: is it fairytale? Current Opinion in Rheumatology. 2017;29(1):103-9.

292. Chu M, Zhu X, Wang C, Rong J, Wang Y, Wang S, et al. The rs4238326 polymorphism in ALDH1A2 gene potentially associated with non-post traumatic knee osteoarthritis susceptibility: a two-stage population-based study. Osteoarthritis and Cartilage. 2017;25(7):1062-7.

293. Evangelou E, Chapman K, Meulenbelt I, Karassa FB, Loughlin J, Carr A, et al. Large‐scale analysis of association between GDF5 and FRZB variants and osteoarthritis of the hip, knee, and hand. Arthritis & Rheumatism. 2009;60(6):1710-21.

294. Valdes AM, Evangelou E, Kerkhof HJ, Tamm A, Doherty SA, Kisand K, et al. The GDF5 rs143383 polymorphism is associated with osteoarthritis of the knee with genome-wide statistical significance. Annals of the Rheumatic Diseases. 2011;70(5):873-5.

295. Suter LG, Smith SR, Katz JN, Englund M, Hunter DJ, Frobell R, et al. Projecting lifetime risk of symptomatic knee osteoarthritis and total knee replacement in individuals sustaining a complete anterior cruciate ligament tear in early adulthood. Arthritis Care & Research. 2017;69(2):201-8.

296. Sharma L, Song J, Felson DT, Cahue S, Shamiyeh E, Dunlop DD. The role of knee alignment in disease progression and functional decline in knee osteoarthritis. JAMA. 2001;286(2):188-95.

297. Cerejo R, Dunlop DD, Cahue S, Channin D, Song J, Sharma L, et al. The influence of alignment on risk of knee osteoarthritis progression according to baseline stage of disease. Arthritis & Rheumatism. 2002;46(10):2632-6.

298. Thomas AC, Hubbard-Turner T, Wikstrom EA, Palmieri-Smith RM. Epidemiology of posttraumatic osteoarthritis. Journal of Athletic Training. 2017;52(6):491-6.

299. Griffin TM, Guilak F. The role of mechanical loading in the onset and progression of osteoarthritis. Exercise and Sport Sciences Reviews. 2005;33(4):195-200.

300. Felson DT. Osteoarthritis as a disease of mechanics. Osteoarthritis and Cartilage. 2013;21(1):10-5.

301. Robinson WH, Lepus CM, Wang Q, Raghu H, Mao R, Lindstrom TM, et al. Low-grade inflammation as a key mediator of the pathogenesis of osteoarthritis. Nature Reviews Rheumatology. 2016;12(10):580.

302. Berenbaum F, Eymard F, Houard X. Osteoarthritis, inflammation and obesity. Current Opinion in Rheumatology. 2013;25(1):114-8.

303. You T, Nicklas BJ. Chronic inflammation: role of adipose tissue and modulation by weight loss. Current Diabetes Reviews. 2006;2(1):29-37.

304. Zhuo Q, Yang W, Chen J, Wang Y. Metabolic syndrome meets osteoarthritis. Nature Reviews Rheumatology. 2012;8(12):729.

305. Thijssen E, Van Caam A, Van Der Kraan PM. Obesity and osteoarthritis, more than just wear and tear: pivotal roles for inflamed adipose tissue and dyslipidaemia in obesity-induced osteoarthritis. Rheumatology. 2015;54(4):588-600.

306. Lotz MK. New developments in osteoarthritis: posttraumatic osteoarthritis: pathogenesis and pharmacological treatment options. Arthritis Research & Therapy. 2010;12(3):1-9.

307. Lieberthal J, Sambamurthy N, Scanzello CR. Inflammation in joint injury and post-traumatic osteoarthritis. Osteoarthritis and Cartilage. 2015;23(11):1825-34.

308. Buckwalter JA, Brown TD, Research R. Joint injury, repair, and remodeling: roles in post-traumatic osteoarthritis. Clinical Orthopaedics and Related Research. 2004;423:7-16.

309. Arden N, Nevitt MC, rheumatology rC. Osteoarthritis: epidemiology. Best Practice & Research Clinical Rheumatology. 2006;20(1):3-25.

310. Loeser RF, Goldring SR, Scanzello CR, Goldring MB. Osteoarthritis: A disease of the joint as an organ. Arthritis & Rheumatism. 2012;64(6):1697-707.

311. Deveza LA, Loeser RF. Is osteoarthritis one disease or a collection of many? Rheumatology. 2018;57(4):iv34-iv42.

312. Castañeda S, Roman-Blas JA, Largo R, Herrero-Beaumont G. Osteoarthritis: a progressive disease with changing phenotypes. Rheumatology 2014;53:13.

313. Goldring MB, Otero M, Plumb DA, Dragomir C, Favero M, El Hachem K, et al. Roles of inflammatory and anabolic cytokines in cartilage metabolism: signals and multiple effectors converge upon MMP-13 regulation in osteoarthritis. European Cells & Materials. 2011;21:202.

314. Mobasheri A, Batt M. An update on the pathophysiology of osteoarthritis. Annals of Physical and Rehabilitation Medicine. Annals of Physical and Rehabilitation Medicine. 2016;59(5-6):333-9.

315. Hermansson M, Sawaji Y, Bolton M, Alexander S, Wallace A, Begum S, et al. Proteomic analysis of articular cartilage shows increased type II collagen synthesis in osteoarthritis and expression of inhibin βA (activin A), a regulatory molecule for chondrocytes. Journal of Biological Chemistry. 2004;279(42):43514-21.

316. Aigner T, Fundel K, Saas J, Gebhard PM, Haag J, Weiss T, et al. Large ‐ scale gene expression profiling reveals major pathogenetic pathways of cartilage degeneration in osteoarthritis. Arthritis & Rheumatism. 2006;54(11):3533-44.

317. Calvo E, Palacios I, Delgado E, Sanchez-Pernaute O, Largo R, Egido J, et al. Histopathological correlation of cartilage swelling detected by magnetic resonance imaging in early experimental osteoarthritis. Osteoarthritis and Cartilage. 2004;12(11):878-86.

318. Troeberg L, Nagase H. Proteases involved in cartilage matrix degradation in osteoarthritis. Biochimica et Biophysica Acta. 2012;1824(1):133-45.

319. Pratta MA, Yao W, Decicco C, Tortorella MD, Liu R-Q, Copeland RA, et al. Aggrecan protects cartilage collagen from proteolytic cleavage. Journal of Biological Chemistry. 2003;278(46):45539-45.

320. Goldring MB. Chondrogenesis, chondrocyte differentiation, and articular cartilage metabolism in health and osteoarthritis. Therapeutic Advances in Musculoskeletal disease. 2012;4(4):269-85.

321. Rolauffs B, Williams JM, Aurich M, Grodzinsky AJ, Kuettner KE, Cole AA, et al. Proliferative remodeling of the spatial organization of human superficial chondrocytes distant from focal early osteoarthritis. Arthritis & Rheumatism. 2010;62(2):489-98.

322. Lorenzo P, Bayliss MT, Heinegård D. Altered patterns and synthesis of extracellular matrix macromolecules in early osteoarthritis. Matrix Biology. 2004;23(6):381-91.

323. Pritzker KP, Gay S, Jimenez SA, Ostergaard K, Pelletier JP, Revell PA, et al. Osteoarthritis cartilage histopathology: grading and staging. Osteoarthritis and Cartilage. 2006;14(1):13-29.

324. Billinghurst RC, Dahlberg L, Ionescu M, Reiner A, Bourne R, Rorabeck C, et al. Enhanced cleavage of type II collagen by collagenases in osteoarthritic articular cartilage. The Journal of Clinical Investigation. 1997;99(7):1534-45.

325. Cawston TE, Young DA. Proteinases involved in matrix turnover during cartilage and bone breakdown. Cell and Tissue Research. 2010;339(1):221.

326. Fosang AJ, Little CB. Drug insight: aggrecanases as therapeutic targets for osteoarthritis. Nature Clinical Practice Rheumatology. 2008;4(8):420-7.

327. Huang K, Wu L. Aggrecanase and aggrecan degradation in osteoarthritis: a review. Journal of International Medical Research. 2008;36(6):1149-60.

328. Fosang AJ, Rogerson FM, East CJ, Stanton H. ADAMTS-5: the story so far. AJ. Fosang et al. European Cells and Materials. 2008;15(1):11-26.

329. Madry H, Luyten FP, Facchini A. Biological aspects of early osteoarthritis. Knee Surgery Sports Traumatology Arthroscopy. 2012;20(3):407-22.

330. Roach H, Aigner T, Soder S, Haag J, Welkerling H. Pathobiology of osteoarthritis: pathomechanisms and potential therapeutic targets. Current Drug Targets. 2007;8(2):271-82.

331. Goldring MB, Goldring SR. Articular cartilage and subchondral bone in the pathogenesis of osteoarthritis. Annals of the New York Academy of Sciences. 2010;1192:230-7.

332. Tetlow LC, Adlam DJ, Woolley DE. Matrix metalloproteinase and proinflammatory cytokine production by chondrocytes of human osteoarthritic cartilage: associations with degenerative changes. Arthritis & Rheumatism. 2001;44(3):585-94.

333. Bluteau G, Conrozier T, Mathieu P, Vignon E, Herbage D, Mallein-Gerin F. Matrix metalloproteinase-1,-3,-13 and aggrecanase-1 and-2 are differentially expressed in experimental osteoarthritis. Biochimica et Biophysica Acta. 2001;1526(2):147-58.

334. Kevorkian L, Young DA, Darrah C, Donell ST, Shepstone L, Porter S, et al. Expression profiling of metalloproteinases and their inhibitors in cartilage. Arthritis & Rheumatism. 2004;50(1):131-41.

335. Tortorella MD, Malfait AM, Deccico C, Arner E. The role of ADAM-TS4 (aggrecanase-1) and ADAM-TS5 (aggrecanase-2) in a model of cartilage degradation. Osteoarthritis and Cartilage. 2001;9(6):539-52.

336. Bau B, Gebhard PM, Haag J, Knorr T, Bartnik E, Aigner T. Relative messenger RNA expression profiling of collagenases and aggrecanases in human articular chondrocytes in vivo and in vitro. Arthritis & Rheumatism. 2002;46(10):2648-57.

337. Sato T, Konomi K, Yamasaki S, Aratani S, Tsuchimochi K, Yokouchi M, et al. Comparative analysis of gene expression profiles in intact and damaged regions of human osteoarthritic cartilage. Arthritis & Rheumatism. 2006;54(3):808-17.

338. Torzilli PA, Bhargava M, Park S, Chen CC. Mechanical load inhibits IL-1 induced matrix degradation in articular cartilage. Osteoarthritis and Cartilage. 2010;18(1):97-105.

339. Buschmann MD, Kim Y-J, Wong M, Frank E, Hunziker EB, Grodzinsky AJ, et al. Stimulation of aggrecan synthesis in cartilage explants by cyclic loading is localized to regions of high interstitial fluid flow. Archives of Biochemistry and Biophysics. 1999;366(1):1-7.

340. Wong M, Siegrist M, Cao X. Cyclic compression of articular cartilage explants is associated with progressive consolidation and altered expression pattern of extracellular matrix proteins. Matrix Biology. 1999;18(4):391-9.

341. Ding L, Heying E, Nicholson N, Stroud NJ, Homandberg GA, Buckwalter J, et al. Mechanical impact induces cartilage degradation via mitogen activated protein kinases. Osteoarthritis and Cartilage. 2010;18(11):1509-17.

342. McGlashan S, Cluett E, Jensen C, Poole C. Primary cilia in osteoarthritic chondrocytes: from chondrons to clusters. Developmental Dynamics. 2008;237(8):2013-20.

343. Loeser RF. Integrins and chondrocyte–matrix interactions in articular cartilage. Matrix Biology. 2014;39:11-6.

344. Lin PM, Chen C-TC, Torzilli PA. Increased stromelysin-1 (MMP-3), proteoglycan degradation (3B3-and 7D4) and collagen damage in cyclically load-injured articular cartilage. Osteoarthritis and Cartilage. 2004;12(6):485-96.

345. Fitzgerald JB, Jin M, Dean D, Wood DJ, Zheng MH, Grodzinsky AJ. Mechanical compression of cartilage explants induces multiple time-dependent gene expression patterns and involves intracellular calcium and cyclic AMP. Journal of Biological Chemistry. 2004;279(19):19502-11.

346. Xu L, Golshirazian I, Asbury BJ, Li Y. Induction of high temperature requirement A1, a serine protease, by TGF-beta1 in articular chondrocytes of mouse models of OA. Histology and Histopathology. 2014;29:609-618.

347. Swingler TE, Waters JG, Davidson RK, Pennington CJ, Puente XS, Darrah C, et al. Degradome expression profiling in human articular cartilage. Arthritis Research & Therapy. 2009;11(3):R96.

348. Polur I, Lee PL, Servais JM, Xu L, Li Y, histopathology. Role of HTRA1, a serine protease, in the progression of articular cartilage degeneration. Histology and Histopathology. 2010;25(5):599.

349. Pap T, Bertrand J. Syndecans in cartilage breakdown and synovial inflammation. Nature Reviews Rheumatology. 2013;9(1):43.

350. Xu L, Peng H, Glasson S, Lee PL, Hu K, Ijiri K, et al. Increased expression of the collagen receptor discoidin domain receptor 2 in articular cartilage as a key event in the pathogenesis of osteoarthritis. Arthritis & Rheumatism. 2007;56(8):2663-73.

351. Goldring MB, Otero M. Inflammation in osteoarthritis. Current Opinion in Rheumatology. 2011;23(5):471.

352. Kokebie R, Aggarwal R, Lidder S, Hakimiyan AA, Rueger DC, Block JA, et al. The role of synovial fluid markers of catabolism and anabolism in osteoarthritis, rheumatoid arthritis and asymptomatic organ donors. Arthritis Research & Therapy. 2011;13(2):1-10.

353. Venn G, Nietfeld J, Duits A, Brennan F, Arner E, Covington M, et al. Elevated synovial fluid levels of interleukin‐6 and tumor necrosis factor associated with early experimental canine osteoarthritis. Arthritis & Rheumatism. 1993;36(6):819-26.

354. Smith MD, Triantafillou S, Parker A, Youssef PP, Coleman M. Synovial membrane inflammation and cytokine production in patients with early osteoarthritis. The Journal of Rheumatology. 1997;24(2):365-71.

355. Song RH, Tortorella MD, Malfait AM, Alston JT, Yang Z, Arner EC, et al. Aggrecan degradation in human articular cartilage explants is mediated by both ADAMTS-4 and ADAMTS-5. Arthritis & Rheumatism. 2007;56(2):575-85.

356. Mehana E-SE, Khafaga AF, El-Blehi SS. The role of matrix metalloproteinases in osteoarthritis pathogenesis: An updated review. Life Sciences. 2019;234:116786.

357. Akhtar N, Rasheed Z, Ramamurthy S, Anbazhagan AN, Voss FR, Haqqi TM, et al. MicroRNA‐27b regulates the expression of matrix metalloproteinase 13 in human osteoarthritis chondrocytes. Arthritis & Rheumatism. 2010;62(5):1361-71.

358. Scanzello CR, Goldring SR. The role of synovitis in osteoarthritis pathogenesis. Bone. 2012;51(2):249-57.

359. Liu-Bryan R, Terkeltaub R. Emerging regulators of the inflammatory process in osteoarthritis. Nature Reviews Rheumatology. 2015;11(1):35.

360. Berenbaum F. Osteoarthritis as an inflammatory disease (osteoarthritis is not osteoarthrosis!). Osteoarthritis and Cartilage. 2013;21(1):16-21.

361. Sellam J, Berenbaum F. The role of synovitis in pathophysiology and clinical symptoms of osteoarthritis. Nature Reviews Rheumatology. 2010;6(11):625-35.

362. Loeser RF. Aging and osteoarthritis: the role of chondrocyte senescence and aging changes in the cartilage matrix. Osteoarthritis and Cartilage. 2009;17(8):971-9.

363. Greene MA, Loeser RF. Aging-related inflammation in osteoarthritis. Osteoarthritis and Cartilage. 2015;23(11):1966-71.

364. Rahmati M, Nalesso G, Mobasheri A, Mozafari M. Aging and osteoarthritis: Central role of the extracellular matrix. Ageing Research Reviews. 2017;40:20-30.

365. Loeser RF, Collins JA, Diekman BO. Ageing and the pathogenesis of osteoarthritis. Nature Reviews Rheumatology. 2016;12(7):412-20.

366. Lotz MK, Otsuki S, Grogan SP, Sah R, Terkeltaub R, D'Lima D, et al. Cartilage cell clusters. Arthritis & Rheumatism. 2010;62(8):2206.

367. Bailey AJ, Mansell JP. Do subchondral bone changes exacerbate or precede articular cartilage destruction in osteoarthritis of the elderly? Gerontology. 1997;43(5):296-304.

368. Buckland-Wright C. Subchondral bone changes in hand and knee osteoarthritis detected by radiography. Osteoarthritis and Cartilage. 2004;12:10-9.

369. Burr DB. Anatomy and physiology of the mineralized tissues: role in the pathogenesis of osteoarthrosis. Osteoarthritis and Cartilage. 2004;12:20-30.

370. Radin EL, Rose RM. Role of subchondral bone in the initiation and progression of cartilage damage. Clinical Orthopaedics and Related Research. 1986(213):34-40.

371. Radin EL, Paul IL, Tolkoff MJ, Rheumatology ROJotACo. Subchondral bone changes in patients with early degenerative joint disease. Arthritis & Rheumatism. 1970;13(4):400-5.

372. Buckland‐Wright J, Macfarlane D, Lynch J, Clark B. Quantitative microfocal radiographic assessment of progression in osteoarthritis of the hand. Arthritis & Rheumatism. 1990;33(1):57-65.

373. Buckland-Wright J, Macfarlane D, Jasani MK, Lynch J. Quantitative microfocal radiographic assessment of osteoarthritis of the knee from weight bearing tunnel and semiflexed standing views. The Journal of Rheumatology. 1994;21(9):1734-41.

374. Bruyère O, Dardenne C, Lejeune E, Zegels B, Pahaut A, Richy F, et al. Subchondral tibial bone mineral density predicts future joint space narrowing at the medial femoro-tibial compartment in patients with knee osteoarthritis. Bone. 2003;32(5):541-5.

375. Carlson CS, Loeser RF, Purser CB, Gardin JF, Jerome CP. Osteoarthritis in cynomolgus macaques III: effects of age, gender, and subchondral bone thickness on the severity of disease. Journal of Bone and Mineral Research. 1996;11(9):1209-17.

376. Carlson CS, Loeser RF, Jayo MJ, Weaver DS, Adams MR, Jerome CP. Osteoarthritis in cynomolgus macaques: a primate model of naturally occurring disease. Journal of Orthopaedic Research. 1994;12(3):331-9.

377. Ding M, Danielsen C, Hvid I. Age-related three-dimensional microarchitectural adaptations of subchondral bone tissues in guinea pig primary osteoarthrosis. Calcified Tissue International. 2006;78(2):113-22.

378. Wang T, Wen C-Y, Yan C-H, Lu W-W, Chiu K-Y. Spatial and temporal changes of subchondral bone proceed to microscopic articular cartilage degeneration in guinea pigs with spontaneous osteoarthritis. Osteoarthritis and Cartilage. 2013;21(4):574-81.

379. Anderson-MacKenzie JM, Quasnichka HL, Starr RL, Lewis EJ, Billingham MEJ, Bailey AJ. Fundamental subchondral bone changes in spontaneous knee osteoarthritis. International Journal of Biochemistry and Cell Biology. 2005;37(1):224-36.

380. Day J, Ding M, Van Der Linden J, Hvid I, Sumner D, Weinans H. A decreased subchondral trabecular bone tissue elastic modulus is associated with pre-arthritic cartilage damage. Journal of Orthopaedic Research. 2001;19(5):914-8.

381. Ding M, Odgaard A, Hvid I, Hvid I. Changes in the three-dimensional microstructure of human tibial cancellous bone in early osteoarthritis. Journal of Bone and Joint Surgery. 2003;85(6):906-12.

382. Karvonen R, Miller P, Nelson D, Granda J, Fernandez-Madrid F. Periarticular osteoporosis in osteoarthritis of the knee. The Journal of Rheumatology. 1998;25(11):2187-94.

383. Bolbos RI, Zuo J, Banerjee S, Link TM, Ma CB, Li X, et al. Relationship between trabecular bone structure and articular cartilage morphology and relaxation times in early OA of the knee joint using parallel MRI at 3T. Osteoarthritis and Cartilage. 2008;16(10):1150-9.

384. Dieppe P, Cushnaghan J, Young P, Kirwan J. Prediction of the progression of joint space narrowing in osteoarthritis of the knee by bone scintigraphy. Annals of the Rheumatic Diseases. 1993;52(8):557-63.

385. McCrae F, Shouls J, Dieppe P, Watt I. Scintigraphic assessment of osteoarthritis of the knee joint. Annals of the Rheumatic Diseases. 1992;51(8):938-42.

386. Hutton C, Higgs E, Jackson P, Watt I, Dieppe P. 99mTc HMDP bone scanning in generalised nodal osteoarthritis. II. The four hour bone scan image predicts radiographic change. Annals of the Rheumatic Diseases. 1986;45(8):622-6.

387. Bettica P, Cline G, Hart DJ, Meyer J, Spector TD. Evidence for increased bone resorption in patients with progressive knee osteoarthritis: longitudinal results from the Chingford study. Arthritis & Rheumatism. 2002;46(12):3178-84.

388. Johnson ML, Gong G, Kimberling W, Recker SM, Kimmel DB, Recker RR. Linkage of a gene causing high bone mass to human chromosome 11 (11q12-13). The American Journal of Human Genetics. 1997;60(6):1326-32.

389. Sniekers YH, Intema F, Lafeber FP, van Osch GJ, van Leeuwen JP, Weinans H, et al. A role for subchondral bone changes in the process of osteoarthritis; a micro-CT study of two canine models. BMC Musculoskeletal Disorders. 2008;9(1):20.

390. Intema F, Sniekers YH, Weinans H, Vianen ME, Yocum SA, Zuurmond AM, et al. Similarities and discrepancies in subchondral bone structure in two differently induced canine models of osteoarthritis. Journal of Bone and Mineral Research. 2010;25(7):1650-7.

391. Intema F, Hazewinkel H, Gouwens D, Bijlsma J, Weinans H, Lafeber F, et al. In early OA, thinning of the subchondral plate is directly related to cartilage damage: results from a canine ACLT-meniscectomy model. Osteoarthritis and Cartilage. 2010;18(5):691-8.

392. Dedrick DK, Goldstein SA, Brandt K, O'Connor B, Goulet RW, Albrecht M. A longitudinal study of subchondral plate and trabecular bone in cruciate ‐ deficient dogs with osteoarthritis followed up for 54 months. Arthritis & Rheumatism. 1993;36(10):1460-7.

393. Brandt KD, Myers SL, Burr D, Albrecht M. Osteoarthritic changes in canine articular cartilage, subchondral bone, and synovium fifty ‐ four months after transection of the anterior cruciate ligament. Arthritis & Rheumatism. 1991;34(12):1560-70.

394. Botter SM, van Osch GJ, Clockaerts S, Waarsing JH, Weinans H, van Leeuwen JP. Osteoarthritis induction leads to early and temporal subchondral plate porosity in the tibial plateau of mice: an in vivo microfocal computed tomography study. Arthritis & Rheumatism. 2011;63(9):2690-9.

395. Hayami T, Pickarski M, Zhuo Y, Wesolowski GA, Rodan GA, Duong LT. Characterization of articular cartilage and subchondral bone changes in the rat anterior cruciate ligament transection and meniscectomized models of osteoarthritis. Bone. 2006;38(2):234-43.

396. Hayami T, Zhuo Y, Wesolowski GA, Pickarski M, Duong LT. Inhibition of cathepsin K reduces cartilage degeneration in the anterior cruciate ligament transection rabbit and murine models of osteoarthritis. Bone. 2012;50(6):1250-9.

397. Botter S, Van Osch G, Waarsing J, Van der Linden J, Verhaar J, Pols H, et al. Cartilage damage pattern in relation to subchondral plate thickness in a collagenase-induced model of osteoarthritis. Osteoarthritis and Cartilage. 2008;16(4):506-14.

398. Batiste DL, Kirkley A, Laverty S, Thain LMF, Spouge AR, Holdsworth DW. Ex vivo characterization of articular cartilage and bone lesions in a rabbit ACL transection model of osteoarthritis using MRI and micro-CT. Osteoarthritis and Cartilage. 2004;12(12):986-96.

399. Pastoureau P, Chomel A, Bonnet J. Evidence of early subchondral bone changes in the meniscectomized guinea pig. A densitometric study using dual-energy X-ray absorptiometry subregional analysis. Osteoarthritis and Cartilage. 1999;7(5):466-73.

400. Kadri A, Ea H, Bazille C, Hannouche D, Liote F, Cohen‐Solal M, et al. Osteoprotegerin inhibits cartilage degradation through an effect on trabecular bone in murine experimental osteoarthritis. Arthritis & Rheumatism. 2008;58(8):2379-86.

401. Boyd SK, Matyas JR, Wohl GR, Kantzas A, Zernicke RF. Early regional adaptation of periarticular bone mineral density after anterior cruciate ligament injury. Journal of Applied Physiology. 2000;89(6):2359-64.

402. Wohl GR, Shymkiw RC, Matyas JR, Kloiber R, Zernicke RF. Periarticular cancellous bone changes following anterior cruciate ligament injury. Journal of Applied Physiology. 2001;91(1):336-42.

403. Boyd SK, Müller R, Zernicke RF. Mechanical and architectural bone adaptation in early stage experimental osteoarthritis. Journal of Bone and Mineral Research. 2002;17(4):687-94.

404. Aizah N, Chong PP, Kamarul T. Early alterations of subchondral bone in the rat anterior cruciate ligament transection model of osteoarthritis. Cartilage. 2019:1947603519878479.

405. Hayami T, Pickarski M, Wesolowski GA, Mclane J, Bone A, Destefano J, et al. The role of subchondral bone remodeling in osteoarthritis: reduction of cartilage degeneration and prevention of osteophyte formation by alendronate in the rat anterior cruciate ligament transection model. Arthritis & Rheumatism. 2004;50(4):1193-206.

406. Huebner JL, Hanest MA, Beekman B, TeKoppele JM, Kraus VB. A comparative analysis of bone and cartilage metabolism in two strains of guinea-pig with varying degrees of naturally occurring osteoarthritis. Osteoarthritis and Cartilage. 2002;10(10):758-67.

407. Ham KD, Loeser RF, Lindgren BR, Carlson CS. Effects of long‐term estrogen replacement therapy on osteoarthritis severity in cynomolgus monkeys. Arthritis & Rheumatism. 2002;46(7):1956-64.

408. Sniekers Y, Weinans H, Bierma-Zeinstra S, Van Leeuwen J, Van Osch G. Animal models for osteoarthritis: the effect of ovariectomy and estrogen treatment–a systematic approach. Osteoarthritis and Cartilage. 2008;16(5):533-41.

409. Hoegh-Andersen P, Tanko LB, Andersen TL, Lundberg CV, Mo JA, Heegaard AM, et al. Ovariectomized rats as a model of postmenopausal osteoarthritis: validation and application. Arthritis Research & Therapy. 2004;6(2):R169-R80.

410. Ham KD, Carlson CS. Effects of estrogen replacement therapy on bone turnover in subchondral bone and epiphyseal metaphyseal cancellous bone of ovariectomized cynomolgus monkeys. Journal of Bone and Mineral Research. 2004;19(5):823-9.

411. Sniekers YH, Weinans H, van Osch GJ, van Leeuwen JP. Oestrogen is important for maintenance of cartilage and subchondral bone in a murine model of knee osteoarthritis. Arthritis Research & Therapy. 2010;12(5):1-12.

412. Bellido M, Lugo L, Roman-Blas JA, Castañeda S, Caeiro JR, Dapia S, et al. Subchondral bone microstructural damage by increased remodelling aggravates experimental osteoarthritis preceded by osteoporosis. Arthritis Research & Therapy. 2010;12(4):R152.

413. Calvo E, Castaneda S, Largo R, Fernández-Valle M, Rodriguez-Salvanes F, Herrero-Beaumont G, et al. Osteoporosis increases the severity of cartilage damage in an experimental model of osteoarthritis in rabbits. Osteoarthritis and Cartilage. 2007;15(1):69-77.

414. Ma H-L, Blanchet T, Peluso D, Hopkins B, Morris E, Glasson S. Osteoarthritis severity is sex dependent in a surgical mouse model. Osteoarthritis and Cartilage. 2007;15(6):695-700.

415. Bellido M, Lugo L, Roman-Blas J, Castaneda S, Calvo E, Largo R, et al. Improving subchondral bone integrity reduces progression of cartilage damage in experimental osteoarthritis preceded by osteoporosis. Osteoarthritis and Cartilage. 2011;19(10):1228-36.

416. Sondergaard BC, Oestergaard S, Christiansen C, Tankó LB, Karsdal MA. The effect of oral calcitonin on cartilage turnover and surface erosion in an ovariectomized rat model. Arthritis & Rheumatism. 2007;56(8):2674-8.

417. Karsdal M, Bay-Jensen A, Henriksen K, Christiansen C. The pathogenesis of osteoarthritis involves bone, cartilage and synovial inflammation: may estrogen be a magic bullet? Menopause International. 2012;18(4):139-46.

418. Brown TD, Radin EL, Martin RB, Burr DB. Finite-Element Studies of Some Juxtarticular Stress Changes Due to Localized Subchondral Stiffening. Journal of Biomechanics. 1984;17(1):11-&.

419. Bultink IE, Lems WF. Osteoarthritis and osteoporosis: what is the overlap? Current Rheumatology Reports. 2013;15(5):328.

420. Klose-Jensen R, Hartlev LB, Boel LWT, Laursen MB, Stengaard-Pedersen K, Keller KK, et al. Subchondral bone turnover, but not bone volume, is increased in early stage osteoarthritic lesions in the human hip joint. Osteoarthritis and Cartilage. 2015;23(12):2167-73.

421. Massicotte F, Lajeunesse D, Benderdour M, Pelletier J-P, Hilal G, Duval N, et al. Can altered production of interleukin-1β, interleukin-6, transforming growth factor-β and prostaglandin E2 by isolated human subchondral osteoblasts identify two subgroups of osteoarthritic patients. Osteoarthritis and Cartilage. 2002;10(6):491-500.

422. Tat SK, Pelletier J-P, Lajeunesse D, Fahmi H, Lavigne M, Martel-Pelletier J. The differential expression of osteoprotegerin (OPG) and receptor activator of nuclear factor κB ligand (RANKL) in human osteoarthritic subchondral bone osteoblasts is an indicator of the metabolic state of these disease cells. Clinical and Experimental Rheumatology. 2008;26(2):295.

423. Tat SK, Pelletier J-P, Lajeunesse D, Fahmi H, Duval N, Martel-Pelletier J. Differential modulation of RANKL isoforms by human osteoarthritic subchondral bone osteoblasts: influence of osteotropic factors. Bone. 2008;43(2):284-91.

424. Lajeunesse D, Pelletier J, Martel-Pelletier J. Osteoporosis and osteoarthritis: bone is the common battleground. Medicographia. 2010;32(4):391-5.

425. Burr DB. The importance of subchondral bone in the progression of osteoarthritis. The Journal of Rheumatology. 2004;70:77-80.

426. Chappard C, Peyrin F, Bonnassie A, Lemineur G, Brunet-Imbault B, Lespessailles E, et al. Subchondral bone micro-architectural alterations in osteoarthritis: a synchrotron micro-computed tomography study. Osteoarthritis and Cartilage. 2006;14(3):215-23.

427. Li BH, Aspden RM. Composition and mechanical properties of cancellous bone from the femoral head of patients with osteoporosis or osteoarthritis. Journal of Bone and Mineral Research. 1997;12(4):641-51.

428. Li BH, Aspden RM. Mechanical and material properties of the subchondral bone plate from the femoral head of patients with osteoarthritis or osteoporosis. Annals of the Rheumatic Diseases. 1997;56(4):247-54.

429. Grynpas MD, Alpert B, Katz I, Lieberman I, Pritzker KPH. Subchondral Bone in Osteoarthritis. Calcified Tissue International. 1991;49(1):20-6.

430. Mansell JP, Bailey AJ. Abnormal cancellous bone collagen metabolism in osteoarthritis. The Journal of Clinical Investigation. 1998;101(8):1596-603.

431. Coats AM, Zioupos P, Aspden RM. Material properties of subchondral bone from patients with osteoporosis or osteoarthritis by microindentation testing and electron probe microanalysis. Calcified Tissue International. 2003;73(1):66-71.

432. Goldring MB, Goldring SR. Articular cartilage and subchondral bone in the pathogenesis of osteoarthritis. Skeletal Biology and Medicine. 2010;1192:230-7.

433. Bailey AJ, Mansell JP, Sims TJ, Banse X. Biochemical and mechanical properties of subchondral bone in osteoarthritis. Biorheology. 2004;41(3‐4):349-58.

434. Mansell JP, Collins C, Bailey AJ. Bone, not cartilage, should be the major focus in osteoarthritis. Nature clinical practice Rheumatology. 2007;3(6):306-7.

435. Couchourel D, Aubry I, Delalandre A, Lavigne M, Martel-Pelletier J, Pelletier JP, et al. Altered mineralization of human osteoarthritic osteoblasts is attributable to abnormal type I collagen production. Arthritis & Rheumatism. 2009;60(5):1438-50.

436. Bailey AJ, Sims TJ, Knott L. Phenotypic expression of osteoblast collagen in osteoarthritic bone: production of type I homotrimer. The International Journal of Biochemistry & Cell Biology. 2002;34(2):176-82.

437. Bailey AJ, Knott L. Molecular changes in bone collagen in osteoporosis and osteoarthritis in the elderly. Experimental Gerontology. 1999;34(3):337-51.

438. Chan TF, Couchourel D, Abed É, Delalandre A, Duval N, Lajeunesse D. Elevated Dickkopf‐2 levels contribute to the abnormal phenotype of human osteoarthritic osteoblasts. Journal of Bone and Mineral Research. 2011;26(7):1399-410.

439. Mansell JP, Tarlton JF, Bailey AJ. Biochemical evidence for altered subchondral bone collagen metabolism in osteoarthritis of the hip. British Journal of Rheumatology. 1997;36(1):16-9.

440. Hernández-Molina G, Neogi T, Hunter DJ, Niu J, Guermazi A, Reichenbach S, et al. The association of bone attrition with knee pain and other MRI features of osteoarthritis. Annals of the Rheumatic Diseases. 2008;67(1):43-7.

441. Reichenbach S, Guermazi A, Niu J, Neogi T, Hunter DJ, Roemer FW, et al. Prevalence of bone attrition on knee radiographs and MRI in a community-based cohort. Osteoarthritis and Cartilage. 2008;16(9):1005-10.

442. Neogi T, Nevitt M, Niu J, Sharma L, Roemer F, Guermazi A, et al. Subchondral bone attrition may be a reflection of compartment-specific mechanical load: the MOST Study. Annals of the Rheumatic Diseases. 2010;69(5):841-4.

443. Roemer FW, Guermazi A, Javaid MK, Lynch JA, Niu J, Zhang Y, et al. Change in MRI-detected subchondral bone marrow lesions is associated with cartilage loss: the MOST Study. A longitudinal multicentre study of knee osteoarthritis. Annals of the Rheumatic Diseases.2009;68(9):1461-5.

444. Roemer FW, Neogi T, Nevitt MC, Felson DT, Zhu Y, Zhang Y, et al. Subchondral bone marrow lesions are highly associated with, and predict subchondral bone attrition longitudinally: the MOST study. Osteoarthritis and Cartilage. 2010;18(1):47-53.

445. Kothari A, Guermazi A, Chmiel JS, Dunlop D, Song J, Almagor O, et al. Within ‐ subregion relationship between bone marrow lesions and subsequent cartilage loss in knee osteoarthritis. Arthritis Care & Research. 2010;62(2):198-203.

446. Taljanovic MS, Graham AR, Benjamin JB, Gmitro AF, Krupinski EA, Schwartz SA, et al. Bone marrow edema pattern in advanced hip osteoarthritis: quantitative assessment with magnetic resonance imaging and correlation with clinical examination, radiographic findings, and histopathology. Skeletal Radiology. 2008;37(5):423-31.

447. Lo G, Hunter D, Nevitt M, Lynch J, McAlindon T. Strong association of MRI meniscal derangement and bone marrow lesions in knee osteoarthritis: data from the osteoarthritis initiative. Osteoarthritis and Cartilage. 2009;17(6):743-7.

448. Hunter DJ, Gerstenfeld L, Bishop G, Davis AD, Mason ZD, Einhorn TA, et al. Bone marrow lesions from osteoarthritis knees are characterized by sclerotic bone that is less well mineralized. Arthritis Research & Therapy. 2009;11(1):R11.

449. Carrino J, Blum J, Parellada J, Schweitzer M, Morrison W. MRI of bone marrow edema-like signal in the pathogenesis of subchondral cysts. Osteoarthritis and Cartilage. 2006;14(10):1081-5.

450. Muratovic D, Findlay D, Cicuttini F, Wluka A, Lee Y, Edwards S, et al. Bone marrow lesions in knee osteoarthritis: regional differences in tibial subchondral bone microstructure and their association with cartilage degeneration. Osteoarthritis and Cartilage. 2019;27(11):1653-62.

451. Tanamas SK, Wluka AE, Pelletier J-P, Martel-Pelletier J, Abram F, Wang Y, et al. The association between subchondral bone cysts and tibial cartilage volume and risk of joint replacement in people with knee osteoarthritis: a longitudinal study. Arthritis Research & Therapy. 2010;12(2):1-7.

452. Bowes MA, McLure SW, Wolstenholme CB, Vincent GR, Williams S, Grainger A, et al. Osteoarthritic bone marrow lesions almost exclusively colocate with denuded cartilage: a 3D study using data from the Osteoarthritis Initiative. Annals of the Rheumatic Diseases. 2016;75(10):1852-7.

453. Felson DT, Chaisson CE, Hill CL, Totterman SM, Gale ME, Skinner KM, et al. The association of bone marrow lesions with pain in knee osteoarthritis. Annals of Internal Medicine.2001;134(7):541-9.

454. Driban JB, Lo GH, Lee JY, Ward RJ, Miller E, Pang J, et al. Quantitative bone marrow lesion size in osteoarthritic knees correlates with cartilage damage and predicts longitudinal cartilage loss. BMC Musculoskeletal Disorders. 2011;12(1):1-10.

455. Zanetti M, Bruder E, Romero J, Hodler J. Bone marrow edema pattern in osteoarthritic knees: correlation between MR imaging and histologic findings. Radiology. 2000;215(3):835-40.

456. Crema MD, Roemer FW, Zhu Y, Marra MD, Niu J, Zhang Y, et al. Subchondral cystlike lesions develop longitudinally in areas of bone marrow edema–like lesions in patients with or at risk for knee osteoarthritis: detection with MR imaging—the MOST study. Radiology. 2010;256(3):855-62.

457. Crema M, Roemer F, Marra M, Niu J, Lynch J, Felson D, et al. Contrast-enhanced MRI of subchondral cysts in patients with or at risk for knee osteoarthritis: the MOST study. European Journal of Radiology. 2010;75(1):e92-e6.

458. Li G, Zheng Q, Landao-Bassonga E, Cheng TS, Pavlos NJ, Ma Y, et al. Influence of age and gender on microarchitecture and bone remodeling in subchondral bone of the osteoarthritic femoral head. Bone. 2015;77:91-7.

459. Chiba K, Nango N, Kubota S, Okazaki N, Taguchi K, Osaki M, et al. Relationship between microstructure and degree of mineralization in subchondral bone of osteoarthritis: a synchrotron radiation μCT study. Journal of Bone and Mineral Research. 2012;27(7):1511-7.

460. Suri S, Walsh DA. Osteochondral alterations in osteoarthritis. Bone. 2012;51(2):204-11.

461. Hu W, Chen Y, Dou C, Dong S. Microenvironment in subchondral bone: predominant regulator for the treatment of osteoarthritis. Annals of the Rheumatic Diseases. 2021;1;80(4):413-22.

462. Walsh DA, McWilliams DF, Turley MJ, Dixon MR, Fransès RE, Mapp PI, et al. Angiogenesis and nerve growth factor at the osteochondral junction in rheumatoid arthritis and osteoarthritis. Rheumatology. 2010;49(10):1852-61.

463. Yuan X, Meng H, Wang Y, Peng J, Guo Q, Wang A, et al. Bone–cartilage interface crosstalk in osteoarthritis: potential pathways and future therapeutic strategies. Osteoarthritis and Cartilage. 2014;22(8):1077-89.

464. Mapp PI, Walsh DA. Mechanisms and targets of angiogenesis and nerve growth in osteoarthritis. Nature Reviews Rheumatology. 2012;8(7):390.

465. Bijlsma JW, Berenbaum F, Lafeber FP. Osteoarthritis: an update with relevance for clinical practice. Lancet. 2011;377(9783):2115-26.

466. Sinusas K. Osteoarthritis: diagnosis and treatment. American Family Physician. 2012;85(1):49-56.

467. Bellamy N, Buchanan WW, Goldsmith CH, Campbell J, Stitt LW. Validation study of WOMAC: a health status instrument for measuring clinically important patient relevant outcomes to antirheumatic drug therapy in patients with osteoarthritis of the hip or knee. Journal of Rheumatology. 1988;15(12):1833-40.

468. Glyn-Jones S, Palmer AJ, Agricola R, Price AJ, Vincent TL, Weinans H, et al. Osteoarthritis. Lancet. 2015;386(9991):376-87.

469. Kellgren JH, Lawrence JS. Radiological assessment of osteo-arthrosis. Annals of the Rheumatic Diseases. 1957;16(4):494-502.

470. Braun HJ, Gold GE. Diagnosis of osteoarthritis: imaging. Bone. 2012;51(2):278-88.

471. Altman R, Asch E, Bloch D, Bole G, Borenstein D, Brandt K, et al. Development of criteria for the classification and reporting of osteoarthritis: classification of osteoarthritis of the knee. Arthritis & Rheumatism. 1986;29(8):1039-49.

472. Bauer D, Hunter D, Abramson S, Attur M, Corr M, Felson D, et al. Classification of osteoarthritis biomarkers: a proposed approach. Osteoarthritis and Cartilage. 2006;14(8):723-7.

473. Palmer A, Brown C, McNally E, Price A, Tracey I, Jezzard P, et al. Non-invasive imaging of cartilage in early osteoarthritis. The Bone & Joint Journal. 2013;95(6):738-46.

474. Pollard T, Gwilym S, Carr AJ. The assessment of early osteoarthritis. Journal of Bone and Joint Surgery. 2008;90(4):411-21.

475. Roemer FW, Crema MD, Trattnig S, Guermazi A. Advances in imaging of osteoarthritis and cartilage. Radiology. 2011;260(2):332-54.

476. Zhang W, Doherty M, Peat G, Bierma-Zeinstra M, Arden N, Bresnihan B, et al. EULAR evidence-based recommendations for the diagnosis of knee osteoarthritis. Annals of the Rheumatic Diseases. 2010;69(3):483-9.

477. Altman R, Alarcon G, Appelrouth D, Bloch D, Borenstein D, Brandt K, et al. The American College of Rheumatology criteria for the classification and reporting of osteoarthritis of the hip. Arthritis & Rheumatism. 1991;34(5):505-14.

478. Altman R, Alarcon G, Appelrouth D, Bloch D, Borenstein D, Brandt K, et al. The American College of Rheumatology criteria for the classification and reporting of osteoarthritis of the hand. Arthritis & Rheumatism. 1990;33(11):1601-10.

479. Liem Y, Judge A, Kirwan J, Ourradi K, Li Y, Sharif M. Multivariable logistic and linear regression models for identification of clinically useful biomarkers for osteoarthritis. Scientific Reports. 2020;10(1):1-12.

480. Mobasheri A, Bay-Jensen A-C, Van Spil W, Larkin J, Levesque M. Osteoarthritis Year in Review 2016: biomarkers (biochemical markers). Otsoearthritis and Cartilage. 2017;25(2):199-208.

481. McAlindon TE, Bannuru RR, Sullivan MC, Arden NK, Berenbaum F, Bierma-Zeinstra SM, et al. OARSI guidelines for the non-surgical management of knee osteoarthritis. Osteoarthritis and Cartilage. Osteoarthritis and Cartilage. 2014;22(3):363-88.

482. Zhang W, Moskowitz RW, Nuki G, Abramson S, Altman RD, Arden N, et al. OARSI recommendations for the management of hip and knee osteoarthritis, part I: critical appraisal

of existing treatment guidelines and systematic review of current research evidence. Osteoarthritis and Cartilage. 2007;15(9):981-1000.

483. Zhang W, Moskowitz RW, Nuki G, Abramson S, Altman RD, Arden N, et al. OARSI recommendations for the management of hip and knee osteoarthritis, Part II: OARSI evidence-based, expert consensus guidelines. Osteoarthritis and Cartilage. 2008;16(2):137-62.

484. Zhang W, Nuki G, Moskowitz RW, Abramson S, Altman RD, Arden NK, et al. OARSI recommendations for the management of hip and knee osteoarthritis: part III: Changes in evidence following systematic cumulative update of research published through January 2009. Osteoarthritis and Cartilage. 2010;18(4):476-99.

485. Bannuru RR, Osani M, Vaysbrot E, Arden N, Bennell K, Bierma-Zeinstra S, et al. OARSI guidelines for the non-surgical management of knee, hip, and polyarticular osteoarthritis. Osteoarthritis and Cartilage. 2019;27(11):1578-89.

486. Kolasinski SL, Neogi T, Hochberg MC, Oatis C, Guyatt G, Block J, et al. 2019 American College of Rheumatology/Arthritis Foundation guideline for the management of osteoarthritis of the hand, hip, and knee. Arthritis & Rheumatology. 2020;72(2):220-33.

487. Fernandes L, Hagen KB, Bijlsma JW, Andreassen O, Christensen P, Conaghan PG, et al. EULAR recommendations for the non-pharmacological core management of hip and knee osteoarthritis. Annals of the Rheumatic Diseases. 2013;72(7):1125-35.

488. Zhang W, Doherty M, Arden N, Bannwarth B, Bijlsma J, Gunther K-P, et al. EULAR evidence based recommendations for the management of hip osteoarthritis: report of a task force of the EULAR Standing Committee for International Clinical Studies Including Therapeutics (ESCISIT). Annals of the Rheumatic Diseases. 2005;64(5):669-81.

489. Bruyère O, Cooper C, Pelletier J-P, Branco J, Brandi ML, Guillemin F, et al. An algorithm recommendation for the management of knee osteoarthritis in Europe and internationally: a report from a task force of the European Society for Clinical and Economic Aspects of Osteoporosis and Osteoarthritis (ESCEO). Seminars in Arthritis and Rheumatism; 2014;44(3):253-263.

490. Bruyère O, Honvo G, Veronese N, Arden NK, Branco J, Curtis EM, et al. An updated algorithm recommendation for the management of knee osteoarthritis from the European Society for Clinical and Economic Aspects of Osteoporosis, Osteoarthritis and Musculoskeletal Diseases (ESCEO). Seminars in Arthritis and Rheumatism; 2019; 49(3):337-350.

491. Gudbergsen H, Boesen M, Lohmander LS, Christensen R, Henriksen M, Bartels EM, et al. Weight loss is effective for symptomatic relief in obese subjects with knee osteoarthritis independently of joint damage severity assessed by high-field MRI and radiography. Osteoarthritis and Cartilage. 2012;20(6):495-502.

492. Jansen MJ, Viechtbauer W, Lenssen AF, Hendriks EJM, de Bie RA. Strength training alone, exercise therapy alone, and exercise therapy with passive manual mobilisation each reduce pain and disability in people with knee osteoarthritis: a systematic review. Journal of Physiotherapy. 2011;57(1):11-20.

493. Fransen M, McConnell S, Harmer AR, Van der Esch M, Simic M, Bennell KL. Exercise for osteoarthritis of the knee. Cochrane Database of Systematic Reviews. 2015;1:CD004376.

494. Escalante Y, Saavedra JM, Garcia-Hermoso A, Silva AJ, Barbosa TM. Physical exercise and reduction of pain in adults with lower limb osteoarthritis: a systematic review. Journal of Back and Musculoskeletal Rehabilitation. 2010;23(4):175-86.

495. Nelson AE, Allen KD, Golightly YM, Goode AP, Jordan JM. A systematic review of recommendations and guidelines for the management of osteoarthritis: The chronic osteoarthritis management initiative of the U.S. bone and joint initiative. Seminars in Arthritis and Rheumatism. 2014;43(6):701-12.

496. Arden NK, Perry TA, Bannuru RR, Bruyère O, Cooper C, Haugen IK, et al. Non-surgical management of knee osteoarthritis: comparison of ESCEO and OARSI 2019 guidelines. Nature Reviews Rheumatology. 2020:1-8.

497. Dowsey M, Nikpour M, Dieppe P, Choong P. Associations between pre-operative radiographic changes and outcomes after total knee joint replacement for osteoarthritis. Osteoarthritis and Cartilage. 2012;20(10):1095-102.

498. Culliford D, Maskell J, Kiran A, Judge A, Javaid M, Cooper C, et al. The lifetime risk of total hip and knee arthroplasty: results from the UK general practice research database. Osteoarthritis and Cartilage. 2012;20(6):519-24.

499. Woolhead G, Donovan J, Dieppe P. Patient expectations and total joint arthroplasty. Journal of Rheumatology. 2003;30(7):1656-7.

500. Jones CA, Beaupre LA, Johnston DW, Suarez-Almazor ME. Total joint arthroplasties: current concepts of patient outcomes after surgery. Rheumatic Diseases Clinics of North America. 2007;33(1):71-86.

501. Rand JA, Trousdale RT, Ilstrup DM, Harmsen WS. Factors affecting the durability of primary total knee prostheses. Journal of Bone and Joint Surgery. 2003;85-A(2):259-65.

502. Soderman P, Malchau H, Herberts P, Zugner R, Regner H, Garellick G. Outcome after total hip arthroplasty: Part II. Disease-specific follow-up and the Swedish National Total Hip Arthroplasty Register. Acta Orthopaedica Scandinavica. 2001;72(2):113-9.

503. Hamel MB, Toth M, Legedza A, Rosen MP. Joint replacement surgery in elderly patients with severe osteoarthritis of the hip or knee: decision making, postoperative recovery, and clinical outcomes. Archives of Internal Medicine. 2008;168(13):1430-40.

504. Parvizi J, Mui A, Purtill JJ, Sharkey PF, Hozack WJ, Rothman RH. Total joint arthroplasty: When do fatal or near-fatal complications occur? Journal of Bone and Joint Surgery. 2007;89(1):27-32.

505. Katz JN. Total joint replacement in osteoarthritis. Best Practice & Research Clinical Rheumatology. 2006;20(1):145-53.

506. Wandel S, Jüni P, Tendal B, Nüesch E, Villiger PM, Welton NJ, et al. Effects of glucosamine, chondroitin, or placebo in patients with osteoarthritis of hip or knee: network meta-analysis. The BMJ. 2010;341.

507. Runhaar J, Rozendaal RM, van Middelkoop M, Bijlsma HJ, Doherty M, Dziedzic KS, et al. Subgroup analyses of the effectiveness of oral glucosamine for knee and hip osteoarthritis: a systematic review and individual patient data meta-analysis from the OA trial bank. Annals of the Rheumatic Diseases. 2017;76(11):1862-9.

508. Henrotin Y, Marty M, Mobasheri A. What is the current status of chondroitin sulfate and glucosamine for the treatment of knee osteoarthritis? Maturitas. 2014;78(3):184-7.

509. Huang Z, Ding C, Li T, Yu SP. Current status and future prospects for disease modification in osteoarthritis. Rheumatology. 2018;57(4):iv108-iv23.

510. Davies PS, Graham SM, MacFarlane RJ, Leonidou A, Mantalaris A, Tsiridis E. Disease-modifying osteoarthritis drugs: in vitro and in vivo data on the development of DMOADs under investigation. Expert Opinion on Investigational Drugs. 2013;22(4):423-41.

511. Qvist P, Bay-Jensen AC, Christiansen C, Dam EB, Pastoureau P, Karsdal MA. The disease modifying osteoarthritis drug (DMOAD): Is it in the horizon? Pharmacological Research. 2008;58(1):1-7.

512. Karsdal MA, Michaelis M, Ladel C, Siebuhr AS, Bihlet AR, Andersen JR, et al. Disease-modifying treatments for osteoarthritis (DMOADs) of the knee and hip: lessons learned from failures and opportunities for the future. Osteoarthritis and Cartilage. 2016;24(12):2013-21.

513. Hunter DJ. Pharmacologic therapy for osteoarthritis--the era of disease modification. Nature Reviews Rheumatology. 2011;7(1):13-22.

514. Tonge D, Pearson M, Jones S. The hallmarks of osteoarthritis and the potential to develop personalised disease-modifying pharmacological therapeutics. Osteoarthritis and Cartilage. 2014;22(5):609-21.

515. Hunter DJ, Losina E, Guermazi A, Burstein D, Lassere MN, Kraus V. A pathway and approach to biomarker validation and qualification for osteoarthritis clinical trials. Current Drug Targets. 2010;11(5):536-45.

516. Innes J, Sharif M, Barr A. Relations between biochemical markers of osteoarthritis and other disease parameters in a population of dogs with naturally acquired osteoarthritis of the genual joint. American Journal of Veterinary Research. 1998;59(12):1530-6.

517. Cope P, Ourradi K, Li Y, Sharif M. Models of osteoarthritis: the good, the bad and the promising. Osteoarthritis and Cartilage. 2019;27(2):230-9.

518. Hart DJ, Mootoosamy I, Doyle DV, Spector TD. The relationship between osteoarthritis and osteoporosis in the general population: the Chingford Study. Annals of the Rheumatic Diseases. 1994;53(3):158-62.

519. Dequeker J, Aerssens J, Luyten FP. Osteoarthritis and osteoporosis: clinical and research evidence of inverse relationship. Aging Clinical and Experimental Research.2003;15(5):426-39.

520. Pogrund H, Rutenberg M, Makin M, Robin G, Menczel J, Steinberg R, et al. Osteoarthritis of the hip joint and osteoporosis: a radiological study in a random population sample in Jerusalem. Clinical Orthopaedics and Related Research. 1982(164):130-5.

521. Foss M, Byers PJAotrd. Bone density, osteoarthrosis of the hip, and fracture of the upper end of the femur. Annals of the Rheumatic Diseases. 1972;31(4):259.

522. Dequeker J, Boonen S, Aerssens J, Westhovens R. Inverse relationship osteoarthritis—osteoporosis: What is the evidence? What are the consequences? Rheumatology. 1996;35(9):813-8.

523. Dretakis EK, Steriopoulos KA, Kontakis GM, Giaourakis G, Economakis G, Dretakis KE. Cervical hip fractures do not occur in arthrotic joints: A clinicoradiographic study of 256 patients. Acta Orthopaedica Scandinavica. 1998;69(4):384-6.

524. Sun S-S, Ma H-L, Liu C-L, Huang C-H, Cheng C-K, Wei H-W. Difference in femoral head and neck material properties between osteoarthritis and osteoporosis. Clinical Biomechanics. 2008;23:S39-S47.

525. Nevitt MC, Lane NE, Scott JC, Hochberg MC, Pressman AR, Genant HK, et al. Radiographic osteoarthritis of the hip and bone mineral density. Arthritis & Rheumatism. 1995;38(7):907-16.

526. Lethbridge-Cejku M, Tobin JD, Scott Jr W, Reichle R, Roy TA, Plato CC, et al. Axial and hip bone mineral density and radiographic changes of osteoarthritis of the knee: data from the Baltimore Longitudinal Study of Aging. The Journal of Rheumatology. 1996;23(11):1943-7.

527. Hochberg MC, Lethbridge-Cejku M, Tobin JD. Bone mineral density and osteoarthritis: data from the Baltimore Longitudinal Study of Aging. Osteoarthritis and Cartilage. 2004;12:45-8.

528. Hochberg MC, Lethbridge‐Cejku M, Scott Jr WW, Reichle R, Plato CC, Tobin JD, et al. Upper extremity bone mass and osteoarthritis of the knees: data from the Baltimore Longitudinal Study of Aging. Journal of Bone and Mineral Research. 1995;10(3):432-8.

529. Hart DJ, Cronin C, Daniels M, Worthy T, Doyle DV, Spector TD, et al. The relationship of bone density and fracture to incident and progressive radiographic osteoarthritis of the knee: the Chingford Study. Arthritis & Rheumatism. 2002;46(1):92-9.

530. Zhang Y, Hannan M, Chaisson C, McAlindon T, Evans S, Aliabadi P, et al. Bone mineral density and risk of incident and progressive radiographic knee osteoarthritis in women: the Framingham Study. Journal of Rheumatology. 2000;27(4):1032-7.

531. Nevitt MC, Zhang Y, Javaid MK, Neogi T, Curtis JR, Niu J, et al. High systemic bone mineral density increases the risk of incident knee OA and joint space narrowing, but not radiographic progression of existing knee OA: the MOST study. Annals of the Rheumatic Diseases. 2010;69(01):163-8.

532. Hardcastle SA, Dieppe P, Gregson CL, Smith GD, Tobias JH. Osteoarthritis and bone mineral density: are strong bones bad for joints? BoneKEy Reports. 2015;4.

533. Bergink A, Uitterlinden A, Van Leeuwen J, Hofman A, Verhaar J, Pols H. Bone mineral density and vertebral fracture history are associated with incident and progressive radiographic knee osteoarthritis in elderly men and women: the Rotterdam Study. Bone. 2005;37(4):446-56.

534. Yoshimura N, Muraki S, Oka H, Mabuchi A, Kinoshita H, Yosihda M, et al. Epidemiology of lumbar osteoporosis and osteoarthritis and their causal relationship—is osteoarthritis a predictor for osteoporosis or vice versa?: the Miyama study. Osteoporosis International. 2009;20(6):999-1008.

535. Verstraeten A, Van Ermen H, Haghebaert G, Nijs J, Geusens P, Dequeker J, et al. Osteoarthrosis retards the development of osteoporosis. Observation of the coexistence of osteoarthrosis and osteoporosis. Clinical Orthopaedics and Related Research. 1991(264):169-77.

536. Dequeker J, Johnell O, Dilsen G, Gennari C, Vaz AL, Lyritis G, et al. Osteoarthritis protects against femoral neck fracture: the MEDOS study experience. Bone 1993;14:51-6.

537. Healey JH, Vigorita V, Lane JM. The coexistence and characteristics of osteoarthritis and osteoporosis. Journal of Bone and Joint Surgery. 1985;67(4):586-92.

538. Im G-I, Kim M-K. The relationship between osteoarthritis and osteoporosis. Journal of Bone and Mineral Metabolism. 2014;32(2):101-9.

539. Geusens PP, van den Bergh JP. Osteoporosis and osteoarthritis: shared mechanisms and epidemiology. Current Opinion in Rheumatology. 2016;28(2):97-103.

540. Hulet C, Sabatier J, Souquet D, Locker B, Marcelli C, Vielpeau C. Distribution of bone mineral density at the proximal tibia in knee osteoarthritis. Calcified Tissue International. 2002;71(4):315-22.

541. Herrero-Beaumont G, Roman-Blas JA, Largo R, Berenbaum F, Castañeda SJAotRD. Bone mineral density and joint cartilage: four clinical settings of a complex relationship in osteoarthritis. Annals of the Rheumatic Diseases. 2011;70(9):1523-5.

542. Arden NK, Nevitt MC, Lane NE, Gore LR, Hochberg MC, Scott JC, et al. Osteoarthritis and risk of falls, rates of bone loss, and osteoporotic fractures. Arthritis & Rheumatism. 1999;42(7):1378-85.

543. Jones G, Nguyen T, Sambrook P, Lord SR, Kelly P, Eisman J. Osteoarthritis, bone density, postural stability, and osteoporotic fractures: a population based study. Journal of Rheumatology. 1995;22(5):921-5.

544. Bergink AP, Van Der Klift M, Hofman A, Verhaar JA, Van Leeuwen JP, Uitterlinden AG, et al. Osteoarthritis of the knee is associated with vertebral and nonvertebral fractures in the elderly: the Rotterdam Study. Arthritis Care & Research. 2003;49(5):648-57.

545. Arden N, Griffiths GO, Hart D, Doyle D, Spector T. The association between osteoarthritis and osteoporotic fracture: the Chingford Study. Rheumatology. 1996;35(12):1299-304.

546. Zhu S, Chen K, Lan Y, Zhang N, Jiang R, Hu J. Alendronate protects against articular cartilage erosion by inhibiting subchondral bone loss in ovariectomized rats. Bone. 2013;53(2):340-9.

547. Strassle B, Mark L, Leventhal L, Piesla M, Li XJ, Kennedy J, et al. Inhibition of osteoclasts prevents cartilage loss and pain in a rat model of degenerative joint disease. Osteoarthritis and Cartilage. 2010;18(10):1319-28.

548. Shirai T, Kobayashi M, Nishitani K, Satake T, Kuroki H, Nakagawa Y, et al. Chondroprotective effect of alendronate in a rabbit model of osteoarthritis. Journal of Orthopaedic Research. 2011;29(10):1572-7.

549. Moreau M, Rialland P, Pelletier J-P, Martel-Pelletier J, Lajeunesse D, Boileau C, et al. Tiludronate treatment improves structural changes and symptoms of osteoarthritis in the canine anterior cruciate ligament model. Arthritis Research & Therapy. 2011;13(3):1-13.

550. Yu D-g, Yu B, Mao Y-q, Zhao X, Wang X-q, Ding H-f, et al. Efficacy of zoledronic acid in treatment of teoarthritis is dependent on the disease progression stage in rat medial meniscal tear model. Acta Pharmacologica Sinica. 2012;33(7):924-34.

551. Zhang L, Hu H, Tian F, Song H, Zhang Y. Enhancement of subchondral bone quality by alendronate administration for the reduction of cartilage degeneration in the early phase of experimental osteoarthritis. Clinical and Experimental Medicine. 2011;11(4):235-43.

552. Muehleman C, Green J, Williams J, Kuettner K, Thonar E-M, Sumner D, et al. The effect of bone remodeling inhibition by zoledronic acid in an animal model of cartilage matrix damage. Osteoarthritis and Cartilage. 2002;10(3):226-33.

553. Behets C, Williams JM, Chappard D, Devogelaer JP, Manicourt DH. Effects of calcitonin on subchondral trabecular bone changes and on osteoarthritic cartilage lesions after acute anterior cruciate ligament deficiency. Journal of Bone and Mineral Research. 2004;19(11):1821-6.

554. Manicourt DH, Altman RD, Williams JM, Devogelaer JP, Druetz‐Van Egeren A, Lenz ME, et al. Treatment with calcitonin suppresses the responses of bone, cartilage, and synovium in the early stages of canine experimental osteoarthritis and significantly reduces the severity of the cartilage lesions. Arthritis & Rheumatism. 1999;42(6):1159-67.

555. Nielsen R, Bay-Jensen A-C, Byrjalsen I, Karsdal M. Oral salmon calcitonin reduces cartilage and bone pathology in an osteoarthritis rat model with increased subchondral bone turnover. Osteoarthrits and Cartilage. 2011;19(4):466-73.

556. Kyrkos M, Papavasiliou K, Kenanidis E, Tsiridis E, Sayegh F, Kapetanos G, et al. Calcitonin delays the progress of early-stage mechanically induced osteoarthritis. In vivo, prospective study. Osteoarthritis and Cartilage. 2013;21(7):973-80.

557. Sampson ER, Hilton MJ, Tian Y, Chen D, Schwarz EM, Mooney RA, et al. Teriparatide as a chondroregenerative therapy for injury-induced osteoarthritis. Science Translational Medicine. 2011;3(101):ra93-ra93.

558. Chang JK, Chang LH, Hung SH, Wu SC, Lee HY, Lin YS, et al. Parathyroid hormone 1–34 inhibits terminal differentiation of human articular chondrocytes and osteoarthritis progression in rats. Arthritis & Rheumatism. 2009;60(10):3049-60.

559. Oestergaard S, Sondergaard BC, Hoegh‐Andersen P, Henriksen K, Qvist P, Christiansen C, et al. Effects of ovariectomy and estrogen therapy on type II collagen degradation and structural integrity of articular cartilage in rats: implications of the time of initiation. Arthritis & Rheumatism. 2006;54(8):2441-51.

560. Pelletier J-P, Kapoor M, Fahmi H, Lajeunesse D, Blesius A, Maillet J, et al. Strontium ranelate reduces the progression of experimental dog osteoarthritis by inhibiting the expression of key proteases in cartilage and of IL-1β in the synovium. Annals of the Rheumatic Diseases. 2013;72(2):250-7.

561. Yu D-g, Ding H-f, Mao Y-q, Liu M, Yu B, Zhao X, et al. Strontium ranelate reduces cartilage degeneration and subchondral bone remodeling in rat osteoarthritis model. Acta Pharmacologica Sinica. 2013;34(3):393-402.

562. Castaneda S, Roman-Blas JA, Largo R, Herrero-Beaumont G. Subchondral bone as a key target for osteoarthritis treatment. Biochemical Pharmacology. 2012;83(3):315-23.

563. Karsdal MA, Sondergaard BC, Arnold M, Christiansen C. Calcitonin affects both bone and cartilage: a dual action treatment for osteoarthritis? Annals of the New York Academy of Sciences. 2007;1117(1):181-95.

564. Karsdal M, Bay-Jensen A, Lories R, Abramson S, Spector T, Pastoureau P, et al. The coupling of bone and cartilage turnover in osteoarthritis: opportunities for bone antiresorptives and anabolics as potential treatments? Annals of the Rheumatic Diseases. 2014;73(2):336-48.

565. Mobasheri AJCrr. The future of osteoarthritis therapeutics: targeted pharmacological therapy. Current Rheumatology Reports. 2013;15(10):364.

566. Cox LGE, van Donkelaar CC, van Rietbergen B, Emans PJ, Ito K. Decreased bone tissue mineralization can partly explain subchondral sclerosis observed in osteoarthritis. Bone. 2012;50(5):1152-61.

567. Finnilä MA, Thevenot J, Aho OM, Tiitu V, Rautiainen J, Kauppinen S, et al. Association between subchondral bone structure and osteoarthritis histopathological grade. Journal of Orthopaedic Research. 2017;35(4):785-92.

568. Bobinac D, Spanjol J, Zoricic S, Maric I. Changes in articular cartilage and subchondral bone histomorphometry in osteoarthritic knee joints in humans. Bone. 2003;32(3):284-90.

569. Roberts BC, Thewlis D, Solomon LB, Mercer G, Reynolds KJ, Perilli E. Systematic mapping of the subchondral bone 3D microarchitecture in the human tibial plateau: Variations with joint alignment. Journal of Orthopaedic Research. 2017;35(9):1927-41.

570. Haberkamp S, Oláh T, Orth P, Cucchiarini M, Madry H. Analysis of spatial osteochondral heterogeneity in advanced knee osteoarthritis exposes influence of joint alignment. Science Translational Medicine. 2020;12(562).

571. Rapagna S, Roberts BC, Solomon LB, Reynolds KJ, Thewlis D, Perilli EJJoOR. Tibial cartilage, subchondral bone plate and trabecular bone microarchitecture in varus‐and valgus‐osteoarthritis versus controls. Journal of Orthopaedic Research. 2020;1–12.

572. Bennell KL, Creaby MW, Wrigley TV, Hunter DJ. Tibial subchondral trabecular volumetric bone density in medial knee joint osteoarthritis using peripheral quantitative computed tomography technology. Arthritis & Rheumatism. 2008;58(9):2776-85.

573. Berglund L, Björling E, Oksvold P, Fagerberg L, Asplund A, Szigyarto CA-K, et al. A genecentric Human Protein Atlas for expression profiles based on antibodies. Molecular & Cellular Proteomics. 2008;7(10):2019-27.

574. Pontén F, Gry M, Fagerberg L, Lundberg E, Asplund A, Berglund L, et al. A global view of protein expression in human cells, tissues, and organs. Molecular Systems Biology. 2009;5(1):337.

575. Collins DH. The pathology of articular and spinal diseases: Edward Arnold; 1949.

576. Collins D, McElligott T. Sulphate (35SO4) uptake by chondrocytes in relation to histological changes in osteo-arthritic human articular cartilage. Annals of the Rheumatic Diseases. 1960;19(4):318.

577. Mankin HJ, Dorfman H, Lippiello L, Zarins A. Biochemical and metabolic abnormalities in articular cartilage from osteo-arthritic human hips. II. Correlation of morphology with biochemical and metabolic data. Journal of Bone and Joint Surgery. 1971;53(3):523-37.

578. Pauli C, Whiteside R, Heras FL, Nesic D, Koziol J, Grogan SP, et al. Comparison of cartilage histopathology assessment systems on human knee joints at all stages of osteoarthritis development. Osteoarthritis and Cartilage. 2012;20(6):476-85.

579. Custers RJH, Creemers LB, Verbout AJ, van Rijen MHP, Dhert WJA, Saris DBF. Reliability, reproducibility and variability of the traditional Histologic/Histochemical Grading System vs the new OARSI Osteoarthritis Cartilage Histopathology Assessment System. Osteoarthritis and Cartilage. 2007;15(11):1241-8.

580. Rutgers M, Van Pelt M, Dhert W, Creemers LB, Saris D. Evaluation of histological scoring systems for tissue-engineered, repaired and osteoarthritic cartilage. Osteoarthritis and Cartilage. 2010;18(1):12-23.

581. Mainil-Varlet P, Aigner T, Brittberg M, Bullough P, Hollander A, Hunziker E, et al. Histological assessment of cartilage repair: a report by the Histology Endpoint Committee of the International Cartilage Repair Society (ICRS). Journal of Bone and Joint Surgery. 2003;85(2):45-57.

582. Mainil-Varlet P, Van Damme B, Nesic D, Knutsen G, Kandel R, Roberts S. A new histology scoring system for the assessment of the quality of human cartilage repair: ICRS II. The American Journal of Sports Medicine. 2010;38(5):880-90.

583. Hoemann C, Kandel R, Roberts S, Saris DB, Creemers L, Mainil-Varlet P, et al. International Cartilage Repair Society (ICRS) recommended guidelines for histological endpoints for cartilage repair studies in animal models and clinical trials. Cartilage. 2011;2(2):153-72.

584. Grogan SP, Barbero A, Winkelmann V, Rieser F, Fitzsimmons JS, O'driscoll S, et al. Visual histological grading system for the evaluation of in vitro–generated neocartilage. Tissue Engineering. 2006;12(8):2141-9.

585. Little C, Smith M, Cake M, Read R, Murphy M, Barry F, et al. The OARSI histopathology initiative–recommendations for histological assessments of osteoarthritis in sheep and goats. Osteoarthritis and Cartilage. 2010;18:S80-S92.

586. Cook J, Kuroki K, Visco D, Pelletier J-P, Schulz L, Lafeber F, et al. The OARSI histopathology initiative–recommendations for histological assessments of osteoarthritis in the dog. Osteoarthritis and Cartilage. 2010;18:S66-S79.

587. Kraus VB, Huebner JL, DeGroot J, Bendele A. The OARSI histopathology initiative–recommendations for histological assessments of osteoarthritis in the guinea pig. Osteoarthritis and Cartilage. 2010;18:S35-S52.

588. Pearson R, Kurien T, Shu K, Scammell B. Histopathology grading systems for characterisation of human knee osteoarthritis–reproducibility, variability, reliability, correlation, and validity. Osteoarthritis and Cartilage. 2011;19(3):324-31.

589. Rout R, McDonnell S, Benson R, Athanasou N, Carr A, Doll H, et al. The histological features of Anteromedial Gonarthrosis—the comparison of two grading systems in a human phenotype of osteoarthritis. The Knee. 2011;18(3):172-6.

590. Ostergaard K, Andersen CB, Petersen J, Bendtzen K, Salter DM. Validity of histopathological grading of articular cartilage from osteoarthritic knee joints. Annals of the Rheumatic Diseases. 1999;58(4):208-13.

591. Johnston JD, Kontulainen SA, Masri BA, Wilson DR. Predicting subchondral bone stiffness using a depth-specific CT topographic mapping technique in normal and osteoarthritic proximal tibiae. Clinical Biomechanics. 2011;26(10):1012-8.

592. Bobinac D, Marinovic M, Bazdulj E, Cvijanovic O, Celic T, Maric I, et al. Microstructural alterations of femoral head articular cartilage and subchondral bone in osteoarthritis and osteoporosis. Osteoarthritis and Cartilage. 2013;21(11):1724-30.

593. Saal A, Gaertner J, Kuehling M, Swoboda B, Klug S. Macroscopic and radiological grading of osteoarthritis correlates inadequately with cartilage height and histologically demonstrable damage to cartilage structure. Rheumatology International. 2005;25(3):161-8.

594. Outerbridge R. The etiology of chondromalacia patellae. The Journal of Bone and Joint Surgery. 1961;43(4):752-7.

595. Yeung P, Zhang W, Wang XN, Yan CH, Chan BP. A human osteoarthritis osteochondral organ culture model for cartilage tissue engineering. Biomaterials. 2018;162:1-21.

596. van den Borne MP, Raijmakers NJ, Vanlauwe J, Victor J, de Jong SN, Bellemans J, et al. International Cartilage Repair Society (ICRS) and Oswestry macroscopic cartilage evaluation scores validated for use in Autologous Chondrocyte Implantation (ACI) and microfracture. Osteoarthritis and Cartilage. 2007;15(12):1397-402.

597. Sharif M, Whitehouse A, Sharman P, Perry M, Adams M. Increased apoptosis in human osteoarthritic cartilage corresponds to reduced cell density and expression of caspase-3. Arthritis & Rheumatism. 2004;50(2):507-15.

598. Bland JM, Altman D. Statistical methods for assessing agreement between two methods of clinical measurement. The Lancet. 1986;327(8476):307-10.

599. Bartlett J, Frost C. Reliability, repeatability and reproducibility: analysis of measurement errors in continuous variables. Ultrasound in Obstetrics and Gynecology. 2008;31(4):466-75.

600. Koo TK, Li MY. A guideline of selecting and reporting intraclass correlation coefficients for reliability research. Journal of Chiropractic Medicine. 2016;15(2):155-63.

601. Gruchy JR, Barnes PJ, Dakin Haché KA. CytoLyt® fixation and decalcification pretreatments alter antigenicity in normal tissues compared with standard formalin fixation. Applied Immunohistochemistry & Molecular Morphology. 2015;23(4):297-302.

602. Bussolati G, Leonardo E. Technical pitfalls potentially affecting diagnoses in immunohistochemistry. Journal of Clinical Pathology. 2008;61(11):1184-92.

603. Waldstein W, Perino G, Gilbert SL, Maher SA, Windhager R, Boettner F. OARSI osteoarthritis cartilage histopathology assessment system: a biomechanical evaluation in the human knee. Journal of Orthopaedic Research. 2016;34(1):135-40.

604. Mantripragada V, Piuzzi N, Zachos T, Obuchowski N, Muschler G, Midura R. Histopathological assessment of primary osteoarthritic knees in large patient cohort reveal the possibility of several potential patterns of osteoarthritis initiation. Current Research in Translational Medicine. 2017;65(4):133-9.

605. Slattery C, Kweon CY. Classifications in brief: outerbridge classification of chondral lesions. Clinical Orthopaedics and Related Research. 2018;476(10):2101.

606. Marinović M, Bazdulj E, Čelić T, Cicvarić T, Bobinac D. Histomorphometric analysis of subchondral bone of the femoral head in osteoarthritis and osteoporosis. Collegium Antropologicum. 2011;35(2):19-23.

607. Zhang Z-M, Jiang L-S, Jiang S-D, Dai L-Y. Differential articular calcified cartilage and subchondral bone in postmenopausal women with osteoarthritis and osteoporosis: two-dimensional analysis. Joint Bone Spine. 2009;76(6):674-9.

608. Zhang Z-M, Li Z-C, Jiang L-S, Jiang S-D, Dai L-Y. Micro-CT and mechanical evaluation of subchondral trabecular bone structure between postmenopausal women with osteoarthritis and osteoporosis. Osteoporosis International. 2010;21(8):1383-90.

609. Li ZC, Dai LY, Jiang LS, Qiu S. Difference in subchondral cancellous bone between postmenopausal women with hip osteoarthritis and osteoporotic fracture: implication for fatigue microdamage, bone microarchitecture, and biomechanical properties. Arthritis & Rheumatism. 2012;64(12):3955-62.

610. Gatenholm B, Lindahl C, Brittberg M, Stadelmann VA. Spatially matching morphometric assessment of cartilage and subchondral bone in osteoarthritic human knee joint with micro-computed tomography. Bone. 2019;120:393-402.

611. Zhang LZ, Zheng HA, Jiang Y, Tu YH, Jiang PH, Yang AL, et al. Mechanical and biologic link between cartilage and subchondral bone in osteoarthritis. Arthritis Care & Research. 2012;64(7):960-7.

612. Ryan M, Barnett L, Rochester J, Wilkinson J, Dall'Ara E. A new approach to comprehensively evaluate the morphological properties of the human femoral head: example of application to osteoarthritic joint. Scientific Reports. 2020;10(1):1-10.

613. Bouxsein ML, Boyd SK, Christiansen BA, Guldberg RE, Jepsen KJ, Muller R. Guidelines for Assessment of Bone Microstructure in Rodents Using Micro-Computed Tomography. Journal of Bone and Mineral Research. 2010;25(7):1468-86.

614. Buie HR, Campbell GM, Klinck RJ, MacNeil JA, Boyd SK. Automatic segmentation of cortical and trabecular compartments based on a dual threshold technique for in vivo micro-CT bone analysis. Bone. 2007;41(4):505-15.

615. Kohler T, Stauber M, Donahue LR, Müller R. Automated compartmental analysis for high-throughput skeletal phenotyping in femora of genetic mouse models. Bone. 2007;41(4):659-67.

616. Perilli E, Parkinson IH, Reynolds KJ. Micro-CT examination of human bone: from biopsies towards the entire organ. Annali Dell'Istituto Superiore di Sanita. 2012;48:75-82.

617. Wen C, Chen Y, Tang H, Yan C, Lu W, Chiu K, et al. Bone loss at subchondral plate in knee osteoarthritis patients with hypertension and type 2 diabetes mellitus. Osteoarthritis and Cartilage. 2013;21(11):1716-23.

618. Chen H, Zhou X, Fujita H, Onozuka M, Kubo K-Y. Age-related changes in trabecular and cortical bone microstructure. International Journal of Endocrinology. 2013;213234.

619. Fazzalari N, Parkinson I. Fractal properties of subchondral cancellous bone in severe osteoarthritis of the hip. Journal of Bone and Mineral Research. 1997;12(4):632-40.

620. Kinney J, Ladd AJ. The relationship between three‐dimensional connectivity and the elastic properties of trabecular bone. Journal of Bone and Mineral Research. 1998;13(5):839-45.

621. Chu L, Liu X, He Z, Han X, Yan M, Qu X, et al. Articular cartilage degradation and aberrant subchondral bone remodeling in patients with osteoarthritis and osteoporosis. Journal of Bone and Mineral Research. 2019;35(3):505-15..

622. Burghardt AJ, Link TM, Majumdar S. High-resolution computed tomography for clinical imaging of bone microarchitecture. Clinical Orthopaedics and Related Research. 2011;469(8):2179-93.

623. Boskey AL, Imbert L. Bone quality changes associated with aging and disease: a review. Annals of the New York Academy of Sciences. 2017;1410(1):93.

624. Chappard D, Baslé M-F, Legrand E, Audran M. Trabecular bone microarchitecture: a review. Morphologie. 2008;92(299):162-70.

625. Recker R, Masarachia P, Santora A, Howard T, Chavassieux P, Arlot M, et al. Trabecular bone microarchitecture after alendronate treatment of osteoporotic women. Current Medical Research and Opinion. 2005;21(2):185-94.

626. Parfitt A, Mathews C, Villanueva A, Kleerekoper M, Frame B, Rao D. Relationships between surface, volume, and thickness of iliac trabecular bone in aging and in osteoporosis.

Implications for the microanatomic and cellular mechanisms of bone loss. The Journal of Clinical Investigation. 1983;72(4):1396-409.

627. Ding M, Hvid I. Quantification of age-related changes in the structure model type and trabecular thickness of human tibial cancellous bone. Bone. 2000;26(3):291-5.

628. Buckland-Wright J, Lynch J, Dave B. Early radiographic features in patients with anterior cruciate ligament rupture. Annals of the Rheumatic Diseases. 2000;59(8):641-6.

629. Zamli Z, Robson Brown K, Sharif M. Subchondral bone plate changes more rapidly than trabecular bone in osteoarthritis. International Journal of Molecular Sciences. 2016;17(9).

630. Zamli Z, Robson Brown K, Tarlton JF, Adams MA, Torlot GE, Cartwright C, et al. Subchondral bone plate thickening precedes chondrocyte apoptosis and cartilage degradation in spontaneous animal models of osteoarthritis. Biomed Research International. 2014;2014:606870.

631. Sanchez C, Deberg MA, Piccardi N, Msika P, Reginster JYL, Henrotin YE. Osteoblasts from the sclerotic subchondral bone downregulate aggrecan but upregulate metalloproteinases expression by chondrocytes. This effect is mimicked by interleukin-6, -1 beta and oncostatin M pre-treated non-sclerotic osteoblasts. Osteoarthritis and Cartilage. 2005;13(11):979-87.

632. Sanchez C, Deberg MA, Bellahcène A, Castronovo V, Msika P, Delcour J-P, et al. Phenotypic characterization of osteoblasts from the sclerotic zones of osteoarthritic subchondral bone. Arthritis & Rheumatism. 2008;58(2):442-55.

633. Sanchez C, Deberg MA, Piccardi N, Msika P, Reginster JYL, Henrotin YE. Subchondral bone osteoblasts induce phenotypic changes in human osteoarthritic chondrocytes. Osteoarthritis and Cartilage. 2005;13(11):988-97.

634. Van der Linden J, Day J, Verhaar J, Weinans H. Altered tissue properties induce changes in cancellous bone architecture in aging and diseases. Journal of Biomechanics. 2004;37(3):367-74.

635. Boivin G, Bala Y, Doublier A, Farlay D, Ste-Marie L, Meunier P, et al. The role of mineralization and organic matrix in the microhardness of bone tissue from controls and osteoporotic patients. Bone. 2008;43(3):532-8.

636. Tassani S, Öhman C, Baruffaldi F, Baleani M, Viceconti M. Volume to density relation in adult human bone tissue. Journal of Biomechanics. 2011;44(1):103-8.

637. Adams GJ, Cook RB, Hutchinson JR, Zioupos P. Bone apparent and material densities examined by cone beam computed tomography and the Archimedes technique: comparison of the two methods and their results. Frontiers in Mechanical Engineering. 2018;3:23.

638. Bouxsein ML, Seeman E. Quantifying the material and structural determinants of bone strength. Best Practice & Research Clinical Rheumatology. 2009;23(6):741-53.

639. Dall'Ara E, Öhman C, Baleani M, Viceconti M. Reduced tissue hardness of trabecular bone is associated with severe osteoarthritis. Journal of Biomechanics. 2011;44(8):1593-8.

640. Paschalis EP, Klaushofer K, Hartmann MA. Material properties and osteoporosis. F1000Research. 2019;8.

641. Dequeker J. Bone and ageing. Annals of the Rheumatic Diseases. 1975;34(1):100.

642. Roschger P, Misof B, Paschalis E, Fratzl P, Klaushofer K. Changes in the degree of mineralization with osteoporosis and its treatment. Current Osteoporosis Reports. 2014;12(3):338-50.

643. McNamara L, Prendergast P, Schaffler M, Interactions N. Bone tissue material properties are altered during osteoporosis. Journal of Musculoskeletal and Neuronal Interactions. 2005;5(4):342.

644. Busse B, Hahn M, Soltau M, Zustin J, Püschel K, Duda GN, et al. Increased calcium content and inhomogeneity of mineralization render bone toughness in osteoporosis: mineralization, morphology and biomechanics of human single trabeculae. Bone. 2009;45(6):1034-43.

645. McNamara L. Perspective on post-menopausal osteoporosis: establishing an interdisciplinary understanding of the sequence of events from the molecular level to whole bone fractures. Journal of the Royal Society Interface. 2010;7(44):353-72.

646. Mashiatulla M, Ross RD, Sumner DR. Validation of cortical bone mineral density distribution using micro-computed tomography. Bone. 2017;99:53-61.

647. Roschger P, Rinnerthaler S, Yates J, Rodan G, Fratzl P, Klaushofer K. Alendronate increases degree and uniformity of mineralization in cancellous bone and decreases the porosity in cortical bone of osteoporotic women. Bone. 2001;29(2):185-91.

648. Ries C, Boese CK, Stürznickel J, Koehne T, Hubert J, Pastor M-F, et al. Age-related changes of micro-morphological subchondral bone properties in the healthy femoral head. Osteoarthritis and Cartilage. 2020;28(11):1437-47.

649. Sanchez C, Deberg MA, Bellahcene A, Castronovo V, Msika P, Delcour JP, et al. Phenotypic characterization of osteoblasts from the sclerotic zones of osteoarthritic subchondral bone. Arthritis & Rheumatism. 2008;58(3):887-.

650. Sanchez C, Mazzucchelli G, Lambert C, Comblain F, DePauw E, Henrotin Y. Comparison of secretome from osteoblasts derived from sclerotic versus non-sclerotic subchondral bone in OA: A pilot study. PLoS One. 2018;13(3):e0194591.

651. Day J, Ding M, Van Der Linden J, Hvid I, Sumner D, Weinans H. A decreased subchondral trabecular bone tissue elastic modulus is associated with pre‐arthritic cartilage damage. Journal of Orthopaedic Research. 2001;19(5):914-8.

652. Bouxsein ML, Boyd SK, Christiansen BA, Guldberg RE, Jepsen KJ, Müller R, et al. Guidelines for assessment of bone microstructure in rodents using micro–computed tomography. Journal of Bone and Mineral Research. 2010;25(7):1468-86.

653. Dall'Ara E, Pahr D, Varga P, Kainberger F, Zysset P. QCT-based finite element models predict human vertebral strength in vitro significantly better than simulated DEXA. Osteoporosis International. 2012;23(2):563-72.

654. Wallace JM. Skeletal hard tissue biomechanics. Basic and applied bone biology: Elsevier; 2019. p. 125-40.

655. Sandy JD, Neame P, Boynton R, Flannery C. Catabolism of aggrecan in cartilage explants. Identification of a major cleavage site within the interglobular domain. Journal of Biological Chemistry. 1991;266(14):8683-5.

656. Sandy JD, Verscharen C. Analysis of aggrecan in human knee cartilage and synovial fluid indicates that aggrecanase (ADAMTS) activity is responsible for the catabolic turnover and loss of whole aggrecan whereas other protease activity is required for C-terminal processing in vivo. Biochemical Journal. 2001;358(3):615-26.

657. Sandy JD, Flannery CR, Neame PJ, Lohmander LS. The structure of aggrecan fragments in human synovial fluid. Evidence for the involvement in osteoarthritis of a novel proteinase which cleaves the Glu 373-Ala 374 bond of the interglobular domain. The Journal of Clinical Investigation. 1992;89(5):1512-6.

658. Sandy J. A contentious issue finds some clarity: on the independent and complementary roles of aggrecanase activity and MMP activity in human joint aggrecanolysis. Osteoarthritis and Cartilage. 2006;14(2):95-100.

659. Glasson SS, Askew R, Sheppard B, Carito BA, Blanchet T, Ma HL, et al. Characterization of and osteoarthritis susceptibility in ADAMTS‐4‐knockout mice. Arthritis & Rheumatism. 2004;50(8):2547-58.

660. Glasson SS, Askew R, Sheppard B, Carito B, Blanchet T, Ma HL, et al. Deletion of active ADAMTS5 prevents cartilage degradation in a murine model of osteoarthritis. Nature. 2005;434(7033):644-8.

661. Stanton H, Rogerson FM, East CJ, Golub SB, Lawlor KE, Meeker CT, et al. ADAMTS5 is the major aggrecanase in mouse cartilage in vivo and in vitro. Nature. 2005;434(7033):648-52.

662. Powell AJ, Little CB, Hughes CEJA, Rheumatology ROJotACo. Low molecular weight isoforms of the aggrecanases are responsible for the cytokine‐induced proteolysis of aggrecan in a porcine chondrocyte culture system. Arthritis & Rheumatism. 2007;56(9):3010-9.

663. Kamm J, Nixon A, Witte T. Cytokine and catabolic enzyme expression in synovium, synovial fluid and articular cartilage of naturally osteoarthritic equine carpi. Equine Veterinary Journal. 2010;42(8):693-9.

664. Pelletier J-P, Boileau C, Boily M, Brunet J, Mineau F, Geng C, et al. The protective effect of licofelone on experimental osteoarthritis is correlated with the downregulation of gene expression and protein synthesis of several major cartilage catabolic factors: MMP-13, cathepsin K and aggrecanases. Arthritis Research & Therapy. 2005;7(5):1-12.

665. Malfait A-M, Liu R-Q, Ijiri K, Komiya S, Tortorella MD. Inhibition of ADAM-TS4 and ADAM-TS5 prevents aggrecan degradation in osteoarthritic cartilage. Journal of Biological Chemistry. 2002;277(25):22201-8.

666. Naito S, Shiomi T, Okada A, Kimura T, Chijiiwa M, Fujita Y, et al. Expression of ADAMTS4 (aggrecanase - 1) in human osteoarthritic cartilage. Pathology International. 2007;57(11):703-11.

667. Zhang E, Yan X, Zhang M, Chang X, Bai Z, He Y, et al. Aggrecanases in the human synovial fluid at different stages of osteoarthritis. Clinical Rheumatology. 2013;32(6):797-803.

668. Van der Kraan P, Van den Berg W. Chondrocyte hypertrophy and osteoarthritis: role in initiation and progression of cartilage degeneration? Osteoarthritis and Cartilage. 2012;20(3):223-32.

669. Mitchell PG, Magna HA, Reeves LM, Lopresti-Morrow LL, Yocum SA, Rosner PJ, et al. Cloning, expression, and type II collagenolytic activity of matrix metalloproteinase-13 from human osteoarthritic cartilage. The Journal of Clinical Investigation. 1996;97(3):761-8.

670. Sandell LJ, Aigner T. Articular cartilage and changes in arthritis: cell biology of osteoarthritis. Arthritis Research & Therapy. 2001;3(2):1-7.

671. Li H, Wang D, Yuan Y, Min J. New insights on the MMP-13 regulatory network in the pathogenesis of early osteoarthritis. Arthritis Research & Therapy. 2017;19(1):248.

672. Huebner JL, Otterness IG, Freund EM, Caterson B, Kraus VB. Collagenase 1 and collagenase 3 expression in a guinea pig model of osteoarthritis. Arthritis & Rheumatism. 1998;41(5):877-90.

673. Wei L, Fleming BC, Sun X, Teeple E, Wu W, Jay GD, et al. Comparison of differential biomarkers of osteoarthritis with and without posttraumatic injury in the Hartley guinea pig model. Journal of Orthopaedic Research. 2010;28(7):900-6.

674. Kamekura S, Hoshi K, Shimoaka T, Chung U, Chikuda H, Yamada T, et al. Osteoarthritis development in novel experimental mouse models induced by knee joint instability. Osteoarthritis and Cartilage. 2005;13(7):632-41.

675. Neuhold LA, Killar L, Zhao W, Sung M-LA, Warner L, Kulik J, et al. Postnatal expression in hyaline cartilage of constitutively active human collagenase-3 (MMP-13) induces osteoarthritis in mice. The Journal of Clinical Investigation. 2001;107(1):35-44.

676. Wang M, Sampson ER, Jin H, Li J, Ke QH, Im H-J, et al. MMP13 is a critical target gene during the progression of osteoarthritis. Arthritis Research & Therapy. 2013;15(1):1-11.

677. Little C, Barai A, Burkhardt D, Smith S, Fosang A, Werb Z, et al. Matrix metalloproteinase 13–deficient mice are resistant to osteoarthritic cartilage erosion but not chondrocyte hypertrophy or osteophyte development. Arthritis & Rheumatism. 2009;60(12):3723-33.

678. Westacott CI, Webb GR, Warnock MG, Sims JV, Elson CJ. Alteration of cartilage metabolism by cells from osteoarthritic bone. Arthritis & Rheumatism. 1997;40(7):1282-91.

679. Prasadam I, Crawford R, Xiao Y. Aggravation of ADAMTS and matrix metalloproteinase production and role of ERK1/2 pathway in the interaction of osteoarthritic subchondral bone osteoblasts and articular cartilage chondrocytes—possible pathogenic role in osteoarthritis. The Journal of Rheumatology. 2012;39(3):621-34.

680. Prasadam I, van Gennip S, Friis T, Shi W, Crawford R, Xiao Y, et al. ERK‐1/2 and p38 in the regulation of hypertrophic changes of normal articular cartilage chondrocytes induced by osteoarthritic subchondral osteoblasts. Arthritis & Rheumatism. 2010;62(5):1349-60.

681. Prasadam I, Friis T, Shi W, Van Gennip S, Crawford R, Xiao Y. Osteoarthritic cartilage chondrocytes alter subchondral bone osteoblast differentiation via MAPK signalling pathway involving ERK1/2. Bone. 2010;46(1):226-35.

682. Zhen G, Wen C, Jia X, Li Y, Crane JL, Mears SC, et al. Inhibition of TGF-β signaling in mesenchymal stem cells of subchondral bone attenuates osteoarthritis. Nature Medicine. 2013;19(6):704.

683. Yang Y, Li P, Zhu S, Bi R. Comparison of early-stage changes of osteoarthritis in cartilage and subchondral bone between two different rat models. PeerJ. 2020;8:e8934.

684. Chen Y, Sun Y, Pan X, Ho K, Li G. Joint distraction attenuates osteoarthritis by reducing secondary inflammation, cartilage degeneration and subchondral bone aberrant change. Osteoarthritis and Cartilage. 2015;23(10):1728-35.

685. Freije JM, Diez-Itza I, Balbín M, Sánchez LM, Blasco R, Tolivia J, et al. Molecular cloning and expression of collagenase-3, a novel human matrix metalloproteinase produced by breast carcinomas. Journal of Biological Chemistry. 1994;269(24):16766-73.

686. Moldovan F, Pelletier JP, Hambor J, Cloutier JM, Martel‐Pelletier J. Collagenase‐3 (matrix metalloprotease 13) is preferentially localized in the deep layer of human arthritic cartilage in situ. In vitro mimicking effect by transforming growth factor β. Arthritis & Rheumatism. 1997;40(9):1653-61.

687. Fernandes JC, Martel-Pelletier J, Lascau-Coman V, Moldovan F, Jovanovic D, Raynauld JP, et al. Collagenase-1 and collagenase-3 synthesis in normal and early experimental osteoarthritic canine cartilage: an immunohistochemical study. Journal of Rheumatology. 1998;25(8):1585-94.

688. Wu W, Billinghurst RC, Pidoux I, Antoniou J, Zukor D, Tanzer M, et al. Sites of collagenase cleavage and denaturation of type II collagen in aging and osteoarthritic articular cartilage and their relationship to the distribution of matrix metalloproteinase 1 and matrix metalloproteinase 13. Arthritis & Rheumatism. 2002;46(8):2087-94.

689. Roach HI, Yamada N, Cheung KS, Tilley S, Clarke NM, Oreffo RO, et al. Association between the abnormal expression of matrix‐degrading enzymes by human osteoarthritic chondrocytes and demethylation of specific CpG sites in the promoter regions. Arthritis & Rheumatism. 2005;52(10):3110-24.

690. Cheung KS, Hashimoto K, Yamada N, Roach HI. Expression of ADAMTS-4 by chondrocytes in the surface zone of human osteoarthritic cartilage is regulated by epigenetic DNA de-methylation. Rheumatology International. 2009;29(5):525-34.

691. Tchetina EV, Squires G, Poole AR. Increased type II collagen degradation and very early focal cartilage degeneration is associated with upregulation of chondrocyte differentiation related genes in early human articular cartilage lesions. The Journal of Rheumatology. 2005;32(5):876-86.

692. Buckwalter J, Mankin HJIcl. Articular cartilage: degeneration and osteoarthritis, repair, regeneration, and transplantation. Instructional Course Lectures. 1998;47:487-504.

693. Gao L, Orth P, Cucchiarini M, Madry H. Effects of solid acellular type-I/III collagen biomaterials on in vitro and in vivo chondrogenesis of mesenchymal stem cells. Expert Review of Medical Devices. 2017;14(9):717-32.

694. Malek S, Köster DV. The Role of Cell Adhesion and Cytoskeleton Dynamics in the Pathogenesis of the Ehlers-Danlos Syndromes and Hypermobility Spectrum Disorders. Frontiers in Cell and Developmental Biology. 2021;21;9:883.

695. Wegst UG, Bai H, Saiz E, Tomsia AP, Ritchie RO. Bioinspired structural materials. Nature Materials. 2015;14(1):23-36.

696. Myllyharju J, Kivirikko KI. Collagens and collagen-related diseases. Annals of Medicine. 2001;33(1):7-21.